

SYNOPSIS

Ph. d. Work On

**BEHAVIOUR OF HELICAL SCREW ANCHORS
IN SANDS**

by

Sanjeev Mukherjee

(Enrolment No: 10914040)

Research Scholar, Deptt. of Civil Engg.



Under the supervision of

Dr. Satyendra Mittal

ASSOCIATE PROFESSOR

DEPARTMENT OF CIVIL ENGINEERING

INDIAN INSTITUTE OF TECHNOLOGY ROORKEE

ROORKEE - 247667 (INDIA)

Feb, 2015

1. INTRODUCTION

The works undertaken in this research activity can be divided in three major areas namely, laboratory experiments to determine compression and pullout capacity, numerical investigation to validate laboratory testing results using software PLAXIS and theoretical formulation for the pullout problem.

2. LABORATORY TESTING

Very elaborate investigations have been conducted to study the performance of helical screw anchor against axial compressive and pullout loads with special attention to the effect of number of helical blades having the same geometrical properties. Various components of testing used are described below. Fig. 1 shows the anchors used in the experiments.



Fig. 1: Helical Screw Anchors



Fig. 2: Rectangular Test Tank

A rectangular test tank made up of steel of height 65 cm with 54 cm width was used to conduct experimental investigations for compressive as well as pullout load testing as shown in Fig. 2. The engineering properties of dry sand collected locally from river Solani bed determined are tabulated in Table 1.

Table 1: Engineering Properties of Soil Used for Laboratory Testing

Soil Characteristics	Classification	G	Φ	e_{min}	e_{max}	γ_{d-min}	γ_{d-max}	C_u	C_c
Values	SP	2.63	38	0.52	0.87	13.76	16.97	3.636	0.49

3. PARAMETER VARIATIONS FOR TESTS

Parameter Variations used for compression and pullout testing are shown in Table 2.

Table 2: Parameter Variations in the Entire Compression & Pullout Testing Program

Parameter Variations	No. of anchors (N_a)	No. of Screw blades in an anchor (n_b)	Embedment depth ratio of anchor (H/B)	Soil Density (kN/m^3)
Compression Tests	1, 2, 3, 4	1, 2, 3	2, 4, 6, 8	15.7

Pullout Tests	1, 2, 3, 4	1, 2, 3	4, 6, 8, 10	15.7
---------------	------------	---------	-------------	------

4. Results of Compression Tests

The Ultimate Compressive Loads obtained from all the tests are shown in Table 3.

Table 3: Ultimate Compressive Loads, Q_{uc} (N)

n_b	H/B	$N_a = 1$	$N_a = 2$	$N_a = 3$	$N_a = 4$
1	2	736	1246	1864	2452
1	4	1589	2698	4022	5346
1	6	2207	3600	5592	6867
1	8	2943	4601	6867	8093
2	2	858	1452	2158	2894
2	4	2649	3649	5886	7357
2	6	3433	5297	7063	9270
2	8	4169	6278	8584	11527

The details of the tests for $n_b = 3$ are provided in the thesis.

5. Results of Pullout Tests

The Ultimate Pullout Loads obtained from all the tests are shown in Table 4.

Table 4: Ultimate Pullout Load, Q_{up} (N)

n_b	H/B	$N_a = 1$	$N_a = 2$	$N_a = 3$	$N_a = 4$
1	2	736	1246	1864	2452
1	4	1589	2698	4022	5346
1	6	2207	3600	5592	6867
1	8	2943	4601	6867	8093
2	2	858	1452	2158	2894
2	4	2649	3649	5886	7357
2	6	3433	5297	7063	9270
2	8	4169	6278	8584	11527

The details of the tests for $n_b = 3$ are provided in the thesis.

6. Generalized Equation Proposed for Multiple Helical Screw Anchors

The ultimate compressive capacity of 2, 3 and 4 no. of anchors has been expressed in terms of ultimate compressive capacity of one anchor which are mentioned below.

$$(Q_{up})_n = N_a(Q_{up})_1^m \dots\dots\dots(1)$$

where $m = 0.87$

The ultimate pullout capacity of 2, 3 and 4 no. of anchors has been expressed in terms of ultimate pullout capacity of one anchor which is mentioned below.

$$(Q_{uc})_n = 2 N_a(Q_{uc})_1 \dots\dots\dots(2)$$

where $m = 0.94$

7. Numerical Investigation (PLAXIS)

To account for the unique geometry of the problem a three-dimensional soil-foundation interaction software program, namely PLAXIS 3D Foundation Suite, was selected. The Mohr-Coulomb model was used to represent the soil behaviour, for which cohesion and friction angle values were obtained through triaxial test results. Structures such as plates and node-to-node anchors had been used in the analysis to represent footing plate, anchor plate and helical screw anchor. Fine mesh was selected for mesh generation. Setup used for analysis through PLAXIS is shown in Fig 3.

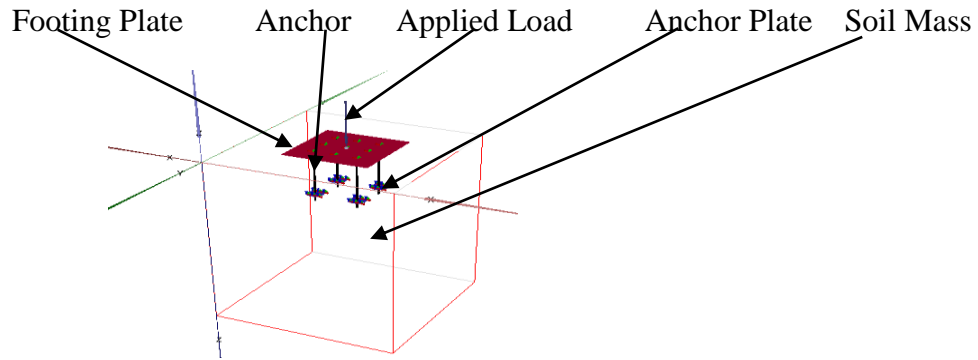


Fig. 3: Position of Various Components in the System

Results obtained from PLAXIS were compared with the laboratory results in non-dimensional form. The differences so obtained are within 10% which indicates that the results obtained from laboratory results can be used to design anchor foundation. Therefore, theoretical formulation has been done on the basis of extensive laboratory work.

Tables 5 and 6 show the comparison for compression and pullout in non-dimensional form respectively. From these tables it is clear that the difference between laboratory test and PLAXIS results is within 10% which can be neglected.

Table 5: Comparison of Non-dimensional Parameter $P_f / (\gamma_a B H \delta_f)$ from Laboratory Experiment and PLAXIS Run for Compression Tests

N_a	n_b	H/B	$P_f / (\gamma_a B H \delta_f)$		%diff
			LAB Test	PLAXIS	
1	1	4	59535.41	65237.04	8.74
1	1	6	40745.87	44934.23	9.32
1	1	8	32319.35	35575.58	9.15
1	2	6	41649.98	45618.69	8.7
1	3	6	41110.74	45918.67	10.47
2	1	6	41881.16	46110.79	9.17
2	2	6	40895.58	45112.13	9.34
2	3	4	65867.37	72999.35	9.77

Table 6: Comparison of Non-dimensional Parameter $P_f / (\gamma_a B H \delta_f)$ from Laboratory Experiment and PLAXIS Run for Pullout Tests

N_a	n_b	H/B	$P_f / (\gamma_a B H \delta_f)$		%diff
			LAB Test	PLAXIS	
1	1	4	59535.41	65237.04	8.74
1	1	6	40745.87	44934.23	9.32
1	1	8	32319.35	35575.58	9.15
1	2	6	41649.98	45618.69	8.7
1	3	6	41110.74	45918.67	10.47
2	1	6	41881.16	46110.79	9.17
2	2	6	40895.58	45112.13	9.34
2	3	4	65867.37	72999.35	9.77

8. Theoretical Formulation

In present work, shallow mode of failure occurs up to H/B=6 and deep mode of failure starts from H/B=8. The forces acting on the anchor were assumed as shown in Fig 4.



Fig. 4: Forces acting on Assumed Failure Surface

The ultimate bearing capacity of shallow helical screw anchors is given by

$$Q_{up} = \frac{\pi\gamma H}{3} (b^2 + r^2 + br) + \frac{\pi\gamma HL(b+r)K'_p}{2} \tan\delta (\tan\phi \cos\theta - \sin\theta) \dots\dots\dots (3)$$

Similarly the ultimate pullout capacity of deep helical screw anchors is given by

$$Q_{up} = \frac{\pi\gamma h_o}{3} (b^2 + r^2 + br) + \pi\gamma r^2 (H - h_o) + \frac{\pi\gamma(b+r)(2H-h_o)K'_p}{2} \tan\delta (\tan\phi \cos\theta - 0.5) \dots\dots\dots (4)$$

The values of ultimate pullout capacity of shallow and deep anchors are calculated for the same parameters as involved in laboratory tests as mentioned in Tables 7 and 8.

Table 7: Comparison of Values of Q_{ult} from Theory and Experiment for Shallow Anchors

H/B	Q_{ult} By Experiment (N)	Q_{ult} By Theory Proposed (N)	% diff
4	93	102	8.82
6	324	294	9.26

Table 8: Comparison of Values of Q_{ult} from Theory and Experiment for Deep Anchors

H/B	Q_{ult} By Experiment (N)	Q_{ult} By Theory Proposed (N)	% diff
8	1079	1129	4.43
10	1717	1753	2.05

9. CONCLUSION

The results obtained from the test indicate that the bearing capacity in compression is much higher than that in tension. The major conclusions of experimental, numerical and theoretical investigations carried out are as given below:

1. With the increase in embedment depth ratio from 2 to 8, the ultimate compressive capacity of helical screw anchor were increased from 981 to 5150 N for no. of anchors equal to 1 and no. of screw blades in an anchor equal to 3. Here the most important observation is that for initial increase in H/B (i.e. for increase in H/B from 2 to 4), the increase in Q_{uc} is 65%, while for further increase in H/B (i.e. for increase in H/B from 6 to 8); the increase in Q_{uc} is 28% which is quite less than earlier increase.

2. With the increase in no. of anchors from 1 to 4, the ultimate compressive capacity of helical screw anchor were increased from 2796 to 7848 N for no. of screw blades in an anchor equal to 3 and embedment depth ratio equal to 4. Here the most important observation is that for initial increase in N_a ; the increase in Q_{uc} is 57% (i.e. for increase in N_a from 1 to 2), while for further increase in N_a ; the increase in Q_{uc} is 19% (i.e. for increase in N_a from 3 to 4) which is less than earlier increase.
3. With the increase inno. of screw blades in an anchor from 1 to 3, the ultimate compressive capacity of helical screw anchor were increased from 5346 to 7848 N for embedment depth ratio H/B equal to 4 and number of anchors N_a equal to 4. Here the most important observation is that for initial increase in n_b ; the increase in Q_{uc} is 27% (i.e. for increase in n_b from 1 to 2), while for further increase in n_b ; the increase in Q_{uc} is 6% (i.e. for increase in n_b from 2 to 3) which is less than earlier increase.
4. It is clear from the above results that the increase in capacity is prominent with the initial increase of these parameters only. There will not be any significant increase in the capacity with further increase in the values of these parameters.
5. With the increase in embedment depth ratio from 4 to 10, the ultimate pullout capacity of helical screw anchor were increased from 441N to 5837 N for no. of anchors equal to 4 and no. of screw blades in an anchor equal to 3. Here the most important observation is that for initial increase in H/B (i.e. for increase in H/B from 4 to 6), the increase in Q_{up} is 73 %, while for further increase in H/B (i.e. for increase in H/B from 8 to 10); the increase in Q_{up} is 37 % which is quite less than earlier increase.
6. With the increase in no. of anchors from 1 to 4, the ultimate pullout capacity of helical screw anchor were increased from 132N to 441 N for no. of screw blades in an anchor equal to 1 and embedment depth ratio equal to 4. Here the most important observation is that for initial increase in N_a ; the increase in Q_{up} is 46% (i.e. for increase in N_a from 1 to 2), while for further increase in N_a ; the increase in Q_{up} is 27% (i.e. for increase in N_a from 3 to 4) which is quite less than earlier increase.
7. With the increase inno. of screw blades in an anchor from 1 to 3, the ultimate pullout capacity of helical screw anchor were increased from 2158N to 3188 N forembedment depth ratio H/B equal to 10 and number of anchors N_a equal to 2. Here

- the most important observation is that for initial increase in n_b ; the increase in Q_{up} is 23 % (i.e. for increase in n_b from 1 to 2), while for further increase in n_b ; the increase in Q_{up} is 12 % (i.e. for increase in n_b from 2 to 3) which is very marginal.
8. It is clear from the above results that the increase in capacity is prominent with the initial increase of parameters only. There will not be any significant increase in the capacity with further increase in the values of these parameters.
 9. The value of angle of internal friction increases from 35° for virgin soil to 48° for soil with 4 nos. of double helical screw anchors.
 10. Apparent coefficient of friction between the anchor and the soil (f^*) which plays an important role in determining the strength of anchors increases with embedment depth ratio and no. of anchors. For compression it increases from 3.73 to 17.58 (increased by almost 371 % with increase in no. of anchors from 1 to 4, embedment depth ratio from 2 to 8 and no. of screw blades in an anchor from 1 to 3) whereas for pullout it increases from 1.39 to 10.02 (increased by almost 620 % with increase in no. of anchors from 1 to 4, embedment depth ratio from 4 to 10 and no. of screw blades in an anchor from 1 to 3).
 11. The difference between PLAXIS and laboratory values are within 10% which is very marginal.
 12. Theoretical formulation is done for ultimate pullout capacity of anchor for single helical screw anchor. By comparison it can be said that the difference between the theoretical and experimental values is minimal. Hence it can be said that for deep depths, the present theory in this paper predicts the ultimate pullout capacity of multiple helical screw anchors with sufficient accuracy.



INDIAN INSTITUTE OF TECHNOLOGY ROORKEE ROORKEE

CANDIDATE'S DECLARATION

I hereby certify that the work which is being presented in the thesis entitled “**BEHAVIOUR OF HELICAL SCREW ANCHORS IN SAND**” in partial fulfilment of the requirements for the award of the Degree of Doctor of Philosophy and submitted in the Department of **Civil Engineering**, of the Indian Institute of Technology Roorkee is an authentic record of my own work carried out during a period from **December, 2010** to **March, 2015** under the supervision of **Dr. Satyendra Mittal, Associate Professor**, Department of **Civil Engineering**, Indian Institute of Technology Roorkee.

The matter presented in this thesis has not been submitted by me for the award of any other degree of this or any other Institute.

(**SANJEEV MUKHERJEE**)

This is to certify that the above statement made by the candidate is correct to the best of my knowledge.

(Satyendra Mittal)
Supervisor

Date:

The Ph.D. Viva-Voce Examination of **Mr. Sanjeev Mukherjee**, Research Scholar, has been held on.....

Chairman, SRC

Signature of External Examiner

This is to certify that the student has made all the corrections in the thesis.

Signature of Supervisor

Head of the Department

ABSTRACT

The design of many engineering structures requires foundation systems to resist both compressive and tensile forces. These types of structures, which may include high rise buildings, chimney towers or transmission towers, are commonly supported by soil anchors. As the uses of anchors increased many-fold in recent years, to support substantial large structure, a greater understanding regarding their behaviour is required. During the last forty years various researchers have proposed approximate techniques to estimate the uplift and compressive capacity of soil anchors. The majority of past research has been experimentally based and, as a result, current design practices are largely based on empirical relationships. In contrast, very few rigorous numerical analyses have been performed to determine the ultimate pull-out and compressive load of anchors.

The study of anchors is complicated by the large number of variables that influence its overall behaviour. These include anchor size, shape, embedment depth and orientation. Apart from these anchor properties, large numbers of soil variables are also there which influence the result greatly. All these variables must be considered in an analysis to achieve correct result. In present research work, a comprehensive study into the behaviour of helical screw anchors is presented. Consideration was given to the wide range of parameters that influence anchor capacity. The aim of the present research was to better understand anchor behaviour and to develop rigorous stability solutions for earth anchors that can be used by design engineers. In the present study, the locally available fine sand collected from Solani River bed was used for laboratory investigations.

A good number of tests were performed by varying number of anchors (1, 2, 3 and 4), number of screw blades in the anchor (1, 2 and 3) and embedment depth ratio (H/B) (for compressive load $H/B = 2, 4, 6$ and 8 and for pullout load $H/B = 4, 6, 8$ and 10). The results obtained from the tests indicate that the bearing capacity in compression is much higher than that in tension.

In compression tests, for initial increase in H/B (i.e. for increase in H/B from 2 to 4), the increase in Q_{uc} was 56%, while for further increase in H/B (i.e. for increase in H/B from 6 to 8); the increase in Q_{uc} was 28% which was quite less than earlier increase. Also, for initial increase in N_a ; the increase in Q_{uc} was 27% (i.e. for increase in N_a from 1 to 2), while for further increase

in N_a ; the increase in Q_{uc} was 20% (i.e. for increase in N_a from 3 to 4) which was less than earlier increase. Similarly, for initial increase in n_b , the increase in Q_{uc} was 27% (i.e. for increase in n_b from 1 to 2), while for further increase in n_b ; the increase in Q_{uc} was 7% (i.e. for increase in n_b from 2 to 3) which was less than earlier increase. It was clear from these test results that ultimate compressive load increases with increases in all these parameters mentioned above but this rate of increase is higher for initial increase than in the later stage.

Similar results were observed for pullout tests also. In pullout tests, for initial increase in H/B (i.e. for increase in H/B from 4 to 6), the increase in Q_{up} was 169%, while for further increase in H/B (i.e. for increase in H/B from 8 to 10); the increase in Q_{up} was 81% which is quite less than earlier increase. Similarly, for initial increase in N_a ; the increase in Q_{up} was 150% (i.e. for increase in N_a from 1 to 2), while for further increase in N_a ; the increase in Q_{up} was 25% (i.e. for increase in N_a from 3 to 4) which was quite less than earlier increase. Also, for initial increase in n_b , the increase in Q_{up} was 60% (i.e. for increase in n_b from 1 to 2), while for further increase in n_b ; the increase in Q_{up} was 25% (i.e. for increase in n_b from 2 to 3) which was quite less than earlier increase. It was clear from the above results that the increase in capacity was prominent with the initial increase of parameters only. There will not be any significant increase in the capacity with further increase in the values of these parameters.

A parametric study was also conducted in the laboratory to ascertain the increase in value of angle of internal friction (Φ) and improved apparent coefficient of friction (f^*) between the anchor and the soil because of insertion of anchors in soil. From this study it was found that the value of angle of internal friction increased from 35° for virgin soil to 48° for soil-anchor system with 4 double helical screw anchors. For compression tests it was found that the value of apparent coefficient of friction increases from 3.73 to 17.58 (increased by almost 371 % with increase in no. of anchors from 1 to 4, embedment depth ratio from 2 to 8 and no. of screw blades in an anchor from 1 to 3). Similarly for pullout tests, the value of apparent coefficient of friction increases from 1.39 to 10.02 (increased by almost 620 % with increase in no. of anchors from 1 to 4, embedment depth ratio from 4 to 10 and no. of screw blades in an anchor from 1 to 3).

Theoretical formulation was also done for ultimate pullout capacity of single helical screw anchor. The difference between the theoretical and experimental value came close to 9% for shallow anchors (for embedment depth ratio of 4 & 6) and 4% for deep anchors (for

embedment depth ratio of 8 & 10). By comparison it can be said that the difference between the theoretical and experimental values is minimal. Hence it can be said that the present theory predicts the ultimate pullout capacity of multiple helical screw anchors with sufficient accuracy.

PLAXIS 3D Foundation Suite was used to verify the findings from the laboratory tests conducted during this investigation. The results obtained by conducting laboratory experiments were compared with the results obtained by conducting PLAXIS runs on the model similar to the one on which laboratory experiments were conducted. The difference between laboratory test and PLAXIS results was within 10% which can be accepted.

ACKNOWLEDGEMENT

At the outset, I would like to express my deep sense of gratitude to **Dr. Satyendra Mittal, Associate Professor, Department of Civil Engineering, IIT Roorkee** for his invaluable guidance, support and encouragement throughout this research work. His painstaking efforts in editing the manuscript and useful suggestions for its improvement are humbly acknowledged.

I would like to thank **Prof. Deepak Kashyap, Professor and Head, Department of Civil Engineering, IIT Roorkee**, for extending every possible help and support during the experimental work. I would also like to express my gratitude to **Prof. D. C. Srivastava, external expert SRC, Prof. Mahendera Singh, SRC member and Prof. N.K. Samadhiya, Chairman SRC** for their support and guidance.

The help and support extended by staff of Soil Mechanics Laboratory of Civil Engineering Department, Geotechnical Engineering Laboratory of IIT Roorkee particularly **Mr. Atma Ram, Mr. Deepak Raj Saxena and Mr. Pitambar** for extending their help and cooperation during the experimental investigations. I am thankful to **Mr. Ombir and Mr. Anand** for their help during arrangement of test set ups and testing process. I would like to express my heartfelt thanks to **Sri Rajiv Chauhan**, former Ph. D. student of Geotechnical engineering section, Civil Engg Department for extending his help and support for organizing and editing this manuscript to make it in a presentable form.

Last, but not the least, I express my deep sense of gratitude to those who were involved directly or indirectly to make my research work successful. It would be unfair if I do not name my wife **Mrs. Tanushree Mukherjee** as a person behind the completion of this research work. She took all the responsibilities of family on my behalf and made it easy for me to concentrate on my research work, in spite of many difficulties. I will be indebted to her throughout my life.

The acknowledgement would remain incomplete without mentioning my daughter **Raina** and son **Arnab**, who bestowed upon me their love and care during course of this research work. I

am deeply indebted to my father **Late Dr. Santosh Kumar Mukherjee**, whose blessings, motivation and inspiration have always provided me high mental support.

Finally, my salutations to All-Pervading Almighty whose Divine Light provided me faith, inspiration, guidance and strength to carry out this research work.

(Sanjeev Mukherjee)

TABLE OF CONTENTS

	Page No.
CANDIDATE’S DECLARATION	i
ABSTRACT	ii
ACKNOWLEDGMENT	v
TABLE OF CONTENTS	vii
LIST OF FIGURES	xii
LIST OF TABLES	xvii
LIST OF NOTATIONS AND SYMBOLS	xix
LIST OF ABBREVIATIONS	xxii
CHAPTER 1 INTRODUCTION	
1.0 BACKGROUND	I-1
1.1 HELICAL SCREW ANCHORS	I-3
1.2 OBJECTIVE OF THE THESIS	I-8
1.3 TEST PROGRAM	I-8
1.4 ORGANISATION OF THESIS	I-8
1.5 LIMITATIONS OF THE PRESENT THESIS	I-9
CHAPTER 2 REVIEW OF LITERATURE	
2.0 HISTORICAL BACKGROUND	II-1
2.1 EARLIER EXPERIMENTAL INVESTIGATIONS	II-3
2.1.1 Compression Loading	II-4
2.1.2 Pullout Loading	II-9
2.2 EARLIER THEORETICAL ANALYSES	II-19

2.2.1	Theoretical Studies for Compression Loading	II-20
2.2.2	Theoretical Studies for Pullout Loading	II-21
2.3	OTHER INVESTIGATIONS	II-35
2.4	COMPRESSIVE CAPACITY VS. PULLOUT CAPACITY	II-36
2.5	GAPS IN STATE OF ART	II-36
2.6	OBJECTIVES OF THE PRESENT STUDY	II-37
 CHAPTER 3 EXPERIMENTAL INVESTIGATION		
3.0	GENERAL	III-1
3.1	LABORATORY TESTS	III-1
3.1.1	Helical Screw Anchors	III-1
3.1.2	Experimental Setup	III-2
3.1.2.1	<i>Test Tank</i>	III-2
3.1.2.2	<i>Loading Frame</i>	III-3
3.1.3	Soil Used in the Study	III-4
3.1.4	Model Test Procedure	III-5
3.1.4.1	<i>Computation of the weight of soil</i>	III-6
3.1.4.2	<i>Preparation and placing of Experimental Soil</i>	III-6
3.1.4.3	<i>Conduct of Experiment</i>	III-6
3.2	RESULTS OF LABORATORY COMPRESSION TESTS	III-7
3.2.1	Experimental Results for Compression Tests	III-8
3.3	RESULTS OF LABORATORY PULLOUT TESTS	III-15
3.3.1	Experimental Results of Pullout Tests	III-16

CHAPTER 4 DISCUSSION ON TEST RESULTS

4.0	INTRODUCTION	IV-1
4.1	DISCUSSION ON COMPRESSION TEST RESULTS	IV-1
4.1.1	Effect of No. of Anchors (N_a)	IV-1
4.1.2	Effect of Embedment Depth Ratio (H/B)	IV-2
4.1.3	Effect of No. of Helical Screws Blades in Anchor (n_b)	IV-3
4.1.4	Ultimate Compressive Capacity of Multiple Anchors	IV-4
	<i>4.1.4.1 Group of Two Anchors</i>	IV-5
	<i>4.1.4.2 Group of Three Anchors</i>	IV-7
	<i>4.1.4.3 Group of Four Anchors</i>	IV-7
4.1.5	Generalized Equation Proposed for Multiple Helical Screw Anchors	IV-8
4.1.6	Limitations of Proposed Equation	IV-10
4.1.7	Comparison of Laboratory and Empirical Values	IV-12
4.1.8	Non-Dimensional Graphs and Design Considerations	IV-13
4.1.9	Design of Anchors using Hyperbolic Curves	IV-13
4.1.10	Parametric Study	IV-17
	<i>4.1.10.1 Increase in the Value of Apparent Coefficient of Friction (f^*)</i>	IV-17
4.1.11	Design Example	IV-17
4.2	DISCUSSION ON PULLOUT TEST RESULTS	IV-20
4.2.1	Effect of No. of Anchors (N_a)	IV-20
4.2.2	Effect of Embedment Depth Ratio (H/B)	IV-20
4.2.3	Effect of No. of Helical Screw Blades in Anchor (n_b)	IV-22

4.2.4	Ultimate Pullout Capacity of Multiple Anchors	IV-23
	<i>4.2.4.1 Group of Two Anchors</i>	IV-24
	<i>4.2.4.2 Group of Three Anchors</i>	IV-24
	<i>4.2.4.3 Group of Four Anchors</i>	IV-25
4.2.5	Generalized Equation Proposed for Multiple Helical Screw Anchors	IV-26
4.2.6	Limitations of Proposed Equation	IV-28
4.2.7	Comparison of Laboratory and Empirical Values	IV-29
4.2.8	Non-Dimensional Graphs and Design Considerations	IV-29
4.2.9	Design of Anchors using Hyperbolic Curves	IV-29
4.2.10	Theoretical Considerations	IV-33
4.2.11	Equations Developed	IV-34
	<i>4.2.11.1 Shallow Anchor</i>	IV-34
	<i>4.2.11.2 Deep Anchor</i>	IV-36
4.2.11	Comparison of Present Work with Published Works	IV-39
	<i>4.2.11.1 Comparison of results with Ghaly (1991)</i>	IV-39
	<i>4.2.11.2 Comparison of results with Malik (2007)</i>	IV-39
4.2.12	Parametric Study	IV-40
	<i>4.2.12.1 Increase in Φ by Plate Load Test</i>	IV-40
	<i>4.2.12.2 Increase in the Value of Apparent Coefficient of Friction (f^*)</i>	IV-41
4.2.13	Design Example	IV-42

CHAPTER 5 NUMERICAL VALIDATION

5.0	INTRODUCTION	V-1
------------	---------------------	-----

5.1	PROBLEM SOLVING WITH PLAXIS 3D	V-1
5.1.1	Defining Soil	V-2
5.1.2	Defining Structure	V-2
5.1.3	Defining Geometric Entities	V-3
5.1.4	Defining Constitutive Model	V-3
	<i>5.1.4.1 Formulation of the Mohr-Coulomb Model</i>	V-4
5.1.5	Initial Conditions	V-5
5.1.6	Mesh Generation	V-5
5.1.7	Defining Loads	V-5
5.1.8	Defining Calculation Phases	V-5
5.1.9	Types of Analysis	V-6
5.1.10	Interpretation and Presentation of Results	V-6
5.2	DESCRIPTION OF THE DEVELOPED PLAXIS 3D MODEL	V-6
5.3	MATERIAL PROPERTIES USED IN THE NUMERICAL ANALYSIS	V-9
5.4	PLAXIS RESULTS FOR COMPRESSION	V-10
5.5	PLAXIS RESULTS FOR PULLOUT	V-13
5.6	COMPARISON OF PLAXIS WITH LABORATORY WORK	V-17
	5.6.1 Comparison with Laboratory Compression Testing	V-19
	5.6.2 Comparison with Laboratory Pullout Testing	V-19
CHAPTER 6 CONCLUSIONS AND RECOMMENDATIONS		
6.0	SUMMARY	VI-1
6.1	COMPRESSIVE CAPACITY OF HELICAL SCREW ANCHORS	VI-2
6.2	PULLOUT CAPACITY OF HELICAL SCREW ANCHORS	VI-3

6.3	NUMERICAL VALIDATION	VI-4
6.4	SCOPE OF FUTURE RESEARCH	VI-4
	LIST OF REFERENCES	1-11
	PAPERS PUBLISHED FROM CURRENT RESEARCH WORK	13
	RESUME	15

LIST OF FIGURES

Fig. No.	Title	Page No.
Fig. 1.1	Helical Anchors	I-3
Fig. 1.2	Helical Anchor Components	I-5
Fig. 1.3	Lead Section	I-7
Fig. 1.4	Extension Section	I-7
Fig. 2.1	Mitchell Screw Pile (a) Screw Pile (b) Screw Pile Used for Moorings in 1836	II-1
Fig. 2.2	Failure of Soil above a Strip Footing Under Uplift Load (After Meyerhof and Adams, 1968)	II-2
Fig. 2.3	Possible Failure Mechanisms of a Multi-Helix Helical Anchor: (a) Individual Bearing Failure and (b) Cylindrical Shear Failure	II-6
Fig. 3.1	Single, Double and Triple Helical Screw Anchor (Lab Test)	III-2
Fig. 3.2	Sketch showing Dimensions of Helical Screw Anchors (a) Single Helical Screw Anchor (b) Double Helical Screw Anchor (b) and (c) Triple Helical Screw Anchor (All Dimensions are in mm)	III-3
Fig. 3.3	Test setup for Testing of 4 Helical Screw Anchors	III-4
Fig. 3.4	Loading Frame	III-4
Fig. 3.5	Grain Size Distribution Curve of Soil Used in Laboratory Tests	III-5
Fig. 3.6	Laboratory Test in Progress for Vertical Helical Screw Anchor	III-7
Fig. 3.7	Compression Test Graphs for 1 No. of Single Helical Screw Anchor	III-9
Fig. 3.8	Compression Test Graphs for 1 No. of Double Helical Screw Anchor	III-10
Fig. 3.9	Compression Test Graphs for 1 No. of Triple Helical Screw Anchor	III-10
Fig. 3.10	Compression Test Graphs for 2 Nos. of Single Helical Screw Anchor	III-11
Fig. 3.11	Compression Test Graphs for 2 Nos. of Double Helical Screw Anchor	III-11
Fig. 3.12	Compression Test Graphs for 2 Nos. of Triple Helical Screw Anchor	III-12
Fig. 3.13	Compression Test Graphs for 3 Nos. of Single Helical Screw Anchor	III-12
Fig. 3.14	Compression Test Graphs for 3 Nos. of Double Helical Screw Anchor	III-13
Fig. 3.15	Compression Test Graphs for 3 Nos. of Triple Helical Screw Anchor	III-13
Fig. 3.16	Compression Test Graphs for 4 Nos. of Single Helical Screw Anchor	III-14
Fig. 3.17	Compression Test Graphs for 4 Nos. of Double Helical Screw Anchor	III-14

Fig. 3.18	Compression Test Graphs for 4 Nos. of Triple Helical Screw Anchor	III-15
Fig. 3.19	Pullout Test Graphs for 1 No. of Single Helical Screw Anchor	III-18
Fig. 3.20	Pullout Test Graphs for 1 No. of Double Helical Screw Anchor	III-18
Fig. 3.21	Pullout Test Graphs for 1 No. of Triple Helical Screw Anchor	III-19
Fig. 3.22	Pullout Test Graphs for 2 Nos. of Single Helical Screw Anchor	III-19
Fig. 3.23	Pullout Test Graphs for 2 Nos. of Double Helical Screw Anchor	III-20
Fig. 3.24	Pullout Test Graphs for 2 Nos. of Triple Helical Screw Anchor	III-20
Fig. 3.25	Pullout Test Graphs for 3 Nos. of Single Helical Screw Anchor	III-21
Fig. 3.26	Pullout Test Graphs for 3 Nos. of Double Helical Screw Anchor	III-21
Fig. 3.27	Pullout Test Graphs for 3 Nos. of Triple Helical Screw Anchor	III-22
Fig. 3.28	Pullout Test Graphs for 4 Nos. of Single Helical Screw Anchor	III-22
Fig. 3.29	Pullout Test Graphs for 4 Nos. of Double Helical Screw Anchor	III-23
Fig. 3.30	Pullout Test Graphs for 4 Nos. of Triple Helical Screw Anchor	III-23
Fig. 4.1	Effect of No. of Anchors for $n_b = 3$, $H/B = 4$ and $N_a = 1, 2, 3$ & 4	IV-2
Fig. 4.2	Effect of Embedment Depth Ratio (H/B) for $n_b=3$, $N_a=1$ and $H/B= 2, 4, 6$ & 8	IV-3
Fig. 4.3	Effect of Screw Blades in Anchors (n_b) for $N=4$, $H/B=4$ and $n_b = 1, 2$ & 3	IV-4
Fig. 4.4	Schematic of Compression Test for a Combination of 2 Anchors (All Dimensions in mm)	IV-5
Fig. 4.5	Ultimate Compressive Capacity of 2 Anchors w.r.t. 1 Anchor	IV-6
Fig. 4.6	Arrangement for Compression Test on a Combination of 3 Anchors (All Dimensions in mm)	IV-7
Fig. 4.7	Ultimate Compressive Capacity of 3 Anchors w.r.t. 1 Anchor	IV-8
Fig. 4.8	Arrangement for Compression Test on a Combination of 4 Anchors (All Dimensions in mm)	IV-9
Fig. 4.9	Ultimate Compressive Capacity of 4 Anchors w.r.t. 1 Anchor	IV-10
Fig. 4.10	Non-Dimensional Compression Test Graph for $N_a=2$, $n_b=2$ and $H/B=2, 4, 6$ & 8	IV-13
Fig. 4.11	Non-Dimensional Compression Test Graph for $N_a=4$ and $n_b= 3$ and $H/B = 2, 4, 6$ & 8	IV-14

Fig. 4.12	Hyperbolic Curve for 2 Nos. of Double Helical Screw Anchors for Compression Tests	IV-16
Fig. 4.13	Hyperbolic Curve for 4 Nos. of Triple Helical Screw Anchors for Compression Tests	IV-16
Fig. 4.14	Pullout Test Graph for $n_b=2$, $H/B=6$ and $N_a=1, 2, 3$ & 4	IV-21
Fig. 4.15	Pullout Test Graph for $n_b=3$, $N_a=4$ and $H/B=4, 6, 8$ & 10	IV-22
Fig. 4.16	Pull-out Test Graph for $N_a=2$, $H/B=6$ and $n_b=1, 2$ & 3	IV-23
Fig. 4.17	Ultimate Pullout Capacity of 2 Anchors w.r.t. 1 Anchor	IV-24
Fig. 4.18	Ultimate Pullout Capacity of 3 Anchors w.r.t. 1 Anchor	IV-25
Fig. 4.19	Ultimate Pullout Capacity of 4 Anchors w.r.t. 1 Anchor	IV-26
Fig. 4.20	Non-Dimensional Lab Pull-out Test Graph for $n_b=1$, $N_a=2$ and $H/B=4, 6, 8$ & 10	IV-30
Fig. 4.21	Non-Dimensional Lab Pull-out Test Graph for $n_b=1$, $N_a=4$ and $H/B=4, 6, 8$ & 10	IV-30
Fig. 4.22	Hyperbolic Curve for 2 Nos. of Single Helical Screw Anchors for Pullout Tests	IV-32
Fig. 4.23	Hyperbolic Curve for 4 Nos. of Single Helical Screw Anchors for Pullout Tests	IV-33
Fig. 4.24	Forces acting on Assumed Failure Surface for Shallow Anchor	IV-35
Fig. 4.25	Forces Acting on Assumed Failure Surface for Deep Anchor	IV-37
Fig. 5.1	Dimension of the Grid Used in PLAXIS	V-7
Fig. 5.2	Position of Various Components in the System	V-8
Fig. 5.3a	Side View of the Mesh generated in PLAXIS	V-8
Fig. 5.3b	Top View of the Mesh generated in PLAXIS	V-9
Fig. 5.4	PLAXIS Run in Compression for $n_b=1$, $H/B=6$ and $N_a=1, 2, 3$ & 4	V-13
Fig. 5.5	PLAXIS Run in Compression for $n_b=1$, $N_a=1$ and $H/B=4, 6$ & 8	V-14
Fig. 5.6	PLAXIS Run in Compression for $N_a=1$, $H/B=6$ and $n_b=1, 2$ & 3	V-14
Fig. 5.7	PLAXIS Run in Pullout for $N_a=2$, $H/B=6$ and $n_b=1, 2$ & 3	V-17
Fig. 5.8	PLAXIS Run in Pullout for $n_b=1$, $N_a=1$ and $H/B=4, 6$ & 8	V-18
Fig. 5.9	PLAXIS Run in Pullout for $n_b=1$, $H/B=6$ and $N_a=1, 2, 3$ & 4	V-18

LIST OF TABLES

Table No.	Title	Page No.
Table 2.1	Earlier Experimental Investigations for Compression Loading	II-6
Table 2.2	Earlier Experimental Investigations for Pullout Loading	II-9
Table 2.3	Earlier Theoretical Analyses for Compression Loading	II-20
Table 2.4	Earlier Theoretical Analyses for Pullout Loading	II-21
Table 3.1	Engineering Properties of Soil Used in Laboratory Experiments	III-5
Table 3.2	Parameter Variations in the Entire Compression Testing Program	III-8
Table 3.3	Ultimate Compressive Loads, Q_{uc} (N)	III-9
Table 3.4	Parameter Variations in the Entire Pullout Testing Program	III-16
Table 3.5	Ultimate Pullout Load, Q_{up} (N)	III-17
Table 4.1	Ultimate Compressive Load of 2, 3 & 4 Anchors Based on Equation 4.4	IV-11
Table 4.2	Comparison of $(Q_{uc})_2$ from Experiments and Equation 4.4	IV-11
Table 4.3	Comparison of $(Q_{uc})_3$ from Experiments and Equation 4.4	IV-12
Table 4.4	Comparison of $(Q_{uc})_4$ from Experiments and Equation 4.4	IV-12
Table 4.5	Values of Constants of Hyperbolic Equation for Compression Tests	IV-15
Table 4.6	Values of f^* for Compression Tests	IV-18
Table 4.7	Ultimate Pullout Capacity of Multiple Anchors from Equation 4.10	IV-27
Table 4.8	Comparison of $(Q_{up})_2$ from Experiments and Equation 4.10	IV-28
Table 4.9	Comparison of $(Q_{up})_3$ from Experiments and Equation 4.10	IV-28
Table 4.10	Comparison of $(Q_{up})_4$ from Experiments and Equation 4.10	IV-29
Table 4.11	Values of Constants of Hyperbolic Equation for Pullout Tests	IV-31
Table 4.12	Comparison of values of Q_{ult} from theory and experiment for shallow anchors	IV-36
Table 4.13	Comparison of values of Q_{ult} from theory and experiment for deep anchors	IV-38
Table 4.14	Comparison of present work with Ghaly (1991)	IV-39
Table 4.15	Comparison of Present Work with Malik (2007)	IV-39
Table 4.16	Difference in present values with Malik (2007)	IV-40
Table 4.17	Values of Φ Obtained after Plate Load Test	IV-41

Table 4.18	Values of f^* for Pullout Tests	IV-41
Table 5.1	Parameters Used in Mohr-Coulomb Model	V-4
Table 5.2	Material Properties of Sand Used in PLAXIS	V-9
Table 5.3	Material Properties of Anchor Plate Used in PLAXIS	V-10
Table 5.4	Material Properties of Footing Plate Used in PLAXIS	V-10
Table 5.5	Material Properties of Node-to-Node Anchor Used in PLAXIS	V-10
Table 5.6	PLAXIS Results of Compression Tests for $N_a=1$	V-11
Table 5.7	PLAXIS Results of Compression Tests for $N_a=2$	V-11
Table 5.8	PLAXIS Results of Compression Tests for $N_a=3$	V-12
Table 5.9	PLAXIS Results of Compression Tests for $N_a=4$	V-12
Table 5.10	PLAXIS Results of Pullout Tests for $N_a=1$	V-15
Table 5.11	PLAXIS Results of Pullout Tests for $N_a=2$	V-15
Table 5.12	PLAXIS Results of Pullout Tests for $N_a=3$	V-16
Table 5.13	PLAXIS Results of Pullout Tests for $N_a=4$	V-16
Table 5.14	Comparison of Non-dimensional Parameter ($P_f/\gamma_d B H \delta_f$) from Laboratory Experiment and PLAXIS Run for Compression Tests	V-19
Table 5.15	Comparison of Non-dimensional Parameter ($P_f/\gamma_d B H \delta_f$) from Laboratory Experiment and PLAXIS Run for Pullout Tests	V-20

LIST OF NOTATIONS AND SYMBOLS

B	Diameter of the screw of the anchor
B'	Width of Footing in Plate Load Test
b	Radius of Screw of Anchor
C_u	Uniformity Coefficient
C_c	Coefficient of Curvature
c	Cohesion
D	Width of the Plate Anchor
G	Specific Gravity
E	Young's Modulus
E_{oed}	Oedometer Modulus
F_c	Uplift Capacity Factor due to Cohesion
F_q	Uplift Capacity Factor due to Surcharge
F_γ	Uplift Capacity Factor due to Unit Weight of Soil
f^*	Apparent Coefficient of Friction
f_s	Average Unit Skin Friction
G	Shear Modulus
H	Embedment Depth of the Anchor
h_o	Height of Assumed Inverted Cone
I_D	Relative Density of Sand
K_o	Coefficient of Earth Pressure at Rest
K_t	Torque Correlation Coefficient
L	Length of the Anchor
L'	Side Length of the Failure Surface Cone
m	Constant
N_a	No. of Anchors
N_q	Bearing Capacity Factor
N_γ	Bearing Capacity Factor
n_b	No. of Screw Blades in an Anchor
P	Load Applied

P_u	Ultimate Failure Load
P_p	Passive Earth Pressure along the Failure Surface
P_f	Failure Load
Q_b	End Bearing Resistance of Anchor
Q_s	Skin Friction along the Anchor Shaft
Q_{uc}	Ultimate Compression Load
$(Q_{uc})_1$	Ultimate Compressive Capacity of a Single Anchor
$(Q_{uc})_2$	Ultimate Compressive Capacity of a Group of 2 anchors
$(Q_{uc})_3$	Ultimate Compressive Capacity of a Group of 3 anchors
$(Q_{uc})_4$	Ultimate Compressive Capacity of a Group of 4 anchors
Q_{up}	Ultimate Pullout Load
$(Q_{up})_1$	Ultimate Pullout Capacity of a Single Anchor
$(Q_{up})_2$	Ultimate Pullout Capacity of a Group of 2 anchors
$(Q_{up})_3$	Ultimate Pullout Capacity of a Group of 3 anchors
$(Q_{up})_4$	Ultimate Pullout Capacity of a Group of 4 anchors
Q_{ut}	Ultimate Tension Load
q	Surcharge Intensity
q_b	Unit Bearing Capacity of Anchor Point of Area A_b
q_u	Ultimate Bearing Capacity
R_i	Interaction Coefficient
S	Spacing between two adjacent Helix Plates
S_{cr}	Critical Spacing between Anchors
S_v	Vertical Spacing between Anchor Plates
T	Shearing Stress developed along the Failure Surface
V	Volume of Truncated Cone within Failure Surface
W	Weight of Sand Wedge within Failure Surface
z	Depth of the Sand Fill Above the Screw of the Anchor
Φ	Angle of Internal Friction of Soil
γ	Unit Weight of Soil
γ_d	Dry Unit Weight of Soil
e_{min}	Minimum Void Ratio of Soil

e_{\max}	Maximum Void Ratio of Soil
γ_{\min}	Minimum Unit Weight, (kN/m ³)
γ_{\max}	Maximum Unit Weight, (kN/m ³)
δ	Average Mobilized Angle of Shear Resistance
δ_f	Displacement at Failure
ν	Poisson's Ratio of Soil
Ψ	Dilation Angle of Soil
ρ	Density of Sand
η_c	Non-Dimensional Efficiency Factor
η_γ	Group Efficiency Factor
σ_m	Mean Principal Stress
λ	Thickness Ratio

LIST OF ABBREVIATIONS

FEM	Finite Element Method
FREQ	Frequency
LL	Liquid Limit
OCR	Over Consolidation Ratio
PI	Plasticity Index
PISA	Power-Installed Screw Anchor
PL	Plastic Limit

BEHAVIOUR OF HELICAL SCREW ANCHORS IN SAND

Ph.D. Thesis

by

SANJEEV MUKHERJEE



**DEPARTMENT OF CIVIL ENGINEERING
INDIAN INSTITUTE OF TECHNOLOGY ROORKEE
ROORKEE – 247667 (INDIA)
MARCH, 2015**

BEHAVIOUR OF HELICAL SCREW ANCHORS IN SAND

A THESIS

*Submitted in partial fulfilment of the
requirements for the award of the degree*

of

DOCTOR OF PHILOSOPHY

in

CIVIL ENGINEERING

by

SANJEEV MUKHERJEE



**DEPARTMENT OF CIVIL ENGINEERING
INDIAN INSTITUTE OF TECHNOLOGY ROORKEE
ROORKEE – 247667 (INDIA)
MARCH, 2015**

**©INDIAN INSTITUTE OF TECHNOLOGY ROORKEE, ROORKEE - 2015
ALL RIGHTS RESERVED**

INTRODUCTION

1.0 BACKGROUND

Ground improvement and soil reinforcement have become necessary in view of shortage of space available and type of structures being constructed globally. Many investigators have done commendable work in the past in this area (Mittal, 2013; Tatsuoka et al., 1995, Puppala et al., 2004, Reddy et al., 2011, Latha and Somwanshi, 2009, Choudhury and Katdare, 2013, Powrie and Cox, 2001, Boominathan and Hari, 2002, Chandra et al., 1984, Madabhushi, 2007, Vanapalli, 2008 etc.).

Initially transmission towers were supported by large-mass concrete blocks where the required uplift capacity was supplied entirely by the self-weight of the concrete. This simple design came at a considerable cost. As a result research was undertaken to find a more economical design solution. The objective of this present research is to develop design of anchor which provides an economical and competitive alternative to the mass foundations.

The purpose of this chapter is to provide the background information regarding helical screw anchors. The design of many engineering structures requires foundation systems to resist compressive, tensile and lateral forces. Their current applications include residential and commercial buildings, bridges, solar farms, light poles, wind turbines, and machine foundations. In such cases, an attractive and economic design solution may be achieved through the use of tension members. In recent decades, their applications in engineering projects have expanded to both support and rehabilitate structures under tensile, compressive and lateral loading. In spite of their current increase in application, the amount of available research and design methodology to date are limited. The majority of relevant research has been focussed solely on the uplift capacity and very limited research has been carried out on predicting the anchor capacity in compression and lateral loading. Due to the increased demand for more complex and efficient designs, it is necessary to better understand the performance characteristics of helical anchors under different loading scenarios and to provide more rigorous design approaches. Therefore, given the lack of

design procedures, the application of helical screw anchors, particularly for the compression case, is also considered in this thesis.

Helical screw anchors are typically fixed to the structure and embedded in the ground to sufficient depth so that they can resist pull-out or compressive forces with safety. Helical screw anchors are a lightweight foundation system designed and constructed specifically to resist any compressive/uplifting force or overturning moment placed on a structure. There are many advantages of using anchors as foundation system. Some of which are outlined below:

- Quick, easy installation possible.
- Immediate loading allowed.
- Small equipments required for installation.
- It is a pre-engineered system.
- It is easily field modified.
- There is direct torque-to capacity correlation.
- Can be installed in any weather.
- Helical screw piles are solution for restricted access sites, can be installed even in high water table and weak surface soils.
- These are environmentally friendly.
- Cause no vibration while driving.
- No concrete is required for such piles.

Fig. 1.1 shows a typical helical screw anchor used in the industry. Current understanding regarding the behaviour of buried foundations, and anchor plates in particular is somewhat unsatisfactory. The complex nature of anchor behaviour, and the sheer number of variables that influence soil compressive and uplift capacity, has meant there are many conflicting theories reported in the literature. Most currently proposed theories have significant underlying assumptions based on experimental observations regarding the likely failure mode of anchors. Unfortunately it would appear that these assumptions are responsible for the general lack of overall agreement on soil compressive and uplift theory. The advantage of using rigorous numerical methods to study anchor behaviour is that a good indication of the likely failure mechanism can be obtained without any assumptions being made in advance.

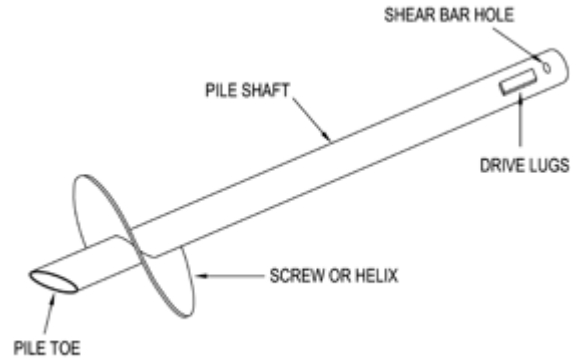


Fig. 1.1: Helical Anchors [Ghaly et al. (1991)]

A laboratory test program had been carried out to examine the compressive and the uplift response of helical screw anchors embedded in cohesionless soil media. Although there are no fully adequate substitutes for full-scale field tests, tests at laboratory scale have the advantage of allowing a close control of at least some of the variables encountered in practice. In this way trends and behaviour patterns observed in the laboratory can be of great value in developing an understanding of performance at larger scales, and mathematical analyses developed in conjunction with laboratory testing may thus be of great value in practice.

The purpose of this chapter is to provide an introduction to the topic of soil anchors and general compressive and uplift capacity, and an overview of the thesis. In this context, the types of anchors currently available and the range of direct applications for soil anchors will be presented.

1.1 HELICAL SCREW ANCHORS

Typically, soil anchors are used to transmit forces from a structure to the soil. Their strength is obtained through the shear strength and dead weight of the surrounding soil. The types of soil anchors used in civil engineering practice vary considerably; however in general, anchors can be divided into four basic categories. These are:

- Plate Anchors
- Screw Anchors
- Grouted Anchors
- Anchor Piles

As the range of applications for anchors expands to include the support of more elaborate and substantially larger structures, a greater understanding of their behaviour is required. The method of load transfer from the anchor to the surrounding soil provides the distinction between these various forms of anchorage. Load can be transferred to the soil through direct bearing (plate anchors, screw anchors), shaft friction (grout injected anchors), or a combination of both direct bearing and shaft friction (anchor piles). Different types of anchors are extensively used depending on magnitude, type of loading, type of structure and subsoil conditions. Anchors are typically constructed from steel or concrete and may be circular (including helical), square or rectangular in shape. The helix can be manufactured in single pitch, multi-variable pitch, and multi-equal pitch. They can be welded, riveted, or bolted to the steel shaft, and the helical blades can be knife edged to facilitate their installation and minimize disturbance to the soil during installation. Anchors may be placed horizontally, vertically, or at an inclined position depending on the load orientation or type of structure requiring support.

There are many advantages of using helical screw anchors over conventional anchors. The main advantage is the rapid installation and immediate loading capabilities that offer cost-saving alternatives to reinforced concrete, grouted anchors and driven piles. Due to enormous advantages being offered by helical screw anchor, these are used in the construction of transmission towers, tall chimneys and underground tanks jetty structures, excavation bracings, mooring systems for ocean surface or submerged platforms. The helical anchor installation causes changes in the soil surrounding the anchor. When a helical anchor is installed into the ground, the soil traversed by the helical plates is sheared and displaced laterally and vertically. As the helical blade moves downward into the ground, the soil experiences torsional and vertical shearing and also radial, vertical, and torsional displacement. Therefore, reductions in the values of some soil parameters have been suggested in the literature to consider the effect of this disturbance.

Previous research has determined that the installation of a screw pile into cohesionless soil causes the lateral displacement of in-situ material, loosening the sand within the cylinder circumscribed by the helices while densifying the sand surrounding the disturbed zone (Mitsch and Clemence 1985). Anchors can be made of steel or concrete whereas helical screw anchors are usually made of steel. Helical screw anchors are made of prefabricated steel screw element

and steel shaft connected together as one unit. The helical screw anchor is installed into the soil by applying torque to their shaft, and with little downward thrusts. Installation generally requires neither removal of soil nor any pre-drilled holes. Installation causes a displacement of soil for most of the part, which causes further densification of the soil around the anchor thus improving the soil properties in the nearby vicinity of the installation path. The installation process is for all practical purposes, vibration free and safer, thus risk to men/material is minimized to a great extent. These features make the helical screw anchor attractive on sites that are environmentally sensitive such as walkways on marshy land.

The screw pile foundation can be utilized in various forms. Helical screw anchors are constructed of three main structural elements: anchor shaft, helices and anchor – structure interface connection as shown in Fig. 1.2.

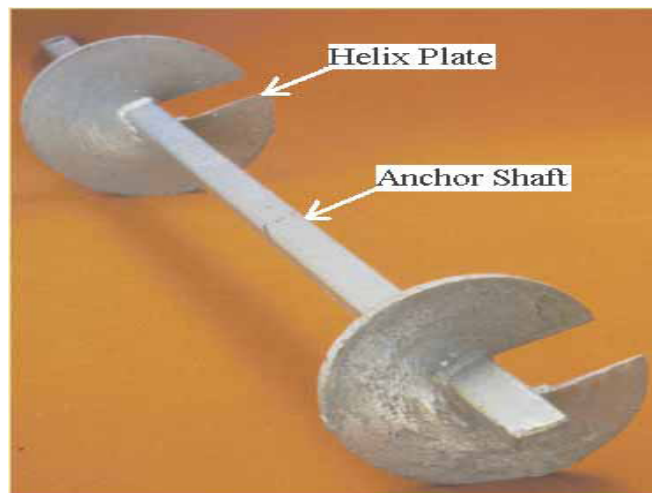


Fig. 1.2: Helical Anchor Components [Malik (2007)]

1.1.1 Anchor shaft

It is composed of structural steel and may be circular or square, hollow or solid. Typical dimension is 40 to 90 mm diameter or width. Expected loads that will result from installation and application normally govern the required size and shape of the shaft. Other factors, such as the method of connecting the anchor to the structure, may also influence the required shaft size and shape.

The anchor shaft has at least four functions -

- a. To provide the required torsional capacity for proper installation
- b. To sustain loads transferred from the helices – during and after installation
- c. To sustain loads transferred from the structure – after installation
- d. To provide the proper connection (interface) to the structure

1.1.2 Helices

Helical screw anchors usually include one to six helices. In the case of multi-helical lead sections, the smaller diameter helix always enters the ground first – followed by larger diameter helices or helices of the same size. The distance between any two helices should be at least three times the diameter of the smaller (or lower) helix. To minimize soil disturbance, helices must be formed to a true helical shape with uniform pitch by matching metal dies.

Helices are constructed of structural steel. The typical thickness of the helices is in the range of 10 to 20 mm, while typical diameters range from 150 to 360 mm. While these dimensions are the most common, helical anchors have been specially manufactured for high compression loading situations with shaft diameters as large as 300 mm and helix diameters as large as 1200 mm.

Helices have at least four functions –

- a. To pull the anchor into the soil to the required depth – during installation
- b. To transfer load into the soil by means of exerting bearing pressure – after installation
- c. To provide the required torsional and bearing capacity – during and after installation
- d. To provide the required strength (welded connection) between the helix and shaft.

1.1.3 Anchor / Structure Interface Connection

Methods of connecting the anchor to the structure depend on the type of structure to be supported. Connections can range from complex welded brackets to holes drilled into the top of the anchor. The major consideration for this connection is to assure that there is a clear transfer of load from the structure to the anchor.

Helical screw anchors are constructed mainly in two sections: lead sections and extension sections. The lead section as shown in Fig. 1.3 (i.e. the first part to enter the ground) is composed of the steel anchor shaft with the helix plates welded to it. Lead sections can have a variety of lengths generally ranging from 250 to 3000 mm. Extension section as shown in Fig. 1.4 may be used to reach deep load-bearing strata. It is used to increase the length of the anchor. Typical lengths of extension sections range from 90 to 300 mm. Both these sections are connected using an overlapping end and a steel pin.



Fig. 1.3: Lead Section [Malik (2007)]



Fig. 1.4: Extension Section [Malik (2007)]

Similar to the total number of helices on an anchor, the total anchor length will also eventually become torque limited. Because helical anchors are screwed into the ground using torque motors, the maximum number of helices on any one anchor eventually becomes limited by the installation torque. For practical purposes, the number of helices on any one anchor should be limited to four or five, with the absolute maximum being eight. It is common that the helix diameter is 2 to 3 times the shaft diameter. Therefore, for the same anchor embedment, shaft diameter and soil strength parameters, a helical anchor with one helix would provide 4 to 9 times the end bearing resistance of a conventional anchor. Consequently, the helical anchor capacity could be either primarily through end-bearing or through a combination of shaft friction and end-bearing.

1.2 OBJECTIVE OF THE THESIS

The objective of this thesis was to study the load transfer phenomena in compression and tension for the purpose of developing a reliable design approach to assist in predicting the capacity of screw piles installed in typical local soils. The design method is supported by the interpretation of results from anchor load tests in laboratory along with the results obtained from numerical analysis. It is hoped that this thesis will achieve its objective of providing guidelines and recommendation for the design of the helical screw anchor installed in cohesionless soil.

1.3 TEST PROGRAM

The present work was organized to conduct compression and pullout tests on a group of one, two, three and four number of single, double and triple helical screw anchors. The soil used was locally available sand collected from bed of Solani River in Roorkee. A total of 100 laboratory tests (Mittal and Shukla, 2013) including 50 compression tests and 50 pullout tests were conducted in Geotechnical Engineering Laboratory of Indian Institute of Technology, Roorkee, India.

1.4 ORGANISATION OF THESIS

The proposed work is organized into six chapters as given below.

Chapter 1 provides an introduction to the entire work carried out in the thesis.

Chapter 2 summarizes a critical review of the available literature detailing the investigations carried out on the compressive and pullout behaviour of helical screw anchors. Both laboratory experiments and theoretical analyses are presented in detail.

Chapter 3 provides the documentation of the anchor testing program carried out in this investigation. This chapter provides the details of the experimental setup, materials used for study and test procedures adopted for the determination of the ultimate compressive and pullout capacity of helical screw anchors. This chapter also presents the results obtained from comprehensive testing program undertaken in this study.

Chapter 4 presents discussion on the test results obtained from compression and pullout laboratory testing.

Chapter 5 presents the numerical validation of the results of compressive and pullout testing using numerical software PLAXIS 3D.

Chapter 6 presents summary, conclusions and scope for future work.

1.5 LIMITATIONS OF THE PRESENT THESIS

This thesis does not address the lateral load-carrying capacity of helical screw anchors, but focusses solely on the determination of static axial (tensile or compressive) screw anchor capacity. A considerable amount of literature exists regarding various methods that have been proposed for the design of screw anchors under uniaxial and lateral loading conditions. The complex load transfer mechanism which exists between any type of anchor and the surrounding soil is still not fully understood by researchers and methods available for the design of deep foundations all contain a certain degree of empirical approximation. Therefore, full-scale load tests are periodically required on anchor installations for most projects in order to verify the predicted load-carrying capacity.

REVIEW OF LITERATURE

2.0 HISTORICAL BACKGROUND

The earliest known use of an anchor foundation was for the support of lighthouses in tidal basins around England. A blind English brick maker, Alexander Mitchell, created design of a screw pile for this purpose in 1836 (Fig. 2.1). In the 1850's, more than 100 Light Houses were constructed along the East Coast, the Florida Coast and the Gulf of Mexico using Screw Pile Foundations.

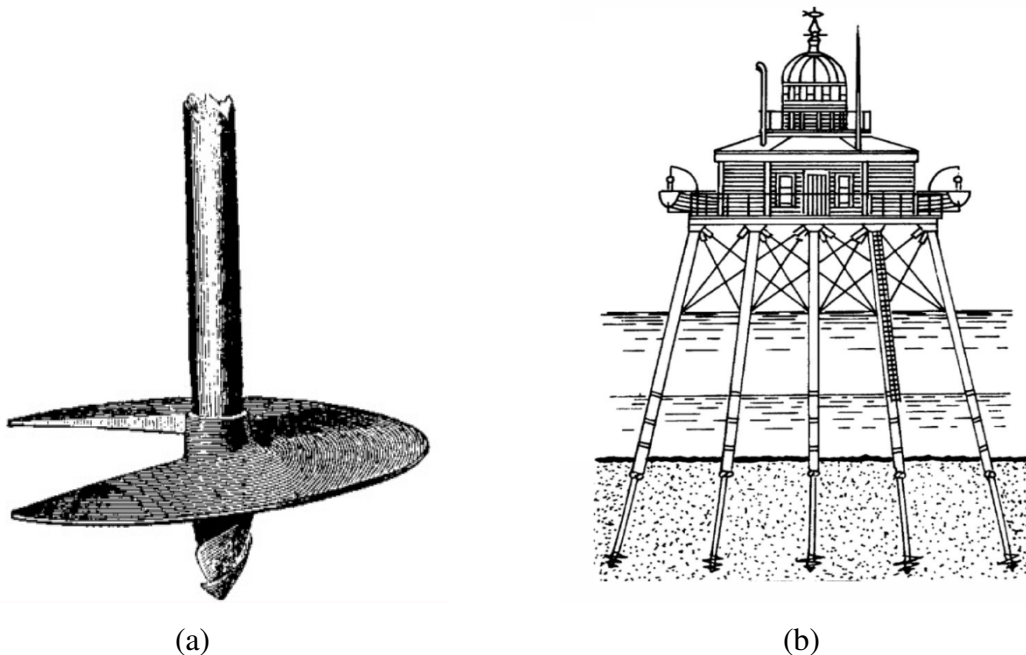


Fig. 2.1: Mitchell Screw Pile

(a) Screw Pile (b) Screw Pile Used for Moorings in 1836

In the 1950s, the A. B. Chance Company introduced the (PISA^{*}) Power-Installed Screw Anchor for resisting tension loads. This anchor consists of a plate or plates, formed into the shape of a helix or one pitch of a screw thread. The plate is attached to a central shaft. The helix plate has its characteristic shape to facilitate installation. Installation is accomplished by applying torque to the anchor and screwing into the soil. The effort to install the anchor is supplied by a torque motor. With the development of tension screw anchor, came the use of the same or similar devices to resist compressive loads. Thus, screw pile foundations came into greater use. Various

sizes and numbers of helices have been used with shafts of varying sections to provide foundations for different applications.

Fig. 2.2 shows a plate anchor having a width D installed to a depth of H . The embedment depth ratio (H/D) is defined as the ratio of the depth of the embedment, H , to the width of the anchor, D . If such an anchor is placed at a relatively shallow depth, the failure surface will extend to the ground surface at ultimate load. This type of behaviour is referred to as shallow anchor condition. With increasing installation depth, the compressibility and deformation of the soil mass above the anchor prevent the failure surface from reaching the ground, and local shear failure in soil located around the anchor will take place. This is referred to as deep anchor condition.

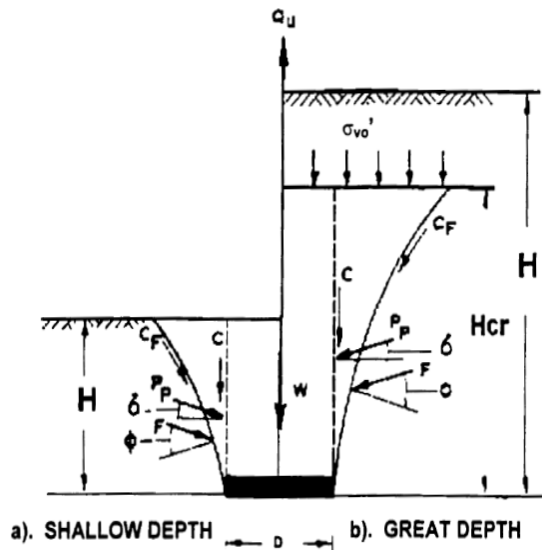


**Fig. 2.2: Failure of Soil above a Strip Footing Under Uplift Load
(After Meyerhof and Adams, 1968)**

In the past few decades, projects that have utilized successfully screw pile foundations include electric utility transmission structures, pipeline supports, building foundations, remedial under pinning, streetlights, walkways in environmentally sensitive areas, dry docks, buried pipelines under water and many others. Research into the behaviour of soil anchors can take two forms, namely experimental or numerical/theoretical based studies. The brief summary of existing research herein has been separated based on this distinction. No attempt is made to present a complete bibliography of all research rather a more selective overall summary of research with greatest relevance to this thesis has been presented. For example, although portions

of the theory underlying the capacity of grouted anchors is also applicable to general soil uplift behaviour, discussion is limited solely to the current thesis topic of helical screw anchors. In addition, contributions made to the behaviour of multiple under-reamed anchors have not been reviewed.

It is clear that the majority of past research has been based on experimental work and as a result, current design practices are largely based on empiricism. In contrast, very few thorough numerical analyses have been performed to determine the ultimate pullout and/or compressive loads of anchors. Of the numerical studies that have been presented in the literature, few can be considered as rigorous. The works prior to 1965 have not been presented in this thesis.

2.1 EARLIER EXPERIMENTAL INVESTIGATIONS

During the past few decades various researchers have conducted laboratory studies to better understand and predict the ultimate capacity of anchors in a range of soil types. Although there are no entirely adequate substitutes for full-scale field testing, tests at laboratory scale have the advantage of allowing close control of at least some of the variables encountered in practice. In this way, trends and behaviour patterns observed in the laboratory can be of great value in developing an understanding of performance at larger scales. In addition, observations made in laboratory testing can be used in conjunction with mathematical analyses to develop semi-empirical theories. These theories can then be applied to solve a wider range of problems.

Experimental investigations into helical screw anchor behaviour have generally adopted one of two approaches; namely, conventional methods under “normal gravity” conditions or “centrifuge systems”. Centrifuge systems use physical scaling laws to match the model and prototype behaviour and can be used to study helical screw anchors. These investigations are based on generating soil stress fields which are in proportion to the size of the model anchors. In this way, a particular anchor size buried at a constant depth can also be used to investigate a range of burial depths simply by varying the stress field. The stress field itself is induced through centrifugal force, as the name suggests. While at rest, the set-up is subjected to a static gravitational force equal to 1g. By rotating the model in a centrifuge motion, gravitational forces greater than 1g can be obtained which generate the required stress field and, in turn, simulate in situ stresses for various burial depths. Unfortunately, because of the significant equipment and set-up costs, only a few research institutions have such a tool at their disposal.

In comparison to centrifuge testing, the more conventional gravity method is generally a cheaper testing alternative due to the ease of set-up and the need for only simple equipment. Quite often, a conventional gravity method can be incorporated into a civil engineering research laboratory by making use of existing equipment. Unfortunately, full scale testing of foundations is costly, time consuming and in most cases unfeasible. For these reasons, testing is generally limited to small scale model tests as these provide a cost effective and convenient alternative. One concern associated with small scale conventional (normal gravity) testing is the presence of scale effects. These are most pronounced for cohesionless granular soils such as sands.

Of course, both methods have advantages and disadvantages associated with them, and these must be borne in mind when interpreting the results from experimental studies of anchor behaviour. The following sections provide a brief summary of past experimental research into the behaviour of helical screw anchors in purely cohesionless soil for compression and pullout loading.

2.1.1 Compression Loading

Till date helical anchors have most commonly been used to resist tensile loads in supporting structures such as transmission towers, dry docks and buried pipelines under water. In recent decades, their applications in engineering projects have exposed to both support and rehabilitate structures under tensile, compressive and lateral loading. Despite its increase in application, the amount of available research and design methodologies to date are relatively limited in comparison with other conventional piling solutions and the majority of relevant research has been focused solely on the uplift condition. Therefore, taking the cue of availability of limited design procedures, the application of helical anchors, particularly for the compression case, has been considered in this thesis.

Helical anchors are increasingly used to support and rehabilitate structures subjected to both tensile and compressive axial loads. The mechanism of load transfer from the deep foundation to the surrounding soil medium is complex, and to date, still not well understood by researchers. Methods available for designing deep foundations contain a certain degree of empirical approximation. Thus, full scale load tests are still required to confirm the prediction of the anchor capacity for most projects and to determine the actual anchor performance.

Helical anchors are used in various projects to provide high compressive, uplift, and lateral capacities for static and dynamic loads. Their current applications include residential and

commercial buildings, bridges, solar farms, light poles, wind turbines, and machine foundations. Due to the increased demand for more complex and efficient designs, it is necessary to better understand the performance characteristics of helical anchors under different loading scenarios and to provide more rigorous design approaches.

Nevertheless, if a vertical anchor is loaded with an axial compressive force in a homogeneous soil, the load is assumed to be carried partly by skin friction and partly through the end bearing resistance. Both components depend on the properties of the soil and the characteristics and method of installing the anchor. In general, most of the design theories proposed for estimating the ultimate anchor capacity, Q_{uc} , consist of the basic components: the end bearing load (or point resistance), Q_b , and the shaft or skin friction load Q_s . The relative contributions of shaft and bearing resistances depend on the embedment depth, soil layering and anchor geometry. The general form for axially loaded single anchors can be expressed as follows:

$$Q_{uc} = Q_b + Q_s = q_b A_b + f_s A_s \dots\dots\dots (2.1)$$

where, Q_{uc} = ultimate anchor compression capacity,

Q_b = end-bearing resistance of the anchor,

Q_s = skin friction developed along the anchor shaft,

q_b = unit bearing capacity of anchor point of area A_b , &

f_s = the average unit skin friction on shaft of area A_s .

The theoretical ultimate compressive capacity of helical anchors is most commonly calculated by employing the limit equilibrium method, i.e., the static equilibrium of the anchor at the onset of failure of the soil around the anchor. The forces transferred from the anchors to the soil are estimated through identification of the failure surface and shape of the failed soil mass. Helical anchors with multiple helices are known to have two possible failure mechanisms: individual bearing failure or cylindrical shear failure as shown in Fig. 2.3.

Till now very few model tests were performed on anchors to investigate compressive loading which is evident from Table 2.1. The works prior to 1965 have not been presented in thesis.

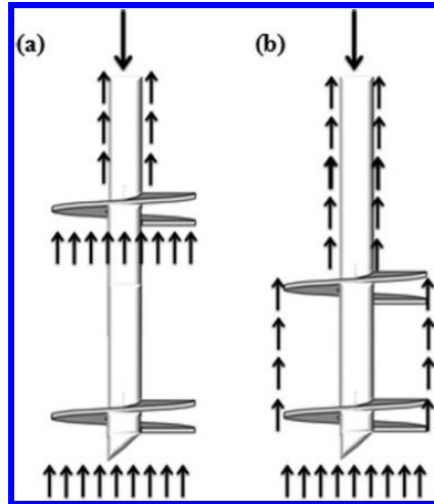


Fig. 2.3: Possible Failure Mechanisms of a Multi-Helix Helical Anchor [Malik (2007)]:
(a) Individual Bearing Failure and (b) Cylindrical Shear Failure

Table 2.1: Earlier Experimental Investigations for Compression Loading

Author	Anchor Properties		Soil Properties	Embedment depth Ratio
	Material & Shape	Size		
Gavin et al. (2014)	Steel & Helical	Shaft Diameter =110 mm, Helix Diameter = 400 mm, Length = 3.07 m, Wall Thickness = 8.5 mm, Helix Thickness = 13 mm, Helix Pitch Angle = 14°	$\gamma = 20 \text{ kN/m}^3$, $\Phi = 42.4^\circ$, $\nu = 0.2$, $e_{\min} = 0.373$, $e_{\max} = 0.733$	6.5
Popadopoulou et al. (2014)	Steel & Helical	Diameter of Helical Plate = 220 mm, Pitch = 76 mm	$\Phi = 25 - 40^\circ$ $\nu = 0.25$	- NM -*
Elsherbiny and Naggar (2013)	Helical Screw	Shaft Diameter = 219 or 273 mm, Helix Diameter = 508 or 610 mm, Wall Thickness = 8.2 or 9.3 mm, No. of Helix = 1	$\Phi = 30^\circ$ $\gamma = 20 \text{ kN/m}^3$ $\Psi = 10^\circ$	10
Sakr (2009)	Helical Screw	Shaft Diameter = 178 mm Helix Diameter = 406 mm Total Length = 5791 mm Thickness of Helix = 19.1 mm	$\Phi = 32^\circ \& 50^\circ$ $\gamma = 19.9 \& 18.1 \text{ kN/m}^3$	12 & 13

Livneh and Naggar (2008)	Helical Screw	Helix Diameter = 200, 250 & 300 mm, Shaft Width = 44.5 mm, Pitch of Screw Thread = 75 mm	$\Phi = 28^\circ$, $c = 10$ kPa, $c_u = 60$ kPa $G = 2.85$, $LL = 29$ $PL = 25$, $PI = 4$	- NM -*
Dash and Pise (2003)	Tubular Steel Piles	Outside Diameter = 25 mm Wall Thickness = 2 mm	$\Phi = 30^\circ$ & 38° , $\gamma = 14$ & 17 kN/m ³ , $I_D = 35$ & 80% , $G = 2.65$, $\delta = 21^\circ$ and 29°	8, 16 & 24

Note: - NM -* : Not mentioned in the paper

Gavin et al. (2014) presented the compression field load test conducted on single helical pile installed in dense sand. They concluded that during compression loading bearing pressure developed beneath the pile helix and pile load response was ductile. They also concluded that the proportion of the total load resistance mobilized as end bearing on the pile helix increased from 74% at displacement of 1% of the helix diameter (normally encountered during service loading) to 90% at displacement of 10% of the helix diameter (mobilization of ultimate pile resistance).

Popadopoulou et al. (2014) conducted full scale in situ tests on helical screw micropile and observed a good agreement between computed and measured ultimate compressive load from these tests. They observed that the ultimate compressive load observed from in-situ tests was lower than the analytical predictions by the Finite Element method. Here overestimation of ultimate compression loads in the analyses was due to the presence of a sandy silt zone below the helical plate, for which probably the shear strength parameters were overestimated from the geotechnical investigation and assumed in the computation.

Elsherbiny and Naggar (2013) investigated the compressive capacity of helical piles in sand and clay by means of field testing and numerical modeling. The numerical models were conducted using the computer program ABAQUS and were calibrated and verified using full-scale load testing data. They observed three distinct regions in the load-settlement curves which were initial linear region, nonlinear region, and final linear region with reduced stiffness. They also observed that the initial linear-elastic region of the load-settlement curve for piles in sand was relatively short with a curvilinear tendency, while piles in clay exhibited a longer linear region with a steep initial slope. They considered the ultimate load criteria as the load applied at the pile head to produce a settlement at the pile head equal to 5% of the helix diameter. Based on the results, they concluded that the theoretical ultimate capacity was much higher than the

interpreted capacity obtained numerically considering the 5%D criterion. This difference was more evident for dense to very dense sands. Therefore, they concluded that the pile design should be governed by settlement requirements to avoid excessive settlement.

Sakr (2009) carried out full-scale pile load testing program using single and double helix piles to investigate their performance under axial compressive, uplift, and lateral loading conditions. They concluded that helical piles with double helixes provided about 40% higher resistance compared with piles with a single helix. They compared the load–settlement curves for single and double helix piles with a spacing ratio S/D of 3 which suggested that the developed load failure mechanism was through the individual helixes. Therefore, they advocated the use of individual helix method for estimating the axial capacities of helical piles (with $S/D= 3$). They compared the compression and uplift capacity and concluded that similar magnitude shaft resistance was developed for both compression and uplift load tests.

Livneh and Naggar (2008) carried out a detailed investigation into the axial performance of square-shaft helical piles. They concluded that the load-deflection curves of the piles exhibit an initial linear segment, followed by a highly nonlinear segment, and finally a near-linear, rapid-failure segment. They concluded that the load transfer mechanism for all piles was predominantly through a tapered cylindrical shear failure surface and bearing of the lead helix in the direction of loading. They developed a method for estimating the axial compressive capacity of helical piles as the sum of the end bearing and cylindrical shearing capacities of the pile. They found that the pile capacity was proportional to the installation torque and they introduced a factor named empirical torque correlation coefficient K_t to predict pile capacity. In compression the value of K_t ranged between 35 and 42 m^{-1} in dense and clayey silt, while in sand the value was greater than 60 m^{-1} . Similarly in tension, the value of K_t ranged between 21.3 and 36.3 m^{-1} . Here the upper range of values corresponded to piles tested in dense silt and sand and the lower range was for piles tested in clayey silt.

Dash and Pise (2003) conducted compression tests and also simultaneous compression and tension tests for the assessment of the effects of compressive load on pull out behaviour of the piles. They concluded that the ultimate compressive capacity increases with the embedment depth and the density of the sand. They also concluded that the net uplift capacity decreases with the increase in the stage of compressive loading. They found that the maximum decrease in uplift capacity is at the 100% stage of compressive loading in both loose and dense sand and at the

identical stage of loading and depth of embedment, the rate of decrease in net uplift capacity is more in loose sand.

2.1.2 Pullout Loading

Helical anchors have generally been used in the construction of structures subject to pullout forces. They are composed of regularly spaced helical steel plates welded to a steel shaft, and installed into soil by applying a torque to the upper end of the shaft by mechanical means. The number and diameters of helical plates are calculated according to the soil characteristics to provide a desired pullout capacity. The ultimate pull-out capacity of helical anchors increases with the number of helices when estimated by the “individual bearing method,” based on Terzaghi (1943) bearing capacity equation. However, field tests have demonstrated that, in certain situations, the amount of increase in the uplift capacity of helical anchors with the increase in the number of helical plates is not as expected. This fact could be observed in the studies by Clemence et al. (1994), Sakr (2009), and Lutenneger (2011).

The helical anchor installation causes changes in the soil surrounding the anchor. When a helical anchor is installed into the ground, the soil traversed by the plates is sheared and displaced laterally and vertically. As the helical blade moves downward into the ground, the soil experiences torsional and vertical shearing, and also radial, vertical, and torsional displacement.

Numerous investigators have performed model tests in an attempt to develop semi-empirical relationships that can be used to estimate the capacity of anchors in cohesionless soil. This is evidenced by the large number of studies shown in Table 2.2. The following section provides a brief summary of past experimental research into the behaviour of anchors in purely cohesionless soil. However, for the sake of brevity, discussions will be limited to those investigations of great relevance to the thesis and/or those seen to have made the most significant contribution to anchor uplift theory.

Table 2.2: Earlier Experimental Investigations for Pullout Loading

Author	Anchor Properties		Soil Properties	Embedment depth Ratio
	Material & Shape	Size		
Gavin et al. (2014)	Steel & Helical	Shaft Diameter = 100 mm, Helix Diameter = 409 mm, Length = 3.07 m, Wall	$\gamma = 20 \text{ kN/m}^3$ $\Phi = 42.4^\circ$ $\nu = 0.2$	H = 2.6 m

		Thickness = 8.5 mm, Helix Thickness = 13 mm, Helix Pitch Angle = 14°	$e_{\min} = 0.373$ $e_{\max} = 0.733$	
Popadopoulos et al. (2014)	Steel & Helical	Diameter of Helical Plate = 220 mm, Pitch = 76 mm	$\Phi = 25 - 40^\circ$ $\nu = 0.25$	- NM -*
Nazir et al. (2014)	Steel & Helical	Shaft Diameter=300–500 mm, Helix Diameter = 100 mm Pitch = 10 mm	- NM -*	1 – 5
Liu et al. (2012)	Steel & Plate	Diameter = 50.8 mm Thickness = 5 mm	$\gamma_{\min} = 13.8 \text{ \& } 14.6$ kN/m ³ , $\gamma_{\max} = 13.8 \text{ \& } 14.6$ kN/m ³ , $\Phi = 30^\circ \text{ \& } 43^\circ$	1 – 9
Lutenegger (2011)	Helical Screw	100, 150, 203 & 254 mm	$\Phi = 33.5^\circ$, $c = 0$ $\gamma = 15.49 \text{ \& } 19.62$ kN/m ³	H = 3 m
Mittal et al. (2010)	Helical Screw	Diameter = 50 mm	$\Phi = 40^\circ$	14 – 22
Kumar & Bhoi (2008)	Strip	Width = 70 mm Length = 360 mm Thickness = 25 mm	$\Phi = 37.4^\circ$, $41.8^\circ \text{ \& } 44.8^\circ$ $\gamma = 17.2, 16.7 \text{ \& } 16.2$ kN/m ³	3, 5 & 7
Kumar & Bhoi (2009)	Strip	Width = 70 mm Length = 360 mm Thickness = 25 mm	$\Phi = 37.4^\circ$, $41.8^\circ \text{ \& } 44.8^\circ$ $\gamma = 17.2, 16.7 \text{ \& } 16.2$ kN/m ³	3, 5 & 7
Kumar & Bhoi (2010)	Strip	Width = 70 mm Length = 360 mm Thickness = 25 mm L/B=5.14	$\Phi = 37.4^\circ$, $41.8^\circ \text{ \& } 44.8^\circ$ $\gamma = 17.2, 16.7 \text{ \& } 16.2$ kN/m ³	3, 5 & 7

Sakai & Tanaka (2007)	Flat Circular Steel Plates	Diameter = 50, 100 & 150 mm Thickness = 5 mm	$e_{max} = 0.98$ $e_{min} = 0.61$	2
Ilamparuthi & Muthukrishnaiah (1999)	Circular Steel Plate Anchor	Diameter = 100 & 150 mm	$\Phi = 33.5^\circ, 38.5^\circ \& 43^\circ$ $\gamma = 15.5, 16.5 \& 17.0$ kN/m ³	0.67 to 7
Ilamparuthi et al. (2002)	Circular Steel Plate Anchor	Diameter = 100, 125, 150, 200, 300 & 400 mm	$\Phi = 34.5^\circ, 38.5^\circ \& 43^\circ$, $e_{min} = 0.46$ $e_{max} = 0.86$, $\gamma = 14.3$ & 18.2 kN/m ³	0.47 – 11.97
Sakai & Tanaka (1998)	Flat Circular Steel Plates	Diameter = 30, 50, 100 & 200 mm Thickness = 5 mm	$\gamma = 16$ kN/m ³ $e_{min} = 0.61$ $e_{max} = 0.98$	1, 2 & 3
Geddes and Murray (1996)	Plate Anchor	Diameter = 50.8 mm L/B=1-10	$\Phi = 43.6^\circ$ $\gamma = 16.5$ kN/m ³	4
Clemence et al. (1994)	Helical Screw Anchor	Diameter = 300mm Thickness = 13 mm Length = 6100 mm	$\Phi = 33^\circ - 34^\circ$, $\gamma = 15.7$ kN/m ³	20
Hanna and Ghaly (1992)	Helical Screw Anchor	Diameter of Screw = 50 mm, Diameter of rod = 16 mm, Pitch of Screw = 15 mm	$\Phi = 31^\circ, 36^\circ \& 42^\circ$ $\gamma = 17.75, 18.74 \& 19.03$ kN/m ³	4 – 16
Ghaly et al. (1991)	Helical Screw Anchor	Diameter of Screw = 50 mm, Diameter of rod = 10 mm, Pitch of Screw = 15 mm	$\Phi = 30^\circ, 35^\circ \& 40^\circ$ $I_D = 35, 50 \& 80\%$ $\gamma = 5.7, 16.2 \& 16.7$ kN/m ³	2 – 16

Ghaly & Hanna (1991)	Helical Screw Anchor	Diameter of Screw = 50 mm, Diameter of rod = 10 mm, Pitch of Screw = 10, 15 & 20 mm, No. of Pitches = 1 & 3	$\Phi = 31^\circ, 36^\circ \text{ \& } 42^\circ$ $I_D = 20, 52 \text{ \& } 83\%$ $\gamma = 17.75, 18.64 \text{ \& } 19.03 \text{ kN/m}^3$	2 - 16
Bouazza & Finlay (1990)	Plate Anchor	Diameter = 37.5 mm Thickness = 3 mm Shaft Diameter = 6 mm	$\Phi = 33.8^\circ, 39^\circ \text{ \& } 43.7^\circ$	2 - 5
Murray & Geddes (1987)	Rectangular & Circular Mild Steel Plate Anchor	Width = 2 in. Diameter = 2 & 3.5 in. Thickness = 0.25 in.	$\Phi = 36^\circ \text{ \& } 44^\circ$ $\rho = 1.56 \text{ \& } 1.68 \text{ mg/m}^3$ $I_D = 0.41 \text{ \& } 0.37$	1 - 10
Mitsch & Clemence (1985)	Helical Screw Anchor	Diameter = 287 mm Length = 2134 mm	$\Phi = 35^\circ - 40^\circ$ $\gamma = 14.9 \text{ \& } 16 \text{ kN/m}^3$	4 & 8
Akinmusuru (1978)	Strip, Rectangular, Square, Circular	Diameter/Width = 50 mm L/B = 2,10	$\Phi = 24^\circ, 35^\circ$	1-10
Das et al. (1976)	Square Circular Plate Anchor	Diameter = 38 - 76 mm	$\Phi = 34^\circ$	1-5
Neely et al. (1973)	Rectangular, Square	Width = 50.8 mm	$\Phi = 38.5^\circ$	1 - 5

* - NM - = Not mentioned in the paper

Gavin et al. (2014) presented the tension field load test conducted on single helical pile installed in dense sand. They concluded that during tension loading bearing pressure develop on the top of the pile helix and pile load response was brittle. They observed that the shaft resistance developed while tension load increased until the normalized pile settlement reached 5% of the helix diameter. Thereafter it remained constant. Finally they concluded that during tension loading, the pile resistance reaches peak value when the normalized pile settlement reach 10% of helix diameter.

Popadopoulou et al. (2014) conducted full scale in situ tests on helical screw micropile and observed a good agreement between computed and measured load from these tests. They observed that for pullout the ultimate load observed from in-situ tests was slightly higher than the analytical predictions by the finite element method.

Nazir et al. (2014) conducted laboratory tests to determine the effect of the embedment ratio, shaft diameter ratio and sand density against the uplift capacity of helical anchor. They concluded that the uplift capacity of helical anchor is in linear relationships with the embedment ratio. They also concluded that the shaft diameter ratio has very little effect whereas the sand density has significant effect on the uplift capacity of helical anchor. In fact, the analysis showed that the uplift capacity of anchor in dense sand was higher in the range between 70% and 90% than the anchor in loose sand. Based on the mode of failure observed in the tests they found that for loose sand local failure happened whereas for dense sand general shear failure occurred in the form of truncated cone.

Liu et al. (2012) presented an experimental investigation on soil deformation around uplift plate anchors in sand by using digital image correlation. They performed a series of model tests to investigate the influence of particle size, soil density, and anchor embedment depth on soil deformation. On the basis of this study, they found that soil deformation and the pullout resistance of plate anchors were substantially influenced by soil density and anchor embedment depth, whereas particle size within the studied range has limited influence. In dense sand, the shape of the failure surface changed from a truncated cone above a shallow anchor to a combined shape of a curved cone and a truncated cone for a deep anchor. In contrast, in loose sand a cone-shaped failure surface was formed within the soil mass above a shallow anchor; however, no

failure surface was observed for a deep anchor, where the compressibility of soil was the dominating factor that influenced the behavior of deep plate anchors in loose sand.

Lutenegger (2011) presented the results of a field investigation on the behaviour of ultimate uplift multi-helix screw anchors in sand. He observed that the transition from cylindrical shear behaviour to individual plate behaviour of cylindrical multi-helix anchors with a fixed number of helical plates in sand occurs at a spacing of about 3. He further concluded that below a plate spacing of 3, the load capacity increases linearly and even at a spacing of 3 and greater, the efficiency is still less than 100%, suggesting that there may be installation effects to consider for helical anchors in sands. He further concluded that the efficiency of multi-helix anchors in sand decreases with the number of helical plates along the shaft. This decrease was more pronounced for closer plate spacing.

Mittal et al. (2010) conducted experimental investigations and concluded that the (a) capacity of screw anchor piles increases with increase in embedment length up to a certain length after which it increases moderately, (b) increase in number of helical plate's results in increase in capacity of screw anchor pile & (c) with the increase in height above ground of applied lateral load above the soil surface, the capacity of screw anchor pile decreases substantially. A theoretical model was developed by incorporating lateral resistance offered by the soil on the shaft of the pile, bearing resistance offered by the soil on the bottom surface of the helical plates, uplift resistance offered by the soil on the top of the helical plates and lateral resistance offered by the soil on the helical plates. It was concluded that this theoretical model predicts the results which are in good agreement with the test results.

Kumar and Bhoi (2008) investigated the interference effect on the vertical load-deformation behaviour of a number of equally spaced strip footings, placed on the surface of dry sand, by using small scale model tests. They demonstrated that the ultimate bearing capacity of a group of multiple strip footings placed on sand increases continuously with decrease in spacing among the footings; the increase in the bearing capacity becomes quite extensive for very small spacing. In contrast, at ultimate failure, the magnitude of the associated settlement was found to increase continuously with decrease in s/B , where s is the spacing between the anchors and B is the width of the strip footing. The interference effect was found to become more extensive for higher friction angle of soil mass.

Kumar and Bhoi (2009) determined the ultimate uplift resistance of a group of multiple strip anchors placed in sand and subjected to equal magnitudes of vertical upward pullout loads by means of a series of small scale model tests. They investigated the effect of interference due to a number of multiple strip anchors placed in a granular medium at different embedment depths. They concluded that the magnitude of the failure load reduces quite extensively with a decrease in the spacing between the anchors. The maximum clear spacing between the anchors, up to which the effect of interference remains still significant, was found to increase invariably with an increase in the depth of the anchor plate.

Kumar and Bhoi (2010) conducted experimental investigations to analyze the effect of interference due to a group of two strip anchors placed in a sandy medium at different embedment depths. They observed that with a decrease in the spacing between the anchors, the magnitude of the failure load reduced quite extensively. From the comparison presented in the paper, it was felt that there is a need to develop a theory for predicting the pullout resistance for a group of anchors which can consider the dependency of the friction angle on the stress level.

Sakai and Tanaka (2007) evaluated the behaviour and scale effect of shallow circular anchors in two-layered sand by comparing the results of a conventional 1 g model test with the results of finite-element analysis. They concluded that in dense sand, uplift resistance decreases after the maximum uplift resistance appears and the softening occurs whereas in loose sand, the uplift resistance is almost constant after the maximum uplift resistance appears and no softening occurs. They also found the formation of shear band originating upward from the edge of the anchor plate into the soil mass which makes an angle of 65° in dense sand, 75° in medium dense and 80° in loose sand.

Ilamparuthi and Muthukrishnaiah (1999) carried out experiments on half-cut models of flat circular and curved anchors embedded at different depths in dry and submerged sand beds of different densities. They observed two types of rupture surface depending on the embedment ratio, one emerging to the surface of the sand bed and the other confined within the sand bed, irrespective of shape of anchor, density of sand bed and dry or submerged condition. They also observed a transition phase that existed between the two types of failure, giving rise to the concept of critical embedment ratio. They observed this critical embedment ratio to be equal to 6.9, 5.8 and 4.9 for dense, medium dense and loose sand beds respectively. They further concluded that the load versus displacement relationship was different for shallow and deep

anchors - a three-phase behaviour for shallow anchors and two-phase behaviour for deep anchors irrespective of density and submergence of the sand bed.

Ilamparuthi et al. (2002) conducted laboratory experiments on half-cut and full-shaped rigid circular anchors. They observed that the uplift capacity is strongly influenced by anchor diameter, embedment ratio, and sand density. They concluded that the load-displacement response is different for shallow and deep anchor conditions, a three-phase behaviour characterizing the shallow case and a two-phase behaviour the deep case. They found that the critical embedment ratio increases with an increase in sand density. They recommended the values as 4.8, 5.9, and 6.8 for loose, medium-dense, and dense sand, respectively, for anchors in the 100 - 150 mm diameter range considered.

Sakai and Tanaka (1998) performed the model tests on shallow anchors having flat circular 0.5 cm thick steel plates with diameter of 30, 50, 100 and 200 mm in dense sand. They concluded that the dimensionless breakout factor first increases with the dimensionless displacement, then decreases after the peak value appears and finally attains the residual value. They further concluded that this peak value decreases with increases in the diameter of the anchor. They also concluded that the scale effect was remarkable with any increase in depth ratio and progressive failure also differed according to embedment ratio.

Geddes and Murray (1996) conducted vertical pullout tests on groups of shallow square anchor plates in row and square configuration in dense sand. They concluded that the load-carrying capacity of a group of anchor plates increases with the spacing between the individual plates up to a limiting critical value. At a critical separation ratio, the maximum efficiency of 100% is reached and continues at that level with further increases in separation. This critical S/B value was valid for all configurations and numbers of plates. They also concluded that the central anchor carries the least load and the outer anchors the greatest.

Clemence et al. (1994) conducted full scale field testing program on helical anchors in sand. They concluded that the uplift behaviour of single helix anchors differ from the multi helix anchors. They also concluded that a large amount of deflection was required to mobilize the maximum load and no clear peak was evident from the load-deflection curves for single helix anchors. So the tests were terminated when the anchors exhibited continual creep under a specific load. However, the load-deflection curves for the double and triple helix anchors exhibited a well defined peak.

Hanna and Ghaly (1992) presented the results of an experimental study on the stress development in sand due to installation and uplifting of helical screw anchors. Based on the results achieved it can be said that the installation and the application of pullout load to a helical screw anchor induce significant increase in lateral and vertical stresses around and in the near vicinity of screw anchor. This increase in lateral and vertical stresses vanishes at distances extending several anchor diameters in the vertical and horizontal direction. They further concluded that the increase in lateral and vertical stresses that take place during the installation procedure is greater for a screw unit with large pitch/diameter ratio i.e. it increases with the increase in helix angle. They also concluded that the rupture surface extends to the sand surface from the screw anchor in case of shallow anchor whereas for deep anchors it is of local nature and does not reach the sand surface.

Ghaly et al. (1991) conducted pullout tests on vertical anchors in sand. The authors concluded that the ultimate pullout load of screw anchors is mainly a function of sand characteristics, anchor diameter and installation depth. They further concluded that relative depth ratio for a given mode of failure depends on the relative density of sand and the diameter of the influence failure circle that appeared on the sand surface during uplift increased with the embedment depth up to a limit beyond which it remained constant when the transit mode of failure takes place. The angle of inclination of the failure cone θ with respect to the vertical does not exceed $2\Phi/3$. The shear strength mobilized along the failure surface of the breakout soil mass is the main resisting factor against the pullout load.

Ghaly and Hanna (1991) conducted experimental study on five models of screw anchors with different geometry to study the effect of shape of the screw anchor on the performance of anchor during installation which primarily depend on geometry of screw anchor, soil properties and installation depth. They concluded that the installation torque required to install a screw anchor increases with the relative density of sand and the installation depth. They further concluded that larger the helix angle the greater the installation torque required to install a screw anchor to a given depth in sands with similar characteristics.

Bouazza and Finlay (1990) performed model anchor pullout tests in two-layered sand. The thickness of each layer was increased to a certain proportion of the anchor diameter and in this investigation it was increased from 1 to 4 anchor diameters. They concluded that the ultimate pullout load depends on the upper thickness ratio (λ) which is the ratio of the upper layer

thickness to the anchor diameter. They proposed that for $\lambda=1$ the ultimate load is independent of the state of the weak layer as dense layer provides most of the strength. Hence for $\lambda=1$, the ultimate pull-out load remains the same whether the upper layer is loose or medium. However, when the thickness of the upper layer (loose or medium) was increased a different phenomenon occurred which depend on the type of upper layer. This observation suggests that the load displacement relationship is governed by the density of the upper layer: the weaker the upper layer, the lower is the ultimate uplift load.

Murray and Geddes (1987) carried out pullout tests on rectangular and circular mild steel plates. They concluded that the dimensionless load coefficient $P/\gamma AH$ and the corresponding displacement at failure increased with increase of H/B ratio and decrease of L/B ratio. They also concluded that the dimensionless load coefficient $P/\gamma AH$ was greater in very dense sand than in medium dense sand but the corresponding displacements were considerably less. They observed significant differences in behaviour between plates embedded in very dense sand and those embedded in medium dense sand. While the dimensionless load coefficient $P/\gamma AH$ was greater in very dense sand, the corresponding displacements were considerably less. For circular plates in very dense sand, there appeared to be a consistent relationship for both the dimensionless load coefficients $P/\gamma AH$ and the corresponding displacements, for all plates tested, when plotted against H/B . Similar relationships did not appear to exist in medium dense sand. The results for vertical uplift in very dense sand suggested that values of $P/\gamma AH$ for a circular plate are on average approximately 1.26 times those for a square plate for $H/B = H/D$.

Mitsch and Clemence (1985) studied the uplift behaviour of helical screw anchors in sand by field and laboratory investigation. The field tests were conducted on full scale anchors whereas laboratory tests were conducted on one-third scale model anchors. They concluded that the failure of multi-helix anchors in sand can be divided into two distinct behaviour based on the embedment depth (H/B) of the anchor and the sand's relative density. They further concluded that anchors with $H/B < 5$ behave as shallow anchors and in this case the failure zone propagated to the soil surface in the form of the truncated cone with a central angle approximately equal to the friction angle (Φ) of the sand. They further concluded that anchors with $H/B > 5$ behaved as deep anchors and in that case the failure zone developed directly above the top helix which did not propagated to the soil surface but was confined to a zone of soil directly above the upper helix of the anchor.

The capacity of deeper vertical anchors was reported by Akinmusuru (1978). Square, circular and rectangular anchors ($L/B= 1, 10$) were tested at embedment ratios ranging from 1 to 10. In a novel attempt to better observe the failure mechanism for anchors at $L/B=10$, the soil was simulated by steel pins (76 mm length) placed to give a friction angle of 24° . The movement of the pins during each test was photographed with the aid of long exposure film. It was observed that at $H/B \geq 6.5$ the failure mechanism does not reach the soil surface and is a near circular shape immediately above the anchor. Although this clearly defines the critical embedment depth, the anchor capacity continued to increase above $H/B \geq 6.5$ and no peak load was observed. For the remaining anchor shapes, Akinmusuru placed the anchors in medium dense sand.

Das et al. (1976) conducted model tests on vertical square plate anchors in loose, medium and dense sands. They expressed the anchor resistance in terms of non-dimensional breakout factor ($N_q = P_u/\gamma AH$). They concluded that for shallow anchors, the breakout factor increases with embedment ratio. But beyond this critical embedment ratio where the anchor behaves as a deep anchor, the breakout factor remains approximately constant. They further concluded that the critical embedment ratio is about 5 for loose sands and increases to about 8 for dense sand.

Neely et al. (1973) reported results for small scale testing on vertical, square and rectangular anchors in sand with a friction angle of 38.5° . Anchors at aspect ratios 1 (square), 2 and 5 were used and embedded up to $H/B= 5$. Very large displacements were observed for square anchors when the embedment ratio was greater than 2. In fact it appears that the load-displacement curves were still increasing when the test was terminated, and an alternative criterion was used to define the ultimate load.

2.2 EARLIER THEORETICAL ANALYSES

In contrast to the variety of experimental results already discussed, very few rigorous numerical analyses have been performed to determine the compressive and pullout capacity of anchors in soil.

While it is essential to verify theoretical solutions with experimental studies wherever possible, results obtained from laboratory testing alone are typically problem specific. This is particularly the case in geomechanics where we are dealing with a highly nonlinear material which often displays pronounced scale effects. As a result, it is often difficult to extend the findings from laboratory research to full scale problems with different material or geometric parameters. Since the cost of performing laboratory tests on each and every field problem

combination is prohibitive, it is necessary to be able to model soil uplift and compressive resistance numerically for the purposes of design.

2.2.1 Theoretical Studies for Compression Loading

The following section provides a brief summary of past theoretical research into the compression behaviour of anchors in purely cohesionless soil.

Table 2.3: Earlier Theoretical Analyses for Compression Loading

Author	Analysis Method	Anchor Properties		Soil Properties	Embedment Depth Ratio
		Material & Shape	Size		
Popadopolou et al. (2014)	Finite Element Method	Steel Helical	Diameter of Helical Plate = 220 mm, Pitch = 76 mm	$\Phi = 25 - 40^\circ$ $\nu = 0.25$	All
Livneh and Naggar (2008)	Finite Element Analysis	Helical Screw	Helix Diameter = 200, 250 & 300 mm, Shaft Width = 44.5 mm, Pitch of Screw Thread = 75 mm	$\Phi = 28^\circ$, $c = 10$ kPa, $c_u = 60$ kPa, $G = 2.85$, $LL = 29$, $PL = 25$, $PI = 4$	All

Popadopolou et al. (2014) investigated the behaviour of helical screw micropiles in axial and horizontal loadings through the finite element method and full scale in situ tests. Based on the distribution of the ultimate compressive axial load along the micropile, they have concluded that the maximum contribution in strength arose from the lower plate. They have also concluded that the compressive load increases slightly with increase in the no. of pitches. Finally they cautioned with the use of theoretical predictions and advised to take into account the influence of the scale of each loaded micropile.

Livneh and Naggar (2008) conducted a comprehensive investigation into the axial performance of square-shaft helical piles with the help of numerical modeling using finite element analysis. The main objective of modelling helical pile behaviour was to define the failure mechanism and load-transfer behaviour for each pile. They assumed two load transfer mechanisms – one is shear resistance derived from a cylindrical failure surface along the inter-helical soil profile and the other is the bearing of the bottom helix on the soil below and

evaluated the contribution of each of these load transfer mechanisms to pile capacity. They concluded that above the top helix, the soil was in tension, which will not contribute significantly to pile capacity, while soil displacements below the bottom helix were attributed to the bearing resistance of this helix. The values of the pile capacity calculated using derived equation was compared with measured field values. The calculated capacities are found to be in good agreement with the measured values to within 12% in all cases.

2.2.2 Theoretical Studies for Pullout Loading

A summary of previous theoretical studies for pullout behaviour of vertical anchors in cohesionless soil is presented in Table 2.4.

Table 2.4: Earlier Theoretical Analyses for Pullout Loading

Author	Analysis Method	Anchor Properties		Soil Properties	Embedment Depth Ratio
		Material & Shape	Size & Roughness		
Popadopolou et al. (2014)	Finite Element Method	Steel Helical	Diameter of Helical Plate = 220 mm, Pitch = 76 mm	$\Phi = 25 - 40^\circ$ $\nu = 0.25$	All
Kumar & Sahoo (2014)	Lower and Upper Bound Finite Element Limit Analysis	Strip Plate	Rough	$\Phi = 0^\circ, 10^\circ, 20^\circ \& 30^\circ$	1 – 7
Kumar & Bhattacharya (2012)	Lower Bound Finite Element Limit Analysis	Strip Plate	- NM -*	$\Phi = 25^\circ, 30^\circ, 35^\circ \& 40^\circ$	1 – 7
Kumar & Sahoo (2012 a)	Upper Bound Finite Element Limit Analysis	Strip Plate	Rough	$\Phi = 0^\circ, 10^\circ, 20^\circ \& 30^\circ$	1 – 10
Kumar & Sahoo (2012 b)	Upper Bound Finite Element Limit Analysis	Strip Plate	Rough	$\Phi = 20^\circ - 45^\circ$	1 – 7

Kumar & Naskar (2012)	Lower Bound Finite Element Limit Analysis	Strip	Rough	$\Phi = 0^{\circ} - 30^{\circ}$	3 - 7
Merifield (2011)	Numerical Modelling: Finite Element	Helical Screw	- NM - *	- NM - *	1 - 10
Khatri and Kumar (2011)	Limit Analysis - Lower Bound	Strip	- NM - *	$\Phi = 25^{\circ} - 40^{\circ}$	- NM - *
Deshmukh et al. (2011)	Kotter's Equation	Strip	- NM - *	ALL	ALL
Mittal et al. (2010)	Analytical	Helical Screw	Helix Diameter = 50 mm	$\Phi = 40^{\circ}$	14 - 22
Tsuha & Aoki (2010)	Analytical	Helical Screw	Diameter of Shaft = 3, 4.5 & 6 mm Diameter of Helix = 10, 15 & 20 mm	$\Phi = 31$ & 41° $\gamma = 15.46$ & 16.3 kN/m^3	All
Deshmukh et al. (2010)	Semi Analytical Method	Strip	- NM - *	- NM - *	< 8
Kumar & Bhoi (2010)	Linear Elastic Finite Element Analysis	Strip	Rough	$\nu = 0.1, 0.2$ & 0.3	3, 5 & 7
Kumar & Kouzer (2009)	Limit Analysis - Upper Bound	Strip	Rough	$\Phi = 40^{\circ}$	1- 6
Koprivica (2009)	Finite Difference Method	Plate	- NM - *	$\Phi = 33^{\circ} - 47^{\circ}$	1 - 7
Kumar & Kouzer	Limit Analysis - Upper Bound	Strip	Rough	$\Phi = 25^{\circ} - 45^{\circ}$	3 & 5

(2008a)					
Kumar & Kouzer (2008b)	Upper Bound Limit Analysis	Strip	- NM -*	$\Phi = 20^\circ - 45^\circ$	1 - 7
Dickin & Laman (2007)	Finite Element Analysis	Strip Anchor	Width = 1 m	$\Phi = 35^\circ \& 51^\circ$	1 - 8
Hanna et al. (2007)	Limit Equilibrium	Helical & Plate Anchor	- NM -*	$\Phi = 25^\circ - 45^\circ$	1 - 8
Sakai & Tanaka (2007)	Finite Element Analysis	Circular Plate	Diameter = 5, 10 & 15 cm	$\Phi = 33^\circ$	2
Kumar (2006)	Elasto-Plastic Finite Element Analysis	Strip Anchor	Width = 0.5 m	$\Phi = 30^\circ - 45^\circ$ $\gamma = 20 \text{ kN/m}^3$	1 - 7
Merifield et al. (2006)	Limit Analysis - Upper and Lower Bound	Plate Anchor	Rough/Smooth	$\Phi = 20^\circ - 40^\circ$	1 - 10
Kumar (2003)	Limit Analysis - Upper Bound	Strip & Circular Plate Anchor	- NM -*	$\Phi = 30^\circ \& 45^\circ$	0 - 6
Sakai & Tanaka (1998)	Finite Element Analysis	Flat Circular Steel Plate Anchor	Diameter = 30, 50, 100 & 200 mm Thickness = 5 mm	$G_s = 2.64$ $e_{\max} = 0.98$ $e_{\min} = 0.61$ $\gamma_d = 1.64 \text{ gm/cc}$	1, 2 & 3
Geddes & Murray (1996)	Limit Analysis - Upper Bound	Strip Inclined Anchor	Rough/Smooth	$\Phi = 43.6^\circ$	1 - 8
SubbaRao &	Method of	Horizontal	Smooth	$\Phi = 25^\circ - 45^\circ$	2 - 8

Kumar (1994)	Characteristics	ntal Strip Anchor s			
Basudhar & Singh (1994)	Limit Analysis - Lower Bound	Strip Anchor	Rough/Smooth	$\Phi = 32^\circ, 35^\circ,$ 38°	1 – 5
Ghaly & Hanna (1994)	Limit Equilibrium	Helical Screw Anchor	- NM - *	$\Phi = 31^\circ - 42^\circ$	4 – 16
Hanna & Ghaly (1994)	Limit Equilibrium	Helical Screw Anchor	- NM - *	$\Phi = 30^\circ - 46^\circ$	2 – 16
Ghaly et al. (1991)	Limit Equilibrium	Helical Screw Anchor	- NM - *	$\Phi = 30^\circ - 40^\circ$	2 - 16
Ghaly & Hanna (1991)	Limit Equilibrium	Helical Screw Anchor	- NM - *	$\Phi = \text{All}$	All
Murray & Geddes (1987)	Limit Analysis & Limiting Equilibrium	Strip, Rectan gular & Circula r	- NM - *	$\Phi = \text{All}$	All
Mitsch & Clemence (1985)	Field and Laboratory Test	Helical Screw Anchor	Diameter = 287 mm Length = 2134 mm	$\Phi = 35^\circ - 40^\circ$ $\gamma = 14.9 \& 16$ kN/m^3	4 & 8
Tagaya et al. (1983)	Elastoplastic Finite Element	Buried Anchor	- NM - *	$\Phi = \text{All}$ $\gamma = 15.8 \text{ kN/m}^3$ $\nu = 0, 0.2 \& 0.4$	All
Rowe & Davis	Elastoplastic	Strip	Smooth	$\Phi = 0 - 45^\circ$	1 - 8

(1982)	Finite Element	Anchor			
Neely et al. (1973)	Limit equilibrium & Method of Characteristics	Strip Anchor	Rough, $\Phi/2^\circ$	$\Phi = 30^\circ - 45^\circ$	1 - 5.5
Meyerhof (1973)	Limit equilibrium – Semi Analytical	Strip Anchor	- NM -*	All	All

* - NM - = Not mentioned in the paper

Popadopolou et al. (2014) investigated the behaviour of helical screw micropiles in axial and horizontal pullout loadings through the finite element method and full scale in situ tests. Based on the distribution of the ultimate pullout axial load along the micropile, they have concluded that the maximum contribution in strength arose from the upper plate. Unlike compression tests for pullout tests they observed a slight decrease in ultimate pullout capacity with the increase in no. of pitches.

Kumar and Sahoo (2014) investigated the vertical uplift resistance of two closely spaced horizontal strip plate anchors embedded in a cohesive-frictional soil, at the same level, by using lower and upper bound theorems of the limit analysis in combination with finite elements and linear optimization. The interference effect on the uplift resistance of the two anchors was evaluated in terms of a non-dimensional efficiency factor (η_c). They concluded that the critical spacing between the two anchors increases with an increase in the values of both H/B and Φ . They further concluded that the reduction in the uplift resistance due to the interference effect increases continuously with a decrease in the values of H/B and increase in the values of Φ . The magnitude of S_{cr} was found to lie in a range of 0.65B - 1.5B with H/B = 1 and 11B - 14B with H/B = 7 for Φ varying from 0 to 30°.

Kumar and Bhattacharya (2012) determined horizontal pullout capacity of a group of two vertical anchors embedded in sand along the same vertical plane in terms of a group efficiency factor, by using the lower bound finite element limit analysis. They analyzed the effect of vertical spacing (S) between the anchor plates on the magnitude of the total group horizontal failure load (P_{uT}) for different combinations of H/B, δ/Φ and Φ . They concluded that the

magnitude of group efficiency factor, η_γ , become maximum for a certain critical S/B, which has been found to lie between 0.5 and 0.8. They further concluded that the magnitude of the group failure load becomes maximum corresponding to a certain critical spacing between the two anchors.

Kumar and Sahoo (2012a) determined vertical uplift resistance for a group of two strip anchor plates attached coaxially to the same vertical tie rod/plate and embedded in a general cohesive-frictional soil by applying the upper bound finite elements limit analysis. They concluded that the value of the uplift capacity factor for a group of two anchors becomes especially quite predominant for greater values of H/B and under fully bonded anchor-soil interface condition. They further concluded that for a given H/B, the magnitude of the uplift factor reaches almost close to the maximum when the upper anchor plate is located midway between the ground surface and the lower anchor plate.

Kumar and Sahoo (2012b) determined horizontal pullout capacity of vertical anchors embedded in sand by using an upper bound finite elements limit analysis. They presented the numerical results in non-dimensional form for various combinations of embedment ratio of the anchor (H/B), internal friction angle (Φ) of sand, and the anchor-soil interface friction angle (δ). They concluded that the magnitude of the pullout factor increases substantially with increases in the embedment ratio, friction angle of sand and anchor-soil interface friction angle. They also concluded that the size of the zone of the influence increases with an increment in the values of H/B, Φ , and δ .

Kumar and Naskar (2012) analyzed the vertical uplift resistance of a group of two coaxial strip anchor plates embedded in a cohesive frictional soil with the application of the lower bound finite element limit analysis. They concluded that a group of two anchors, as compared to a single isolated anchor, always provides a greater magnitude of F_c for $\Phi < 20^\circ$ and with $H/B \geq 3$. The magnitude of F_c reaches close to the maximum when the upper anchor plate is located midway between the ground surface and the lower anchor plate. On the other hand, for a purely frictional material, the magnitude of the uplift resistance (F_γ) for two anchors and a single anchor remains almost identical as long as the position of the lower anchor plate in the group is kept the same as that of a single anchor.

Merifield (2011) used numerical modelling techniques to understand the behaviour of multiplate circular anchor foundation in clay soils. They presented a practical design framework

for multiplate helical anchor foundations replacing existing semiempirical design methods that are inadequate and have been found to be excessively under- or overconservative. They avoided the need to apply bearing capacity theory that was derived initially for surface footings, to the problem of anchor uplift.

Khatri and Kumar (2011) analyzed the effect of anchor width on the uplift ultimate resistance of strip anchors using the lower bound theorem of limit analysis in conjunction with finite element analysis and linear programming. An iterative stepwise procedure to incorporate the dependence of Φ on σ_m , was adopted. They observed that with a decrease in width of the anchor (i) the magnitude of uplift capacity increases continuously and (ii) the magnitude of the collapse pressure decrease quite substantially. They also observed that compared with shallow anchors the scale effect becomes more pronounced for deep anchors.

Deshmukh et al. (2011) investigated the theoretical analysis net uplift capacity of horizontal strip anchor in cohesionless soil using Kotter's equation. They proposed a simple method as no charts or graphs are required in this method. They assumed a planar failure surface at a characteristic angle with the ground surface and compared the results so obtained with the available experimental results for dense to loose cohesionless soil with the maximum embedment ratio of 8. They concluded that the present method predicts the net uplift capacity of horizontal strip anchor very well and their predicted values are very close to the experimental results for 93% cases. The comparison of results with available theoretical solutions show that, proposed method makes better prediction for anchor embedment ratio less than 8 in dense cohesionless soil.

Mittal et al. (2010) developed a model to determine lateral load capacity of screw anchor piles. In this model, the following forces have been considered to act on helical pile: (1) Lateral resistance offered by soil on the shaft of the pile, (2) Bearing resistance offered by soil on the bottom surface of the helical plates, (3) Uplift resistance offered by soil on the top of the helical plates & (4) Lateral resistance offered by soil on the helical plates. They compared the lateral capacities from the empirical equation developed by considering the earlier forces and experiments conducted. The comparison showed good agreement.

Tsuha and Aoki (2010) evaluated the physical relationship between the uplift capacity and installation torque of deep helical piles in sand by developing a simplified theoretical relationship. They verified the result by centrifuge physical modeling. They compared the

measured values of the empirical torque correlation factor (K_T) with the field and laboratory results reported in the literature. From this comparison they concluded that magnitude of K_T decreases with the increase in pile dimensions and also sand friction angle.

Deshmukh et al. (2010) proposed an analytical method based on Kötter's equation for estimating the net uplift capacity of a horizontal rectangular/square shallow anchor in cohesionless soil. They obtained a closed form solution for the uplift capacity with no requirement of any charts or tables. The proposed method considers failure surface in the form of frustum of a trapezoid making an angle with the horizontal which depends on angle of shearing resistance, Φ . No assumptions are required regarding coefficient of earth pressure and the predictions of this method show a very close agreement with experimental results. The results of theoretical predictions are compared with the experimental results and the field test. It leads to the predictions that are very close to experimental values in 80% cases.

Kumar and Bhoi (2010) examined the effect of the spacing of anchors on their elastic settlements based on linear elastic finite element analysis for closely spaced strip anchors. It was noted that for a given applied load on each anchor, the elastic settlements increase continuously with a decrease in the spacing between the anchors. It was also noted that the effect of the interference of anchors leads to an increase in the settlements for the same magnitude of the load applied on each anchor. As compared to two anchors case, the effect of the interference has been found to be more predominant for the case of multiple anchors. The effect of the Poisson ratio of the medium in all the cases was found to be very marginal.

Kumar and Kouzer (2009) examined vertical uplift resistance of two interfering rigid rough strip anchors embedded horizontally in sand at shallow depths using an upper bound theorem of limit analysis in combination with finite elements and linear programming. In this analysis the effect of the spacing between the anchors was studied in detail for different embedment ratios of anchors. They concluded that the vertical uplift capacity of the anchors reduces quite significantly with a decrease in the spacing between the anchors. They also concluded that when the clear spacing (S) between the anchors is approximately greater than $2d \tan \Phi$, no interference effect exists. They also observed that the soil mass lying above the anchor and encompassed within rupture surfaces on either side of the anchor moves almost as a single rigid unit with the velocity same as that of the velocity of the anchor itself.

Koprivica (2009) presented theoretical and numerical methods for determination of the uplift behaviour of horizontal anchor plates loaded by a vertical tension force, for plane and spatial axially-symmetrical strain conditions. The final results of this paper were analytical expressions and diagrams of the bearing capacity of shallow anchors in sand which enabled relatively simple calculation of bearing capacity, which is independent of the angle of the shearing resistance, relative density and embedment ratio. The given expressions, diagrams and anchor shaft appearance in the soil represented the influence of nonlinear failure stress envelope parameters which together with relative density, give a quality aspect to the possible solution of a capacity problem of the anchor plates in sand loaded by vertical tension in the conditions of plane and axially-symmetrical strains.

Kumar and Kouzer (2008a) examined the variation of the uplift resistance for a group of two and multiple horizontal strip anchors placed in sand and subjected to vertical uplift load by using an upper-bound limit analysis and with the employment of a rigid wedge collapse mechanism, bounded by planar rupture surfaces. They concluded that when the clear spacing (S) between the anchors is greater than $2d\tan\Phi$, no interference of the anchors occurs. On the other hand, for $S < 2d\tan\Phi$, the uplift resistance of the anchors reduces substantially with a decrease in the spacing between the anchors. The uplift resistance for a group of interfering multiple anchors was found always to be smaller than that for a group of two anchors.

Kumar and Kouzer (2008b) examined the uplift capacity of rigid horizontal anchors placed in sand using an upper bound limit analysis in combination with finite elements and linear programming. They expressed the collapse load in terms of non-dimensional uplift factor F_γ which was found to increase continuously with an increase in both the embedment depth ratio and friction angle of sand. They observed that the influence of friction angle on the pullout resistance is greater at higher embedment ratios. Even though their analysis considered the development of plastic strains within elements in all cases, it had been noticed that the soil mass lying above the anchor remains rigid and a planar rupture surface emanating from the anchor edge and making an angle Φ with the vertical developed.

Dickin and Laman (2007) have conducted physical and computational studies to investigate the uplift response of 1 m wide strip anchors. For this study they used Hardening Soil Model available in software PLAXIS to describe the non-linear sand behaviour and to model strip anchor. The analyses were carried out using a plane strain model for anchors in both loose

and dense sand. The variation of uplift load with displacement from the PLAXIS analyses showed generally good agreement in the pre-peak region with the physical modelling obtained from the centrifuge for all anchor depths. They concluded that uplift resistances increased significantly with both embedment ratio and sand packing.

Hanna et al. (2007) presented analytical models to predict the pullout capacity and the load–displacement relationship for shallow single vertical helical and plate anchors in sand. They developed empirical expression to determine the critical depth of anchors, which depends on the diameter of the anchor base and the angle of shearing resistance of the sand. The predicted values by the proposed theory compared well with the experimental and field data of single and multi helix, plate anchors and belled piles in loose and medium-dense sand. The predicted load–displacement curves for these anchors by the proposed theory compared well with the results produced by other theories available in the literature.

Sakai and Tanaka (2007) evaluated the uplift resistance and the scale effect of a shallow circular anchor in a two layered sand bed by comparing the results of a conventional 1 g model test with the results of an elastoplastic finite-element analysis with shear band effect. They employed yield function corresponding to the Mohr-Coulomb model and a plastic potential function geometrically represented by the Drucker-Prager model to analyze quadrilateral isoparametric element using finite element analysis. They concluded that the finite-element analysis show good agreement with experimental results. Calculated maximum uplift resistance, displacement corresponding to the maximum uplift resistance and residual uplift resistance coincide with the observed experimental results. They further concluded that in dense sand softening occurs after maximum uplift resistance is achieved whereas in loose sand no softening occurs.

Kumar (2006) examined the load displacement relationship of shallow rigid strip anchors embedded in sands and subjected to uplift pressures by using the elasto-plastic finite element method. The magnitudes of F_γ , the non-dimensional uplift factor, as well as the displacements of anchor at failure were found to increase with the increases in the values of the anchor embedment ratio and the angle of shearing resistance of soils. The influence of the friction angle on the pullout resistance was found to be more considerable at higher embedment ratios. He concluded that even at complete collapse, the soil mass lying just vertically above the anchor remained more or less non plastic. The failure of the anchor occurred on account of the

development of a thin curved plastic shear zone emerging from the bottom of the anchor and then extending up to the ground surface.

Using upper and lower bound theorems of limit analysis, Merifield et al. (2006) presented the results of a rigorous numerical study to estimate the ultimate pullout load for vertical and horizontal plate anchors in frictional soils. They considered the effects of soil friction angle, soil dilation, anchor embedment depth and anchor roughness. Anchor roughness was found to have significant effect on the capacity of vertical anchors. Soil dilation was found to have significant effect on the anchor capacity.

Kumar (2003) determined the vertical uplift resistance of shallow strip and circular plate anchor buried horizontally using the upper bound theorem of limit analysis. He established uplift capacity factors f_γ and f_q due to the effects of soil unit weight and surcharge respectively. He concluded that the uplift resistance due to soil unit weight for anchors embedded in dense sand underlying loose sand is more than that of anchors in loose sand underlying dense sand. They also found that this difference is quite significant for the case when the two layers have the same thickness. However, they found that the surcharge component remain unaffected by the relative positions of the layers. They concluded that the uplift factors for circular anchors are much higher than strip anchors.

Sakai and Tanaka (1998) studied the uplift resistance of a shallow anchor in dense sand using elastoplastic finite-element analysis. The finite element analysis employed a constitutive model in which non-associative strain hardening-softening elasto-plastic material was assumed. In their analysis, they evaluated the scale effect observed in the behaviour of a shallow circular anchor with dry sand by comparing 1 g model with the finite element analysis. The load-displacement curves by the finite element analysis showed good agreement with experimental results. They further concluded that the scale effect was remarkable with the increase in h/D and progressive failure differed according to h/D . At $h/D=1$, as the progressive failure was not remarkable, the scale effect was similar between the conventional 1 g test and the centrifugal test. But in case of $h/D=3$, the scale effect was remarkable on conventional 1 g test compared to centrifugal test.

Geddes and Murray (1996) carried out model-scale pullout tests on groups of square anchor plates in row and square configurations placed at a constant dry density. They concluded that all the load-displacement curves for different numbers of anchors and configurations may be

reduced to a single curve by normalizing them with respect to peak load values. They further concluded that the efficiency of the group of anchors increases with the increase in the separation of anchors and at a critical separation ratio of 2.9 the maximum efficiency of 100% is reached. They also concluded that in a group end anchors carry the greatest loads and the central anchor the least load.

SubbaRao and Kumar (1994) proposed a theory for vertical uplift capacity of shallow horizontal strip anchors in a general $c-\Phi$ soil based on method of characteristics and assuming a largely log-spiral failure surface. They established uplift capacity factors F_c , F_q and F_γ for the effects of cohesion, surcharge, and density respectively as functions of embedment ratio λ and angle of friction Φ . They concluded that for any embedment ratio F_γ increased by 1.5 to 2 times with an increase in Φ from 25° to 45° whereas it increased by threefold as the embedment ratio increased from 2 to 8 for any particular value of Φ . The theory was shown to be capable of predicting accurately anchor pullout behaviour in clays and also in loose and medium-dense sands. In dense to very dense sands, its predictions appeared to be slightly conservative.

Basudhar and Singh (1994) used finite element method to predict the lower bound for the break-out factor of smooth and rough horizontal and vertical anchors. They concluded that the break-out factors increases with increase in embedment depth ratio of the anchor. They also concluded that the break-out factors are substantially higher for rough anchors than for smooth anchors.

Ghaly and Hanna (1994) developed theoretical models to calculate the uplift capacity of vertical screw anchors. In these models, the limit equilibrium technique was employed together with Kotter's differential equation to calculate the shear stresses acting on the observed log-spiral surface of failure. They simplified the developed theory by introducing weight and shear factors for shallow and deep anchors. They presented these factors in simple graphs as functions of the angle of shearing resistance of the sand and the relative depth ratio of the anchor. A comparison of the theoretical values and the present experimental results, as well as the field data reported in the literature on the uplift capacity of screw anchors, showed good agreement.

Hanna and Ghaly (1994) developed a theory to predict the ultimate pullout capacity of group of anchors with different configurations utilizing the theoretical model developed in a companion paper. They concluded that the uplift capacity of a group of shallow vertical screw anchors comprises of three components, namely self-weight of the group, weight of sand within

the rupture surface and shear stresses acting on the rupture surface. Transition and deep groups of anchors with locally developed rupture surfaces were subjected to further resistance to uplift due to surcharge pressure. Comparison between theoretical and experimental results showed good agreement in the case of loose and medium sands and satisfactory agreement in the case of dense sand. They proposed an empirical equation based on theory and experimental data to mathematically quantify the effect of densification on the angle of shearing resistance of the sand.

Using the limit equilibrium technique together with the assumed failure planes, Ghaly et al. (1991) developed a theoretical model to predict the ultimate pullout capacity of the anchors in sand which considered the effect of sand characteristics, anchor diameter and installation depth. Using this theoretical model, the ultimate pullout load of screw anchors installed in sand was predicted. Good agreement existed between the present theoretical and experimental results as well as field results reported in the literature. A simplified equation was proposed from which the modified coefficient of passive earth pressure can be calculated. Design charts were presented from which the ratio δ/Φ and the value of K'_0 could be estimated for an anchor installed to a given depth in sand whose angle of shearing resistance is known.

Ghaly and Hanna (1991) presented theoretical studies on the torque required to install helical screw anchors in sand. They established a torque factor in terms of the parameters affecting the torque value and proposed a correlation between this factor and the uplift capacity factor. They concluded that the main forces affecting the torque magnitude are the frictional resistance exerted on the anchor's shaft and the locally compacted column of sand overlying the screw blade and the bearing resistance exerted on the screw blades. They established a torque factor incorporating all the parameters affecting the torque magnitude and proposed a correlation between the uplift capacity factor and the torque factor. A comparison of installation torque from theoretical predictions and experimental results showed very good agreement.

Murray and Geddes (1987) adopted upper bound limit analysis approach based on the theory of plasticity to estimate ultimate uplift resistance of a strip anchor. They assumed that the failure boundaries consist of two straight lines inclined outwards at an angle Φ to the vertical at the plate edges. They concluded that an increase in surface roughness increase the ultimate uplift resistance. They analyzed circular anchor also and drawn conclusion similar to those for strip anchors. The theoretical solutions for strip and circular anchors examined have shown a scatter

of plots, in some cases showing very poor correlation with the experimental results. These discrepancies can probably be attributed to some extent to an inability to describe mathematically the stress history or degree of overconsolidation of the sand arising from the sand placement techniques.

Mitsch and Clemence (1985) examined the pullout capacity of helical anchor in sand theoretically and found that the failure of multi-helix anchor follow two distinct behaviour pattern based on the embedment ratio of anchor (H/B) and the sand's relative density. They concluded that with relative density ranging from 47% to 90% and $H/B < 5$, the anchors behave as a shallow anchor and anchors with $H/B > 5$ behave as a deep anchor. For shallow anchor the failure zone propagated to the soil surface in the form of truncated cone with a central angle approximately equal to the friction angle (Φ) of the sand. And for deep anchors, the failure zone developing directly above the top helix did not propagated to the soil surface rather was confined to a zone of soil directly above the upper helix. They proposed that the pullout capacity is equal to the sum of the bearing resistance of the top helix, the frictional resistance acting on a cylinder of sand formed between the helices and friction on the anchor shaft. They calculated the uplift capacity of the anchor based on the proposed equation which showed excellent agreement with the measured capacities.

Tagaya et al. (1983) performed analysis of the pullout resistance of buried anchor by a elastoplastic finite element analysis program based on Lade's constitutive equation to clarify ground stresses, maximum pullout resistance etc. They compared the results with the three-dimensional centrifuge testing. They concluded that the jaky's equation to obtain initial stress gives a greater pullout resistance for $\Phi < 35^\circ$ and for the analysis of the shallow anchor a region extending to the side three times more than the anchor width must be considered.

Rowe and Davis (1982) described a theoretical investigation of anchors in cohesionless soils which considered the effect of anchor embedment, soil friction angle, soil dilatancy, initial stress state and anchor roughness for vertical anchors. Their theoretical solution was based on an elasto-plastic finite element analysis using a soil structure interaction theory. The soil was assumed to have a Mohr-Coulomb failure criterion and either an associated or non-associated flow rule. The theoretical results were presented in the form of design charts which could be used in hand calculations to obtain an estimate of anchor capacity for a wide range of anchor geometries and soil types.

Neely et al. (1973) used both a trial failure surface approach and the method of characteristics to analyze a vertical strip anchor in a cohesionless material. In the first method, a trial surface was adopted which consisted of a combination of straight lines and logarithmic spirals. It was assumed initially that the soil above the level of the top of the anchor would act as a simple surcharge. This was defined as the “Surcharge method of analysis”. However, since this approach ignores the shearing resistance of the soil above the anchor, the approach was modified by incorporating the strength of the soil above the anchor through what was termed an equivalent free surface. It should be noted that although the analysis adopted in this method represents a more analytical attempt to predict the ultimate capacity of vertical anchors than any preceding work, the proposed methods ignore the active stress distribution behind the anchor and the kinematic behaviour of the material. Consequently the results are considered as approximate only.

This paper by Meyerhof (1973) is widely referred when considering the capacity of anchors. It is, however, based on two key assumptions; namely, the shape of the failure surface and the distribution of stress along the failure surface. Even so, the theory presented by Meyerhof has been found to give reasonable estimates for a wide range of anchor problems.

2.3 OTHER INVESTIGATIONS

A number of authors have conducted laboratory research to study the effects of initial stress state like Hanna and Carr (1971), Hanna et al. (1972) and Hanna & Ghaly (1992). They have demonstrated that the stress history of sand can significantly affect the load carrying capacity of an anchor. Laboratory tests were conducted on sands with an overconsolidation ratio (OCR) as high as 14, but no attempt was made to mathematically quantify the effect of OCR on the uplift capacity.

This shortcoming was addressed by Hanna and Ghaly (1992) who conducted experimental pullout tests on circular screw anchors in sand to determine the effects of the coefficient of earth pressure at rest (K_0) and OCR. Although this study was limited to helical screw type anchors, a number of interesting observations were reported. Firstly, the Authors revealed it was inherently difficult to reconstruct a residual stress profile in the laboratory that closely models what is observed in the field. It was discovered that by compacting the sand in layers inside a sand chamber, a deposit is created in which the OCR increases with depth. This is

not what is observed in a naturally occurring deposit. Secondly, it was suggested that the anchor capacity increases with increasing OCR.

2.4 COMPRESSIVE CAPACITY VS. PULLOUT CAPACITY

Dash and Pise (2003) conducted detailed laboratory tests to assess the effects of compressive load on uplift capacity of piles. They concluded that the stage of compressive loading is a significant parameter influencing the net uplift capacity of a pile. They further concluded that the net uplift capacity decreases with the increase in the stage of compressive loading. Also at the identical stage of loading and depth of embedment the rate of decrease of net uplift capacity is more in loose sand. The decrease in net uplift capacity may be due to the reduction in soil–pile friction angle δ caused by the presence of compressive loading, which has been exhibited by the proposed logical approach. An assumption of a decrease in soil-pile friction angle, and using Chattopadhyay and Pise’s method (1986) predicts uplift capacity of piles which are remarkably closer to the experimental values.

Trofimendkov and Mariupolskii (1965) conducted a series of field compression and tension tests using screw piles with various soil types. About two hundred piles were installed in soft to hard clays as well as loose to medium dense sands with pile helix diameter ranging from 0.45 to 1.5 m to a depth up to 7 m. The test results indicated that the compression capacity was 1.4 to 1.5 times higher than the uplift capacity. The author concluded that in the compression tests, the bearing plate was pressing on undisturbed soil, and the density of a typical soil increases with depth. A design procedure was proposed based on the test results and the author concluded that the ultimate bearing capacity in compression tests is 1.3 times more than that of a screw pile in the pulling out tests. Therefore, the compression to tension capacity ratio can be expressed as:

$$Q_{uc} = 1.3 Q_{ut} \dots\dots\dots (2.1)$$

where, Q_{uc} = ultimate anchor compression capacity

Q_{ut} = ultimate anchor tension capacity

2.5 GAPS IN STATE OF ART

A number of conclusions can be drawn from the foregoing review into helical screw anchor research:

- (1) The majority of past research has been experimentally based, as evidenced by the large number of studies shown in Tables 2.1 & 2.2. Unfortunately, results obtained from

- laboratory testing are typically problem specific and are difficult to extend to field problems with different material or geometric parameters. Moreover, lack of reported experimental data often makes comparisons with theory difficult.
- (2) Very few rigorous numerical studies have been undertaken to determine anchor behaviour. It is generally agreed that existing theories do not adequately describe the behaviour of anchor plates. Most methods of analysis are based upon the initial assumption of a particular failure mode (limit equilibrium method and upper bound limit analysis). Given that few attempts have been made to accurately monitor internal soil deformations under laboratory conditions, the validity of the assumed failure mechanisms remain largely unproven. A rigorous numerical study of soil anchors using advanced numerical methods is clearly needed.
 - (3) Most of the work is done for clayey soils. Work on sandy soil is rare. Moreover, no attempt has been made to determine the capacity of anchors in inhomogeneous purely cohesionless soil, as it may also be a common field characteristic.
 - (4) Most of the work is done for single anchors. Literature on interference effect on the pullout capacity of a group of closely spaced anchors is scanty.
 - (5) Most of the work is done for uplift and lateral loads. Work on compressive loads had been least researched.
 - (6) Most anchor studies have been concerned with either vertical or horizontal resistance. However, anchors are frequently placed at orientations somewhere between horizontal and vertical depending on the type of application and load orientation (i.e. transmission tower foundations). The effect of anchor inclination on the pullout capacity needs to be investigated.

2.6 OBJECTIVES OF THE PRESENT STUDY

With the understanding of the gaps mentioned above, present work has been undertaken to develop

- (a) understanding of multiplate anchor behaviour and their failure mechanisms
- (b) understanding of the interference effect on the compressive and pullout capacity of a group of closely spaced anchors
- (c) design methodology and framework in the form of equations and design charts in terms of soil properties, loads required etc.

EXPERIMENTAL INVESTIGATIONS

3.0 GENERAL

Very elaborate investigations have been conducted to study the performance of helical screw anchor against axial compressive and pullout loads with special attention to the effect of number of helical blades having the same geometrical properties. To not take into account the effect of spacing between the helix blades on the performance against compressive and pullout loading on multi-helix screw anchor, helical blades were kept in continuation with each other. The tests were carried out at different depths of installation to delve into performance of helical screw anchor at different depths of embedment.

The definitive method of determining allowable compressive and pullout capacity for helical screw anchor is to perform large-scale field tests. However, this type of testing is not common due to high costs and logistics of applying loads of high magnitude and very often tests have to be terminated well before failure as the actual ultimate anchor loads are significantly higher than the anticipated values. An alternative to field-testing is to perform model tests in a laboratory to understand physical phenomenon occurring, and to develop methods of analysis and design.

3.1 LABORATORY TESTS

3.1.1 Helical Screw Anchors

Three types of helical screw anchors having same geometrical properties of helical blade, but having varying number of pitches, i.e. no. of blades without any spacing have been used in the present work. These anchors each having 1, 2, 3 helical blades are termed as ‘single helical screw anchor’, ‘double helical screw anchor’ and ‘triple helical screw anchor’ respectively. These are shown in Fig. 3.1 and Fig. 3.2.

These anchors (made of mild steel) were machine made as one unit with no welded, riveted or bolted joints, thus side effects of these joints on the anchor performance did not come into play. The outer diameter of the helix was 50 mm, while shaft diameter was 16 mm which was comparatively smaller which resulted in minimizing the effects of shaft on the anchor

performance. The thickness of the blade was very thin (≈ 2 mm). All the anchors were having conical end of an apex angle of 90° . Length of each anchor was 510 mm. On the other end of the anchor threads were made for facilitating attachment with tie rod. Tie rods, made of mild steel with 16 mm diameter were used to facilitate tests at different depths. The weight of the whole anchor assembly was negligible as compared to pullout load subjected, hence neglected.



Fig. 3.1: Single, Double and Triple Helical Screw Anchor (Lab Test)

3.1.2 Experimental Setup

3.1.2.1 Test Tank

A square test tank was used to conduct experimental investigations for compressive as well as pullout load testing as shown in Fig. 3.3. The tank dimension was 750 X 750 X 650 mm which was so chosen that there is no boundary effect to anchors. While conducting tests on a pair of helical anchors, this boundary effect along with the effect of interference between two anchors is also taken into consideration. Thus to prevent these effects the clear spacing between the two anchor rods were kept as $2.5 \times B$ and the clear spacing between anchor and the wall of the tank

was kept as $5 \times B$. This is done in the past by many investigators e.g. Ghaly et al. (19910, Kumar and Bhoi (2009) and Merifield (2011).

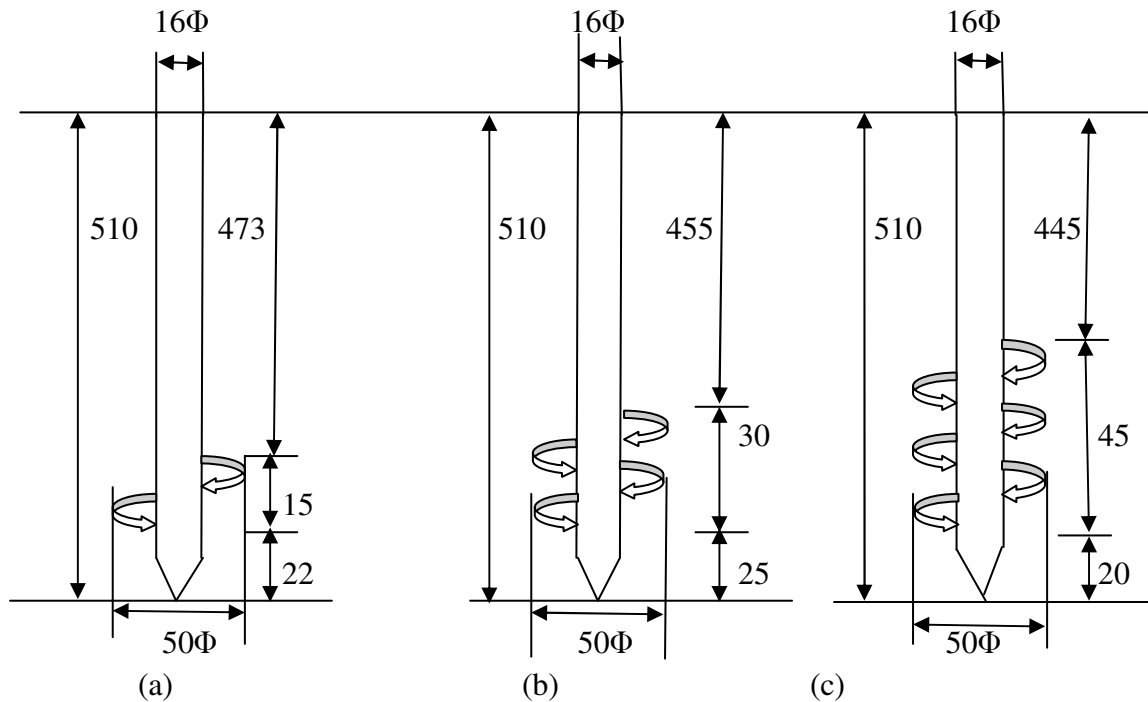


Fig. 3.2: Sketch Showing Dimensions of Helical Screw Anchors (a) Single Helical Screw Anchor (b) Double Helical Screw Anchor and (c) Triple Helical Screw Anchor (All Dimensions are in mm)

3.1.2.2 Loading Frame

Loading frame consisted of a vertical frame with broad base which is useful in increasing the stability as shown in Fig. 3.4. On this frame a long channel was attached. A reaction frame was attached at the center of this channel. This reaction frame was attached with the help of 2 rectangular plates along with four rods at its center. There are two knobs on one side of reaction frame and a rod protruding from the bottom of the reaction frame. This rod was moved by rotating the knobs with the help of a Jack to apply the load. A proving ring was attached beneath this reaction frame as shown in Fig. 3.3 to measure the load applied. A footing was attached to the proving ring with the help of an extension rod. Beneath this footing, anchors were attached with the help of nut and bolt system.

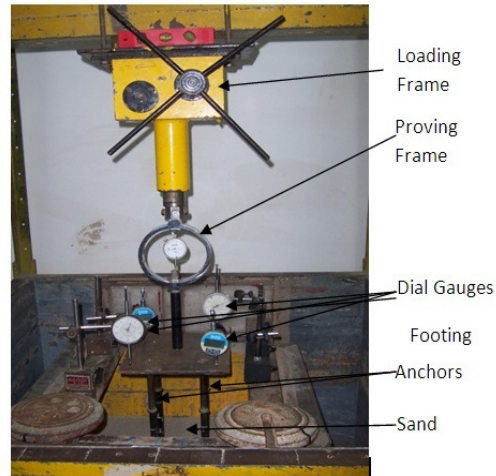


Fig. 3.3: Test setup for Testing of 4 Helical Screw Anchors



Fig. 3.4: Loading Frame

3.1.3 Soil Used in the Study

Soil used was locally collected soil, procured from the bed of Solani River in Roorkee. The grain size distribution curve of the soil is shown in Fig. 3.5. As per Indian Standard (IS: 1498-1970: reaffirmed 1987) Classification System, the soil was classified as poorly graded sand (SP). The maximum and minimum void ratios were determined as per procedures laid down in Indian Standard IS: 2720 (Part XIV, 1968). The engineering properties of the sand obtained by conducting various laboratory tests on the soil are shown in Table 3.1 (Mittal & Shukla, 2013).

Table 3.1: Engineering Properties of Soil Used in Laboratory Experiments

Soil Characteristics	Values
Specific Gravity, G	2.63
Relative Density	75%
Angle of Internal Friction, Φ	38°
Cohesion, c	0 kPa
Minimum Void Ratio, e_{\min}	0.52
Maximum Void Ratio, e_{\max}	0.87
Minimum Dry Unit Weight, $\gamma_{d-\min}$	13.76 kN/m ³
Maximum Dry Unit Weight, $\gamma_{d-\max}$	16.97 kN/m ³
Uniformity Coefficient, C_u	3.64
Coefficient of Curvature, C_c	0.49
Soil Classification	SP

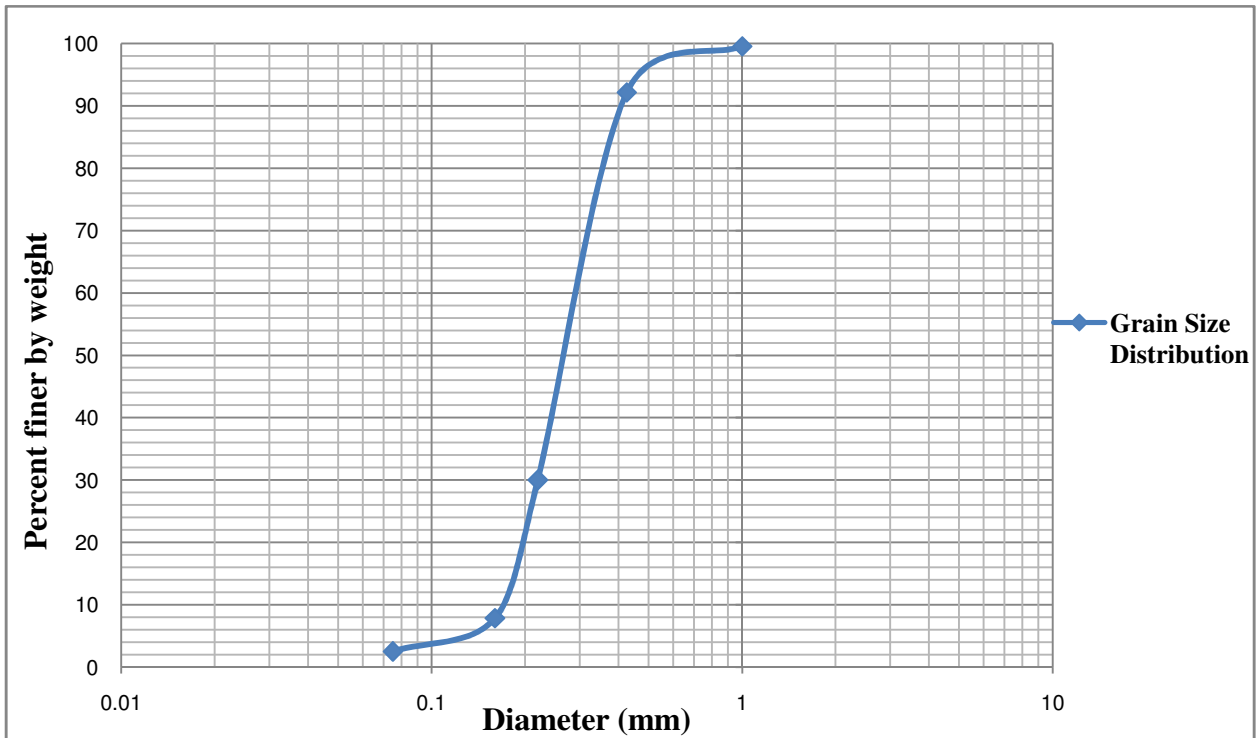


Fig. 3.5: Grain Size Distribution Curve of Soil Used in Laboratory Tests

3.1.4 Model Test Procedure

Ultimate compressive capacity had been measured with anchors installed in the soil at four depth ratios $(H/B) = 2, 4, 6, 8$ whereas ultimate pullout capacity has been measured with anchors installed in the soil at four depth ratios $(H/B) = 4, 6, 8, 10$, where H is the depth of

embedment of bottom of helical screw part of the anchor from soil surface and B is the diameter of the helix. To eliminate boundary effect a clear distance of $2.5B = 2.5 \times 0.05 = 0.125$ m, was provided between the anchor and the wall of the tank center-to-center.

3.1.4.1 Computation of the weight of soil

As the minimum and maximum unit weights of the sand were found to be 13.76 and 16.97 kN/m³ respectively, a unit weight of 15.7 kN/m³ was selected to represent medium dense sand. Hence a known weight of soil was placed in the tank of known volume to maintain a uniform density of 15.7 kN/m³.

3.1.4.2 Preparation and placing of Experimental Soil

Soil was air dried before placing in the tank. Special care had been given to the soil so that the soil was dried uniformly.

The prepared soil sample was weighed in batches and was laid in the test tank in 50.0 mm thick layers. Each layer was compacted using wooden and iron hammers in a measured quantity of blow to achieve uniform density of 15.7 kN/m³. Here 25 blows were imparted for each layer. These numbers of blows were achieved by doing several trials separately in a tank to achieve the desired density. During the course of testing many times density was cross checked by weighing the quantity of sand accommodated in tank. For this marking had been done along the height of the tank at every 10 cms. Since the tank size was known (75 cm X 75 cm), therefore, sand accommodated in each 10 cm height was 88.3 kg. After placing the soil to the required thickness the helical screw anchor with all the accessories attached was placed at the center of the tank and was kept vertical.

Thereafter prepared soil was placed and compacted in the test tank for remaining depth in the similar manner as done before. In the study carried out by Malik (2007) it was seen that there is hardly any remarkable change in the compressive/pullout strength of anchors in freshly filled soil for pre-buried or post-buried anchor. Furthermore, it was experienced during tests that maintaining the verticality of anchor in post-buried situation was difficult particularly in the case of multiple anchors. However it is agreeable that in the field, certainly the anchor shall be post-buried, and it shall be stable due to already consolidated soil for many years.

3.1.4.3 Conduct of Experiment

On the top of anchor, a plate was kept and dial gauges were fixed on top of it. For measurement of axial displacement, one dial gauge at each corner of the plate was fixed as shown in Fig. 3.6. The plate was connected to the proving ring with the help of an extension rod. Load was continuously increased with the help of proving ring in smaller steps of 50 Kg till failure when dial gauges showed continuous increase in displacement without any further application of loads. The deflections were recorded by dial gauges and load displacements curves were plotted.



Fig. 3.6: Laboratory Test in Progress for Vertical Helical Screw Anchor

3.2 RESULTS OF LABORATORY COMPRESSION TESTS

While the capacity of screw anchors to carry axial compression loading has historically been under-utilized, screw anchors have recently begun serving in many of the same capacities as conventional concrete anchors, and have been used to provide axial compression capacities in excess of 1000 kN for permanent structures. If a vertical anchor is loaded with an axial

compressive force in a homogeneous soil, the load is assumed to be carried partly by skin friction and partly through the anchor bearing resistance. Both components depend on the properties of the soil and the characteristics and method of installing the anchor.

The cylindrical failure surface between the top and bottom helices of a multi-helix anchor loaded in compression is formed in the same manner as when loaded in tension, because the formation of this surface is largely a consequence of the anchor geometry and the pattern of soil disturbance during its installation. The shear resistance of cohesionless soil is sensitive to the soil disturbance due to the anchor installation process. The screwing action may loosen the soil surrounding the anchor. Therefore, the disturbed soil strength property above the top helix (anchor in tension) is much lower than the soil below the bottom helix that is less disturbed (anchor in compression). Consequently, the ultimate capacity in compression is much higher than the ultimate capacity in tension for screw anchors installed in cohesionless soil.

Exhaustive experimental investigations have been conducted to study and find information about the performance of helical screw anchor against axial compressive load, with special attention to effect of number of helical blades having the same geometric properties. Total 48 tests were conducted by varying various parameters such as no. of anchors (N_a), no. of screw blades in an anchor (n_b) and embedment depth of the anchor (H/B). In all the tests the density of the sand was kept constant. All the values of these parameters considered for the testing are listed in Table 3.2.

Table 3.2: Parameter Variations in the Entire Compression Testing Program

No. of anchors (N_a)	No. of Screw blades in the anchor (n_b)	Embedment depth of anchor (H/B)	Soil Density (kN/m^3)
1, 2, 3, 4	1, 2, 3	2, 4, 6, 8	15.7

Here the main objective was to study the effect of helical screw anchor properties rather than soil. Therefore, the soil density was kept constant throughout the investigation and anchor properties e.g. no. of screw blades in an anchor and no. of anchors were varied.

3.2.1 Experimental Results for Compression Tests

Displacement readings were taken with every increment of load to get load displacement curves. It was observed that with increase in compressive load, rate of increase in displacement increases till it fails finally.

For the entire tests, axial compressive load and axial displacement graphs were plotted and ultimate compressive Load (Q_{uc}) was found when displacement became infinity at that particular load. At this point, load-displacement curve became asymptotic to the displacement axis. The load vs. displacement curves for single, double and triple helical screw anchors are displayed in Fig. 3.7 to Fig. 3.18. The Ultimate Compressive Loads for all the tests are shown in Table 3.3.

Table 3.3: Ultimate Compressive Loads, Q_{uc} (N)

n_b	H/B	$(Q_{uc})_1$ (N)	$(Q_{uc})_2$ (N)	$(Q_{uc})_3$ (N)	$(Q_{uc})_4$ (N)
1	2	736	1246	1864	2452
1	4	1589	2698	4022	5346
1	6	2207	3600	5592	6867
1	8	2943	4601	6867	8093
2	2	858	1452	2158	2894
2	4	2649	3649	5886	7357
2	6	3433	5297	7063	9270
2	8	4169	6278	8584	11527
3	2	981	1687	2551	3286
3	4	2796	4395	6376	7848
3	6	3679	5641	7554	10104
3	8	5150	7495	10497	13244

Based on the above results, the curves have been plotted to highlight the influence of various factors on the ultimate compressive capacity and displacement.

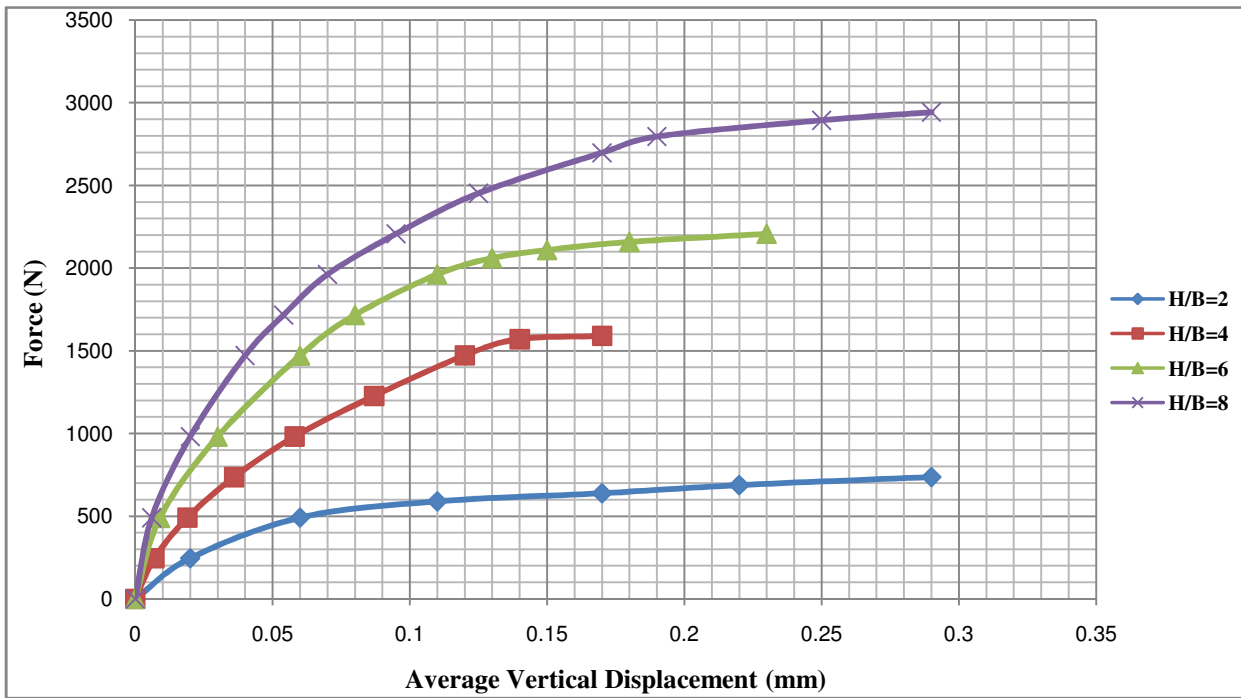


Fig. 3.7: Compression Test Graphs for 1 No. of Single Helical Screw Anchor

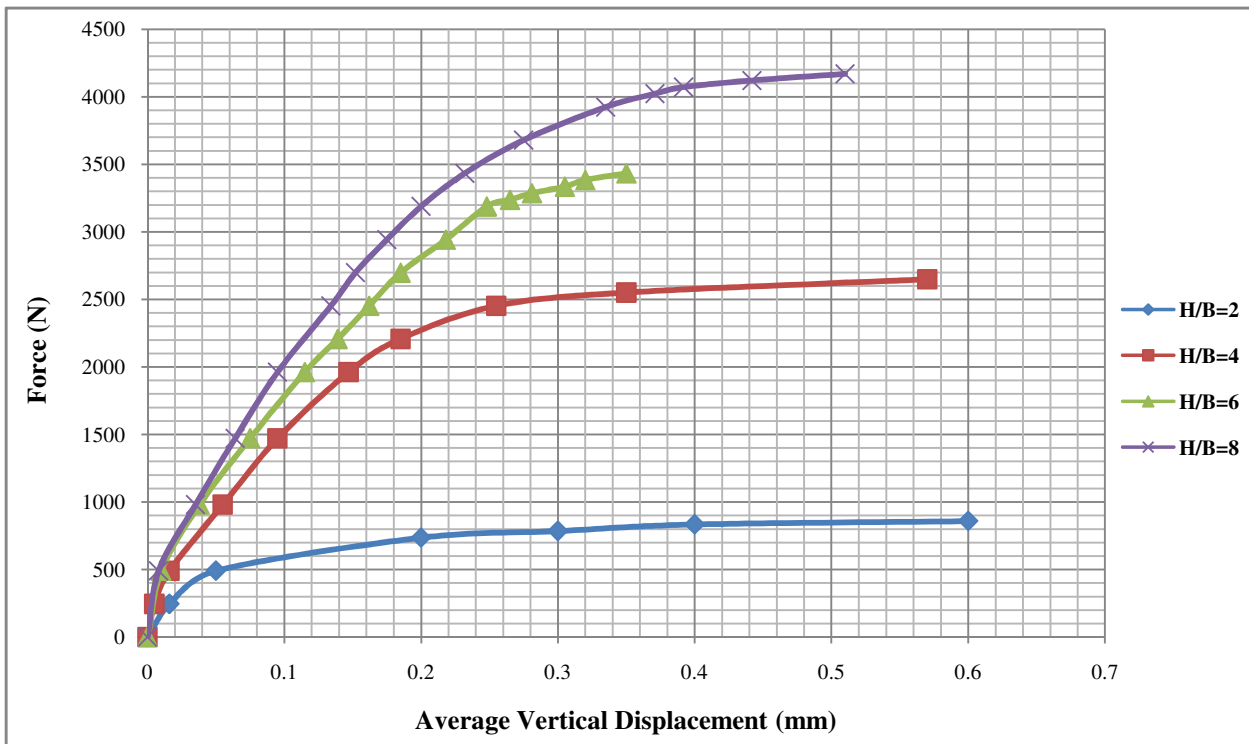


Fig. 3.8: Compression Test Graphs for 1 No. of Double Helical Screw Anchor

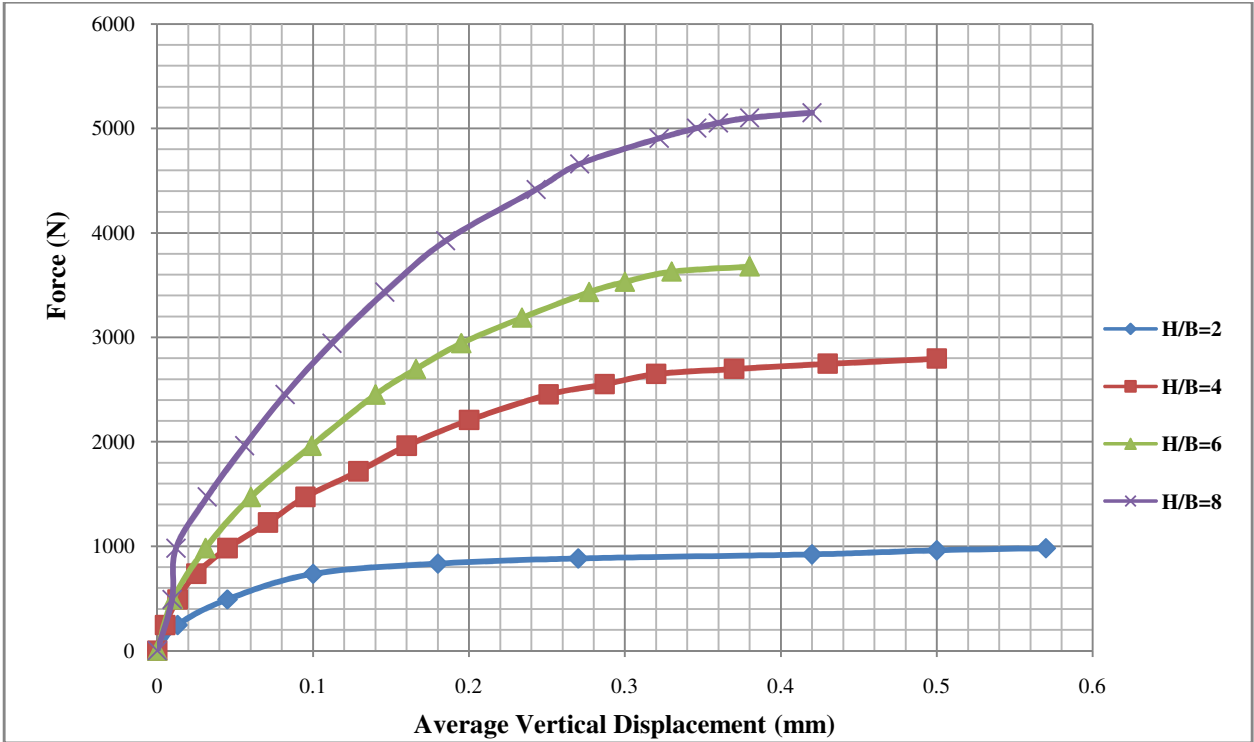


Fig. 3.9: Compression Test Graphs for 1 No. of Triple Helical Screw Anchor

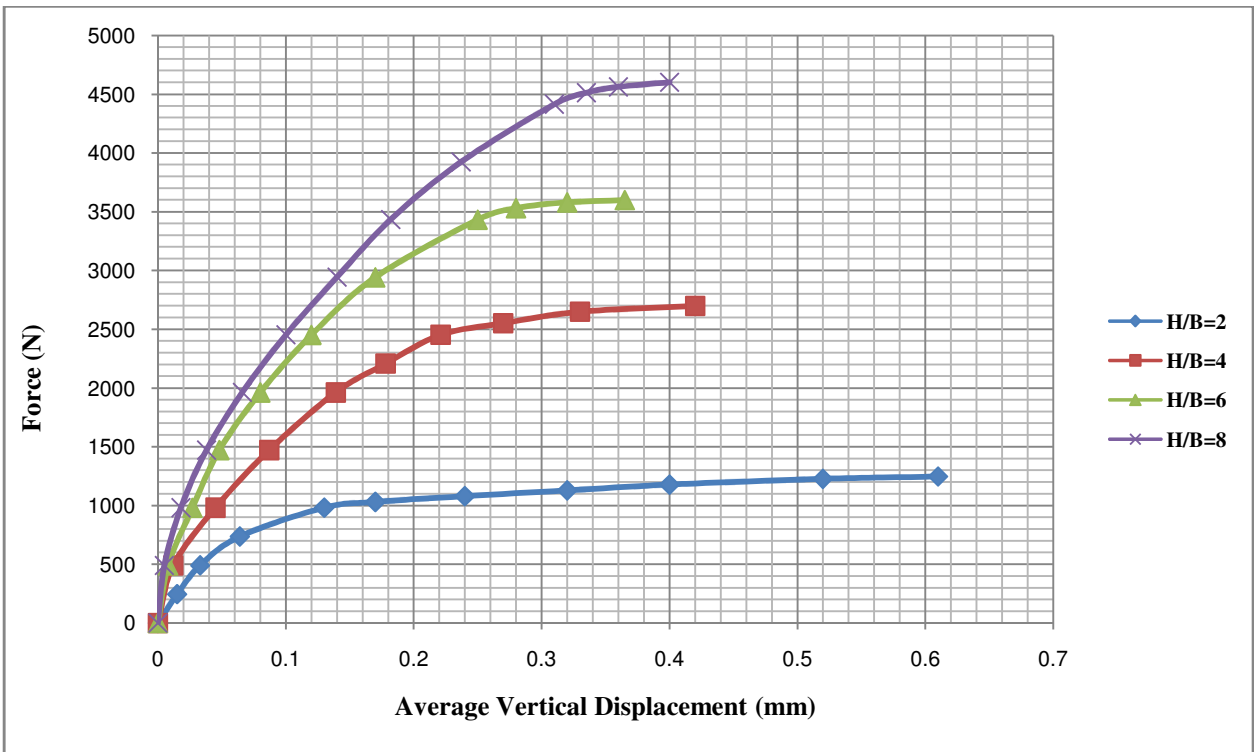


Fig. 3.10: Compression Test Graphs for 2 Nos. of Single Helical Screw Anchor

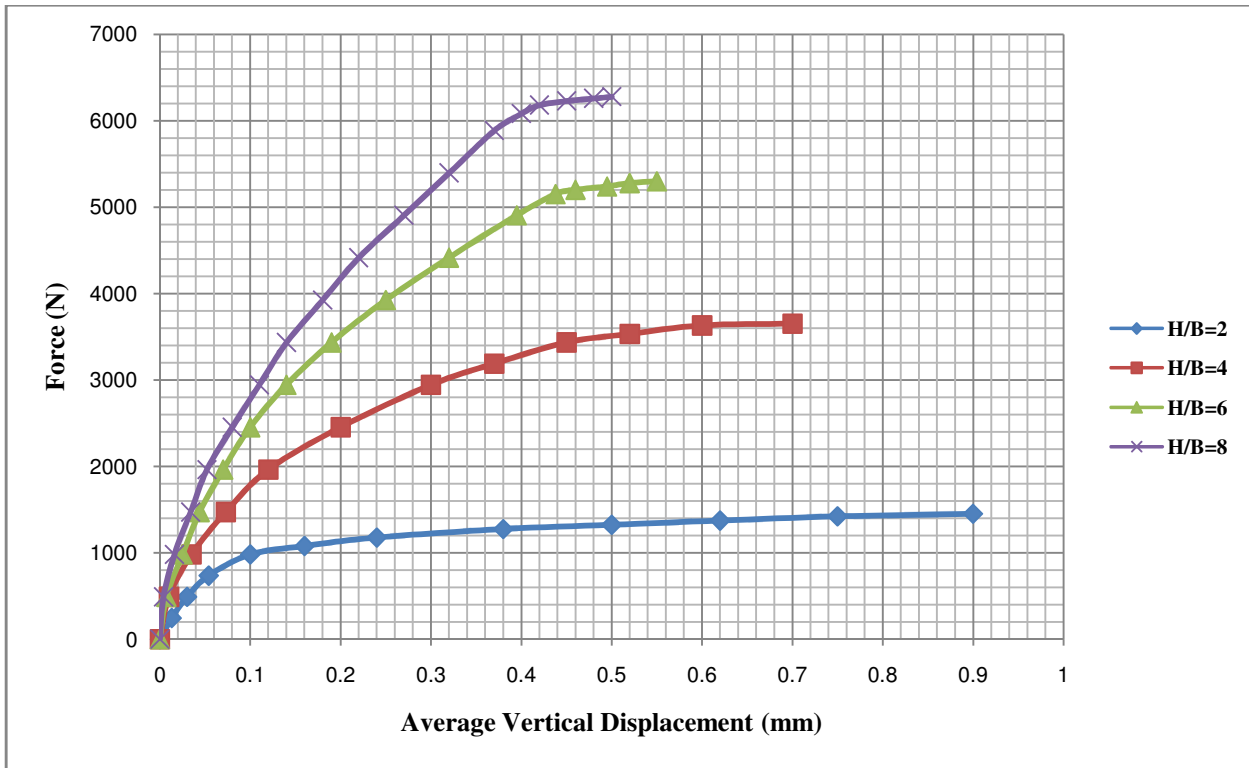


Fig. 3.11: Compression Test Graphs for 2 Nos. of Double Helical Screw Anchor

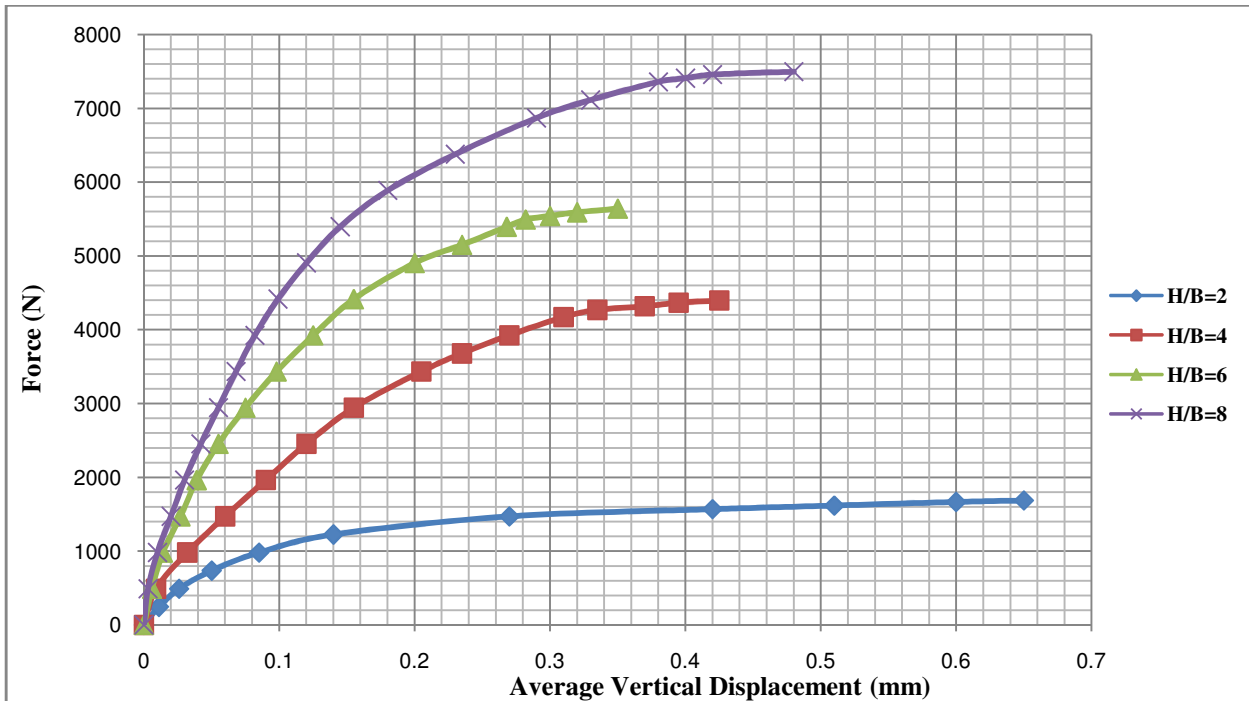


Fig. 3.12: Compression Test Graphs for 2 Nos. of Triple Helical Screw Anchor

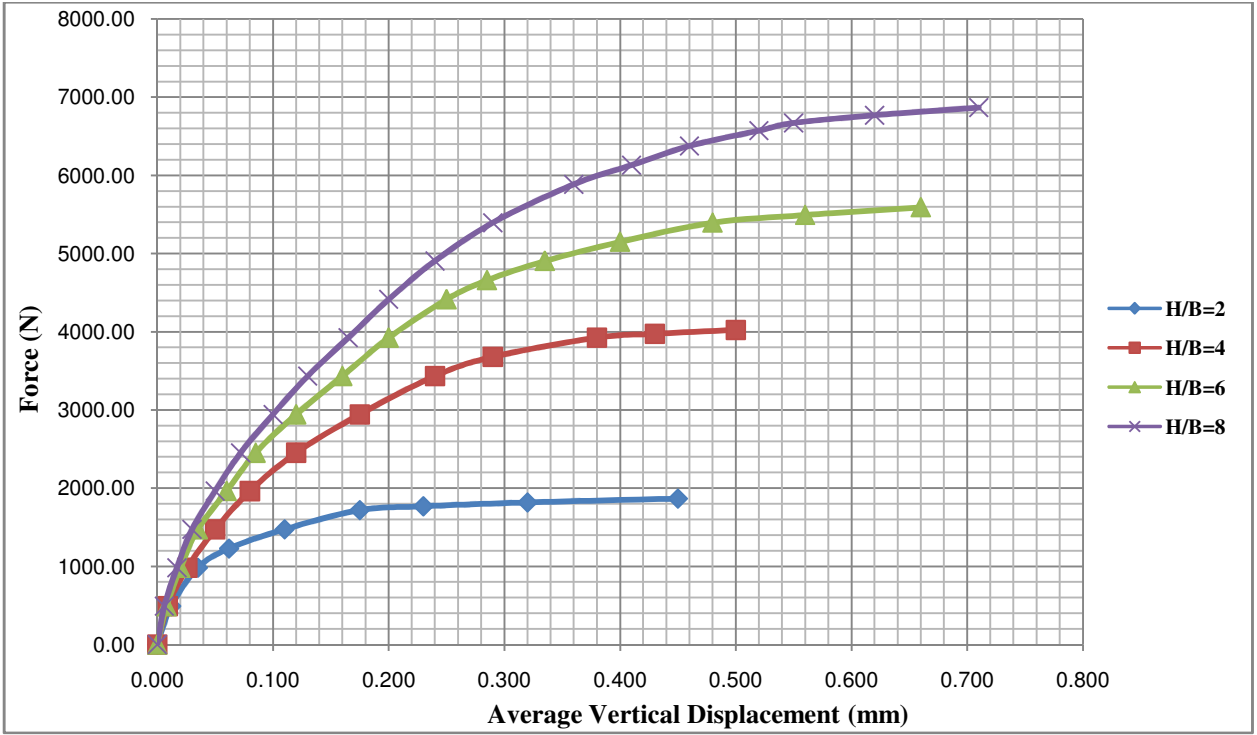


Fig. 3.13: Compression Test Graphs for 3 Nos. of Single Helical Screw Anchor

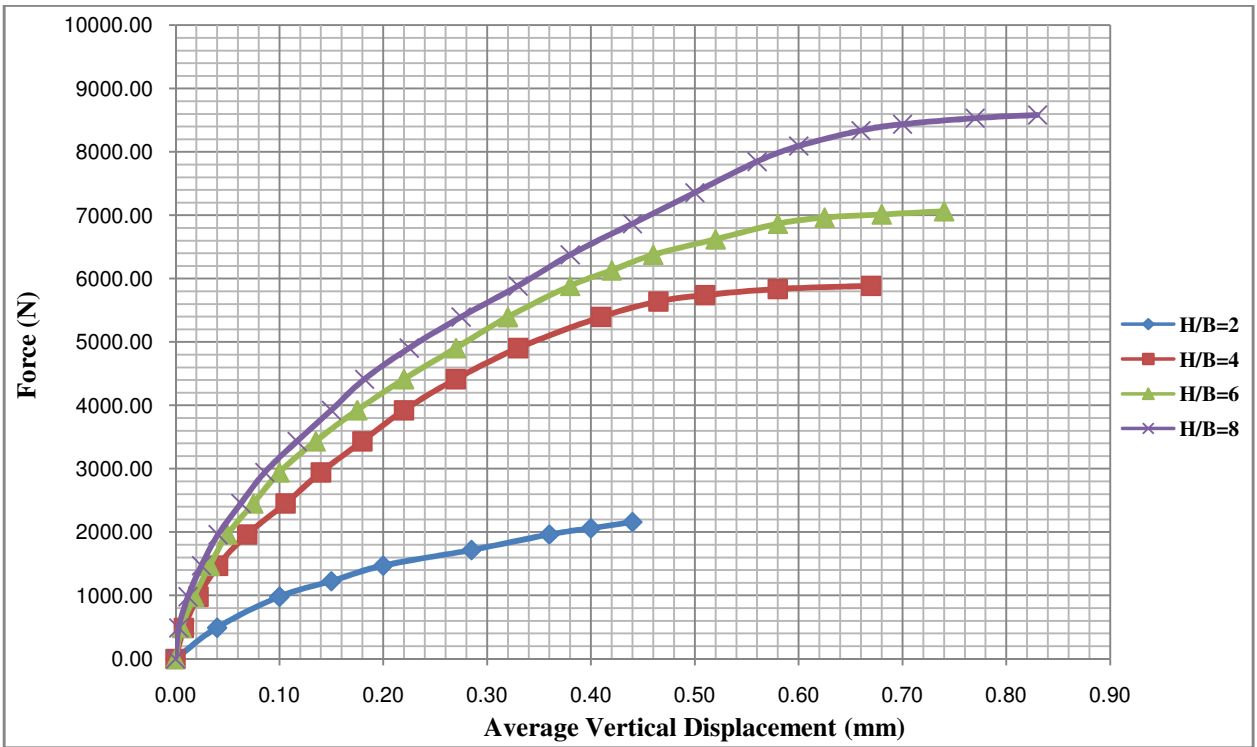


Fig. 3.14: Compression Test Graphs for 3 Nos. of Double Helical Screw Anchor

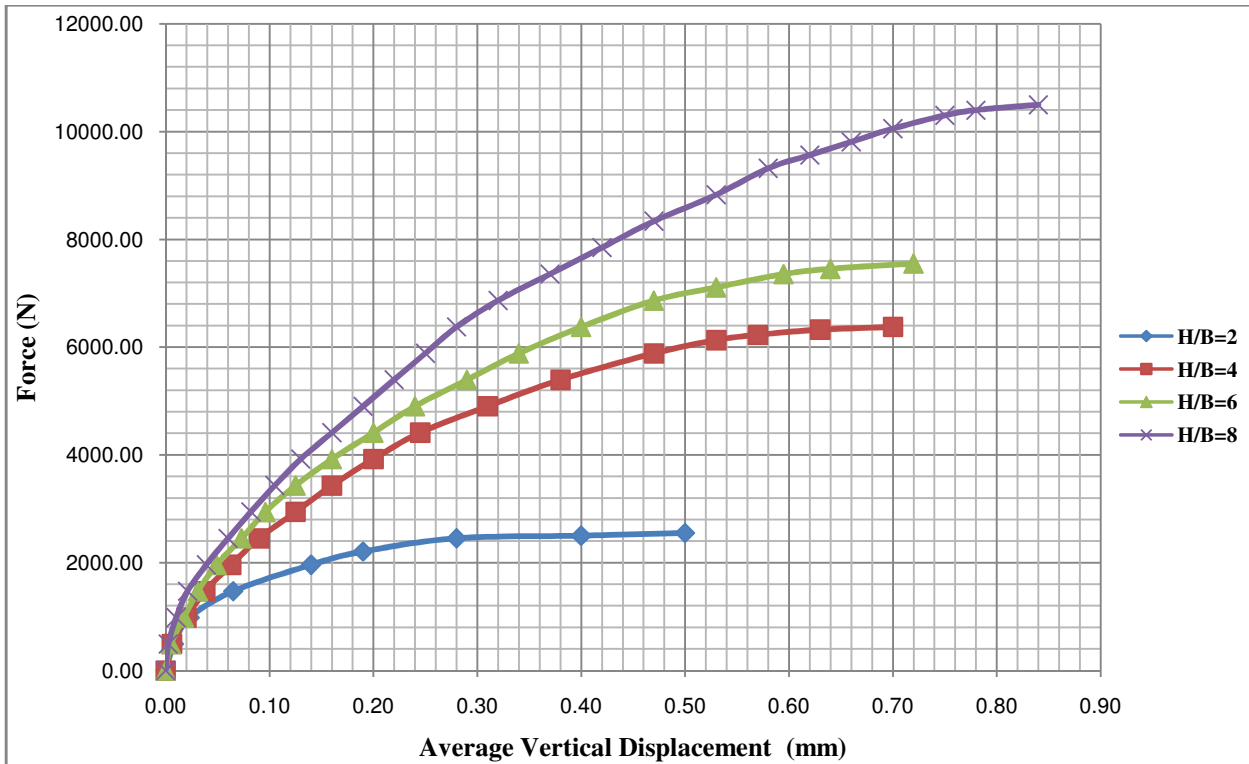


Fig. 3.15: Compression Test Graphs for 3 Nos. of Triple Helical Screw Anchor

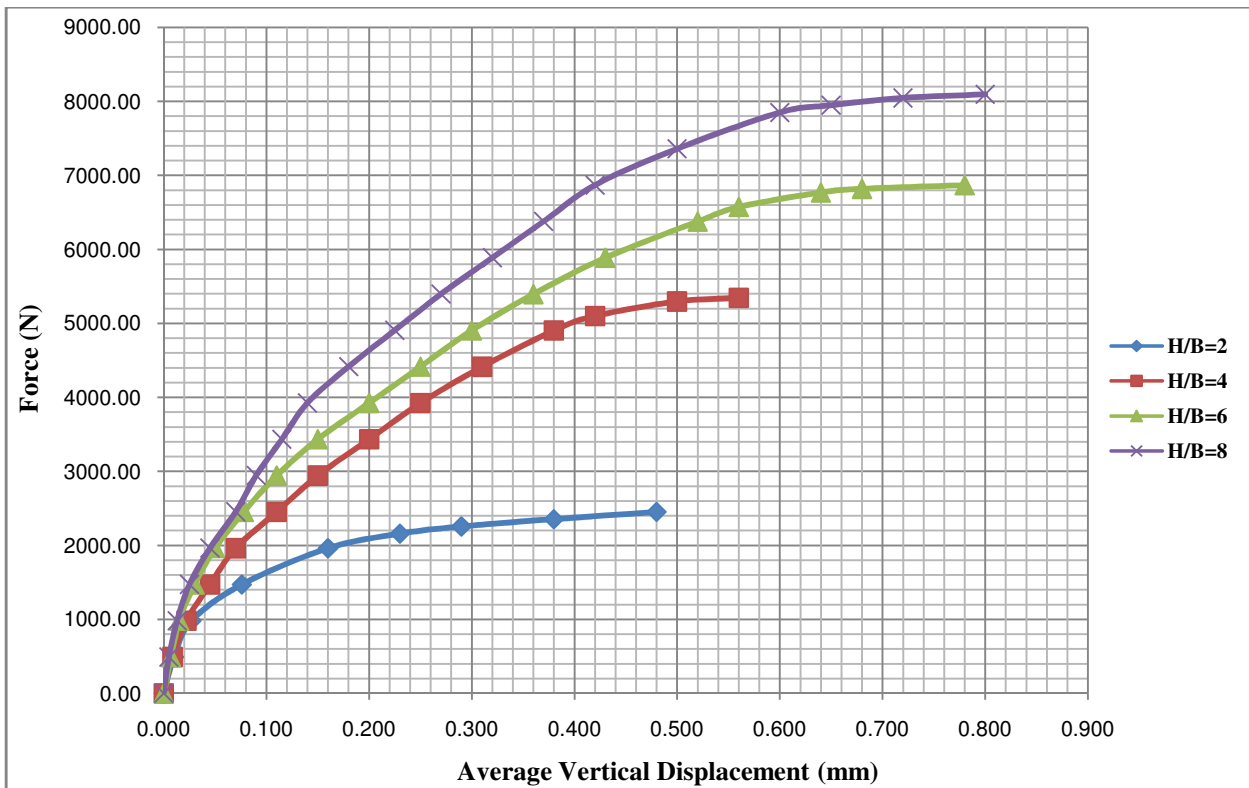


Fig. 3.16: Compression Test Graphs for 4 Nos. of Single Helical Screw Anchor

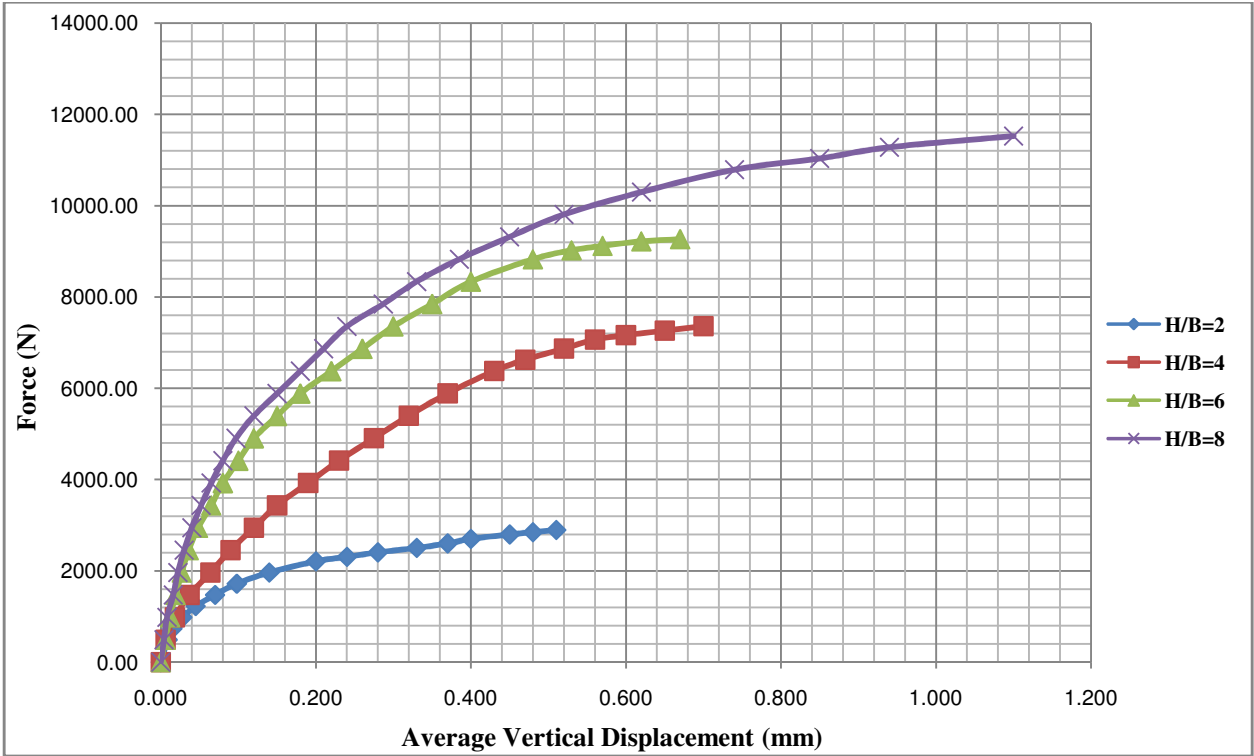


Fig. 3.17: Compression Test Graphs for 4 Nos. of Double Helical Screw Anchor

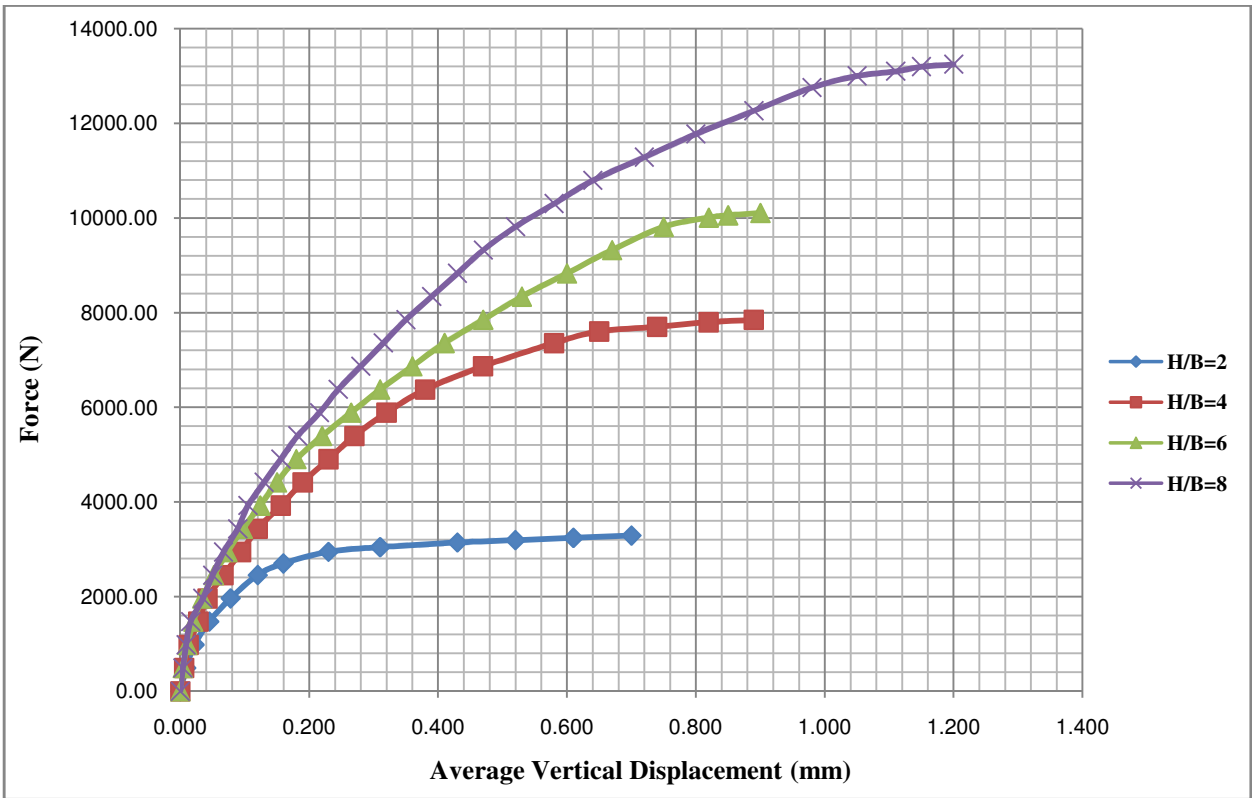


Fig. 3.18: Compression Test Graphs for 4 Nos. of Triple Helical Screw Anchor

3.3 RESULTS OF LABORATORY PULLOUT TESTS

Many geotechnical designs require knowledge of soil uplift resistance where the foundations must withstand tensile forces. Such situations are common to both land and marine environments and arise, for example, from wave action on offshore structures, wind loading on high mast transmission towers and buoyancy forces on buried pipelines. In the present research program exhaustive experimental investigations have been conducted to study and find information about the performance of helical screw anchor against axial pullout load, with special attention to effect of number of helical blades having the same geometric properties.

It is observed from various available theoretical and experimental research studies that the vertical uplift resistance of anchors in a group reduces quite significantly with a decrease in the spacing between the anchors. The aim of the present research is to determine experimentally the vertical pullout resistance of a group of two, three and four helical screw anchors subjected to failure simultaneously at the same magnitudes of the failure loads. A group of helical screw anchors, each having width B , are embedded at clear spacing (s). All the anchors are placed at the same depth (H) in sand with horizontal free surface; the embedment ratio for each of the anchors becomes equal to H/B , where B is the diameter of the anchor blade. It is assumed that all the anchors are loaded to failure simultaneously exactly at the same magnitude of the failure load.

Total 48 tests were conducted by varying various parameters such as no. of anchors (N_a), no. of screw blades in an anchor (n_b) and embedment depth of the anchor (H/B). In all the tests the density of the sand was kept constant. All the values of these parameters considered for the testing are listed in Table 3.4.

Table 3.4: Parameter Variations in the Entire Pullout Testing Program

No. of anchors (N_a)	No. of Screw blades in the anchor (n_b)	Embedment depth of anchor (H/B)	Soil Density (kN/m^3)
1, 2, 3, 4	1, 2, 3	4, 6, 8, 10	15.7

Here the main objective was to study the effect of helical screw anchor properties rather than soil. Therefore, the soil density was kept constant throughout the investigation and anchor properties e.g. no. of screw blades in an anchor and no. of anchors were varied.

3.3.1 Experimental Results of Pullout Tests

The aim of the present research is to determine experimentally the vertical pullout resistance of a group of two, three and four helical screw anchors subjected to failure simultaneously at the same magnitudes of the failure loads. A group of helical screw anchors, each having diameter B, are embedded at clear spacing (s). All the anchors are placed at the same depth (H) in sand with horizontal free surface; the embedment ratio for each of the anchors becomes equal to H/B, where B is the diameter of the anchor blade. It is assumed that all the anchors are loaded to failure simultaneously exactly at the same magnitude of the failure load.

Displacement readings were taken with every increment of load to get load displacement curves. It was observed that with increase in pullout load, rate of increase in displacement increases till it fails. Loads were applied until a relative displacement of 20% of the plate diameter was achieved or the anchors failed by rapid pull-out, whichever occurred first.

For all the tests, axial pullout load and axial displacement graphs were plotted and ultimate pullout load (Q_{up}) was obtained when displacement became infinity at that particular load. At this point, load-displacement curve became asymptotic to the displacement axis. The load vs. displacement curves for single, double and triple helical screw anchors are displayed in Fig. 3.19 to Fig. 3.30. The ultimate pullout loads for all the tests are shown in Table 3.5.

Based on the results shown in Table 3.5, the curves have been plotted to highlight the influence of various factors on the ultimate pullout capacity and displacement.

Table 3.5: Ultimate Pullout Load, Q_{up} (N)

n_b	H/B	$(Q_{up})_1$	$(Q_{up})_2$	$(Q_{up})_3$	$(Q_{up})_4$
1	4	93	137	221	294
1	6	373	539	760	991
1	8	1079	1545	2060	2747
1	10	1717	2158	3823	4513
2	4	118	196	280	392
2	6	491	638	956	1275
2	8	1226	1619	2296	3139
2	10	1962	2796	4415	5101
3	4	132	226	319	441
3	6	638	824	1246	1668
3	8	1472	1839	2747	3679
3	10	2256	3188	4689	5837

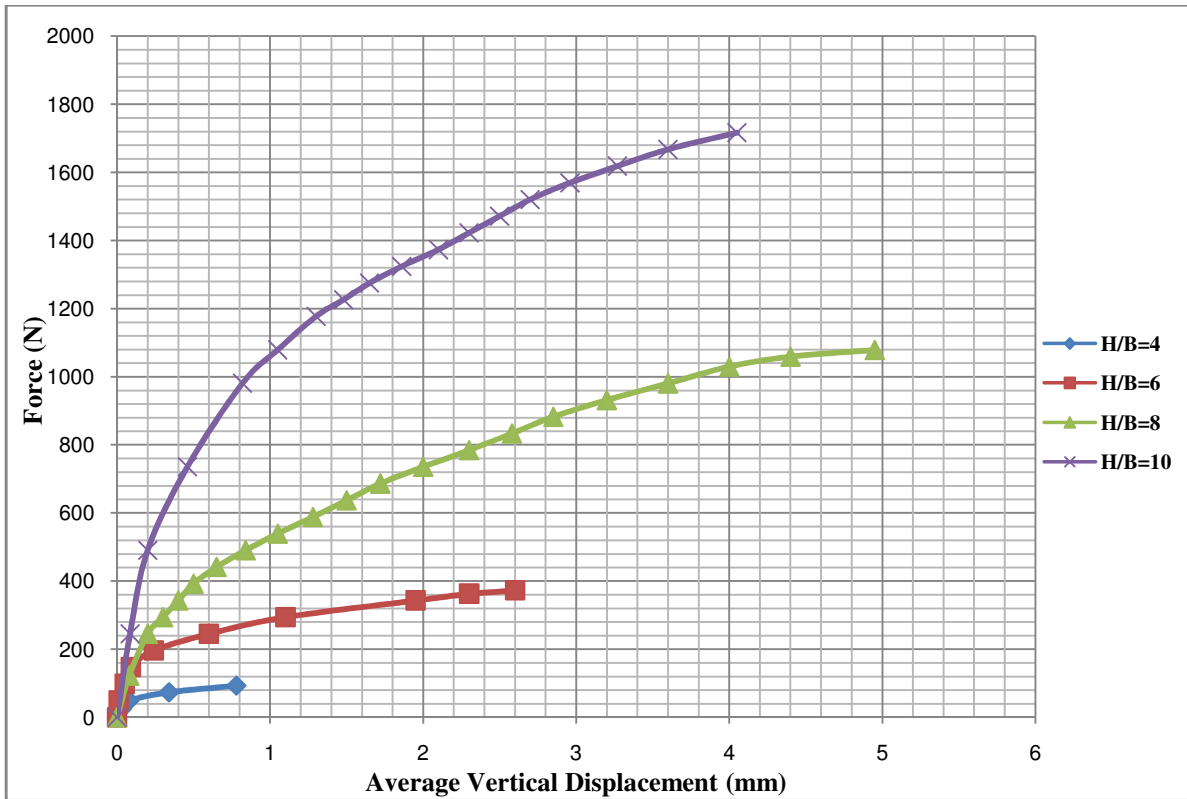


Fig. 3.19: Pullout Test Graphs for 1 No. of Single Helical Screw Anchor

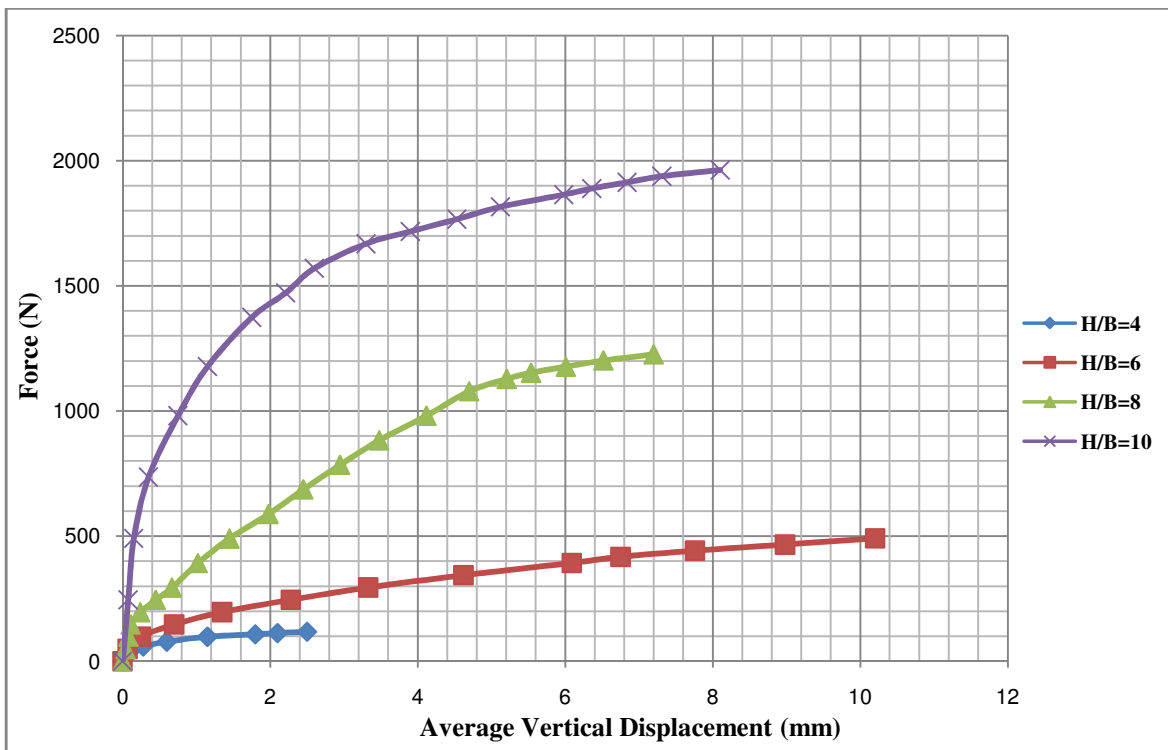


Fig. 3.20: Pullout Test Graphs for 1 No. of Double Helical Screw Anchor

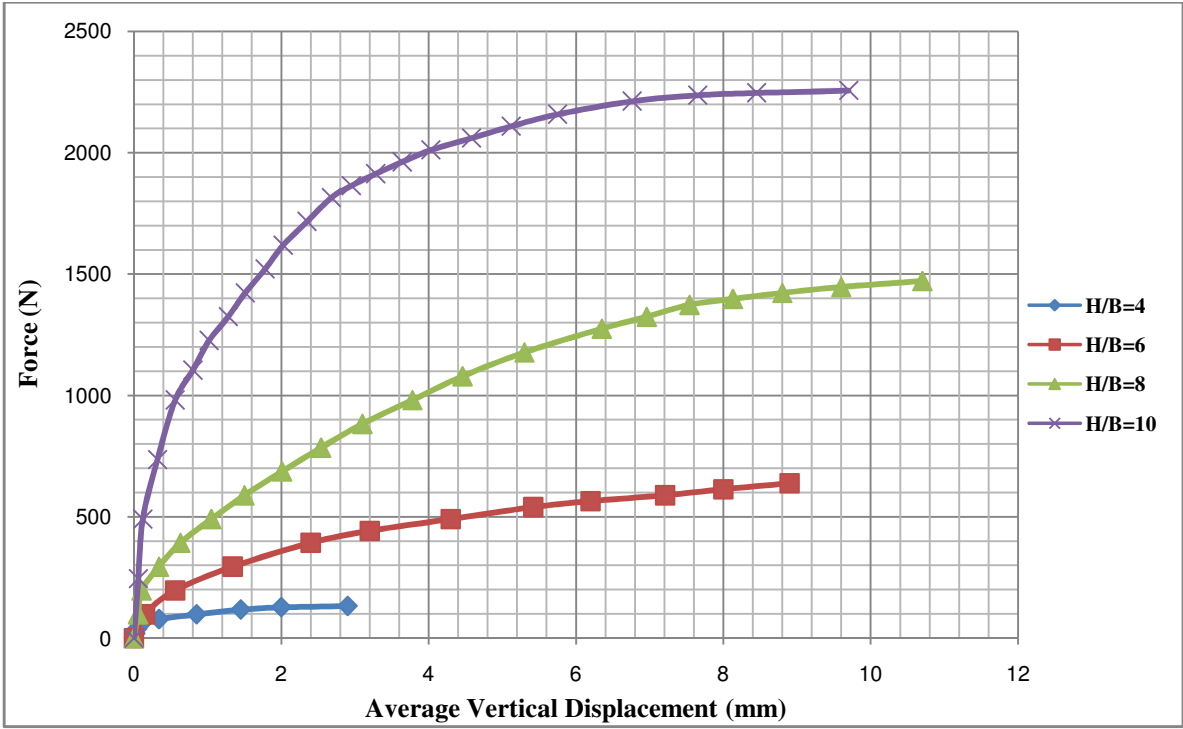


Fig. 3.21: Pullout Test Graphs for 1 No. of Triple Helical Screw Anchor

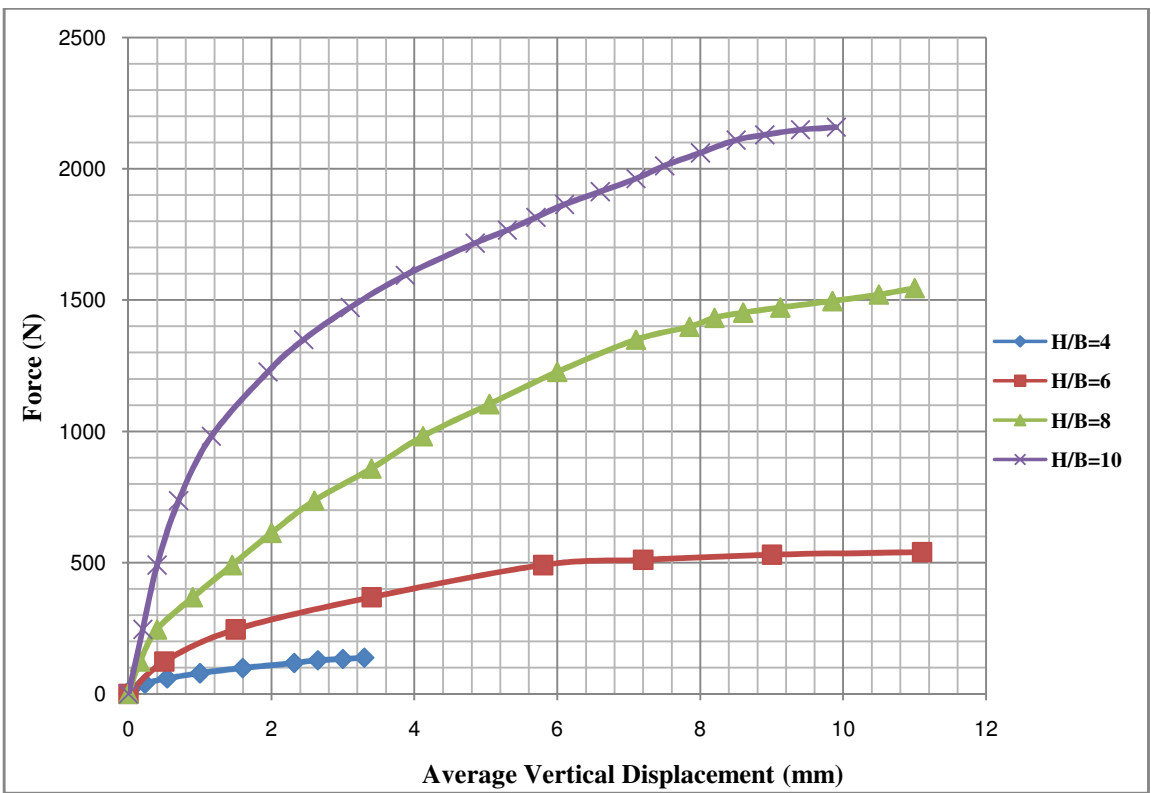


Fig. 3.22: Pullout Test Graphs for 2 Nos. of Single Helical Screw Anchor

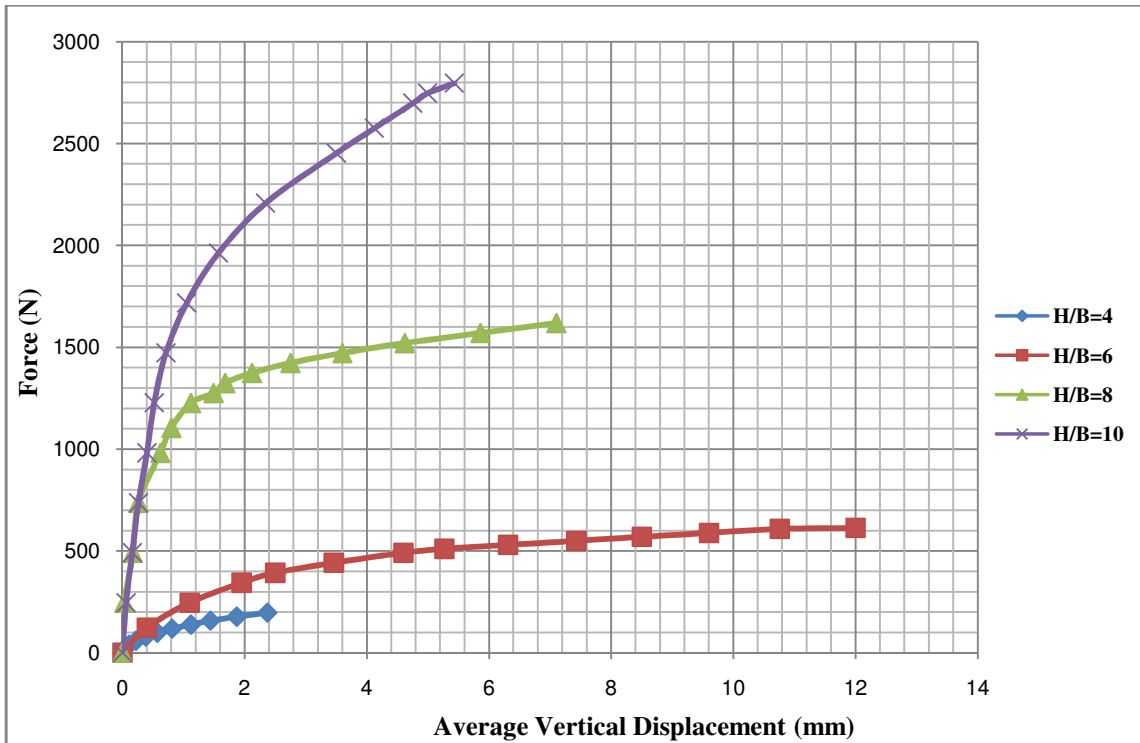


Fig. 3.23: Pullout Test Graphs for 2 Nos. of Double Helical Screw Anchor

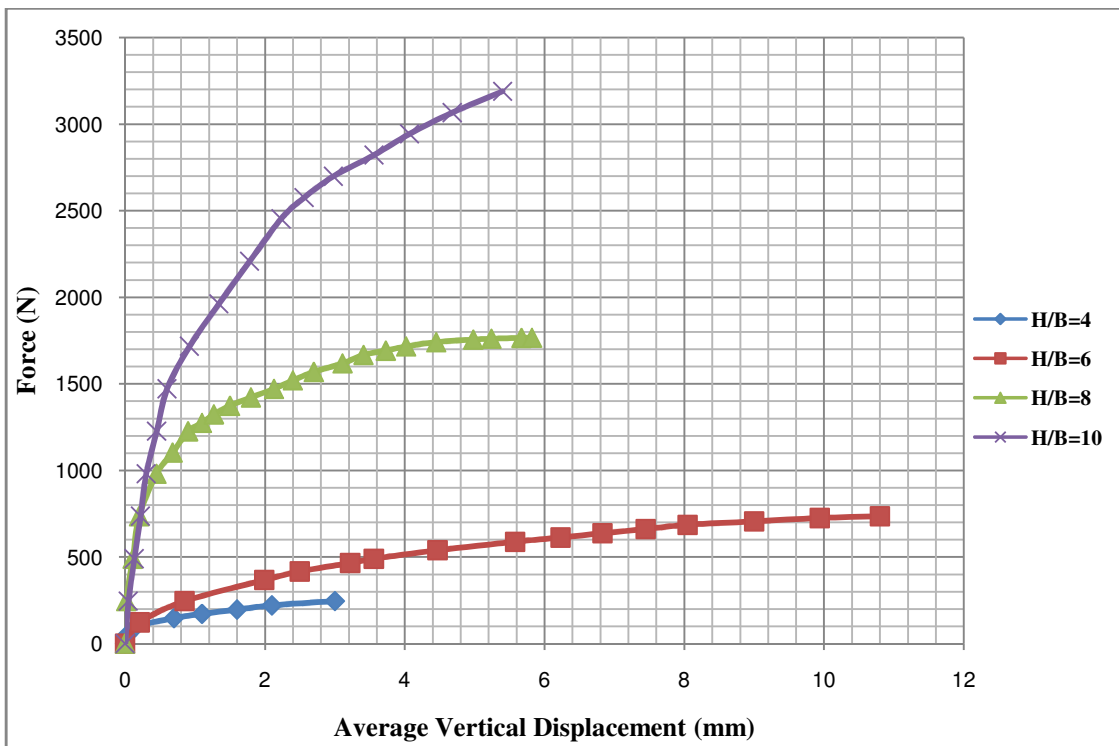


Fig. 3.24: Pullout Test Graphs for 2 Nos. of Triple Helical Screw Anchor

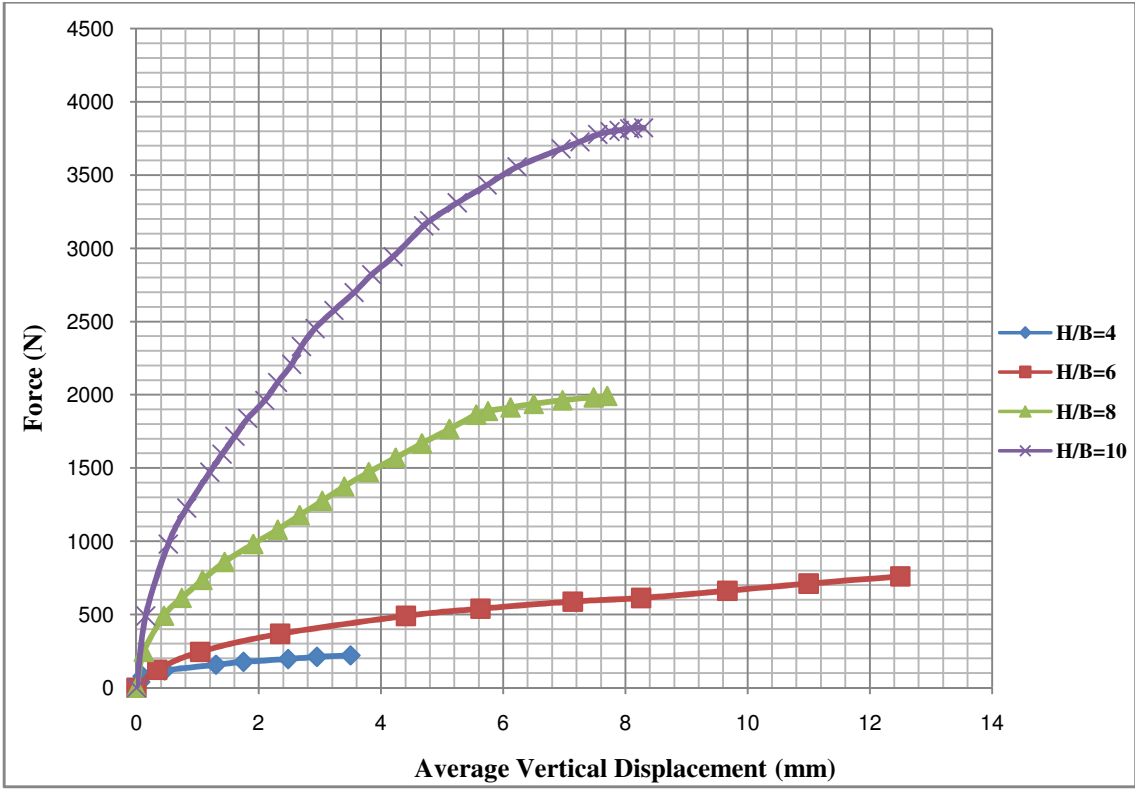


Fig. 3.25: Pullout Test Graphs for 3 Nos. of Single Helical Screw Anchor

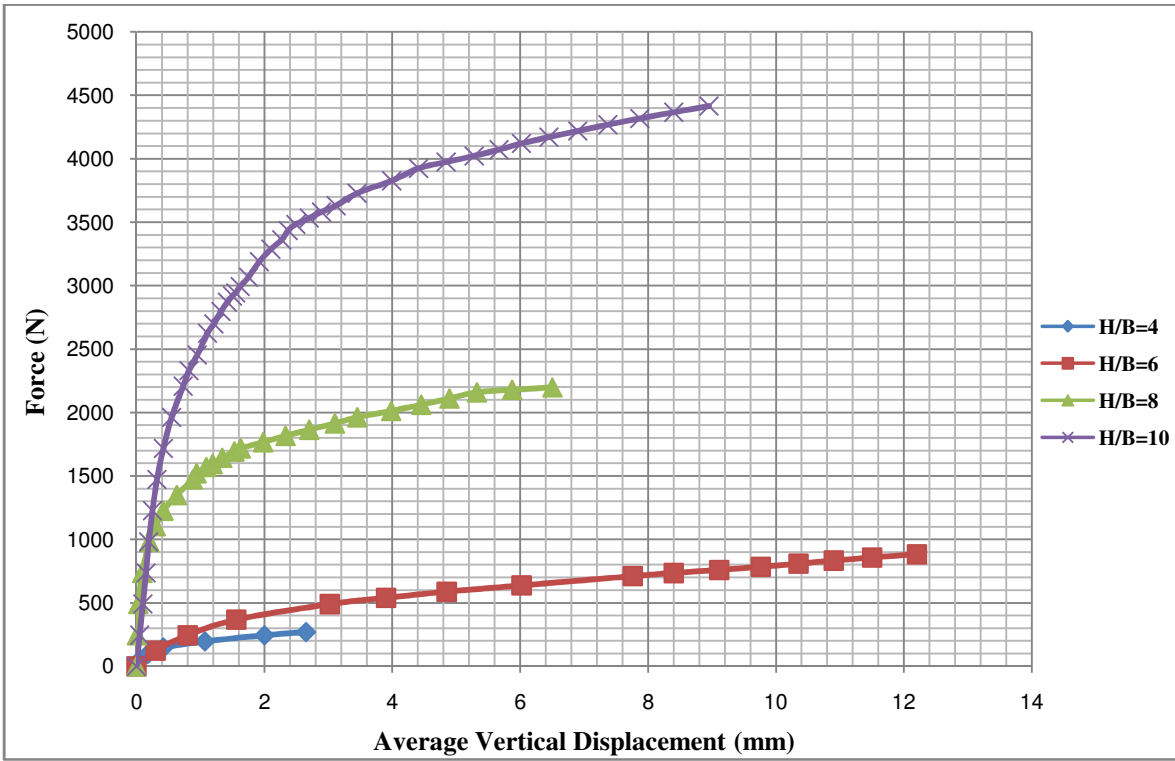


Fig. 3.26: Pullout Test Graphs for 3 Nos. of Double Helical Screw Anchor

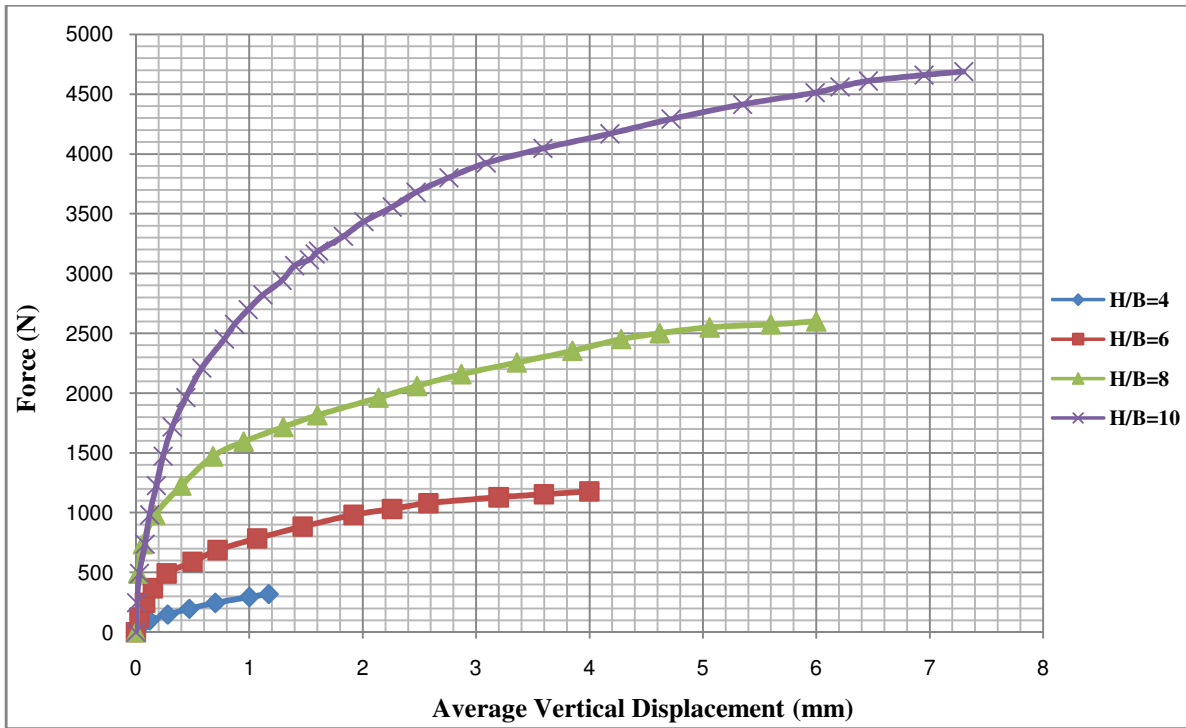


Fig. 3.27: Pullout Test Graphs for 3 Nos. of Triple Helical Screw Anchor

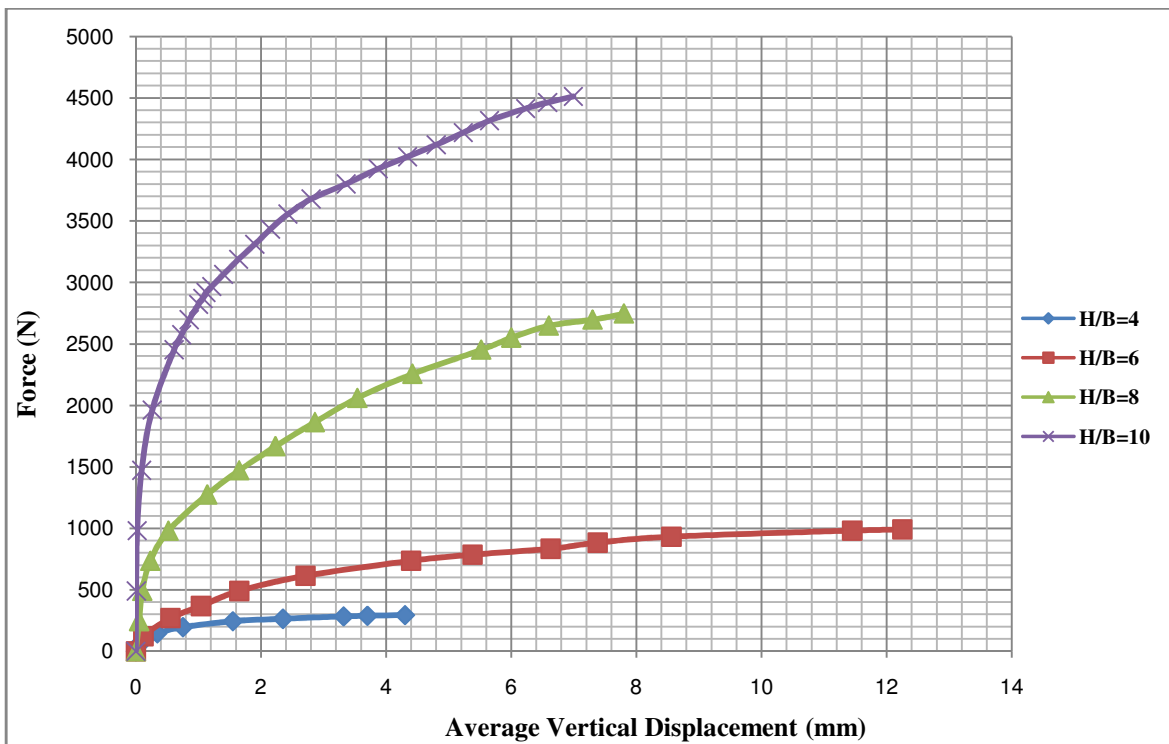


Fig. 3.28: Pullout Test Graphs for 4 Nos. of Single Helical Screw Anchor

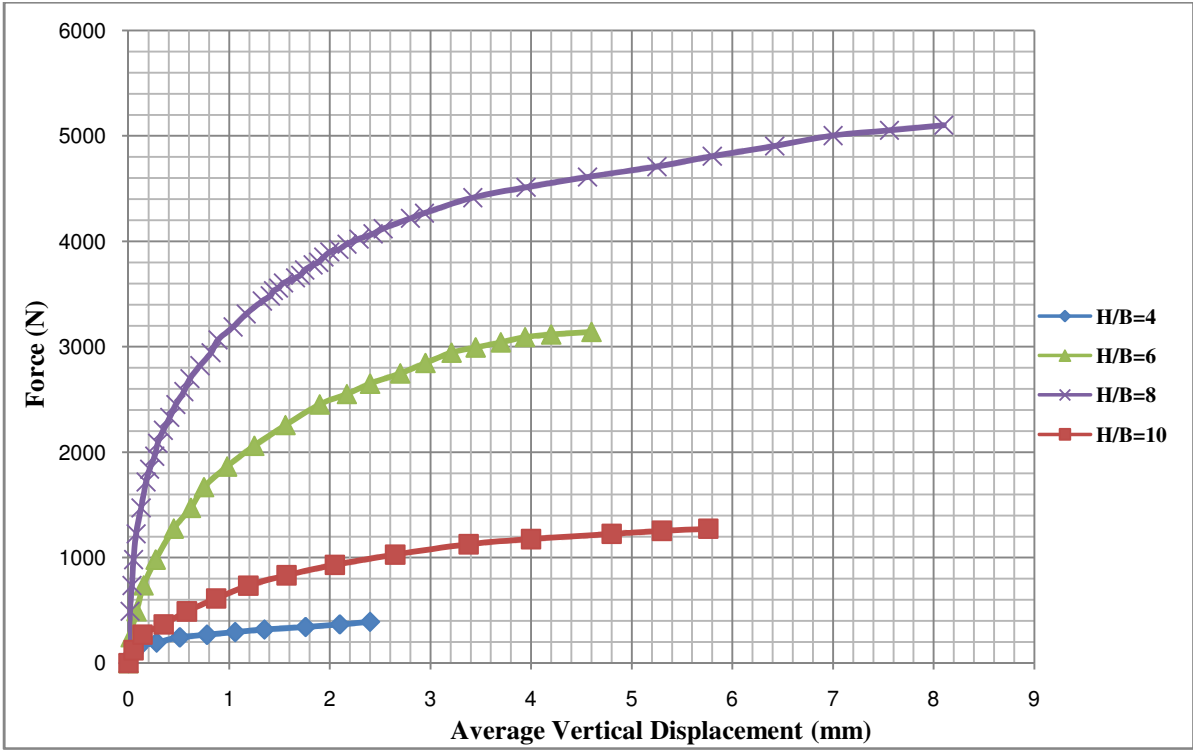


Fig. 3.29: Pullout Test Graphs for 4 Nos. of Double Helical Screw Anchor

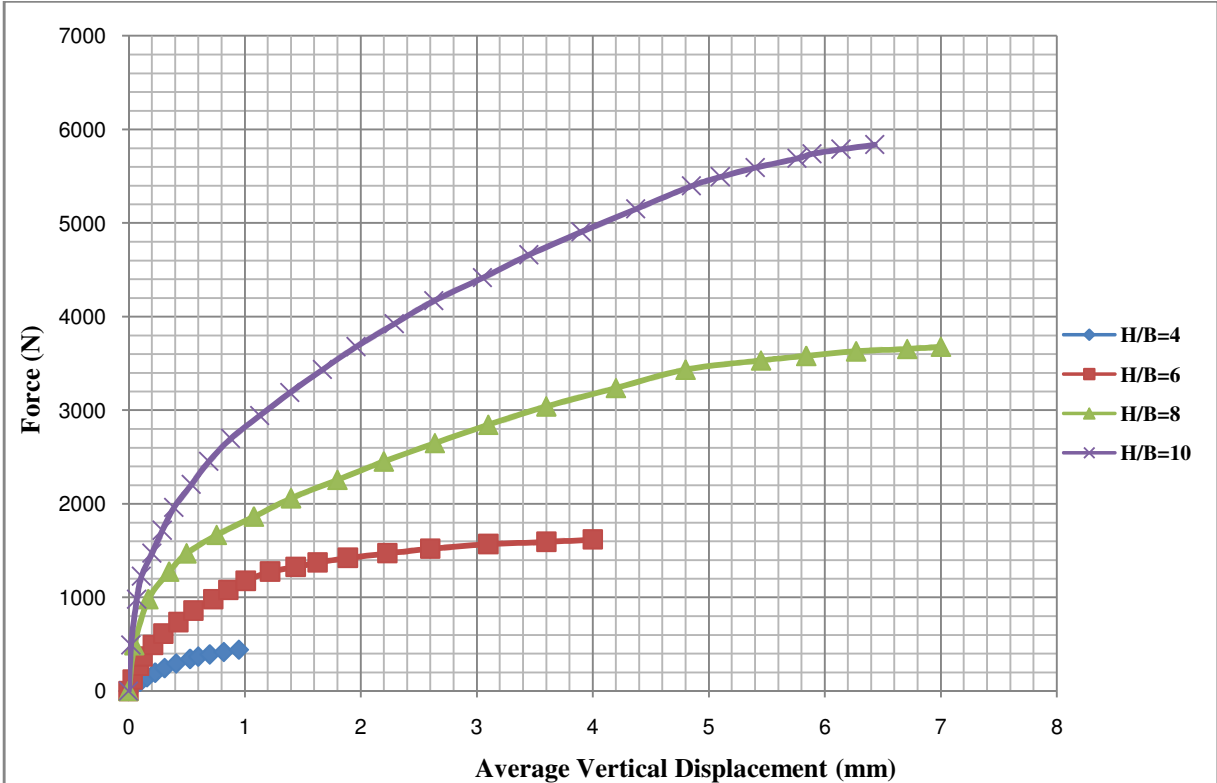


Fig. 3.30: Pullout Test Graphs for 4 Nos. of Triple Helical Screw Anchor

DISCUSSION ON TEST RESULTS

4.0 INTRODUCTION

Here discussions on compressive and pullout laboratory test results are presented separately.

4.1 DISCUSSION ON COMPRESSION TEST RESULTS

The compression tests were conducted to study the effect of various parameters like number of helical blades (n_b), installation depth (H) and number of anchors (N_a) in a group. Special attention had been given to number of anchors as it was very difficult to test more than one anchor in laboratory as well as in the field.

A large amount of deflection was required to mobilize the maximum load and no peak compressive load was evident from the load-deflection curves. The tests were terminated, however, when the anchor exhibited continual creep under a specific load. A well-defined peak compressive load was, therefore, difficult to precisely define. A best fitted equation has been developed based on the test results, for actual design of anchors.

4.1.1 Effect of No. of Anchors (N_a)

Fig. 4.1 displays plot of ultimate compressive load versus deformation for 1, 2, 3 and 4 no. of helical anchors maintaining anchor properties constant. By using double tangent method, it is found that the ultimate compressive capacity increases from 2796 N for 1 anchor to 7848 N for 4 anchors for no. of screw blades in an anchor equal to 3 and embedment depth ratio equal to 4. The ultimate compressive capacity increases from 2796 N to 4395 N for increase in N_a from 1 to 2 whereas it increases from 6376 N to 7848 N for increase in N_a from 3 to 4. Hence for initial increase in H/B (i.e. for increase in H/B from 2 to 4), the increase in Q_{uc} is 57 %, while for further increase in H/B (i.e. for increase in H/B from 6 to 8); the increase in Q_{uc} is 19 % which is quite less than earlier increase. Therefore, it is clear that, though ultimate compressive load increases with increase in no. of anchors (N_a), however rate of increase is higher for initial increase in N_a than that of later increase in N_a . This indicates that with further increase in N_a no

significant gain in compressive capacity will be obtained; rather it attains a constant value or has a very insubstantial increase after some further increase in N_a .

This is one of the important conclusions of this study. It was seen that the anchor capacity does not increase linearly as we increase the number of blades, number of anchors and embedment depth ratio. This is almost in line with the tests conducted on single or group of anchors. In case of group of anchors, the anchor capacity is not sum of individual capacity of each anchor. This is also reported by Ghaly et al. (1991), Hanna and Ghaly (1994), Ilamparuthi et al. (2002), Kumar and Kouzer (2008).

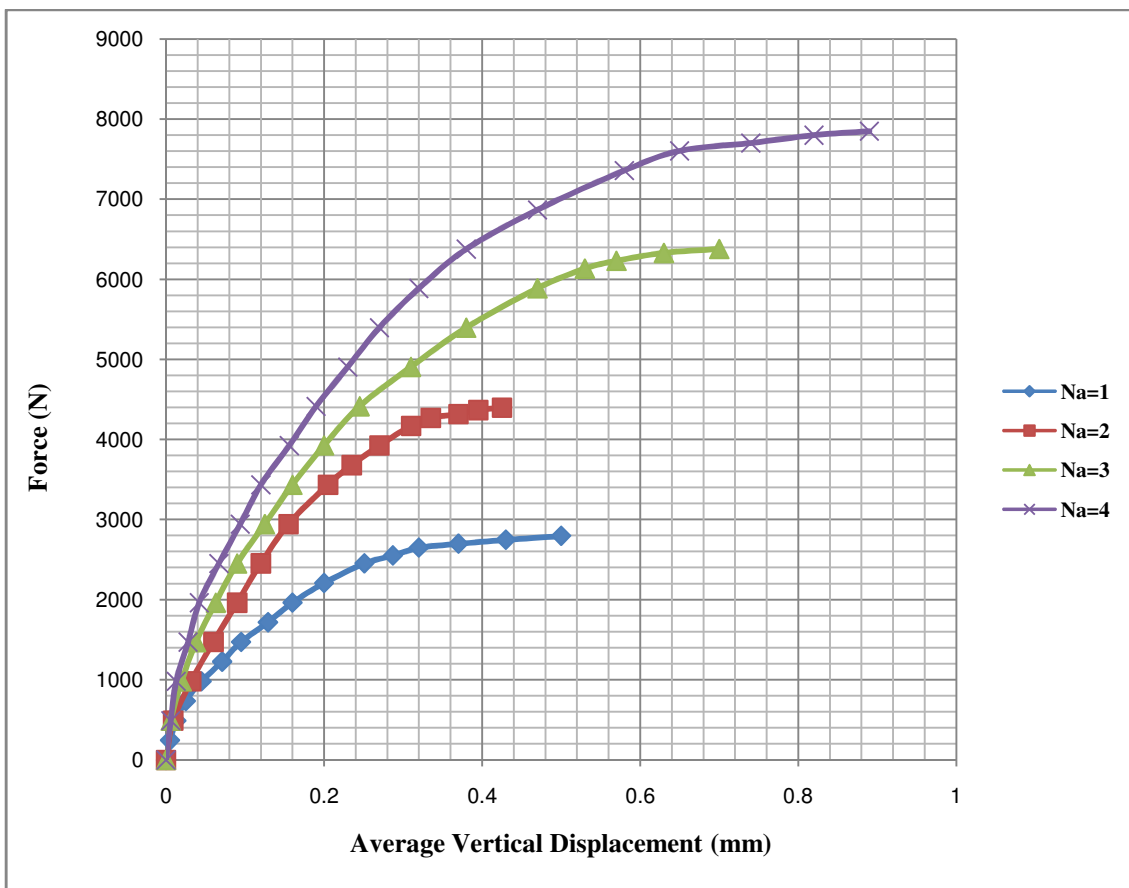


Fig. 4.1: Effect of No. of Anchors for $n_b = 3$, $H/B = 4$ and $N_a = 1, 2, 3$ & 4

4.1.2 Effect of Embedment Depth Ratio (H/B)

Fig. 4.2 displays plot of ultimate compressive load (Q_{uc}) versus deformation for H/B ratio of 2, 4, 6 & 8 maintaining anchor properties constant. It is observed that ultimate compressive capacity increases from 981 N for H/B ratio of 2 to 5150 N for H/B ratio of 8 for no. of anchors

equal to 1 and no. of screw blades in an anchor equal to 3. By using double tangent method, it is found that ultimate compressive capacity increases from 981 N to 2796 N for increase in H/B ratio from 2 to 4 whereas it increases from 3679 N to 5150 N for increase in H/B ratio from 6 to 8. Hence for initial increase in H/B (i.e. for increase in H/B from 2 to 4), the increase in Q_{uc} is 65%, while for further increase in H/B (i.e. for increase in H/B from 6 to 8); the increase in Q_{uc} is 28% which is quite less than earlier increase. Therefore, it is clear that, though ultimate compressive load increases with increase in H/B ratio, however rate of increase is higher for initial increase in H/B ratio than that of later increase in H/B ratio. This indicates that with further increase in H/B ratio, no significant gain in compressive capacity will be obtained; rather it attain a constant value or have a very insubstantial increase after some further increase in H/B ratio.

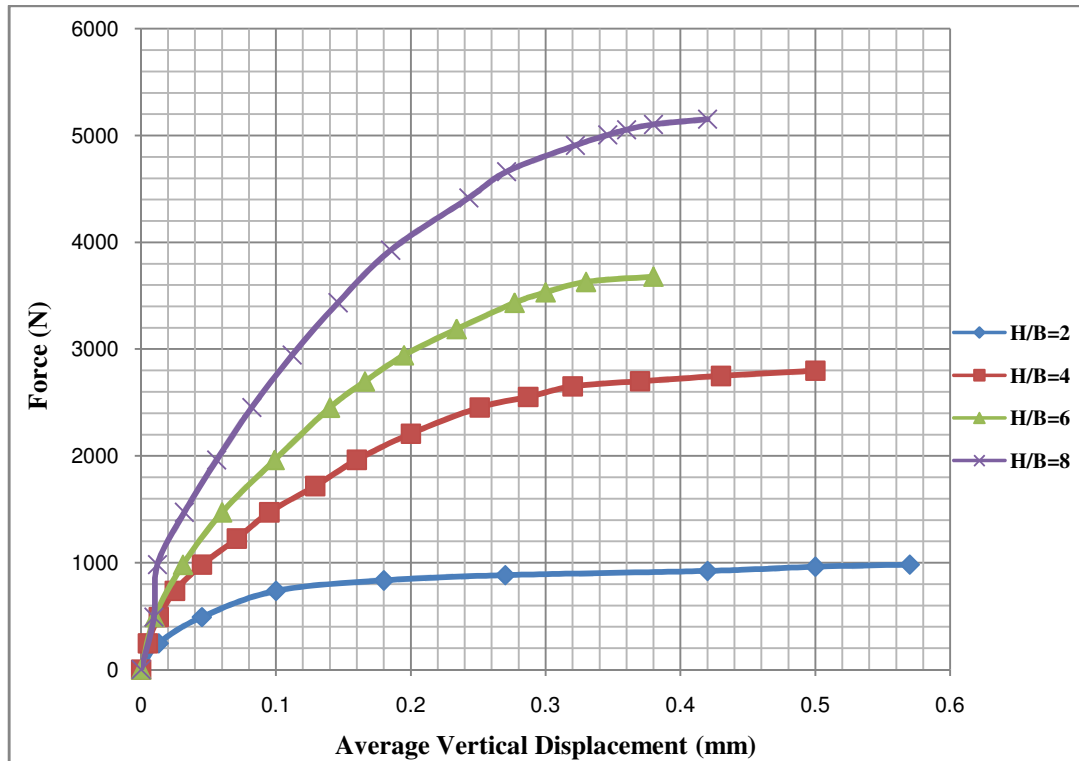


Fig. 4.2: Effect of Embedment Depth Ratio (H/B) for $n_b=3$, $N_a=1$ and H/B= 2, 4, 6 & 8

4.1.3 Effect of No. of Helical Screws Blades in Anchor (n_b)

Fig. 4.3 displays plot of ultimate compressive load (Q_{uc}) versus deformation for no. of helical screws in anchor, $n_b=1, 2$ & 3 maintaining H/B ratio constant. It is observed that with an increase in n_b , Q_{uc} increases. By using double tangent method, it is found that the ultimate

compressive capacity increases from 5346 N for $n_b=1$ to 7848 N for $n_b=3$ for embedment depth ratio H/B equal to 4 and number of anchors N_a equal to 4. The ultimate compressive capacity increases from 5346 N to 7357 N for increase in n_b from 1 to 2 whereas it increases from 7357 N to 7848 N for increase in n_b from 2 to 3. Hence for initial increase in n_b , the increase in Q_{uc} is 27% (i.e. for increase in n_b from 1 to 2), while for further increase in n_b ; the increase in Q_{uc} is 6% (i.e. for increase in n_b from 2 to 3) which is less than earlier increase. Hence it is clear that, ultimate compressive load increases very marginally with increase in no. of screws in anchors (n_b). This indicates that there is no significant change in ultimate compressive capacity with the change in the helical screws in anchor. In few of the cases, a reverse trend is also seen. However this can be attributed to an experimental error.

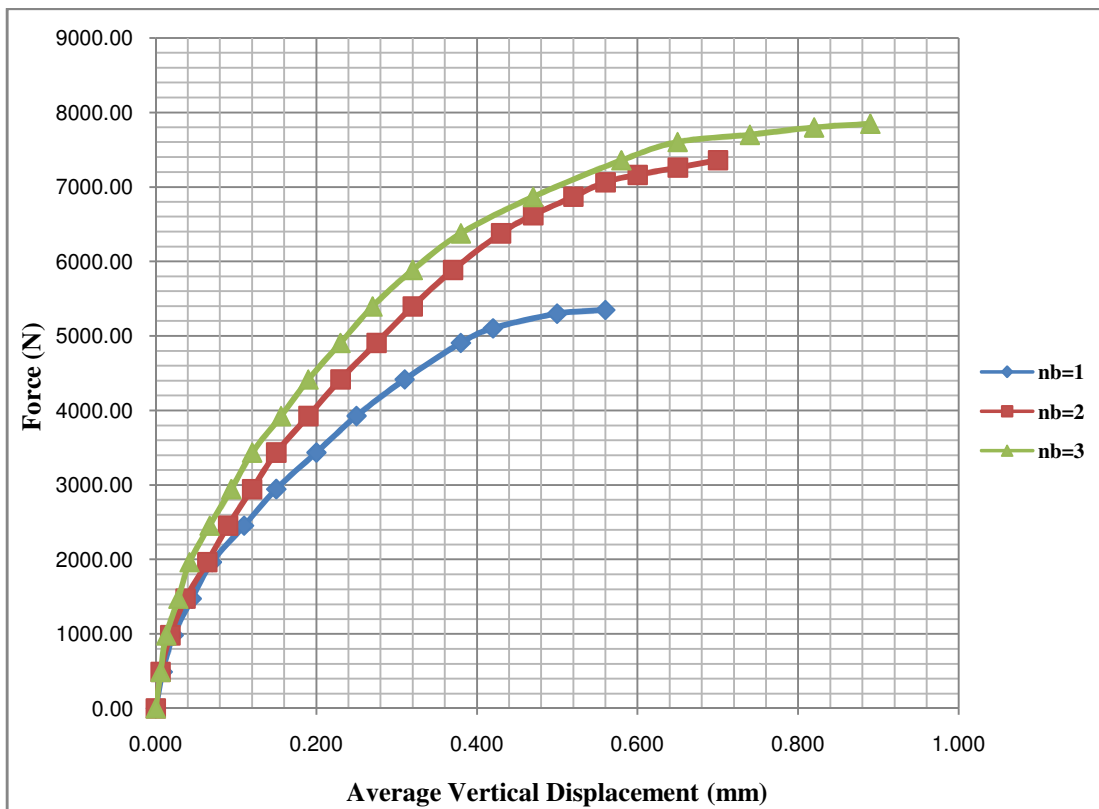


Fig. 4.3: Effect of Screw Blades in Anchors (n_b) for $N=4$, $H/B=4$ and $n_b=1, 2$ & 3

4.1.4 Ultimate Compressive Capacity of Multiple Anchors

In the present experimental investigation, the experiments were carried out on a group of 2, 3 and 4 number of anchors arranged in linear, equilateral triangle and square pattern respectively. An attempt has been made to express the ultimate compressive capacity of multiple

anchors in terms of one anchor. This is because it is relatively easy to test one anchor compared to more than one anchors either in the laboratory or in the field. Also it is much easier to analyze one anchor compared to multiple anchors. Keeping this point in mind the graphs of ultimate pullout capacity of multiple anchors with respect to single anchor have been plotted as shown in Figs. 4.5, 4.7 & 4.9 respectively.

4.1.4.1 Group of Two Anchors

The set-up of anchors for testing of two numbers of anchors at a time is shown in Fig. 4.4. Here in the figure, all the dimensions are mentioned in millimeters. Here diameter of the hole is 10 mm and the clear distance between two holes (center-to-center) is kept as $2.5 \times B$.

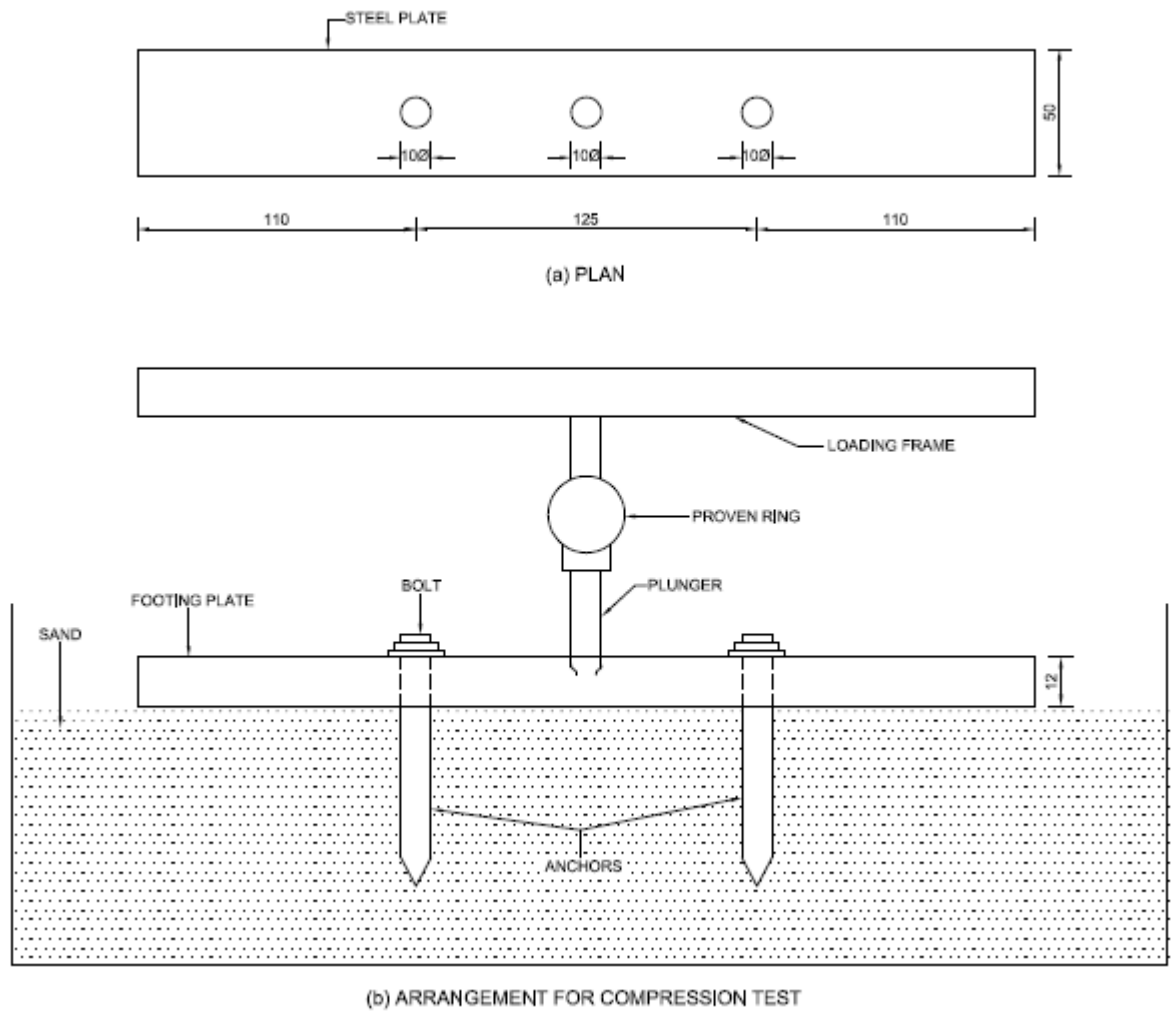


Fig. 4.4: Schematic of Compression Test for a Combination of 2 Anchors

(All Dimensions in mm)

where B is the diameter of the screw of the anchor to avoid interference of anchors on each other

The graph of ultimate compressive load of 2 anchors versus 1 anchor is shown in Fig. 4.5. The firm line (straight line) illustrates the best fit line. R² function is also mentioned in the graph, which is close to 1. Based on this curve an equation to calculate ultimate compressive load of 2 anchors with respect to 1 anchor has been proposed. The equation to calculate the ultimate compressive capacity of a group of 2 anchors, (Q_{uc})₂, comes out as

$$(Q_{uc})_2 = 3.0169(Q_{uc})_1^{0.9158} \dots\dots\dots (4.1)$$

where, (Q_{uc})₁= ultimate compressive capacity of a single anchor &
 (Q_{uc})₂=ultimate compressive capacity of a group of 2 anchors

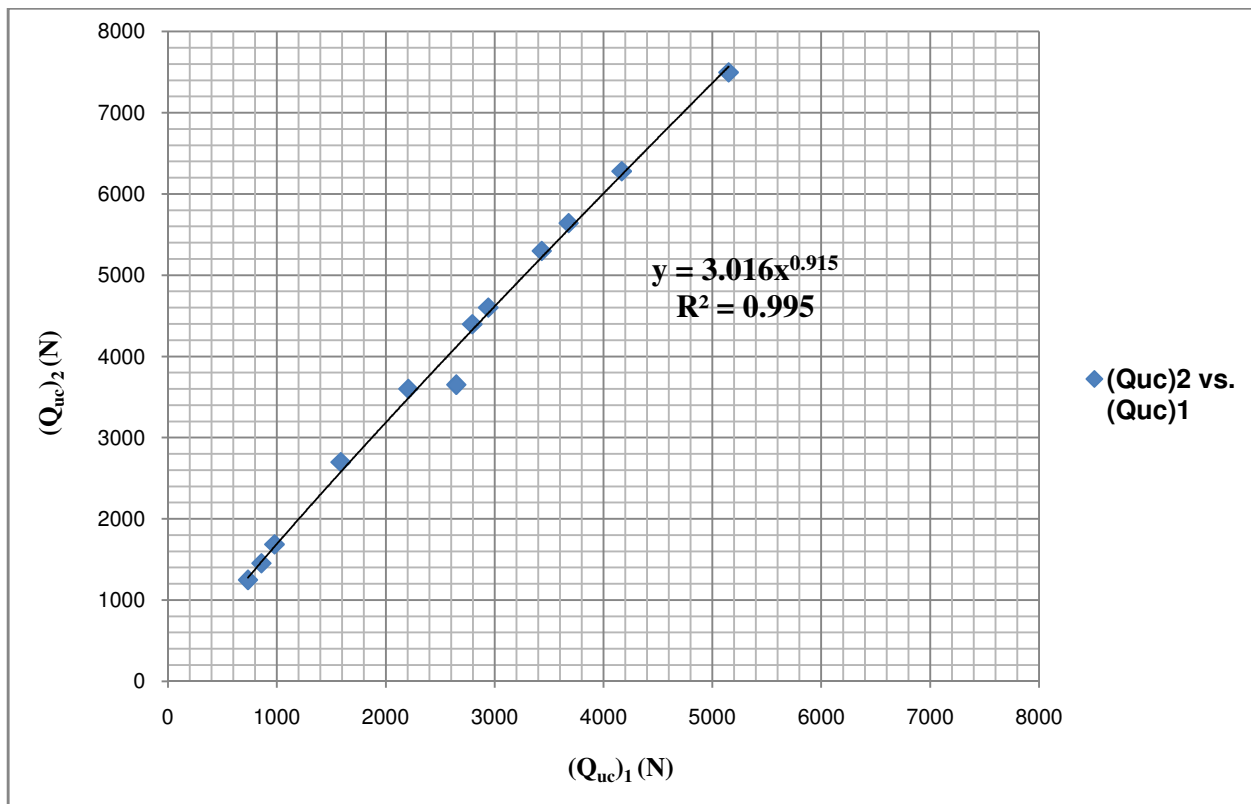


Fig. 4.5: Ultimate Compressive Capacity of 2 Anchors w.r.t. 1 Anchor

4.1.4.2 Group of Three Anchors

The set-up of anchors for testing of three numbers of anchors at a time is shown in Fig. 4.6. The graph of ultimate compressive load of 3 anchors versus 1 anchor has been plotted as shown in Fig. 4.7. Based on this curve an equation to calculate ultimate compressive load of 3 anchors with respect to 1 anchor has been proposed. The equation to calculate the ultimate compressive capacity of a group of 3 anchors, $(Q_{uc})_3$, comes out as

$$(Q_{uc})_3 = 6.3212(Q_{uc})_1^{0.8688} \dots\dots\dots(4.2)$$

where, $(Q_{uc})_1$ = ultimate compressive capacity of a single anchor &
 $(Q_{uc})_3$ = ultimate compressive capacity of a group of 3 anchors

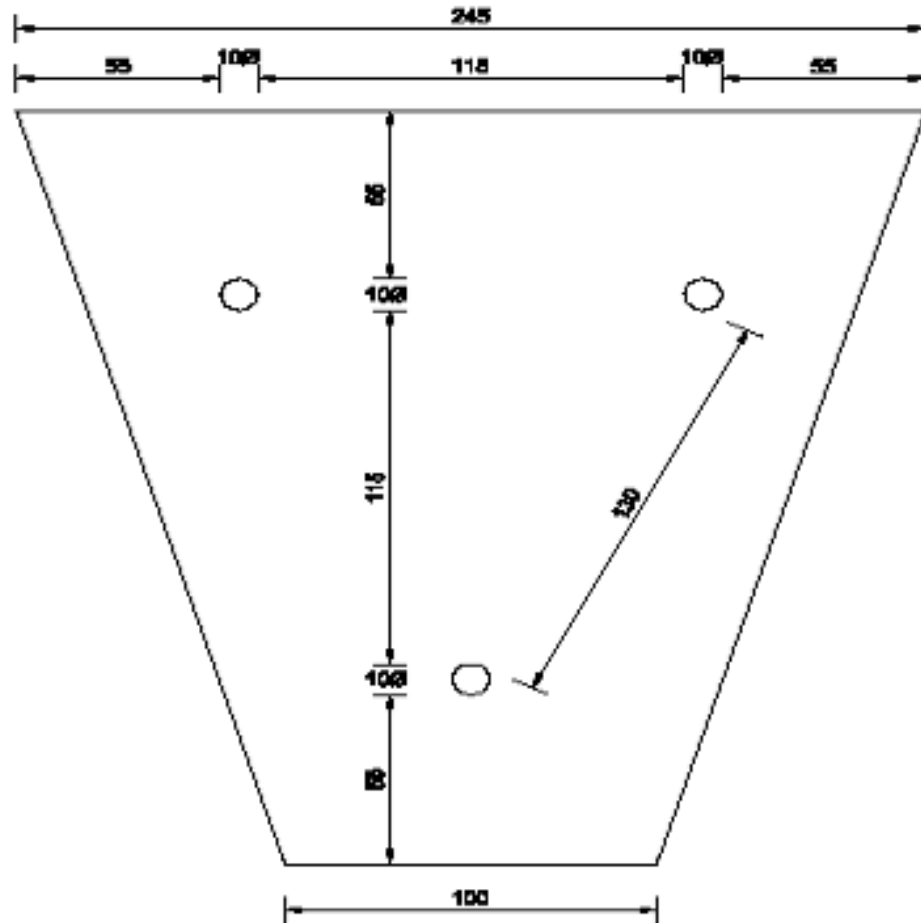


**Fig. 4.6: Arrangement for Compression Test on a Combination of 3 Anchors
 (All Dimensions in mm)**

4.1.4.3 Group of Four Anchors

The set-up of anchors for testing of four numbers of anchors at a time is shown in Fig. 4.8. The graph of ultimate compressive load of 4 anchors versus 1 anchor has been plotted as shown in Fig. 4.9. Based on this curve an equation to calculate ultimate compressive load of 4 anchors with respect to 1 anchor has been proposed. The equation to calculate the ultimate compressive capacity of a group of 4 anchors, $(Q_{uc})_4$, comes out as

$$(Q_{uc})_4 = 9.2251(Q_{uc})_1^{0.8521} \dots\dots\dots(4.3)$$

where, $(Q_{uc})_1$ = ultimate compressive capacity of a single anchor &
 $(Q_{uc})_4$ =ultimate compressive capacity of a group of 4 anchors

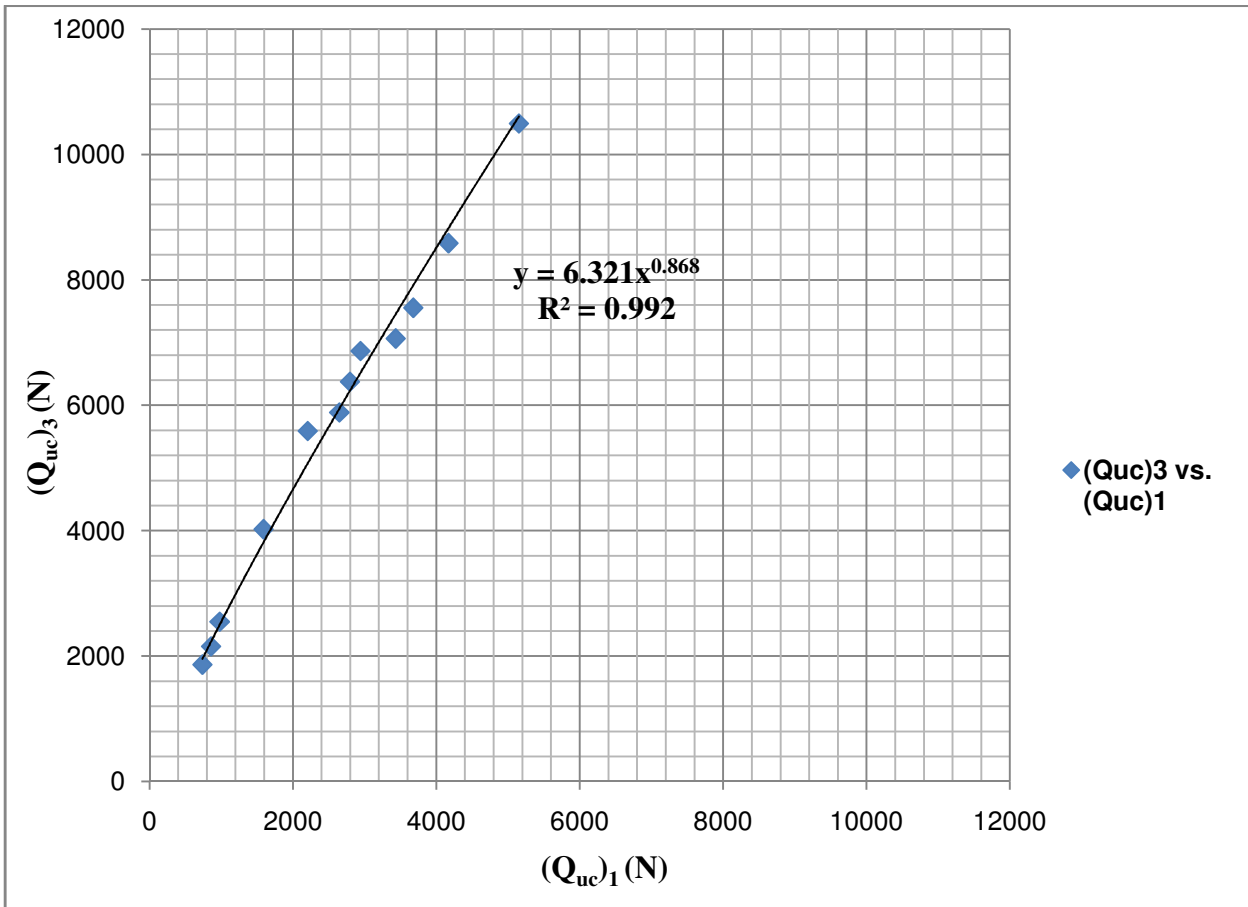
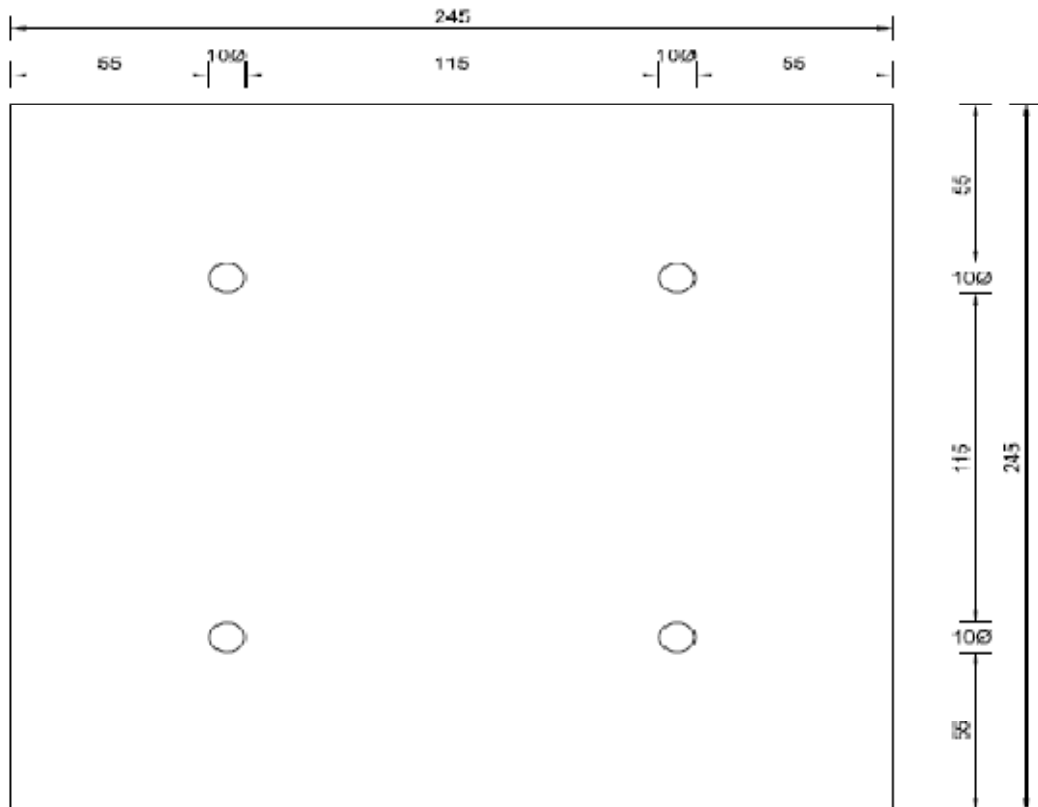


Fig. 4.7: Ultimate Compressive Capacity of 3 Anchors w.r.t. 1 Anchor

4.1.5 Generalized Equation Proposed for Multiple Helical Screw Anchors

The ultimate compressive capacity of 2, 3 and 4 no. of anchors has been expressed in terms of ultimate compressive capacity of one anchor. To achieve this, graphs of ultimate compressive capacity of 2, 3 and 4 no. of anchors vs. ultimate compressive capacity of 1 anchor have been plotted as shown in Figs. 4.5, 4.7 and 4.9 respectively. From these three graphs equations of ultimate compressive capacity of multiple anchors with respect to one anchor have been derived as shown in Equations 4.1, 4.2 and 4.3.



**Fig. 4.8: Arrangement for Compression Test on a Combination of 4 Anchors
(All Dimensions in mm)**

Because of similarity of the equations derived for 2, 3 & 4 no. of anchors w.r.t. 1 anchor, a single equation for determining ultimate compressive capacity of multiple anchors in terms of 1 anchor have been proposed.

$$(Q_{uc})_n = 2 N_a(Q_{uc})_1 \dots\dots\dots(4.4)$$

where, $(Q_{uc})_n$ = Ultimate Compressive Capacity of Multiple Anchors
 where $n = 2, 3$ and 4 in present study

$(Q_{uc})_1$ = Ultimate Compressive Capacity of 1 Anchor

N_a = No. of Anchors = 2, 3 or 4 for 2, 3 or 4 no of anchors

m = a constant whose value is proposed as 0.87

By assuming the values of m and n as mentioned above, the values of ultimate compressive capacity of 2, 3 and 4 number of helical screw anchors have been computed using Equation 4.4 as mentioned in Table 4.1.

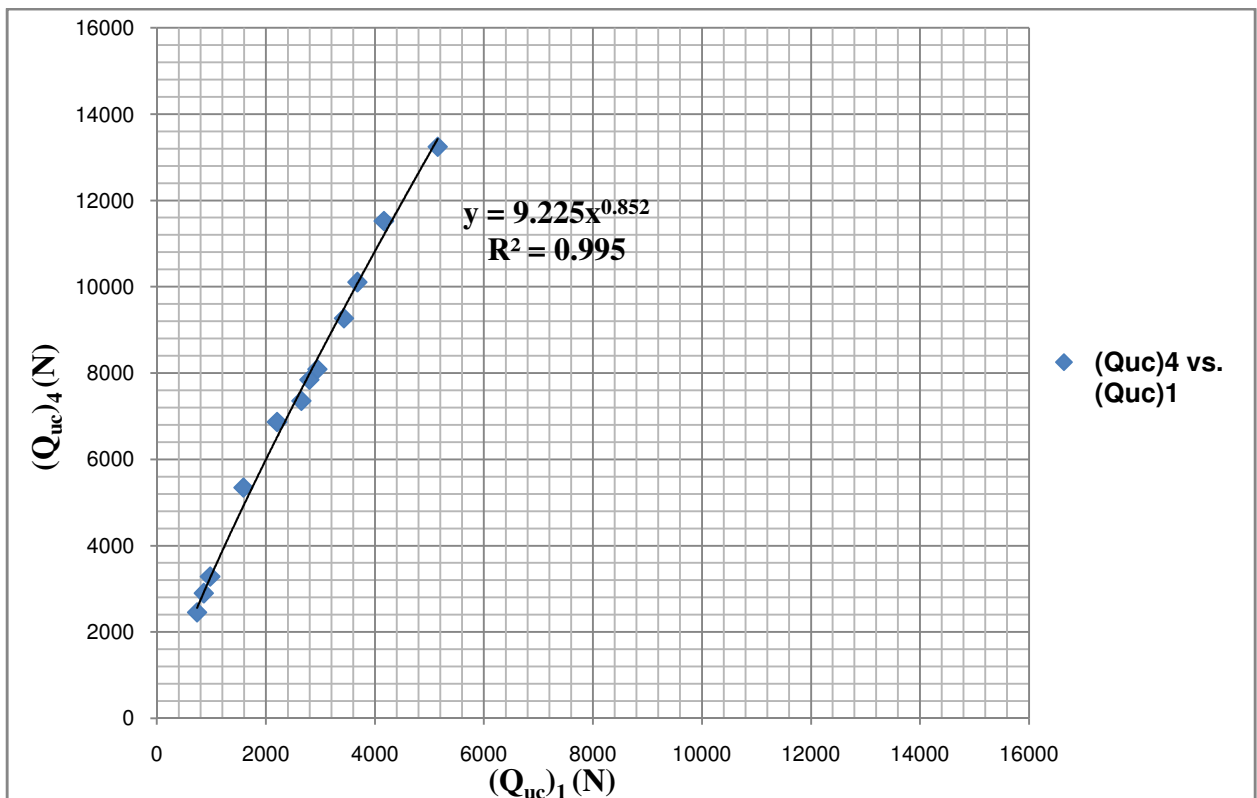


Fig. 4.9: Ultimate Compressive Capacity of 4 Anchors w.r.t. 1 Anchor

Now two sets of values of ultimate compressive capacity of 2, 3 and 4 number of helical screw anchors are available – one from the experimental investigation carried out in the laboratory, and the other from the equations proposed for multiple number of helical screw anchors. To assess the validity of proposed equation, the percentage difference between the two values have been calculated which are tabulated in Tables 4.3, 4.4 and 4.5 for 2, 3 and 4 number of anchors respectively. From these tables, it is clear that the difference between the experimental value and the value obtained from the proposed equation is within 10% only. Hence it can be said that the proposed equation calculates the ultimate compressive capacity of multiple helical screw anchors to a greater degree of satisfaction.

4.1.6 Limitations of Proposed Equation

There are several limitations of the proposed empirical equation which are listed below.

1. This is presuming that embedment depth, diameter and material of the anchor are same in all the tests.
2. All the soil properties i.e. relative density and angle of internal friction are same in all the tests.

Table 4.1: Ultimate Compressive Load of 2, 3 & 4 Anchors Based on Equation 4.4

n_b	H/B	$(Q_{uc})_2$ (N)	$(Q_{uc})_3$ (N)	$(Q_{uc})_4$ (N)
1	2	1248.08	1872.12	2496.16
1	4	2438	3657	4876
1	6	3244.64	4866.96	6489.28
1	8	4167.8	6251.7	8335.6
2	2	1426.24	2139.36	2852.48
2	4	3803.12	5704.68	7606.24
2	6	4765.36	7148.04	9530.72
2	8	5642.72	8464.08	11285.44
3	2	1602.56	2403.84	3205.12
3	4	3986.08	5979.12	7972.16
3	6	5061.08	7591.62	10122.16
3	8	6781.6	10172.4	13563.2

Table 4.2: Comparison of $(Q_{uc})_2$ from Experiments and Equation 4.4

n_b	H/B	$(Q_{uc})_2$ from Lab Exp. (N)	$(Q_{uc})_2$ from Eq. 4.4 (N)	% diff
1	2	1246	1248.08	0.16
1	4	2698	2438	9.64
1	6	3679	3244.64	9.86
1	8	4660	4167.8	9.41
2	2	1452	1426.24	1.79
2	4	3649	3803.12	4.05
2	6	5739	4765.36	10.04
2	8	7014	5642.72	10.11
3	2	1687	1602.56	5.04
3	4	4660	3986.08	9.31
3	6	6131	5061.08	10.28
3	8	8338	6781.6	9.51

Table 4.3: Comparison of $(Q_{uc})_3$ from Experiments and Equation 4.4

n_b	H/B	$(Q_{uc})_3$ from Lab Exp. (N)	$(Q_{uc})_3$ from Eq. 4.4 (N)	% diff
1	2	1864	1872.12	0.43
1	4	4022	3657	9.07
1	6	5592	4866.96	12.96
1	8	6867	6251.7	8.95
2	2	2158	2139.36	0.88
2	4	5886	5704.68	3.07
2	6	7063	7148.04	1.19
2	8	8584	8464.08	1.4
3	2	2551	2403.84	5.76
3	4	6376	5979.12	6.23
3	6	7554	7591.62	0.5
3	8	10497	10172.4	3.1

Table 4.4: Comparison of $(Q_{uc})_4$ from Experiments and Equation 4.4

n_b	H/B	$(Q_{uc})_4$ from Lab Exp. (N)	$(Q_{uc})_4$ from Eq. 4.4 (N)	% diff
1	2	2452	2496.16	1.76
1	4	5346	4876	8.79
1	6	6867	6489.28	5.5
1	8	8093	8335.6	2.91
2	2	2894	2852.48	1.45
2	4	7357	7606.24	3.27
2	6	9270	9530.72	2.74
2	8	11527	11285.44	2.1
3	2	3286	3205.12	2.46
3	4	7848	7972.16	1.55
3	6	10104	10122.16	0.18
3	8	13244	13563.2	2.35

4.1.7 Comparison of Laboratory and Empirical Values

Now two sets of values of Q_{uc} had been obtained - one from experimental investigation and the other from proposed Equation 4.4. The values of Q_{uc} from both these methods had been calculated and listed in Tables 4.3, 4.4 and 4.5. From these tables, it is clear that the difference between the ultimate compressive capacity calculated from proposed equation and the experiments done at the laboratory are minimal. Hence an anchor foundation having multiple anchors could be safely designed with the value of ultimate compressive capacity of single anchor and using Equation 4.4.

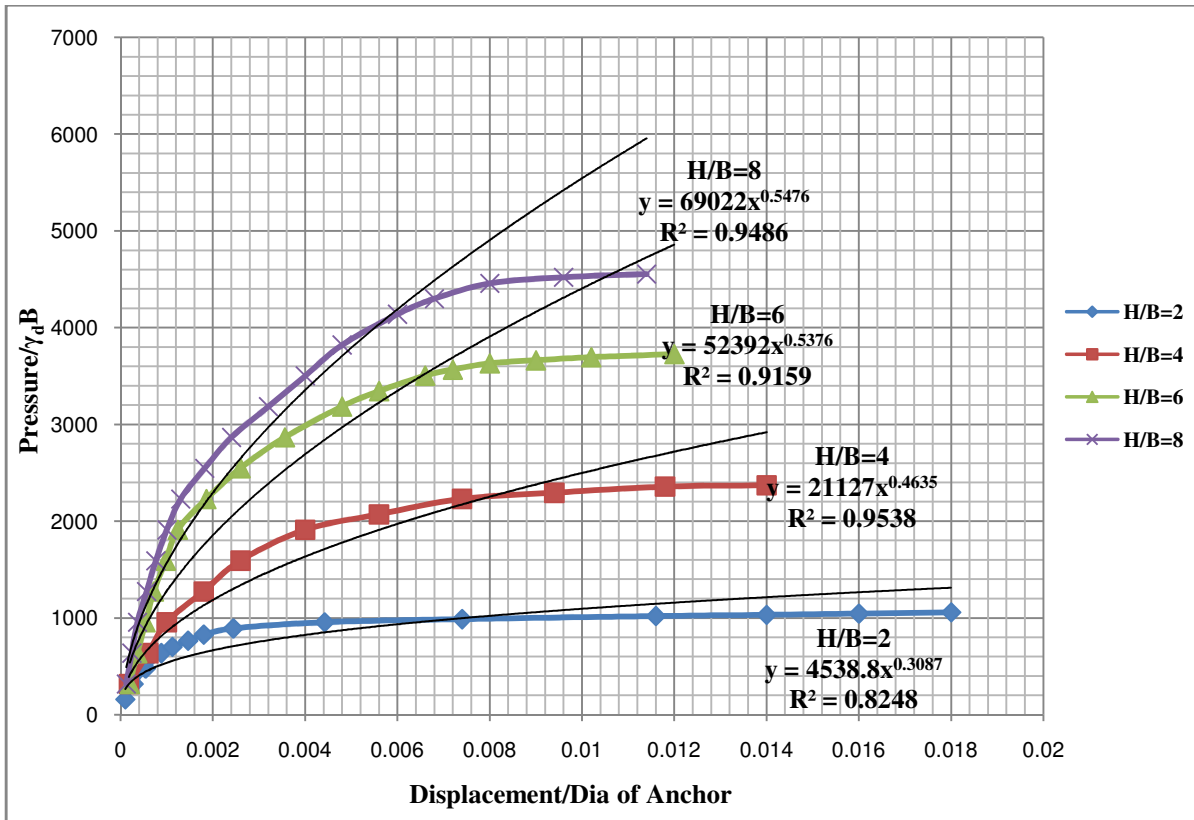


Fig. 4.10: Non-Dimensional Compression Test Graph for $N_a=2$, $n_b=2$ and $H/B=2, 4, 6$ & 8

4.1.8 Non-Dimensional Graphs and Design Considerations

To design an anchor foundation load - displacement graph in non-dimensional form is needed. The non-dimensional graphs were plotted using power functions as adopted by Kumar (2006). Similar approach had been adopted by Mittal and Mukherjee (2013). During this research work several non-dimensional graphs have been plotted. Two such graphs are shown in Figs. 4.10 and 4.11.

4.1.9 Design of Anchors using Hyperbolic Curves

The non-dimensional graphs presented above have been further normalized in hyperbolic form by dividing the load axis with the displacement axis and plotting the graph with this against the displacement axis. This rendered the graph as straight line which can be used for design purposes. All non-dimensional graphs were normalized in this way and equations of these straight lines were obtained. It was found that all the straight lines were similar in nature of the form

$$\frac{\Delta}{B} = \frac{C_1 \left(\frac{P}{\gamma B}\right)}{[1 - C_2 \left(\frac{P}{\gamma B}\right)]} \dots\dots\dots (4.5)$$

where, Δ = displacement of anchor,

B = diameter of the helical screw of the anchor,

P = load applied,

γ = unit weight of sand,

C_1 and C_2 = constants

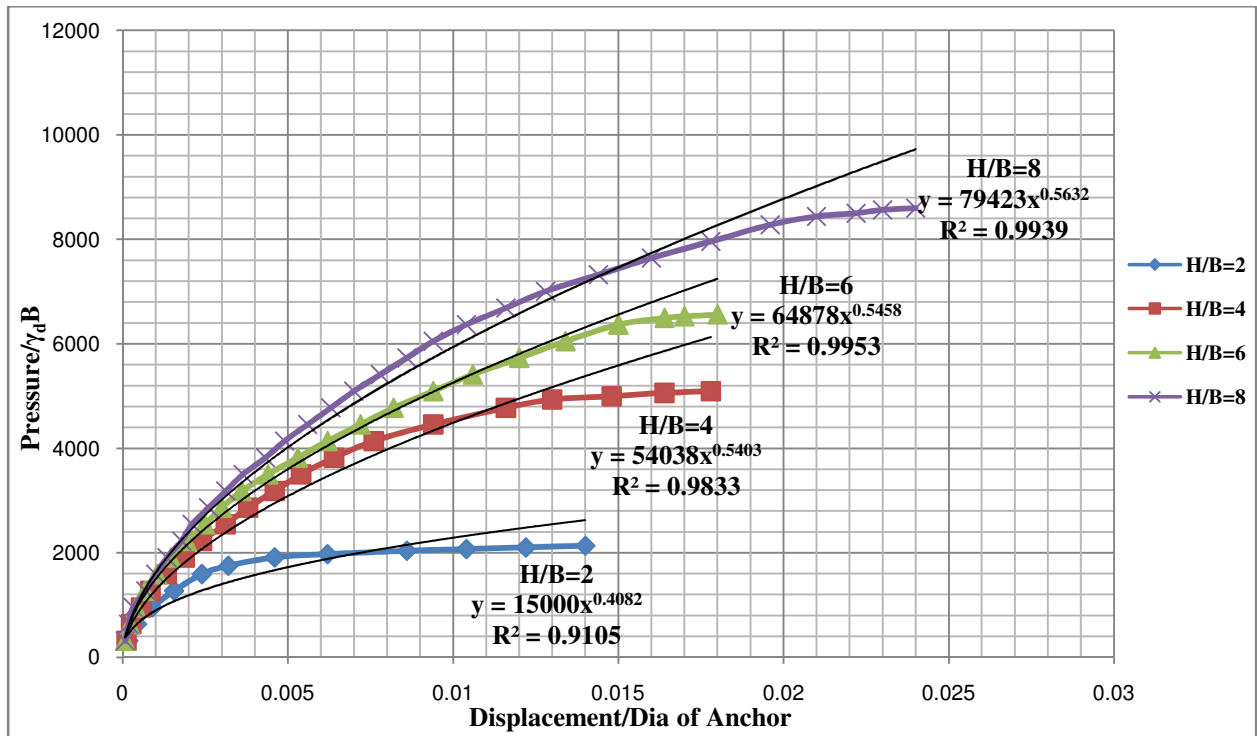


Fig. 4.11: Non-Dimensional Compression Test Graph for $N_a=4$ and $n_b= 3$ and $H/B = 2, 4, 6$ & 8

The values of these constants C_1 and C_2 have been calculated for all the tests are summarized in the Table 4.5 below. With the help of Equation 4.5 and values of constants given in Table 4.5, one can easily calculate the value of displacement/diameter of screw blade of anchor and design an anchor foundation as described in the following paragraph.

With the help of Figs. 4.12 or 4.13 an anchor foundation for a particular structure for compressive load can be easily designed. For a particular structure the values of load getting applied and acceptable deformation level will be known. A particular diameter of anchor to be used for that foundation can be assumed based on the experience and prevalent market condition. For this assumed load and diameter of the anchor, the value of (Pressure/ $\gamma_d B$) can be calculated. Using this value Deformation/Diameter of anchor can be calculated from hyperbolic equations of the curves generated as shown in the Figs. 4.12 or 4.13 and values of constants as mentioned in Table 4.5 for an assumed H/B ratio. The deformation which this particular foundation will experience can be calculated by multiplying this value with the assumed diameter of anchor. For safety purposes this deformation must be within the acceptable level of deformation.

Table 4.5: Values of Constants of Hyperbolic Equation for Compression Tests

H/B	$N_a=1$		$N_a=2$		$N_a=3$		$N_a=4$	
	C_1	C_2	C_1	C_2	C_1	C_2	C_1	C_2
$n_b=1$								
2	2×10^{-6}	0.0018	1×10^{-6}	0.0011	6×10^{-7}	0.0008	6×10^{-7}	0.0006
4	9×10^{-7}	0.0007	9×10^{-7}	0.0005	7×10^{-7}	0.0003	7×10^{-7}	0.0002
6	5×10^{-7}	0.0006	6×10^{-7}	0.0003	6×10^{-7}	0.0002	6×10^{-7}	0.0002
8	4×10^{-7}	0.0004	6×10^{-7}	0.0003	6×10^{-7}	0.0002	6×10^{-7}	0.0002
$n_b=2$								
2	2×10^{-6}	0.0017	1×10^{-6}	0.001	2×10^{-6}	0.0005	7×10^{-7}	0.0005
4	8×10^{-7}	0.0005	9×10^{-7}	0.0004	7×10^{-7}	0.0002	7×10^{-7}	0.0002
6	9×10^{-7}	0.0003	7×10^{-7}	0.0002	6×10^{-7}	0.0002	4×10^{-7}	0.0001
8	8×10^{-7}	0.0003	6×10^{-7}	0.0002	6×10^{-7}	0.0001	4×10^{-7}	0.0001
$n_b=3$								
2	1×10^{-6}	0.0015	1×10^{-6}	0.0008	5×10^{-7}	0.0006	5×10^{-7}	0.0004
4	9×10^{-7}	0.0005	8×10^{-7}	0.0002	7×10^{-7}	0.0002	6×10^{-7}	0.0002
6	8×10^{-7}	0.0003	4×10^{-7}	0.0002	6×10^{-7}	0.0002	6×10^{-7}	0.0001
8	6×10^{-7}	0.0002	3×10^{-7}	0.0002	6×10^{-7}	0.0001	6×10^{-7}	0.0009

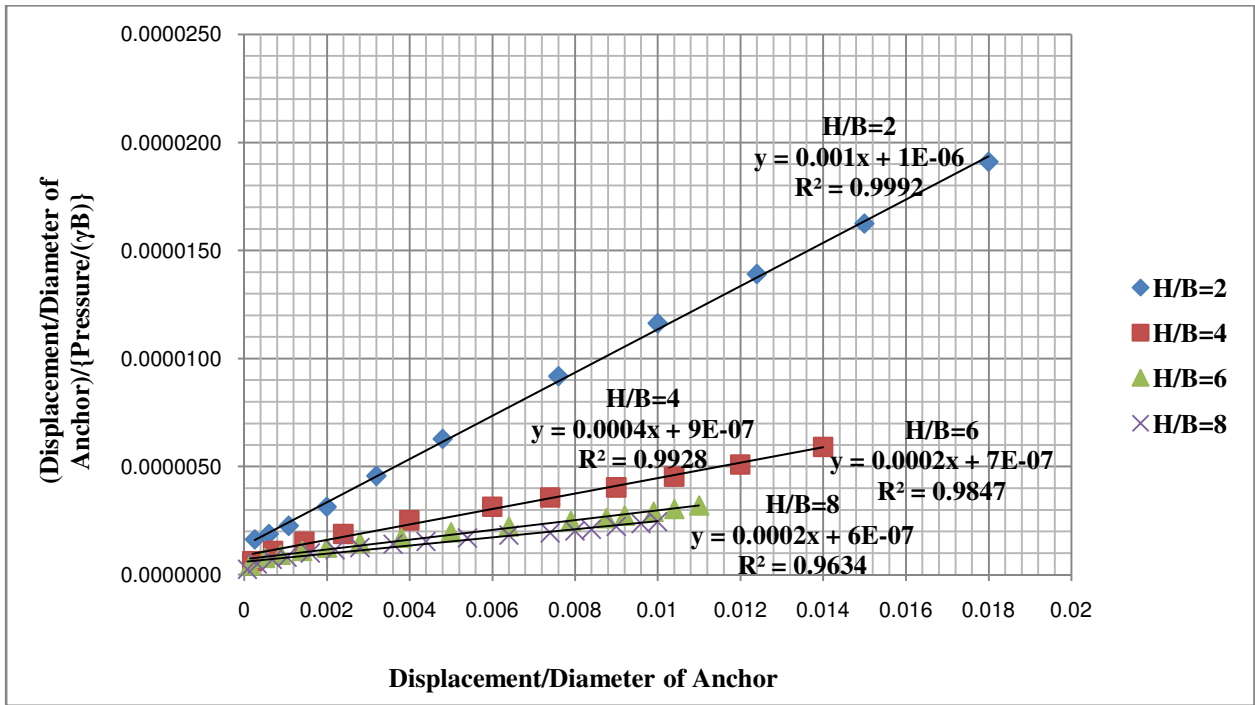


Fig. 4.12: Hyperbolic Curve for 2 Nos. of Double Helical Screw Anchors for Compression Tests

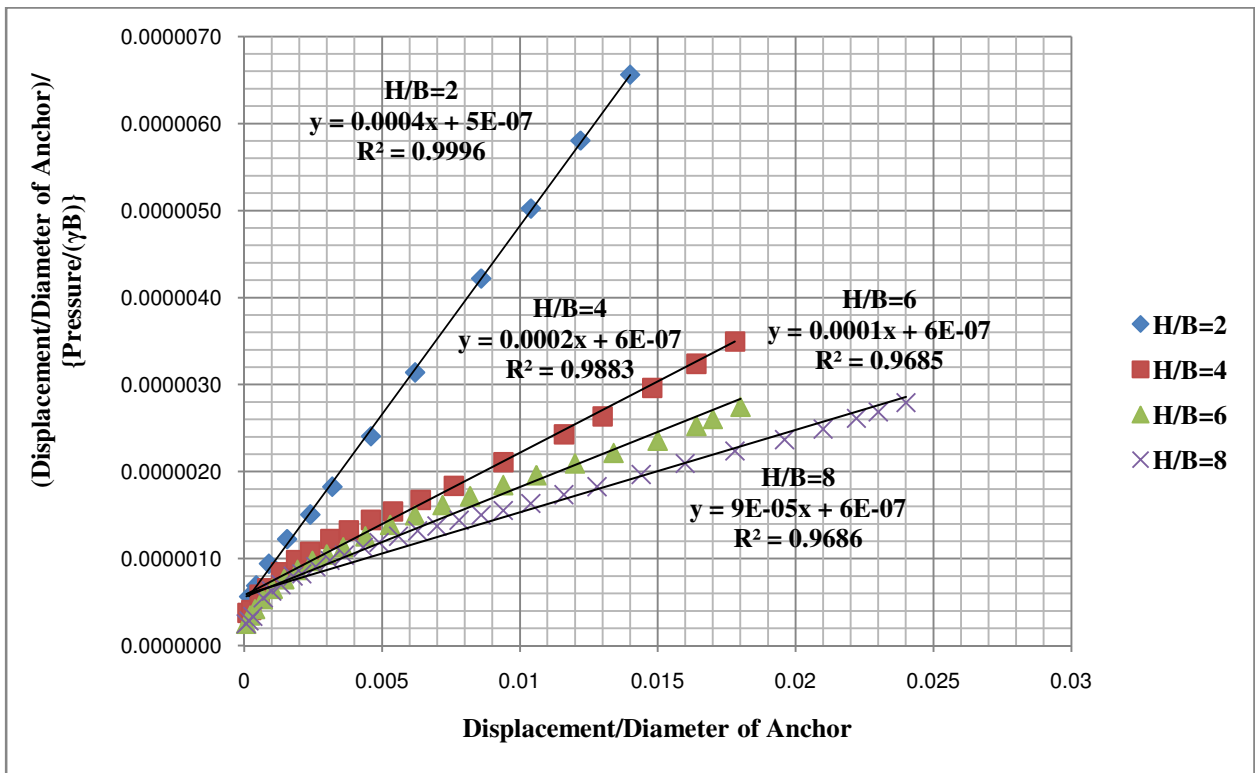


Fig. 4.13: Hyperbolic Curve for 4 Nos. of Triple Helical Screw Anchors for Compression Tests

4.1.10 Parametric Study

4.1.10.1 Increase in the Value of Apparent Coefficient of Friction (f^*)

Apparent coefficient of friction between the anchor and the soil (f^*) plays an important role in determining the strength of anchors. This is a very important parameter in the design of anchor as the force transfer from anchor to soil is through the friction mobilized at the interface. Value of f^* calculated from compression tests are tabulated in Table 4.6.

The compressive resistance is defined as the force mobilized along the length of the anchor which lies beyond the failure surface when an assumed failure surface cuts a layer of soil anchor. From the load deflection curve obtained from conducting compression test, the compressive load responsible for failure is computed from Equation 4.4. From this failure load the apparent coefficient of friction is determined as follows.

$$f^* = \frac{P}{\{\pi BL(\gamma_d z + q)\}} \dots\dots\dots (4.6)$$

where, f^* is the apparent coefficient of friction, P is the failure load, B is the diameter of screw blade of the anchor, L is the embedded length of the anchor, γ_d is the dry unit weight of soil, z is the depth of the sand fill above the screw of the anchor and q is surcharge intensity, if any.

Compressive resistance of the anchor or value of apparent coefficient of friction is influenced by several factors such as properties of soil, roughness and stiffness of the anchor, boundary conditions of the test, diameter and length of the anchor and normal stress acting on the anchor.

4.1.11 Design Example

Problem: Design a helical screw anchor to withstand compressive load of 200 kN by using present methodology.

The soil properties are as follows:

$c = 0$, $\Phi = 38^\circ$, $\gamma_d = 15.7 \text{ kN/m}^3$, Classification of soil is SP.

Solution: Given, proposed compressive load, Q = 200 kN

Assuming acceptable deformation of the structure = 8 mm

Designing this anchor system for two and four number of anchors:

Table 4.6: Values of f^* for Compression Tests

n_b	H/B	f^*			
		$N_a=1$	$N_a=2$	$N_a=3$	$N_a=4$
1	2	10.98	9.09	9.09	8.98
1	4	9.18	7.66	7.62	7.59
1	6	6.73	5.51	5.58	5.14
1	8	5.52	4.29	4.21	3.73
2	2	13.84	11.62	11.48	11.67
2	4	15.96	10.86	11.68	10.95
2	6	10.79	8.88	7.29	7.17
2	8	8	6.64	5.42	5.46
3	2	16.91	14.3	14.49	13.92
3	4	17.58	14.38	13.12	12.11
3	6	11.91	9.73	7.99	8.02
3	8	10.12	8.05	6.75	6.39

(A) If 2 numbers of anchors can be used as a group, then assuming anchor diameter as 200mm

Cross sectional area of each anchor, $A = 0.0314 \text{ m}^2$

Since design load is 200 kN, hence pressure,

$$P = 200 / 0.0314 = 6369.43 \text{ kN/m}^2$$

$$\text{Therefore, } \frac{P}{\gamma B} = \frac{6369.43}{15.7 \times 0.2} = 2028.48$$

For $H/B = 4$ and $n_b = 2$ (i.e. for Double Helical Screw Anchor), from Fig. 4.10, the hyperbolic equation is

$$\begin{aligned} \frac{\delta}{B} &= \frac{0.0000009 * \frac{P}{\gamma B}}{1 - 0.0004 * \frac{P}{\gamma B}} \\ &= \frac{0.0000009 * 2028.48}{1 - (0.0004 * 2028.48)} \\ &= 0.00968 \end{aligned}$$

Deformation/diameter of anchor = 0.00968

Therefore, System Deformation = 0.00968 x 200 = 1.936 mm < 8 mm

which is within acceptable level of deformation

Hence this system can be designed with 2 nos. of double helical screw anchor having diameter of screws as 200 mm installed at H/B = 4 i.e. at 0.8 m below the soil surface.

(B) If 4 numbers of anchors can be used as a group, then assuming anchor diameter as 200 mm.

Cross sectional area of each anchor, $A = 0.0314 \text{ m}^2$

Since design load is 200 kN, hence pressure,

$$P = 200 / 0.0314 = 6369.43 \text{ kN/m}^2$$

$$\text{Therefore, } \frac{P}{\gamma B} = \frac{6369.43}{15.7 * 0.2} = 2028.48$$

For H/B = 2 and $n_b = 3$ (i.e. for Triple Helical Screw Anchor), from Fig. 4.11, the hyperbolic equation is

$$\begin{aligned} \frac{\delta}{B} &= \frac{0.0000005 * \frac{P}{\gamma B}}{1 - 0.0004 * \frac{P}{\gamma B}} \\ &= \frac{0.0000005 * 2028.48}{1 - (0.0004 * 2028.48)} \\ &= 0.00125 \end{aligned}$$

Deformation/diameter of anchor = 0.00125

Therefore, System Deformation = 0.00125 x 200 = 0.25 mm < 8 mm

which is within acceptable level of deformation

Hence this system can be designed with 4 nos. of triple helical screw anchor having diameter of screws as 200 mm installed at $H/B = 2$ i.e. at 0.4 m below the soil surface.

4.2 DISCUSSION ON PULLOUT TEST RESULTS

Like compression tests, the pullout tests were also conducted to study the effect of parameters like number of helical blades (n_b), installation depth (H) and number of anchors (N_a) in a group. Displacement readings were taken with every increment of load to get load vs. displacement curves. It was observed that with increase in pullout load, rate of increase in displacement increases till it fails. Loads were applied until a relative displacement of 10% of the helix diameter was achieved or the anchors failed by rapid pull-out, whichever occurred first.

4.2.1 Effect of No. of Anchors (N_a)

Fig. 4.14 displays a typical plot of ultimate pullout load versus deformation for no. of helical anchors of 1, 2, 3 and 4 maintaining anchor properties and embedment depth constant. Fig. 4.14 displays the result for no. of screw blades in anchor $n_b=3$, H/B ratio of 4 and no. of anchors $N_a=1, 2, 3$ & 4.

By using double tangent method, it is found that the ultimate pullout capacity increases from 132 N for $N_a=1$ to 441 N for $N_a=4$ for double helical screw anchor for embedment depth ratio equal to 4. This increase is from 132 N to 245 N for $N_a=1$ to $N_a=2$ whereas from 319 N to 441 N for $N_a=3$ to $N_a=4$. Hence for initial increase in N_a , the increase in Q is 46%, while for further increase in N_a the increase in Q is 27% which is quite less than earlier increase. Hence it is clear that, though ultimate pullout load increases with increase in no. of anchors (N_a), however rate of increase is higher for initial increase in N_a than that of later increase in N_a . This indicates that with further increase in N_a , no significant gain in pullout capacity will be obtained; rather it attains a constant value or has a very insubstantial increase after some further increase in N_a .

4.2.2 Effect of Embedment Depth Ratio (H/B)

Two distinct categories of anchors have been identified on the basis of their embedment depth. These are shallow and deep anchors. In the former the anchor is installed close to the surface of the soil, and the failure surface in the soil extends from the tip of the anchor to the ground surface with significant surface movements. An increase in depth of embedment results

in another type of failure in which the failure surface does not extend to the surface but instead forms locally around the anchor. This type of failure exemplifies the deep anchor mode.

Fig. 4.15 displays plot of ultimate pullout load (Q_{up}) versus deformation for H/B ratio of 4, 6, 8 & 10 maintaining anchor properties constant. Fig. 4.15 displays the result for no. of screw blades in anchor $n_b=3$, no. of anchors $N_a=4$ and H/B ratio = 4, 6, 8 and 10. By using double tangent method, it is found that the ultimate pullout capacity increase from 441 N to 5837 N for increase in H/B ratio from 4 to 10. This increase in Q is from 441 N to 1619 N for increase in H/B from 4 to 6 and from 3679 N to 5837 N for increase in H/B from 8 to 10. Hence for initial increase in N_a , the increase in Q_{up} is 73%, while for further increase in N_a the increase in Q_{up} is 37% which is quite less than earlier increase. Hence it is clear that, though ultimate pullout load increases with increase in depth ratio, however rate of increase is higher for initial increase in H/B than that of later increase in H/B.

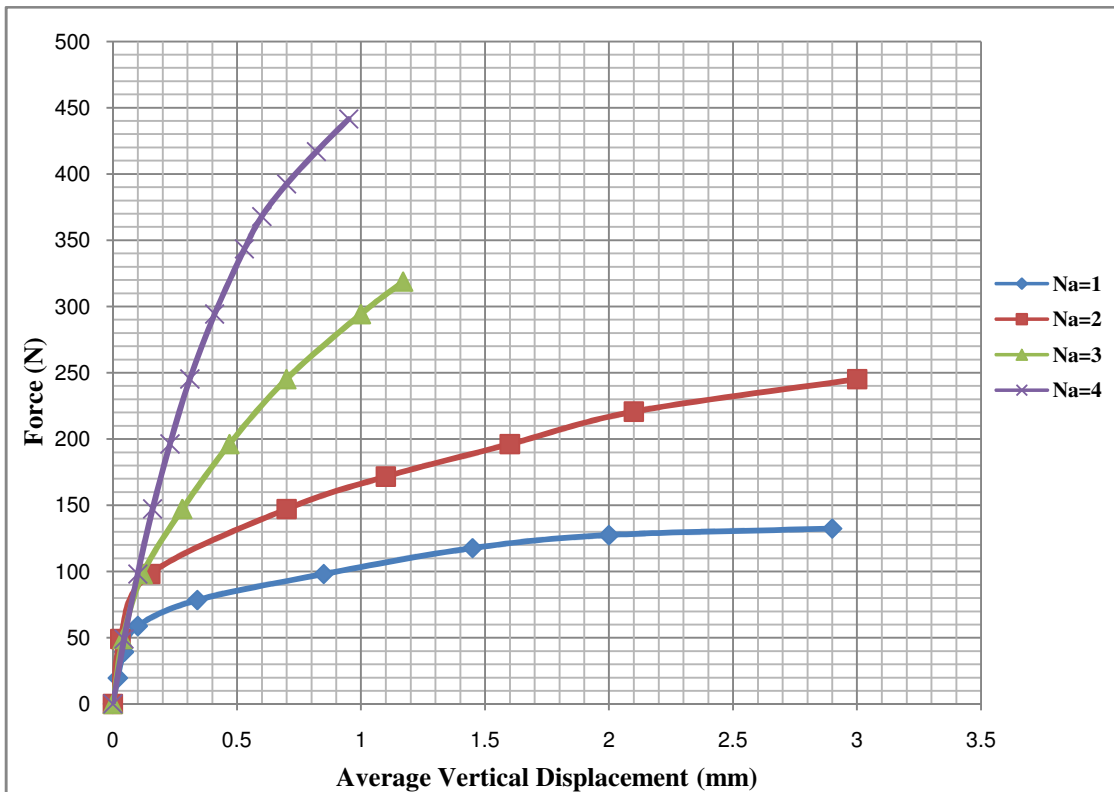


Fig. 4.14: Pullout Test Graph for $n_b=2$, H/B=6 and $N_a=1, 2, 3$ & 4

This indicates that with further increase in installation depth, no significant gain in pullout capacity will be obtained; rather it attains a constant value or has a very insubstantial increase after some further increase in installation depth.

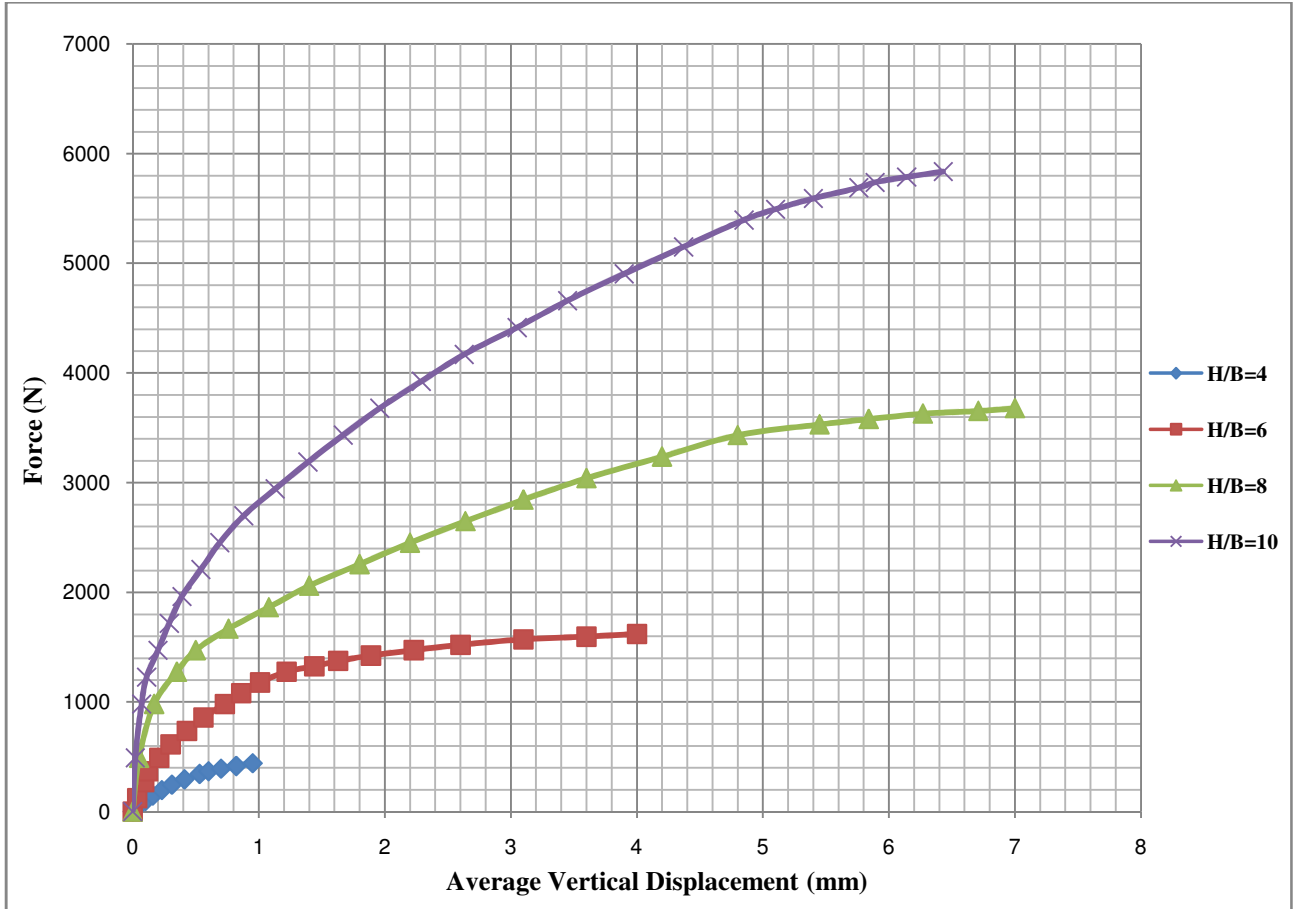


Fig. 4.15: Pullout Test Graph for $n_b = 3$, $N_a = 4$ and $H/B = 4, 6, 8$ & 10

4.2.3 Effect of No. of Helical Screw Blades in Anchor (n_b)

Fig. 4.16 displays plot of ultimate pullout load versus deformation for no. of helical screws in anchor, $n_b=1, 2$ and 3 maintaining H/B ratio and no. of anchors constant. Fig. 4.16 displays the result for no. of anchors $N_a=2$, H/B ratio = 10 and no. of screw blades in anchor $n_b = 1, 2$ and 3 . It is observed that with an increase in n_b , Q_{up} increases. In general this increase in pullout capacity is more for initial increase in no. of helical blades (n_b), than for subsequent increase in no. of helical blades but with a less amount.

By using double tangent method, it is found that the increase in ultimate pullout capacity is from 2158 N to 3188 N for increase in n_b from 1 to 3 . This increase in Q_{up} is from 2158 N to

2796 N for increase in n_b from 1 to 2 and from 2796 N to 3188 N for increase in n_b from 2 to 3. Hence for initial increase in n_b , the increase in Q_{up} is 22.82%, while for further increase in n_b the increase in Q_{up} is 12.29% which is minimal. Hence it can be argued that number of screw blades does not have much significance in the load carrying capacity of anchor.

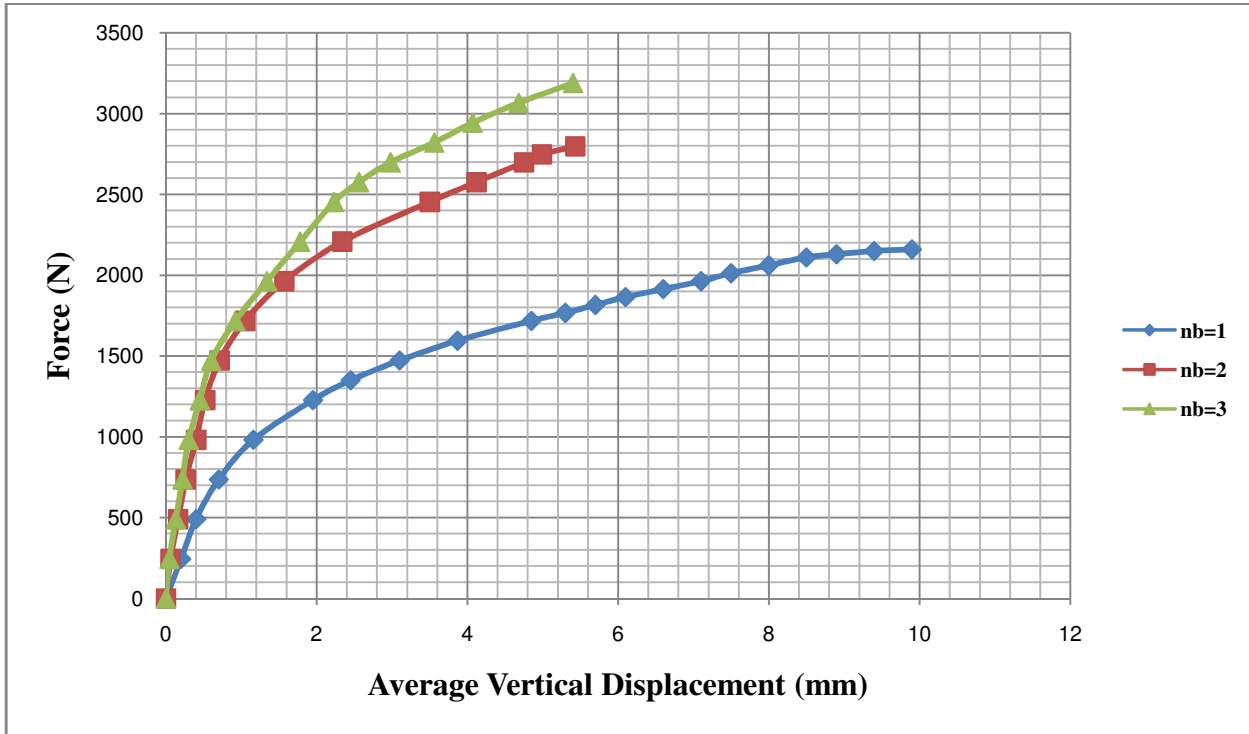


Fig. 4.16: Pull-out Test Graph for $N_a = 2$, $H/B = 10$ and $n_b = 1, 2 \text{ \& } 3$

4.2.4 Ultimate Pullout Capacity of Multiple Anchors

Similar to compression testing, in pullout testing also experiments were carried out on a group of 2, 3 and 4 number of anchors arranged in linear, equilateral triangle and square pattern respectively. An attempt has been made to express the ultimate pullout capacity of multiple anchors in terms of one anchor. The diagrammatic representation of these tests for compression tests has been given in Section 4.1.4 of this thesis. For pullout tests also these details are the same. Hence they have not been repeated here. The graphs of ultimate pullout capacity of multiple anchors with respect to single anchor have been plotted as shown in Figs. 4.17, 4.18 and 4.19 respectively.

4.2.4.1 Group of Two Anchors

The set-up of anchors for testing of two numbers of anchors at a time is shown in Fig. 4.4. The graph of ultimate pullout load of 2 anchors versus 1 anchor is shown in Fig. 4.17.

Based on this curve an equation to calculate ultimate compressive load of 2 anchors with respect to 1 anchor is proposed. The equation to calculate the ultimate compressive capacity of a group of 2 anchors, $(Q_{up})_2$, comes out as

$$(Q_{up})_2 = 2.2113 (Q_{up})_1^{0.9281} \dots\dots\dots (4.7)$$

where, $(Q_{up})_1$ = ultimate pullout capacity of 1 anchor &

$(Q_{up})_2$ = ultimate pullout capacity of 2 anchors

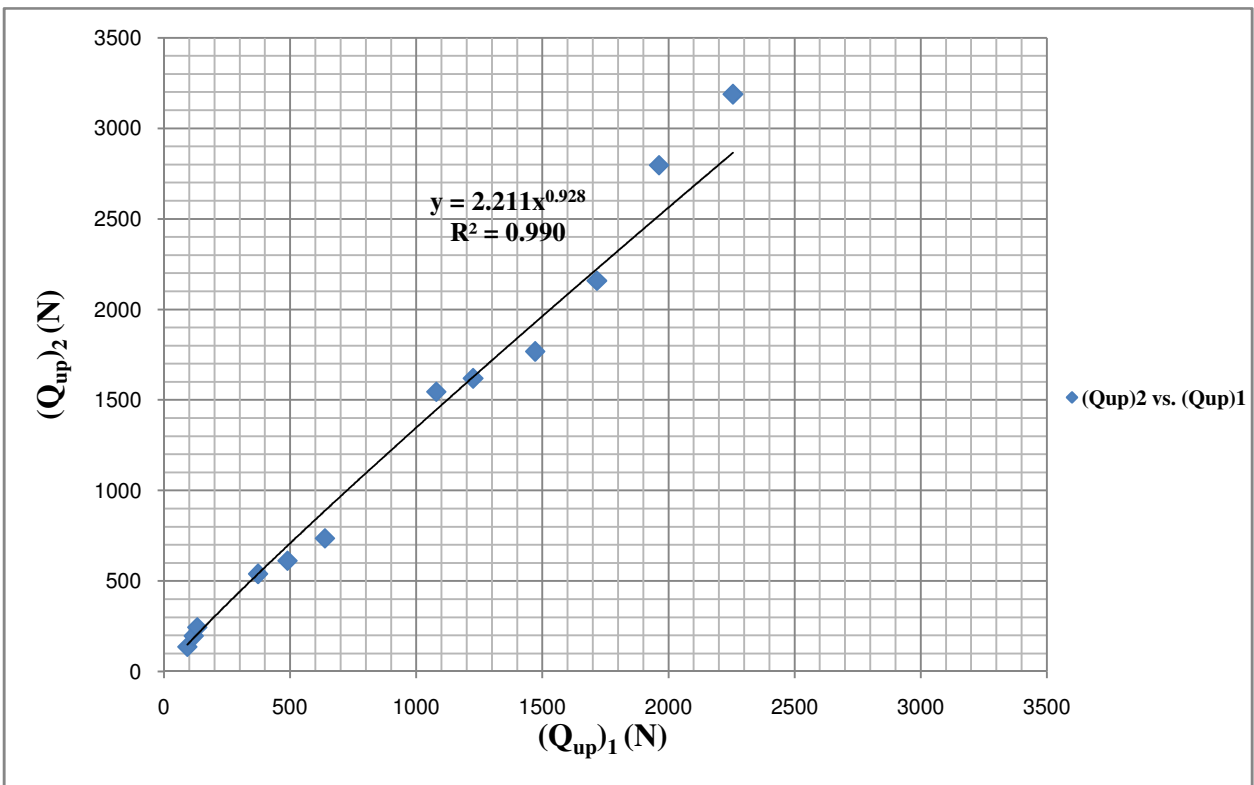


Fig. 4.17: Ultimate Pullout Capacity of 2 Anchors w.r.t. 1 Anchor

4.2.4.2 Group of Three Anchors

The set-up of anchors for testing of three numbers of anchors at a time is shown in Fig. 4.6. The graph of ultimate pullout load of 3 anchors versus 1 anchor was plotted as shown in Fig.

4.18. Based on this curve an equation to calculate ultimate compressive load of 3 anchors with respect to 1 anchor is proposed. The equation to calculate the ultimate compressive capacity of a group of 3 anchors, $(Q_{up})_3$, comes out as

$$(Q_{up})_3 = 2.8525 (Q_{up})_1^{0.9482} \dots\dots\dots (4.8)$$

where, $(Q_{up})_1$ = ultimate pullout capacity of 1 anchor &

$(Q_{up})_3$ = ultimate pullout capacity of 3 anchors

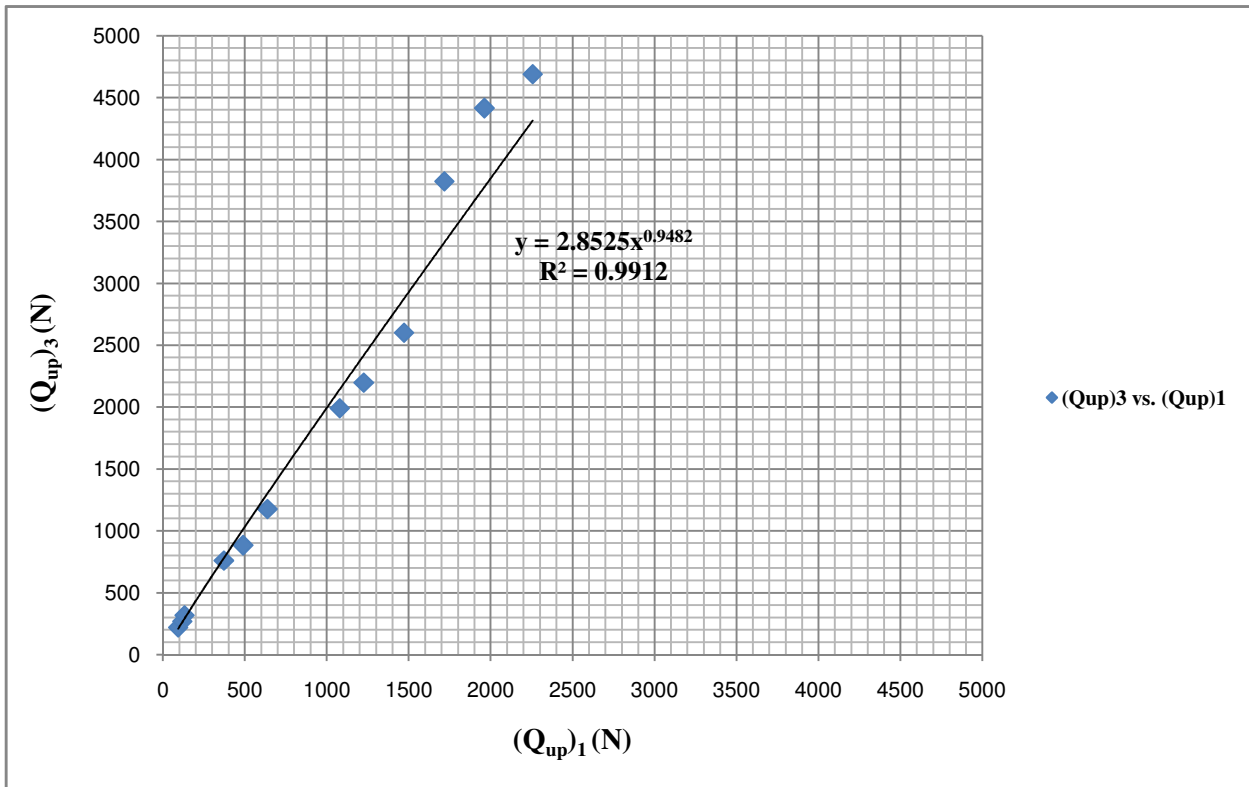


Fig. 4.18: Ultimate Pullout Capacity of 3 Anchors w.r.t. 1 Anchor

4.2.4.3 Group of Four Anchors

The set-up of anchors for testing of four numbers of anchors at a time is shown in Fig. 4.8. The graph of ultimate pullout load of 4 anchors versus 1 anchor was plotted as shown in Fig. 4.19. Based on this curve an equation to calculate ultimate pullout load of 4 anchors with respect to 1 anchor is proposed. The equation to calculate the ultimate pullout capacity of a group of 4 anchors, $(Q_{up})_4$, comes out as

$$(Q_{up})_4 = 4.6658 (Q_{up})_1^{0.9168} \dots\dots\dots (4.9)$$

where, $(Q_{up})_1$ = ultimate pullout capacity of 1 anchor &
 $(Q_{up})_4$ = ultimate pullout capacity of 4 anchors

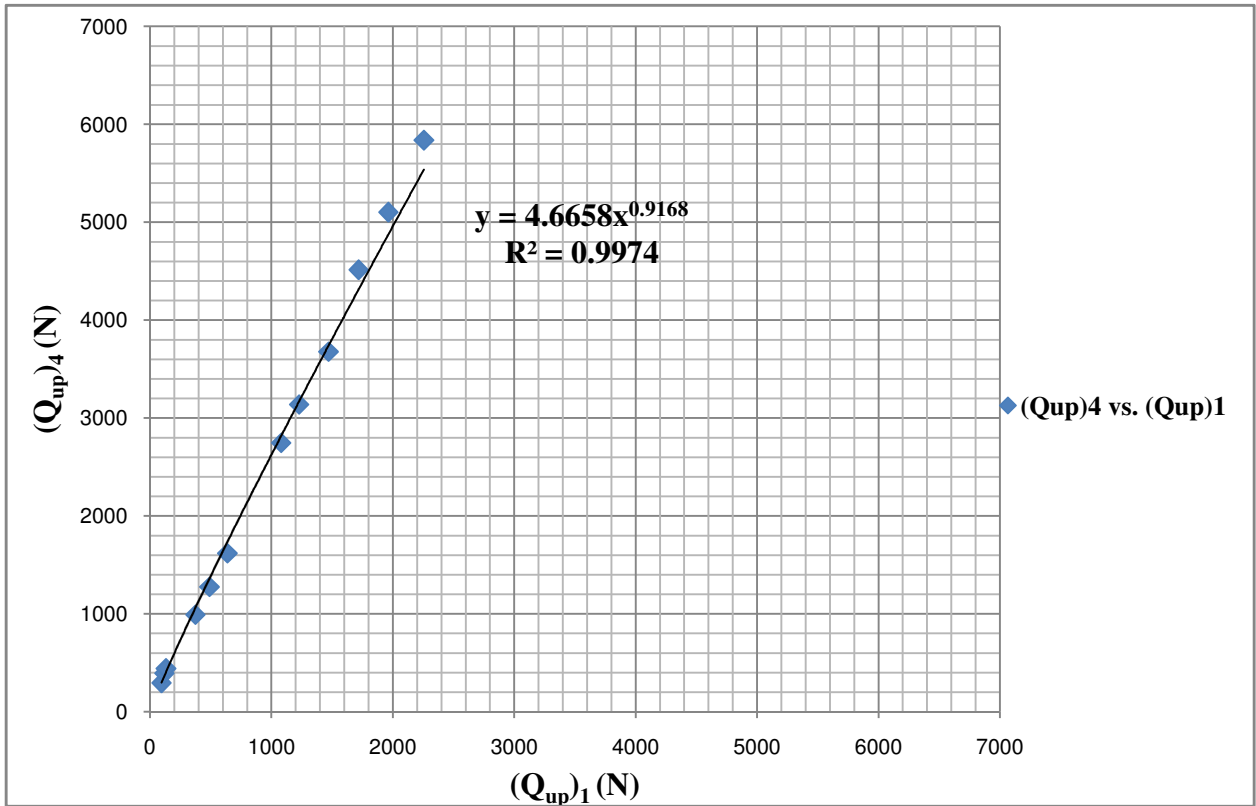


Fig. 4.19: Ultimate Pullout Capacity of 4 Anchors w.r.t. 1 Anchor

4.2.5 Generalized Equation Proposed for Multiple Helical Screw Anchors

The ultimate pullout capacity of 2, 3 and 4 no. of anchors has been expressed in terms of ultimate pullout capacity of one anchor. The graphs of ultimate pullout capacity of 2, 3 and 4 no. of anchors vs. ultimate pullout capacity of 1 anchor have been plotted as shown in Figs. 4.17, 4.18 and 4.19 respectively. From these three graphs equations of ultimate compressive capacity of multiple anchors with respect to one anchor have been derived as shown in Equations 4.7, 4.8 and 4.9.

Because of similarity of the above equations, a single equation has been proposed for determining ultimate pullout capacity of multiple anchors in terms of 1 anchor.

$$(Q_{up})_n = N_a(Q_{up})_1^m \dots\dots\dots (4.10)$$

where, $(Q_{up})_n$ = Ultimate Pullout Capacity of Multiple Anchors

where $n = 2, 3 \text{ \& } 4$ in our study

$(Q_{up})_1$ = Ultimate Pullout capacity of 1 Anchor

N_a = No. of Anchors = 2, 3 or 4 for 2, 3 or 4 no of anchors and,

m = a constant whose value is proposed as 0.94

By assuming the values of m and n as mentioned above, the values of ultimate pullout capacity of 2, 3 and 4 number of helical screw anchors has been computed using Equation 4.10 as mentioned in Table 4.6.

Now two sets of values of ultimate pullout capacity of 2, 3 and 4 number of helical screw anchors are available - one from the experimental investigation carried out in the laboratory, and the other from the equations proposed for multiple number of helical screw anchors as mentioned in Equation 4.10. To assess the validity of proposed equation, the percentage difference between the two values have been calculated which are tabulated in Tables 4.7, 4.8 and 4.9 for 2, 3 and 4 number of anchors respectively. From these tables it is clear that the difference between the experimental value and the value obtained from the proposed equation is within variations of 10% only. Hence it can be said that the proposed equation calculates the ultimate pullout capacity of multiple helical screw anchors within the acceptable limits.

Table 4.7: Ultimate Pullout Capacity of Multiple Anchors from Equation 4.10

n_b	H/B	$(Q_{up})_2$	$(Q_{up})_3$	$(Q_{up})_4$
1	4	148.28	222.42	296.56
1	6	554.82	832.23	1109.64
1	8	1521.94	2282.91	3043.88
1	10	2366.26	3549.39	4732.52
2	4	185.92	278.88	371.84
2	6	718.98	1078.47	1437.96
2	8	1718.28	2577.42	3436.56
2	10	2685.92	4028.88	5371.84
3	4	206.8	310.2	413.6
3	6	923.86	1385.79	1847.72
3	8	2042.96	3064.44	4085.92
3	10	3066.92	4600.38	6133.84

Table 4.8: Comparison of $(Q_{up})_2$ from Experiments and Equation 4.10

n_b	H/B	$(Q_{up})_2$ from Lab Exp. (N)	$(Q_{up})_2$ from Eq. (4.10) (N)	% diff
1	4	137	148.28	3.52
1	6	539	554.82	2.97
1	8	1545	1521.94	8.15
1	10	2158	2366.26	1.73
2	4	196	185.92	9.69
2	6	613	718.98	9.29
2	8	1619	1718.28	1.17
2	10	2796	2685.92	10.95
3	4	245	206.8	19.59
3	6	736	923.86	15.01
3	8	1767	2042.96	6.95
3	10	3188	3066.92	10.95

4.2.6 Limitations of Proposed Equation

There are several limitations of the proposed empirical equation which are listed below.

1. This is presuming that embedment depth, diameter and material of the anchor are same.
2. All the soil properties i.e. relative density and angle of internal friction are same.

Table 4.9: Comparison of $(Q_{up})_3$ from Experiments and Equation 4.10

n_b	H/B	$(Q_{up})_3$ from Lab Exp. (N)	$(Q_{up})_3$ from Eq. (4.0) (N)	% diff
1	4	221	212.565	3.82
1	6	760	784.38	3.06
1	8	1991	2128.92	6.48
1	10	3823	3294.63	13.81
2	4	270	265.89	1.48
2	6	883	1013.7	12.89
2	8	2197	2400.51	8.46
2	10	4414	3734.73	15.38
3	4	319	295.44	7.38
3	6	1177	1299.12	9.39
3	8	2600	2848.89	8.74
3	10	4689	4258.53	9.18

Table 4.10: Comparison of $(Q_{up})_4$ from Experiments and Equation 4.10

n_b	H/B	$(Q_{up})_4$ from Lab Exp. (N)	$(Q_{up})_4$ from Eq. (4.10) (N)	% diff
1	4	294	283.42	3.6
1	6	991	1045.84	5.17
1	8	2747	2838.56	3.21
1	10	4513	4392.84	2.66
2	4	392	354.52	9.56
2	6	1275	1351.6	5.67
2	8	3139	3200.68	1.94
2	10	5101	4979.64	2.37
3	4	441	393.92	10.66
3	6	1619	1732.16	6.52
3	8	3679	3798.52	3.13
3	10	5837	5678.04	2.8

4.2.7 Comparison of Laboratory and Empirical Values

Now two sets of values of Q_{up} are available – one from experimental investigation and the other from proposed Equation 4.10. Q_{up} from both these methods have been calculated and listed in Tables 4.7, 4.8 and 4.9. From these tables it is clear that the difference between the ultimate pullout capacity calculated from proposed equation and the experiments done at the laboratory are minimal. So an anchor foundation with multiple anchors can be safely designed with the value of ultimate pullout capacity of single anchor and proposed Equation 4.10.

4.2.8 Non-Dimensional Graphs and Design Considerations

To design an anchor foundation load - displacement graph in non-dimensional form is required. Several non-dimensional graphs have been plotted in this work for variations of no. of anchors, embedment depth ratio and no of screw blades in the anchor. Two such graphs plotted for two and four number of anchors are shown in Figs. 4.20 and 4.21 respectively.

4.2.9 Design of Anchors using Hyperbolic Curves

The non-dimensional graphs presented above have been further normalized in hyperbolic form by dividing the load axis with the displacement axis and plotting the graph with this against the displacement axis. This rendered the graph as straight line which can be used for design

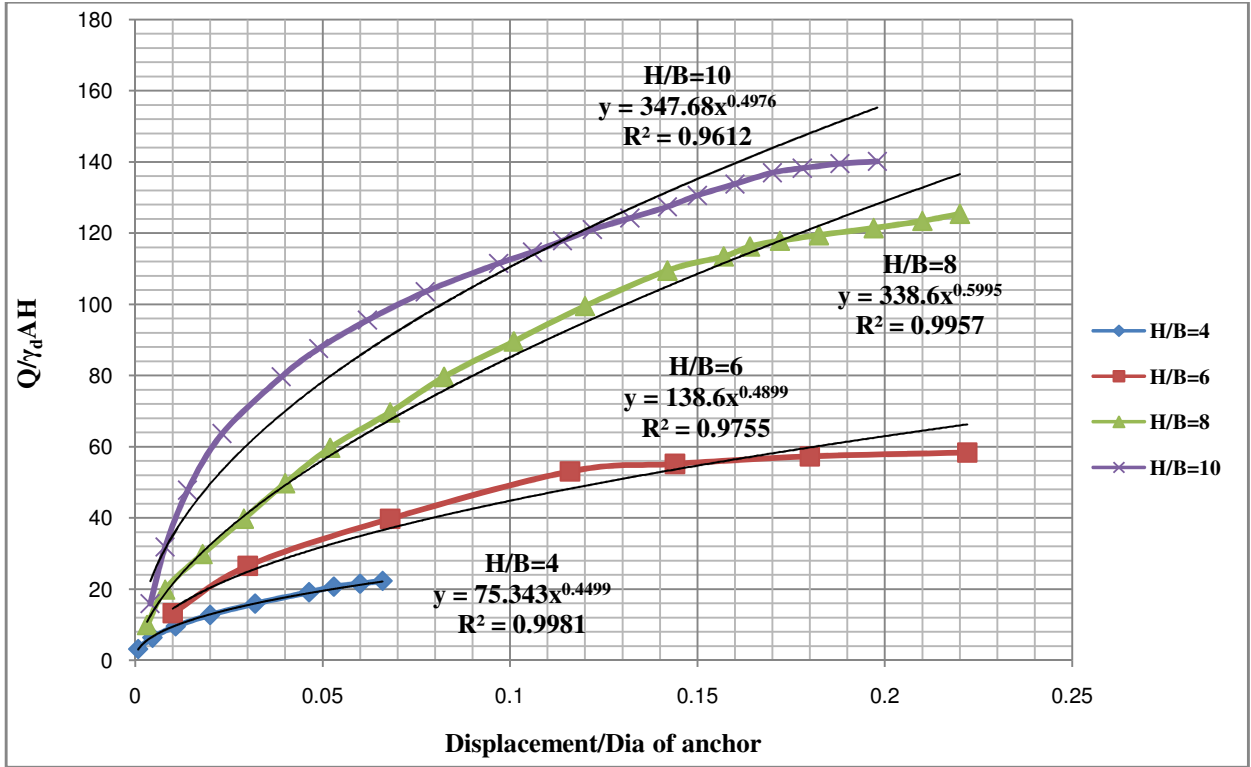


Fig. 4.20: Non-Dimensional Lab Pull-out Test Graph for $n_b=1$, $N_a=2$ and $H/B=4, 6, 8 \text{ \& } 10$

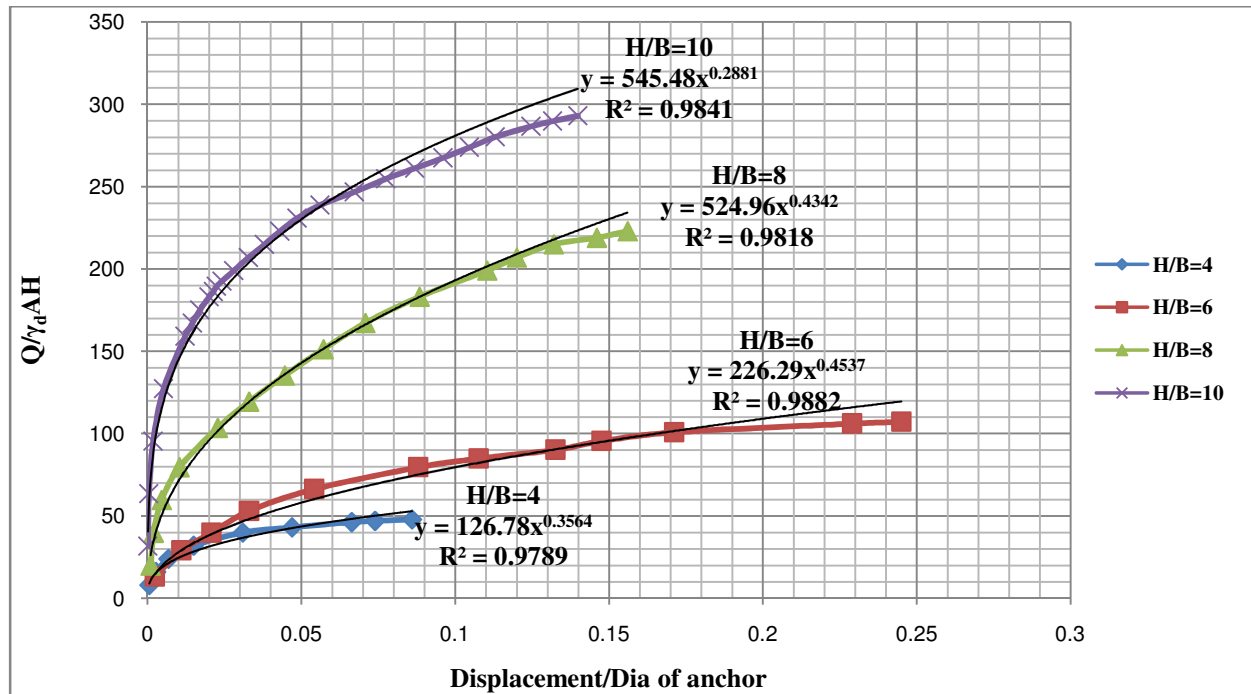


Fig. 4.21: Non-Dimensional Lab Pull-out Test Graph for $n_b=1$, $N_a=4$ and $H/B=4, 6, 8 \text{ \& } 10$

purposes. All non-dimensional graphs were normalized in this way and equation of these straight lines obtained. Two such graphs plotted for two and four number of anchors are shown in Figs. 4.22 and 4.23 respectively.

It was found that all the straight lines were similar in nature which can be described in the following form

$$\frac{\Delta}{B} = \frac{C_1 \left(\frac{Q}{\gamma AH}\right)}{[1 - C_2 \left(\frac{Q}{\gamma AH}\right)]} \dots\dots\dots (4.11)$$

- where, Δ = displacement of anchor,
- B = diameter of the helical screw of the anchor,
- P = load applied,
- γ = unit weight of sand, and
- C_1 and C_2 = constants

The values of these constants C_1 and C_2 calculated for all the tests are summarized in Table 4.10 as shown below.

Table 4.11: Values of Constants of Hyperbolic Equation for Pullout Tests

H/B	N _a =1		N _a =2		N _a =3		N _a =4	
	C ₁	C ₂	C ₁	C ₂	C ₁	C ₂	C ₁	C ₂
n_b=1								
2	0.0001	0.0592	0.0006	0.0381	0.0002	0.0262	0.0001	0.0197
4	0.00007	0.0271	0.0007	0.0139	0.0006	0.0104	0.0003	0.0082
6	0.0002	0.0095	0.0005	0.0058	0.0003	0.0046	0.0001	0.0041
8	0.0001	0.0078	0.0002	0.006	0.0002	0.003	0.00004	0.0033
n_b=2								
2	0.0003	0.0476	0.0003	0.026	0.0002	0.0206	0.00007	0.0153
4	0.0007	0.0168	0.0004	0.0086	0.0006	0.0088	0.00008	0.0042
6	0.0004	0.0079	0.0001	0.0031	0.00004	0.0055	0.00003	0.0017
8	0.0001	0.0073	0.00003	0.0019	0.00006	0.0032	0.00001	0.0012
n_b=3								
2	0.0002	0.0446	0.0002	0.0238	0.0001	0.0149	0.0001	0.0082
4	0.0004	0.0126	0.0005	0.0104	0.00007	0.0072	0.00006	0.005
6	0.0003	0.0071	0.00006	0.0065	0.00005	0.0045	0.00006	0.003
8	0.0001	0.0062	0.00008	0.0043	0.00004	0.0031	0.00004	0.0019

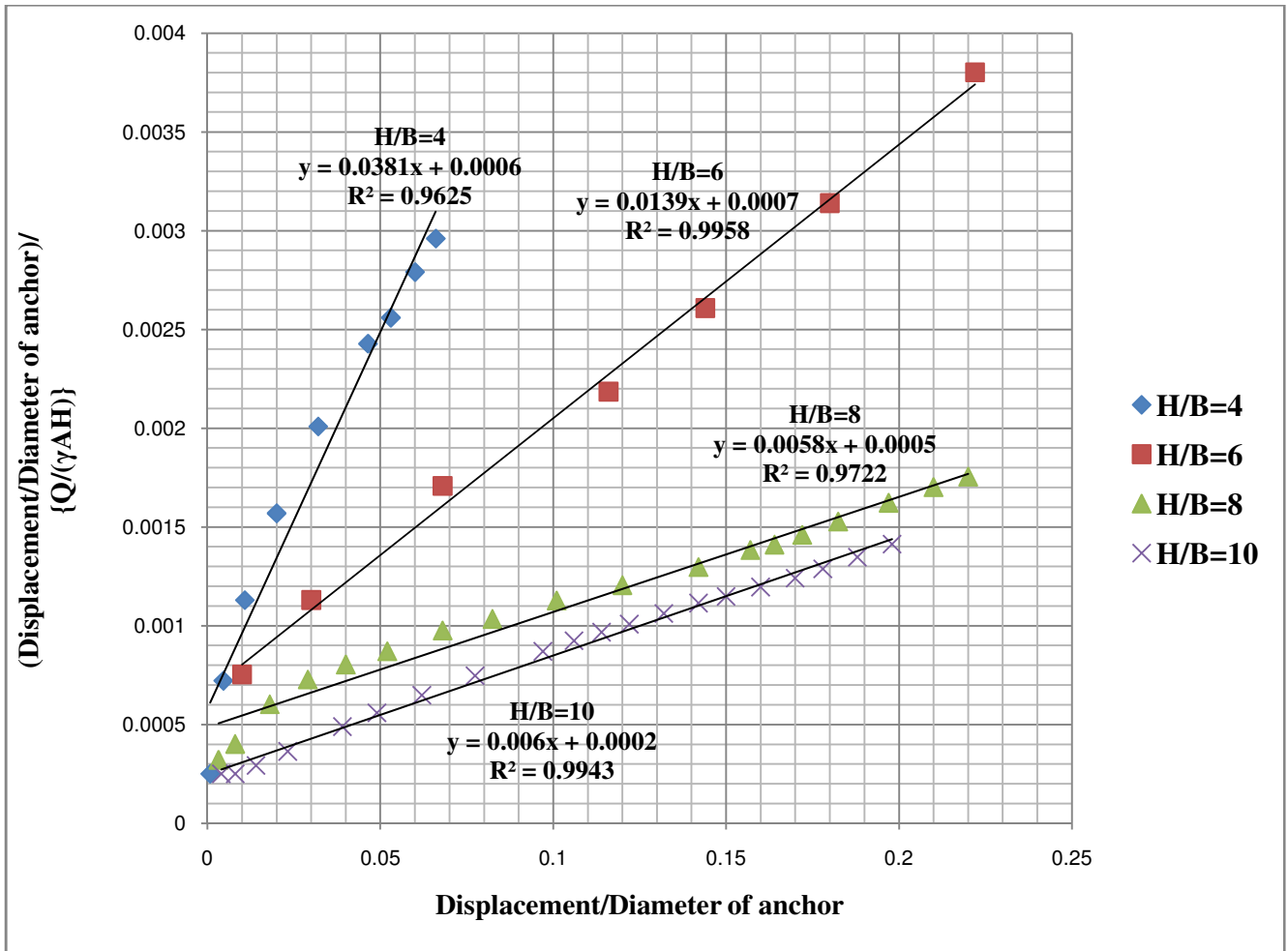


Fig. 4.22: Hyperbolic Curve for 2 Nos. of Single Helical Screw Anchors for Pullout Tests

With the help of Equation 4.11 and values of constants given in Table 4.10, one can easily calculate the value of (deformation / diameter of screw blade of anchor).

With the help of Figs. 4.22 or 4.23 an anchor foundation for a particular structure for pullout load can be easily designed. For designing a particular structure the values of load getting applied and acceptable deformation level will be known. Based on the experience and prevalent market conditions, a particular diameter of anchor to be used for this foundation can be assumed. For this load and assumed diameter of the anchor, the value of $(Q/\gamma_d AH)$ can be calculated. With the help of hyperbolic curves drawn as shown in Figs. 4.22 or 4.23 the value of Deformation/Diameter of anchor can be calculated from hyperbolic equations of the curves generated as shown in the Figs. 4.22 or 4.23 and values of constants as mentioned in Table 4.5 for an assumed H/B ratio. The deformation which this particular foundation will experience can

be calculated by multiplying this value with the assumed diameter of anchor. For safety purposes this deformation must be within the acceptable level of deformation.

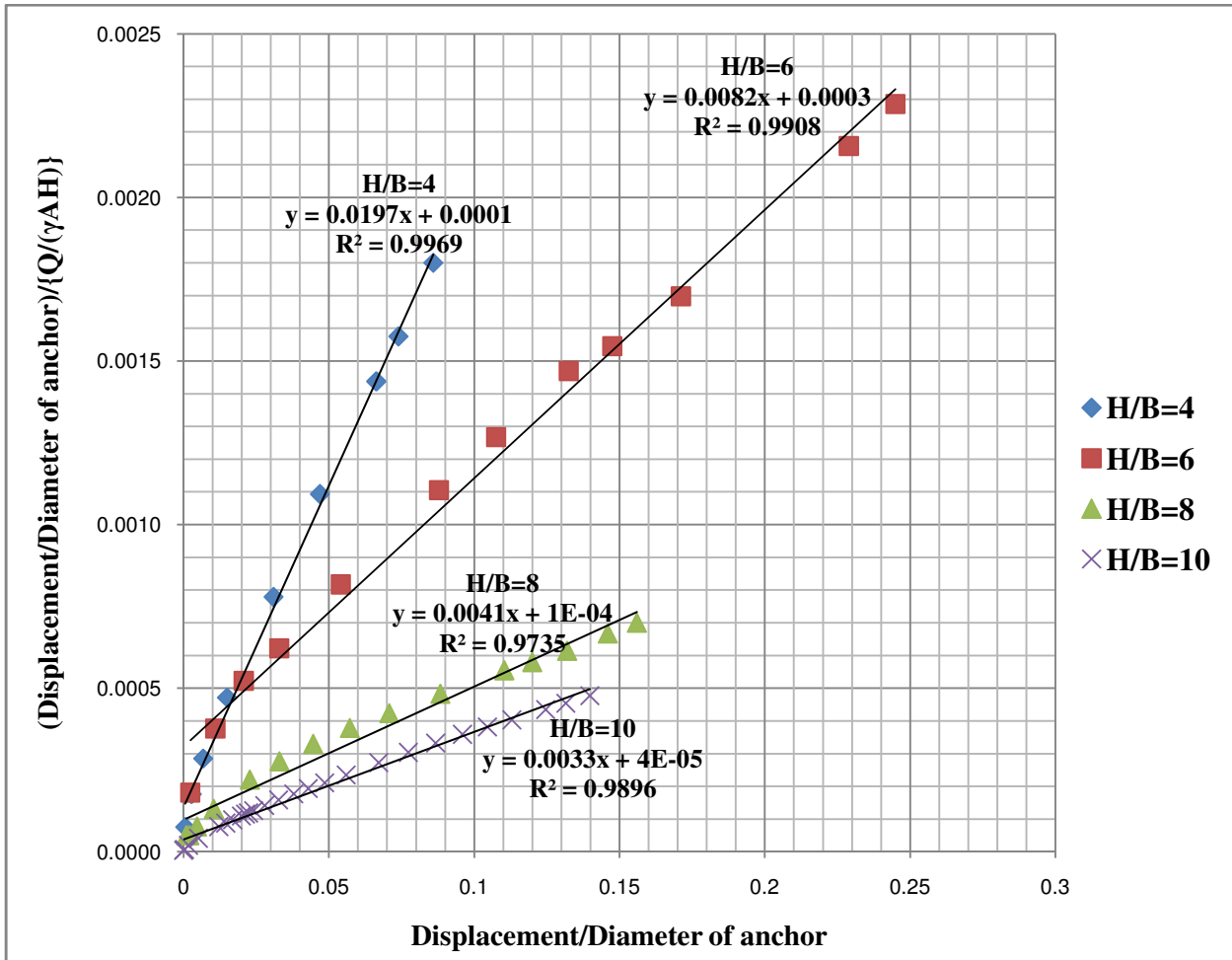


Fig. 4.23: Hyperbolic Curve for 4 Nos. of Single Helical Screw Anchors for Pullout Tests

4.2.10 Theoretical Considerations

The uplift behaviour of screw anchors depends on

1. Angle of shearing resistance of sand, and
2. Installation depth of the screw anchor

There are generally two types of failure.

1. General Shear Failure: For anchors installed to shallow depths, failure surface is a curved surface inclined outwards and reaches sand surface.

2. Local Shear Failure: For anchors installed to deep depths, failure surface is similar to general shear failure but it forms completely inside the sand and no movements were recorded on the sand surface.

In present work, shallow mode of failure occurs up to $H/B=6$ and deep mode of failure starts from $H/B=8$. Ilamparuthi et al. (2002) proposed values of critical embedment ratio of 4.8, 5.9 and 6.8 for loose, medium dense and dense sand, respectively. This matches very well with the present finding that shallow mode of failure occurs up to $H/B=6$ for medium dense sand.

Determination of actual failure surface is very difficult. The curved actual failure surface was assumed as planar failure surface inclined at an angle $\theta (=2\phi/3)$ to the vertical as suggested by Ghaly et al. (1991). Following assumptions were made in the present analysis:

1. The sand is homogeneous, isotropic and behaves in a nonlinear stress strain relationship.
2. The blades of the screw anchor are thin and rigid so that its deformation is negligible.
3. The weight of the screw anchor is negligible.

4.2.11 Equations Developed

4.2.11.1 Shallow Anchor

Here various components are defined as below.

Q_{up} = ultimate pullout load

V = Volume of truncated cone within failure surface

W = weight of sand wedge within failure surface

P_p = passive earth pressure along the failure surface

T = Shearing stress developed along the failure surface

Φ = angle of shearing resistance of the sand

δ = average mobilized angle of shearing resistance on the assumed plane of failure

b = radius of screw of anchor

r = radius of influence failure circle on the sand surface

L = side length of the failure surface cone

θ = surface inclination angle of inverted failure cone with respect to the vertical

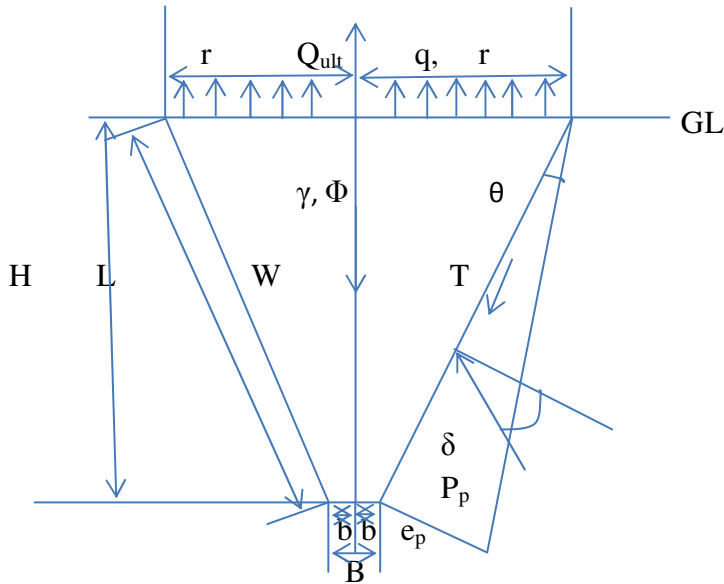


Fig. 4.24: Forces acting on Assumed Failure Surface for Shallow Anchor

The various forces acting on the failure soil wedge are:

- Weight of sand wedge within the failure surface

$$\text{➤ } V = \pi H \frac{(b^2 + r^2 + br)}{3} \dots\dots\dots(4.12)$$

$$\text{➤ } W = \gamma V = \pi \gamma H \frac{(b^2 + r^2 + br)}{3} \dots\dots\dots(4.13)$$

- Passive earth pressure for unit perimeter of inverted cone

$$\text{➤ } e_p = \gamma K'_p H \dots\dots\dots(4.14)$$

$$\text{➤ } P'_p = 0.5 e_p L = 0.5 \gamma H K'_p L \dots\dots\dots(4.15)$$

$$\text{where, } K'_p = \frac{(1 + \sin\phi)}{(1 - \sin\phi)}$$

- Summation of passive earth pressure on assumed failure surface

$$\text{➤ } P_p = P'_p \{ \pi(b + r) \tan\delta \} \dots\dots\dots (4.16)$$

- Shearing stress developed along the failure surface
 - $T = c + P_p \tan \varphi$ (4.17)

For cohesionless soil $c = 0$, hence

- $T = P_p \tan \varphi = P'_p \{ \pi(b + r) \tan \delta \} \tan \varphi$ (4.18)

- For equilibrium, $\Sigma V = 0$
 - $W + T \cos \theta = P_p \sin \theta + \pi B^2 q$ (4.19)

- Putting the values of W , T & P_p in the above equation and mentioning

$$q = q_{up} = \text{ultimate pullout load} = \frac{Q_{up}}{\pi B^2}, \text{ we get}$$

- $Q_{up} = \frac{\pi \gamma H}{3} (b^2 + r^2 + br) + \frac{\pi \gamma H L (b+r) K'_p}{2} \tan \delta (\tan \varphi \cos \theta - \sin \theta)$ (4.20)

In Equation (4.20) there are 4 unknowns namely r , θ , δ and K'_p . These values are calculated based on the tables and graphs provided by Ghaly et al. (1991). Based on the values obtained from Ghaly's tables and graphs, the values of ultimate load came out as shown in the Table 4.12.

Table 4.12: Comparison of values of Q_{up} from theory and experiment for shallow anchors

H/B	Q_{up} by Experiment (N)	Q_{up} by Theory Proposed (N)	% diff
4	93	102	8.82
6	324	294	9.26

4.2.11.2 Deep Anchor

Here the remaining components are as defined below.

- N = downward force due to vertical earth pressure
- h_0 = height of assumed inverted cone

The various forces acting on the failure soil wedge are:

- Weight of sand wedge within the failure surface
 - $V = \pi h_o \frac{(b^2+r^2+br)}{3}$ (4.21)
 - $W = \pi \gamma h_o \frac{(b^2+r^2+br)}{3}$ (4.22)
- Downward force on anchor due to vertical earth pressure
 - $P_o = \gamma(H - h_o)$ (4.23)
 - $N = P_o \pi r^2 = \gamma \pi r^2 (H - h_o)$ (4.24)
- Passive earth pressure for unit perimeter of inverted cone
 - $e_{p1} = P_o K'_p = \gamma(H - h_o) K'_p$ (4.25)
 - $e_{p2} = \gamma H K'_p$ (4.26)
 - $P'_p = 0.5(e_{p1} + e_{p2})L = 0.5\gamma K'_p(2H - h_o)L$ (4.27)

where, $K'_p = \frac{(1+\sin\phi)}{(1-\sin\phi)}$

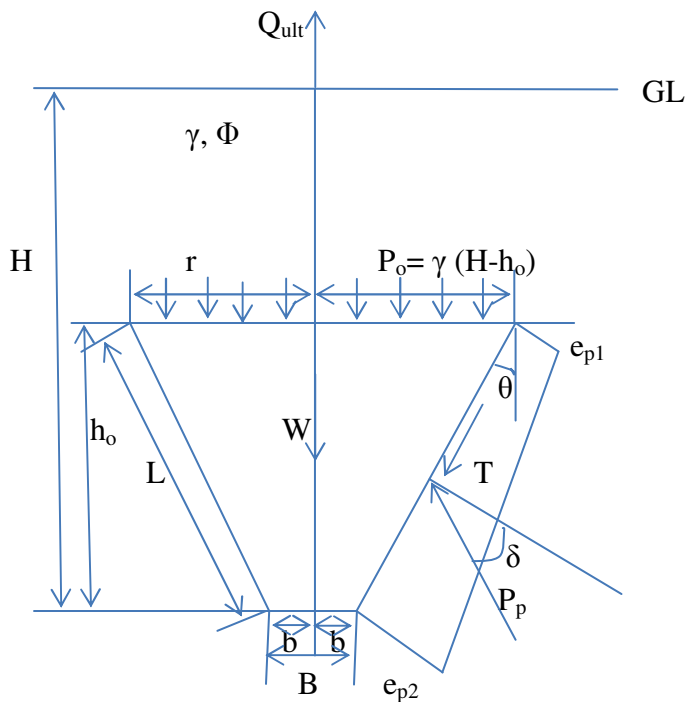


Fig. 4.25: Forces Acting on Assumed Failure Surface for Deep Anchor

- Summation of passive earth pressure on assumed failure surface
 - $P_p = P'_p \pi(b + r)\tan\delta = 0.5\pi\gamma K'_p L(b + r)(2H - h_o)\tan\delta$ (4.28)

- Shearing stress developed along the failure surface
 ➤ $T = c + P_p \tan \varphi$ (4.29)

- For cohesionless soil $c = 0$, hence
 ➤ $T = P_p \tan \varphi = 0.5\pi\gamma K'_p L(b + r)(2H - h_o)\tan\delta\tan\varphi$(4.30)

- For equilibrium, $\Sigma V = 0$
 ➤ $W + T\cos\theta + N = P_p\sin\theta + \pi B^2 q$(4.31)

- Putting the values of W , T , N & P_p in the above equation and mentioning

$q = q_{up} = \text{ultimate load intensity} = \frac{Q_{up}}{\pi B^2}$, we get

$$Q_{up} = \frac{\pi\gamma h_o}{3}(b^2 + r^2 + br) + \pi\gamma r^2(H - h_o) + \frac{\pi\gamma(b + r)(2H - h_o)K'_p}{2}\tan\delta(\tan\varphi \cos\theta - 0.5)$$

..... (4.32)

In Equation (4.32) there are 4 unknowns namely r , θ , δ and K'_p . These values are calculated based on the tables and graphs provided by Ghaly et al. (1991). Based on the values obtained from Ghaly's graphs and tables, the values of ultimate load came out as shown in Table 4.13.

Table 4.13: Comparison of values of Q_{up} from theory and experiment for deep anchors

H/B	(Q_{up})By Experiment (N)	(Q_{up})By Theory Proposed (N)	% diff
8	1079	1129	4.43
10	1717	1753	2.05

Here from Tables 4.12 and 4.13 it is clear that the differences between ultimate pullout capacity values obtained from laboratory tests and from theory proposed are within 10% which is negligible. Hence it can be said that the present theory predicts the ultimate pullout capacity of single helical anchor safely.

4.2.11 Comparison of Present Work with Published Works

4.2.11.1 Comparison of results with Ghaly et al. (1991)

Table 4.14 below presents the comparison of present work with Ghaly et al. (1991). In Ghaly's experiments, unit weight of sand was taken as 16.7 kN/m^3 and angle of internal friction as 40° . But in the present investigation, unit weight of sand was taken as 15.7 kN/m^3 and angle of internal friction as 38° . To compare results from both the investigations, soil having same property was taken for the present experimental investigation and experiments were conducted. From Table 4.14 it can be said that both the results matches very well.

Table 4.14: Comparison of Present Work with Ghaly (1991)

H/B	Q_u from Ghaly et al. (1991) * (N)	Q_u from Present Experiment (N)	% diff
4	233	210	9.87
6	613	554	9.62
8	981	1079	9.08
10	1570	1716	8.51

* Note: -Values taken for medium pitch screw in medium dense sand.

4.2.11.2 Comparison of results with Malik (2007)

Table 4.15 presents the comparison of the present work with Malik (2007). From Table 4.15 it is clear that the values match very well for shallower depth i.e. for H/B ratio of 4 & 6. Only at greater depth i.e. at H/B ratio of 8 the values differ. Malik (2007) got lower values because of lower values of specific gravity, angle of internal friction and unit weight as shown in Table 4.16.

Table 4.15: Comparison of Present Work with Malik (2007)

H/B	$Q/\gamma AH$ Malik (2009)	$Q/\gamma AH$ (Present Work)	% diff
Single Helical Screw Anchor			
4	17.13	15.13	11.67
6	42.93	47.77	10.13
8	56.74	87.59	35.22
Double Helical Screw Anchor			
4	18.03	15.92	13.25
6	46.24	53.08	12.89
8	58.98	89.58	34.16

Triple Helical Screw Anchor			
4	19.47	19.91	2.2
6	50.5	55.74	9.4
8	62.16	119.44	47.96

Table 4.16: Difference in present values with Malik (2007)

Characteristics	Values in Malik (2009)	Values in present investigation
Specific Gravity at 27° C	2.55	2.63
Angle of Internal Friction	36°	38°
Average unit wt. (kN/m ³)	14.7	15.7

4.2.12 Parametric Study

Parametric study was conducted to determine the increase in angle of internal friction and improved apparent coefficient of friction (f^*) between the anchor and the soil because of insertion of anchors in soil.

4.2.12.1 Increase in Φ by Plate Load Test

Anchors installed in the soil increases the value of ϕ which results in increase in strength of the soil. This increase in the value of ϕ can be calculated from the plate load test. The plate load tests were conducted on virgin soil and also on soil with 1, 2, 3 and 4 double helical screw anchors. A plate of dimension 150 x 150 mm was fixed on the top of the anchor with the help of nuts and bolts. Ultimate bearing capacity for surface footing was computed from the equation

$$q_u = 0.4 \gamma_d B' N_\gamma \dots\dots\dots(4.33)$$

where, q_u = ultimate bearing capacity, N_γ = bearing capacity factor, B' = width of the footing plate (150 mm x 150 mm) and γ_d = dry unit weight of soil = 16 kN/m³.

From the test results and using Eq. (4.33) the value of N_γ has been calculated. After calculating N_γ , value of Φ can be read from Saran (2006). The values of N_γ and corresponding values of Φ are given in Table 4.17.

Table 4.17: Values of Φ Obtained after Plate Load Test

Test Condition	q_u	N_γ	Φ
Virgin Soil	47.96	49.95	35.16
Soil with 1 Anchor	174.42	181.69	42.23
Soil with 2 Anchors	283.41	295.22	45.24
Soil with 3 Anchors	392.4	408.75	46.39
Soil with 4 Anchors	566.8	590.42	48.24

From Table 4.17, it is clear that value of Φ increased from 35° for virgin soil to 48° for this equivalent material with 4 double helical screw anchors.

4.2.12.2 Increase in the Value of Apparent Coefficient of Friction (f^*)

Apparent coefficient of friction between the anchor and the soil (f^*) plays an important role in determining the strength of anchors. This is a very important parameter in the design of anchor as the force transfer from anchor to soil is through the friction mobilized at the interface. Value of f^* is calculated for Pullout tests. Its values are tabulated in Table 4.18.

Table 4.18: Values of f^* for Pullout Tests

n_b	H/B	f^*			
		$N_a=1$	$N_a=2$	$N_a=3$	$N_a=4$
1	4	1.34	1.02	1.07	1.06
1	6	2.14	1.53	1.44	1.41
1	8	3.29	2.3	2.05	2.06
1	10	3.22	1.99	2.34	2.08
2	4	1.95	1.6	1.49	1.57
2	6	2.99	1.9	1.9	1.89
2	8	3.88	2.51	2.37	2.43
2	10	3.78	2.65	2.78	2.41
3	4	2.28	1.95	1.82	1.86
3	6	4.02	2.53	2.57	2.58
3	8	4.76	2.92	2.91	2.92
3	10	4.44	3.08	3.02	2.82

The pull-out resistance is defined as the force mobilized along the length of the anchor which lies beyond the failure surface when an assumed failure surface cuts a layer of soil anchor.

From the load deflection curve obtained from conducting pull-out test, the pull out load responsible for failure is computed from Equation 4.34. From this failure load the apparent coefficient of friction is determined as follows.

$$f^* = \frac{P_u}{\{\pi BL(\gamma_d z + q)\}} \dots\dots\dots (4.34)$$

where f^* is the apparent coefficient of friction, P_u is the ultimate failure load, B is the diameter of screw blade of the anchor, L is the embedded length of the anchor, γ_d is the dry unit weight of soil, z is the depth of the sand fill above the screw of the anchor and q is surcharge intensity, if any.

Pull-out resistance of the anchor or value of apparent coefficient of friction is influenced by several factors such as properties of soil, roughness and stiffness of the anchor, boundary conditions of the test, diameter and length of the anchor and normal stress acting on the anchor.

4.2.13 Design Example

Problem: Design a helical screw anchor to withstand pullout load of 100 kN by using present methodology.

The soil properties are as follows:

$c = 0$, $\Phi = 38^\circ$, $\gamma_d = 15.7 \text{ kN/m}^3$, Classification of soil is SP.

Solution: Given, Proposed Compressive Load, $Q = 100 \text{ kN}$

Assuming acceptable deformation of the structure = 8 mm

Designing this anchor system for two and four number of anchors:

(A) If 2 no. of anchors can be used, then assuming anchor diameter as 300 mm

Cross Sectional Area of Anchor, $A = 0.07 \text{ m}^2$

$$\frac{Q}{\gamma A} = \frac{100}{15.7 * 0.07} = 90.99$$

Assuming Embedment Depth Ratio, $H/B = 8$

Hence, $H = 8 \times 0.3 = 2.4 \text{ m}$

$$\frac{Q}{\gamma A H} = \frac{90.99}{2.4} = 37.91$$

For $H/B = 8$ and $n_b = 1$, from Fig. (4.20) the hyperbolic equation is

$$\begin{aligned}\frac{\delta}{B} &= \frac{0.0005 \frac{Q}{\gamma_{AH}}}{1 - 0.0058 \frac{Q}{\gamma_{AH}}} \\ &= \frac{0.0005 \times 37.91}{1 - (0.0058 \times 37.91)} \\ &= 0.0243\end{aligned}$$

Hence, deformation/diameter of anchor = 0.0243

Therefore, Deformation = 0.0243 x 300 = 7.29 mm < 8 mm

which is within acceptable level of deformation

Hence this system can be designed with 2 numbers of single helical screw anchor having diameter of screws as 300 mm installed at H/B = 8 i.e. at 2.4 m below the soil surface.

(B) If 4 no. of anchors can be used, then assuming anchor diameter as 200 mm.

Cross Sectional Area of Anchor, A = 0.0314 m²

$$\frac{Q}{\gamma A} = \frac{100}{15.7 * 0.0314} = 202.85 \text{ m}$$

Assuming using Embedment Depth Ratio, H/B=8

$$H = 8 \times 0.2 = 1.6 \text{ m}$$

$$\frac{Q}{\gamma_{AH}} = \frac{202.85}{1.6} = 126.78$$

For H/B = 8 and n_b = 1, from Fig. (4.21) the hyperbolic equation is

$$\begin{aligned}\frac{\delta}{B} &= \frac{0.0001 \frac{Q}{\gamma_{AH}}}{1 - 0.0041 \frac{Q}{\gamma_{AH}}} \\ &= \frac{0.0001 \times 126.78}{1 - (0.0041 \times 126.78)}\end{aligned}$$

$$= 0.0264$$

Hence, deformation/diameter of anchor = 0.0264

Therefore, Deformation = $0.0264 \times 200 = 5.28 \text{ mm} < 8 \text{ mm}$

which is within acceptable level of deformation

Hence this system can be designed with 4 nos. of single helical screw anchor having diameter of screws as 200 mm installed at $H/B = 8$ i.e. at 1.6 m below the soil surface.

NUMERICAL VALIDATION

5.0 INTRODUCTION

Numerical methods are useful for solving problems of stress/strain deformation prediction and analysis. The main objective of modeling helical anchor behaviour was to define the failure mechanism and load transfer behaviour. Upon calibration-verification with the experimental data, FEM provided insight into the effects of anchor loading on the surrounding soil. Based on the findings of the model and full-scale load test results, a methodology for calculating the anchor capacity was developed.

To account for the unique geometry of the problem a three-dimensional soil-foundation interaction software program, namely PLAXIS 3D Foundation Suite, was selected. This software was selected as it was used by many investigators to model helical screw and plate anchors like Popadopoulou et al. (2014), Abdelghany and Naggar (2013), Ismail and Shahin (2012), Livneh and Naggar (2008), Dickin and Naggar (2007) and many more. PLAXIS 3D is a three-dimensional finite element program, developed to perform deformation and stability analysis for various types of geotechnical applications. It uses a convenient graphical user interface that enables users to quickly generate a geometric model and finite element mesh. Soil mass under loading can be subjected to self-weight, external forces, in-situ stresses, temperature fluctuations, fluid pressures, pre-stressing and dynamic forces etc. as the model developed in the present investigation is under static point load, therefore, only this sort of modeling will be dealt in this chapter. This software was chosen for the modeling of problem and validation purpose. At the end, a comparison between the results obtained from PLAXIS 3D and that of experimental results had been presented. All the information given about modeling with PLAXIS 3D is fully derived from manuals (e.g. theory, reference, material models, scientific etc.).

5.1 PROBLEM SOLVING WITH PLAXIS 3D

The problem of static analysis in geotechnical engineering could be solved using PLAXIS 3D that includes defining soil and structure parameters, defining constitutive model, initial conditions, mesh generation, loading and interpretation and presentation of results. All of these are described under the following headings.

5.1.1 Defining Soil

In PLAXIS, the modeling process is completed in five modes which are separated into geometry and calculation modes. All the changes to geometry (such as creation, relocation, modification or removal of entities) are only possible in geometry mode. Geometry mode is further subdivided into two modes - soil mode for defining soil stratigraphy, general water levels and the initial conditions of the soil layers and structure mode for defining geometric entities as well as structural elements and forces.

The soil stratigraphy is defined in the soil mode using the borehole feature of the program. Boreholes are locations in the draw area at which the information on the position of soil layers and the water table is given. If multiple boreholes are defined, PLAXIS 3D automatically interpolates between the boreholes, and derives the position of soil layers from the borehole information. Each defined soil layer is used throughout the whole model contour. In other words, all soil layers appear in all boreholes.

In order to simulate the behaviour of the soil, a suitable material model and appropriate material properties must be assigned to the geometry. In PLAXIS soil properties are collected in material datasets and the various datasets are stored in a material database. Therefore, for our work a linearly elastic perfectly plastic model namely Mohr-Coulomb Failure Criteria was selected from those available in PLAXIS to describe the non-linear sand behaviour in the work.

5.1.2 Defining Structure

Geometric entities, structural elements and boundary conditions are defined in the structure mode. The soil layer created in the soil mode appears in the draw area in the structure mode but it cannot be modified in the structure mode. For structures also, a suitable material model and appropriate material properties must be assigned to a particular structure. Different types of structures have different parameters and therefore different types of data sets. From the database, a data set can be assigned to one or more clusters. For structures (like beams, plates etc.) the system is similar, but different types of structures have different parameters and, therefore, different type of data sets. PLAXIS 3D distinguishes between material data sets for soils and interfaces and different types of structures like plates, beams, geogrids, embedded piles and anchors.

Several assigning tools are available in PLAXIS to modify the geometry of the structure by changing the location or the orientation of the object in the model or by creating higher objects with a higher dimension e.g. from lines to surfaces or from surfaces to volumes. A structure can be moved, rotated or extruded. Points, lines and surfaces can be extruded to create lines, surfaces and volumes correspondingly.

5.1.3 Defining Geometric Entities

The geometric entities are the basic components of the physical model. Features such as structures, loads etc., can be assigned to geometric entities. There are several geometric entities available in PLAXIS which are points, lines, polycurves, surfaces and volumes. Several advanced features are available in PLAXIS 3D to be assigned to a structure. The geometric entities as well as the structural elements and forces in the project are defined in the structure mode. Advanced options for modifying geometric entities in the model are also available.

5.1.4 Defining Constitutive Model

The mechanical behaviour of soils may be modeled at various degree of accuracy. There are eleven built-in material models in PLAXIS 3D. Each model is developed keeping in mind the specific type of constitutive behaviour exhibited by the geological material. The simplest material model in PLAXIS 3D is based on Hooke's law for isotropic linear elastic behaviour. This model is available under the name Linear Elastic model, but it is also the basis of other models. Hooke's law can be given by the equation:

$$\begin{pmatrix} \epsilon_{xx}^e \\ \epsilon_{yy}^e \\ \epsilon_{zz}^e \\ \gamma_{xy}^e \\ \gamma_{yz}^e \\ \gamma_{zx}^e \end{pmatrix} = 1/E_u \begin{pmatrix} 1 & -\nu_u & -\nu_u & 0 & 0 & 0 \\ -\nu_u & 1 & -\nu_u & 0 & 0 & 0 \\ -\nu_u & -\nu_u & 1 & 0 & 0 & 0 \\ 0 & 0 & 0 & 2+2\nu_u & 0 & 0 \\ 0 & 0 & 0 & 0 & 2+2\nu_u & 0 \\ 0 & 0 & 0 & 0 & 0 & 2+2\nu_u \end{pmatrix} \begin{pmatrix} \sigma_{xx} \\ \sigma_{yy} \\ \sigma_{zz} \\ \sigma_{xy} \\ \sigma_{yz} \\ \sigma_{zx} \end{pmatrix} \dots\dots\dots (5.1)$$

The Mohr-Coulomb Failure Criteria represents a first-order approximation of soil or rock behaviour. This model is the most applicable for general engineering studies involving soil mass.

The present study uses Mohr-Coulomb Failure Criteria which finds applicability in modeling of soil and rock mechanics. The material properties for this model are elastic shear modulus, elastic bulk modulus, angle of internal friction, cohesion, adhesion, tension and dilation.

5.1.4.1 Formulation of the Mohr-Coulomb Failure Criteria

The Mohr-Coulomb yield condition is an extension of Coulomb’s friction law to general state of stress. In fact, this condition ensures that Coulomb’s friction law is obeyed in any plane within a material element. The full Mohr-Coulomb yield condition consists of six yield functions when formulated in terms of principal stresses. In addition to the yield functions, six plastic potential functions are also defined for the Mohr-Coulomb Failure Criteria. PLAXIS implements the exact form of the full Mohr-Coulomb Failure Criteria for the intersection of two yield surfaces using a sharp transition from one yield surface to another. For stress states within the yield surface, the behaviour is elastic and obeys Hooke’s law for isotropic linear elasticity.

The linear elastic perfectly-plastic Mohr-Coulomb Failure Criteria requires a total five parameters which can be obtained from basic tests on soil samples. These parameters with their standard units are listed in Table 5.1 below. Here instead of using Young’s modulus as a stiffness parameter, alternative stiffness parameters can be used which are Shear Modulus and Oedometer Modulus.

Table 5.1: Parameters Used in Mohr-Coulomb Failure Criteria

Notation	Parameters	Unit
E	Young’s Modulus	[kN/m ²]
v	Poisson’s Ratio	[-]
C	Cohesion	[kN/m ²]
Φ	Angle of Internal Friction	[°]
Ψ	Dilatancy Angle	[°]
G	Shear Modulus	[kN/m ²]
E _{oed}	Oedometer Modulus	[kN/m ²]

5.1.5 Initial Conditions

Many analysis problems in geotechnical engineering require the specification of a set of initial stresses. The initial stresses in a soil body are influenced by the weight of the soil, the water conditions and the history of its formation. The stress state is usually characterized by an initial vertical effective stress ($\sigma'_{v,0}$). The initial horizontal effective stress ($\sigma'_{h,0}$) is related to the initial vertical effective stress by the coefficient of lateral earth pressure (K_0) as ($\sigma'_{h,0} = K_0 \times \sigma'_{v,0}$). In PLAXIS, initial stresses may be generated by using the K_0 procedure or by using Gravity Loading.

5.1.6 Mesh Generation

PLAXIS 3D allows for a fully automatic mesh generation procedure in which geometry is divided into volume elements and compatible structural elements, if applicable. The mesh generation takes full account of the position of the geometry entities in the geometry model, so that the exact position of the layers, loads and structures is accounted for in the finite element mesh. The mesh should be sufficiently fine to obtain accurate numerical results. On the other hand, very fine meshes should be avoided since this will lead to excessive calculation times. PLAXIS incorporates a fully automatic mesh generation procedure, in which the geometry is divided into elements of basic element type, and compatible structural elements. Five different mesh densities are available in PLAXIS ranging from very coarse to very fine.

5.1.7 Defining Loads

Loads are features that can be assigned to geometric entities. There are various types of loads available in PLAXIS which can be used for analysis purpose. They are point load, line load, surface load and dynamic load.

5.1.8 Defining Calculation Phases

Finite element calculations can be divided into several sequential calculation phases. Each calculation phase corresponds to particular loading or construction stage. The order of calculation phases is defined by selecting the parent phase first and then adding the remaining phases in their order of execution.

5.1.9 Types of Analysis

The first step in PLAXIS analysis is defining a calculation type of a phase. The options available are KO procedure and Gravity loading for the initial phase and Plastic, Consolidation, Safety and Dynamic for other phases. In PLAXIS, initial stresses may be generated by using the KO procedure or by using Gravity loading.

5.1.10 Interpretation and Presentation of Results

During a 3D finite element deformation analysis, information about the calculation process is presented in a separate window and load-displacement curve for one of the pre-selected nodes for curves is shown. The presented graph may be used to roughly evaluate the progress of the calculation. After the calculation process is finished, the results can be seen in the output program by selecting the appropriate phase.

The main output quantities of a finite element calculation are the displacements and stresses. In addition, when a finite element model involves structural elements, the structural forces in these elements are also calculated. The Deformed mesh is a plot of the finite element model in the deformed shape. The deformation options for the structure are available in the deformations menu. The user may select total displacements, phase displacements or incremental displacements based on their requirements. For each item a further selection can be made among the displacement vectors \mathbf{u} and the individual displacement components u_x , u_y and u_z .

Forces available from the Forces menu for the plates are – axial forces N_1 and N_2 , shear forces Q_1 and Q_2 and moments M_{11} , M_{22} and M_{12} . For node-to-node anchor output is the anchor force expressed in the unit of force on the nodes of the anchor. The load-displacement curves can be used to visualize the relationship between the applied loading and the resulting displacement of a certain point in the geometry.

5.2 DESCRIPTION OF THE DEVELOPED PLAXIS 3D MODEL

In order to carry out finite element analysis using PLAXIS 3D program, a three dimensional model of anchor assembly has been generated to represent the soil-anchor assembly in the field. This geometry model consists of node-to-node anchor, anchor plate and footing plate. This is done in two tab sheets (Geometry modes) of the input program which are Soil and

Structures. The mesh generation is done in the Mesh tab. At the last calculation is done in Calculation mode in two tab sheets namely Water Levels and Staged Construction. Since in our problem soil is completely dry and water has no role so Water Levels tab sheet is not used at all.

Because of the symmetry of the system, full model has been taken for simulation. To compare well with the Laboratory Testing, the size of the grid in PLAXIS is kept same as the size of the test tank in laboratory testing which are 750 x 750 x 650 mm. Fig.5.1 shows the dimension of the grid used in PLAXIS. Set up of all the components in PLAXIS has been accomplished as shown in Fig. 5.2. This figure shows the position of the various components used in PLAXIS which are node-to-node anchor, anchor plate, footing plate and the soil mass. After creating the geometry of the problem the mesh has been generated. This model was analyzed using all the five types of mesh categories available in PLAXIS ranging from very coarse to very fine. Very coarse mesh gives results very fast but the result is not convergent and reliable. Very fine mesh gives accurate result but take lots of time to analyze even a simple problem. Keeping complexity of the present problem in mind, we have used fine mesh throughout in our analysis which is shown in Fig. 5.3a.

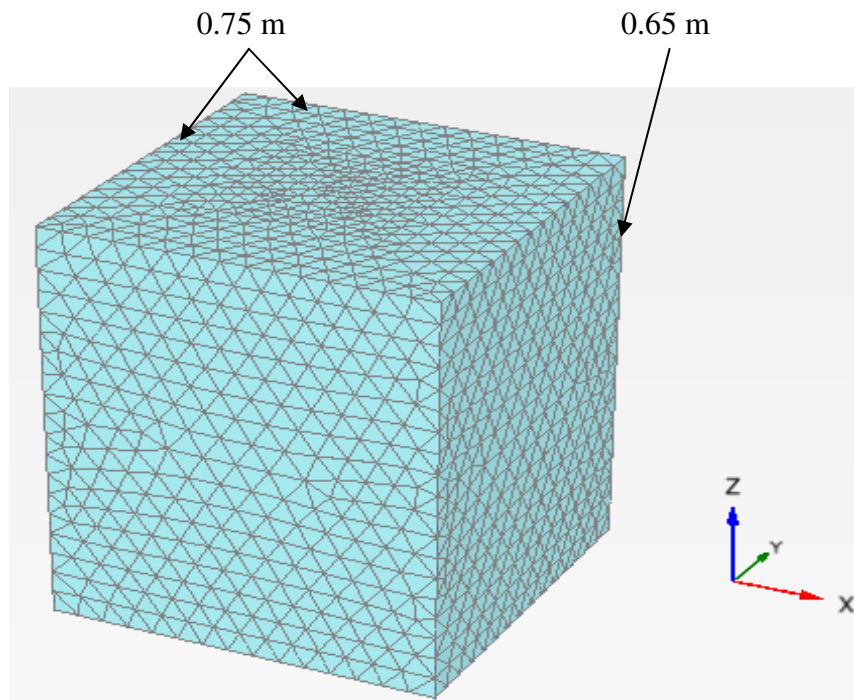


Fig. 5.1: Dimension of the Grid Used in PLAXIS

The numerical model was constructed to match the full scale geometry of the anchor in all regards excluding the helical shape of the bearing plates, which were modeled as circular discs rather than pitched plates. It was not possible to model helical anchor in PLAXIS despite several efforts. The available literature by Livneh and Naggar (2008) also reveals that authors had modeled helical screw anchor as circular disc rather than pitched plates. The helical screw anchor is represented by node-to-node anchor coupled with a circular plated attached to it. The Mohr-Coulomb Failure Criteria was used to represent the soil behaviour, for which cohesion and friction angle values were obtained through triaxial test results. This model was used by Livneh and Naggar (2008) and Popadopoulou et al. (2014) for modeling sand. The same had been adopted in the present research work also. Values of soil parameters used in the investigation are shown in Table 5.2. In PLAXIS soil/structure interface behaviour may be modeled using parameters generated using an interaction coefficient, R_i defined as the ratio between the shear strength of soil/structure interface and the corresponding shear strength of the soil. Fully rough interface conditions, $R_i = 1$, were assumed in this study. This value was taken as suggested by Dickin and Laman (2007). The present problem was simulated with a range of values of R_i from 0.7 to 1 and had been observed that its value hardly affects the pullout capacity. Hence the value of R_i was taken as 1 in the entire thesis. The side view and the top view of the mesh generated have been shown in Figs. 5.3a and 5.3b.

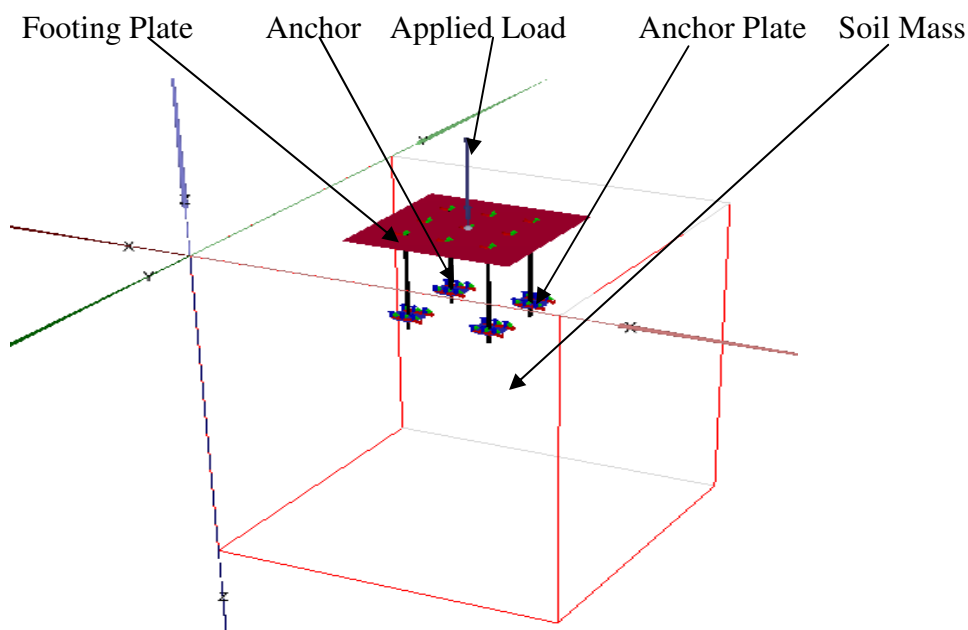


Fig. 5.2: Position of Various Components in the System

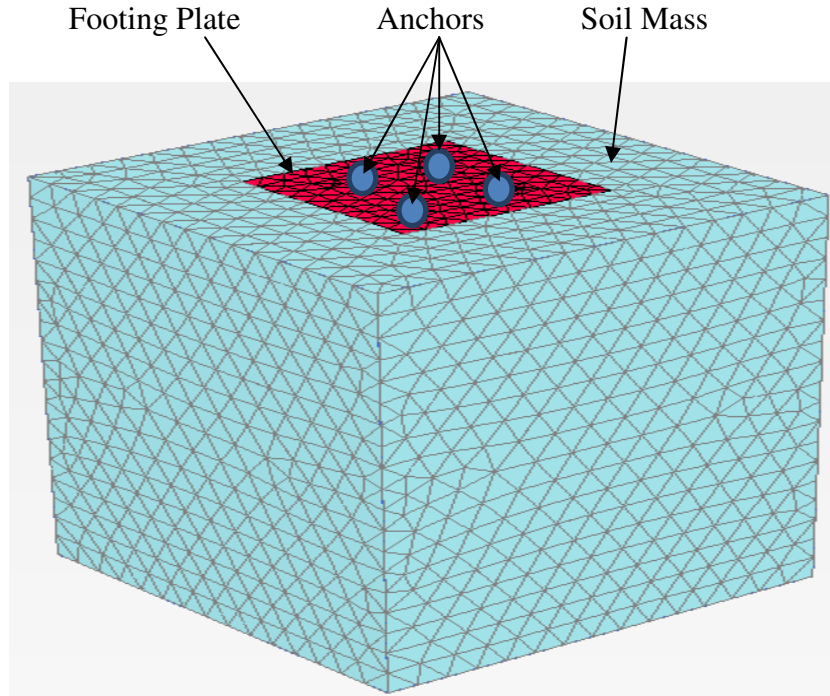


Fig. 5.3a: Side View of the Mesh Generated in PLAXIS

Here boundary conditions adopted are as mentioned below.

- (1) Vertical model boundaries with their normal in x -direction (i.e., parallel to the y - z plane) are fixed in the x -direction ($u_x = 0$) and free in y - and z -directions.
- (2) Vertical model boundaries with their normal in z -direction (i.e., parallel to the x - y plane) are fixed in the z -direction ($u_z = 0$) and free in x - and y -directions.
- (3) The model bottom boundary is fixed in all directions ($u_x = u_y = u_z = 0$).
- (4) The “ground surface” of the model is free in all directions.

Load was applied vertically on the top of anchor, downward for compression tests and upward for pullout tests.

5.3 MATERIAL PROPERTIES USED IN THE NUMERICAL ANALYSIS

The shear strength parameters i.e. density, angle of internal friction and Young’s modulus for the numerical simulation were obtained from the Triaxial Shear tests as mentioned in Mittal and Shukla (2013). The values of Poisson’s ratios were assumed meeting the requirements from the available literature. The material properties of sand, footing plate, anchor plate and node-to-

node anchor used in PLAXIS are provided in Tables 5.2, 5.3, 5.4 and 5.5 respectively as suggested by Ranjan and Rao (2000).

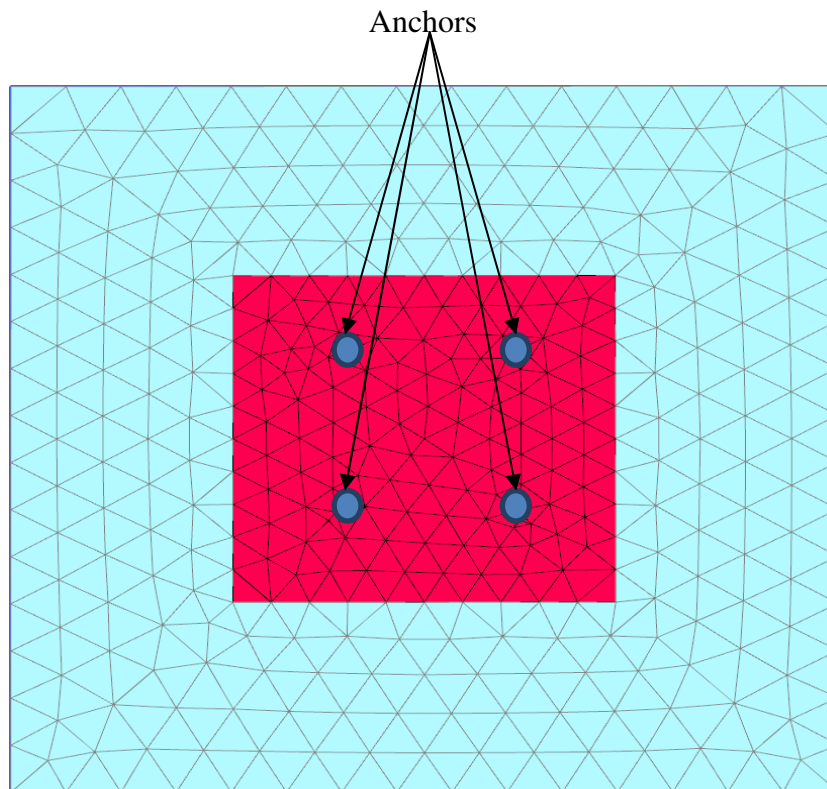


Fig. 5.3b: Top View of the Mesh Generated in PLAXIS

Table 5.2: Material Properties of Sand Used in PLAXIS

Type of Soil	Medium Dense	Dense
c (Pa)	0	0
Φ (°)	32 & 36	38 & 40
γ (kN/m³)	13.73, 15.7 & 17.66	13.73, 15.7 & 17.66
v	0.3	0.4
E (MPa)	40	65

Table 5.3: Material Properties of Anchor Plate Used in PLAXIS

Diameter (m)	0.005
Thickness (m)	0.002
Unit Weight (kN/m³)	77

Young's Modulus of Elasticity (kN/m²)	200 x 10 ⁶
Poisson's Ratio	0.303

Table 5.4: Material Properties of Footing Plate Used in PLAXIS

Width (m)	0.25
Thickness (m)	0.016
Unit Weight (kN/m³)	77
Young's Modulus of Elasticity (kN/m²)	200 x 10 ⁶
Poisson's Ratio	0.303

Table 5.5: Material Properties of Node-to-Node Anchor Used in PLAXIS

Parameter	Name	Node-to-node Anchor	Unit
Material Type	Type	Elastic	-
Axial Stiffness	EA	6.5 x 10 ⁶	kN

5.4 PLAXIS RESULTS FOR COMPRESSION

The numerical investigations were carried out by taking the various components having material properties as described in Tables 5.2, 5.3, 5.4 and 5.5. In PLAXIS, compression tests were carried out for embedment depth ratio of 4, 6 and 8. PLAXIS results for compression are shown in Tables 5.6, 5.7, 5.8 and 5.9. Based on the results shown in these tables, load-displacement curves were plotted to highlight variation in ultimate compressive capacity with the variation in no. of anchors, embedment depth ratio and no. of screw blades in the anchor as shown in Figs. (5.4), (5.5) and (5.6).

Table 5.6: PLAXIS Results of Compression Tests for N_a=1

n_b	H/B	Φ (Degree)	γ_d (kN/m³)	Failure Load, P_f (N)
1	8	32	13.73	2466
1	6	36	15.7	5488
1	8	38	15.7	6690
1	4	40	17.66	12735
2	4	40	17.66	12090

2	6	36	15.7	5580
2	6	38	15.7	7112
2	8	32	13.73	2470
3	4	40	17.66	12420
3	6	36	15.7	5502
3	6	38	15.7	6984
3	8	32	13.73	2442

Table 5.7: PLAXIS Results of Compression Tests for $N_a=2$

n_b	H/B	Φ (Degree)	γ_d (kN/m^3)	Failure Load, P_f (N)
1	8	36	13.73	5200
1	6	38	15.7	7536
1	4	40	17.66	11670
2	4	32	15.7	2780
2	6	40	13.73	9540
2	6	38	15.7	7288
2	8	36	17.66	6600
3	4	32	15.7	2784
3	4	38	15.7	6888
3	4	40	17.66	12705
3	6	36	15.7	5190
3	8	32	13.73	2448

Table 5.8: PLAXIS Results of Compression Tests for $N_a=3$

n_b	H/B	Φ (Degree)	γ_d (kN/m^3)	Failure Load, P_f (N)
1	2	32	15.7	2670
1	2	40	17.66	12045
1	4	32	15.7	2817
1	4	40	13.73	10155
1	6	38	15.7	8330
1	6	40	17.66	11820
1	8	36	13.73	5300
2	2	32	15.7	2674
2	6	40	17.66	13620
2	8	36	13.73	4805

2	8	38	15.7	7227
3	4	32	15.7	2808
3	4	38	15.7	7792
3	6	40	17.66	10875
3	8	36	13.73	5256

Table 5.9: PLAXIS results of Compression Tests for $N_a=4$

n_b	H/B	Φ (Degree)	γ_d (kN/m^3)	Failure Load, P_f (N)
1	4	32	13.73	2467
1	4	36	15.7	6032
1	4	38	15.7	7608
1	6	38	15.7	7389
1	6	40	13.73	9090
1	6	40	17.66	12075
1	8	40	17.66	13335
2	4	32	15.7	2832
2	6	40	13.73	8700
2	8	36	17.66	6699
2	8	38	15.7	7032
3	4	32	15.7	2817
3	4	38	15.7	8210
3	6	32	17.66	12900
3	6	36	17.66	6804
3	6	40	13.73	8450
3	6	40	15.7	9890
3	6	40	17.66	12870
3	8	32	17.66	3405

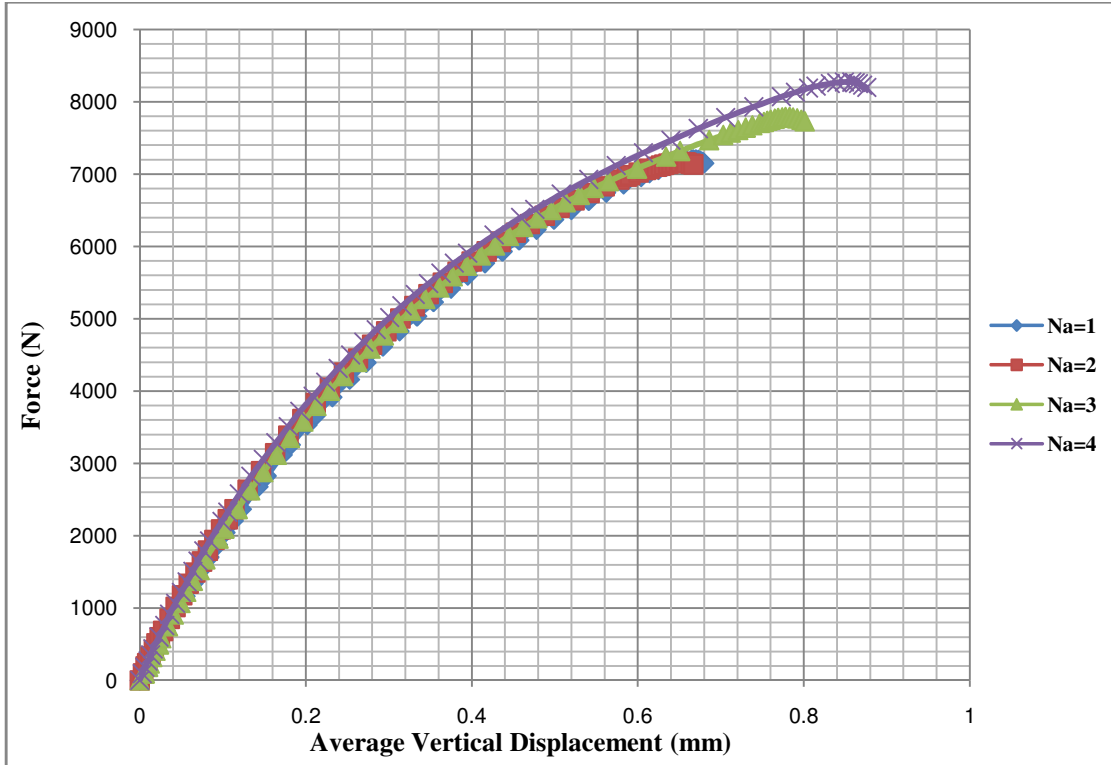


Fig. 5.4: PLAXIS Run in Compression for $n_b = 1$, $H/B=6$ and $N_a = 1, 2, 3$ & 4

5.5 PLAXIS RESULTS FOR PULLOUT

The numerical investigations were carried out by taking the various components same as taken as for compression case. In PLAXIS, pullout tests were carried out for embedment depth ratio of 4, 6 and 8. PLAXIS results for pullout are shown in Tables 5.10, 5.11, 5.12 and 5.13. Based on the PLAXIS results shown in these tables, load-displacement curves were plotted to highlight variation in ultimate pullout capacity with the variation in no. of anchors, embedment depth ratio and no. of screw blades in the anchor as shown in Figs. 5.7, 5.8 and 5.9.

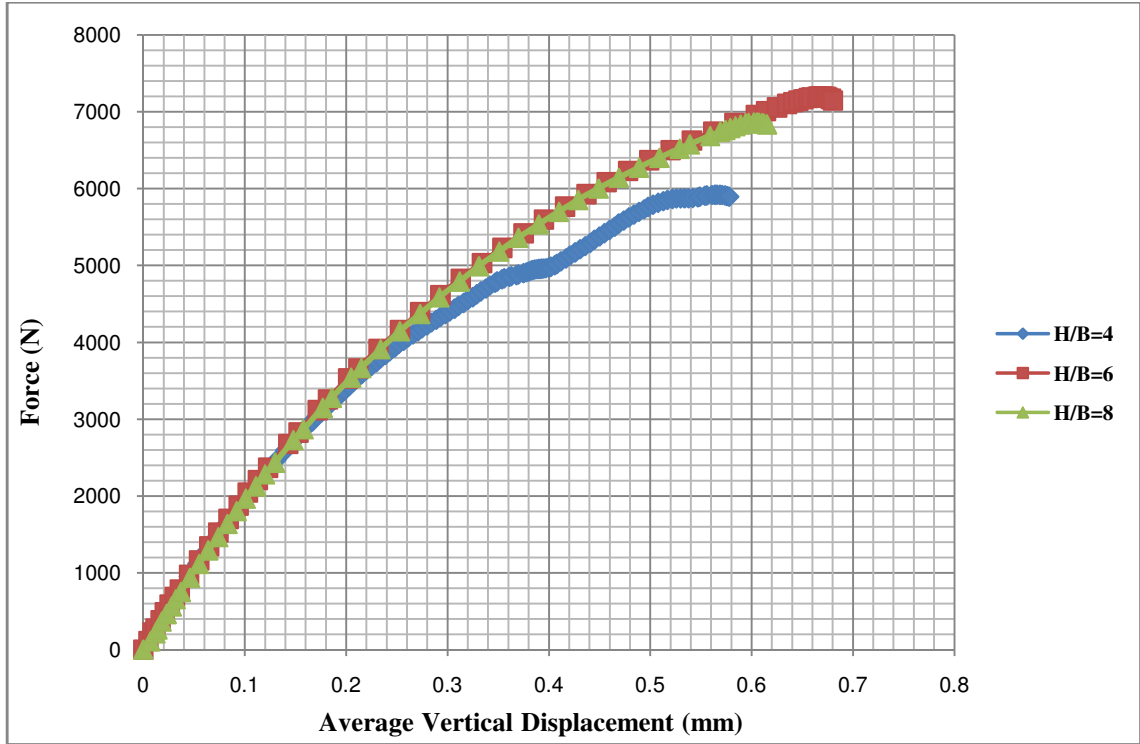


Fig. 5.5: PLAXIS Run in Compression for $n_b = 1$, $N_a = 1$ and $H/B = 4, 6$ & 8

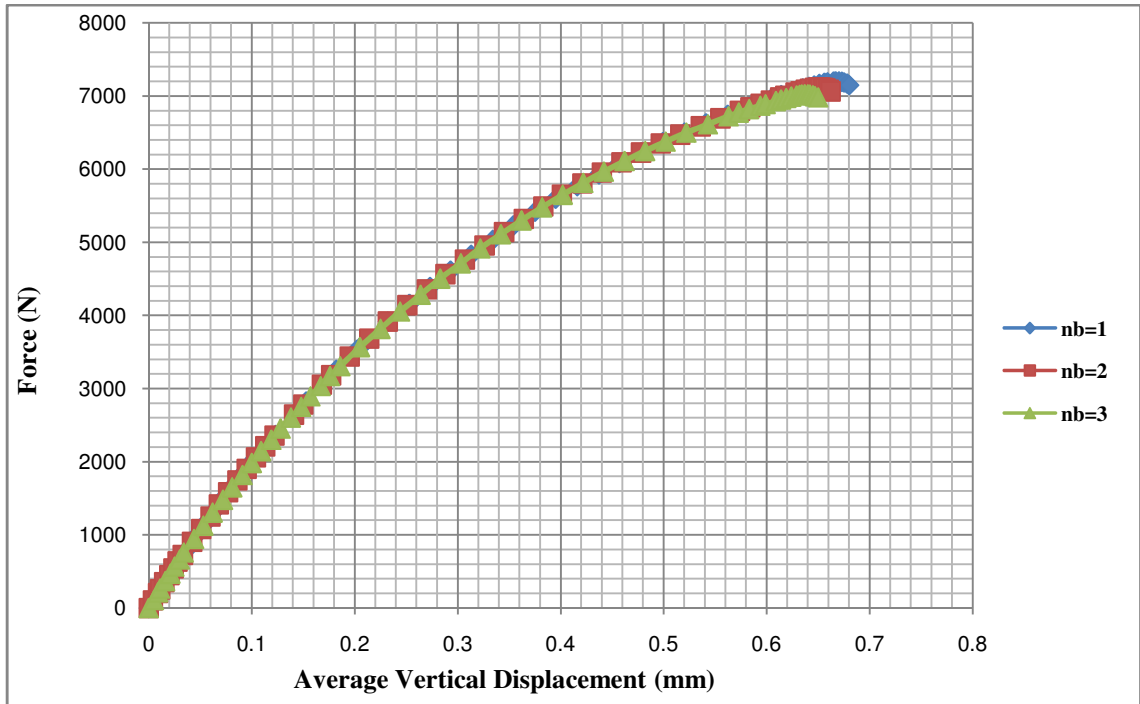


Fig. 5.6: PLAXIS Run in Compression for $N_a = 1$, $H/B = 6$ and $n_b = 1, 2$ & 3

Table 5.10: PLAXIS Results of Pullout Tests for $N_a=1$

n_b	H/B	Φ (Degree)	γ (kN/m^3)	Failure Load, P_f (N)
1	4	40	17.66	123
1	6	36	15.7	158
1	8	32	13.73	150
1	8	38	15.7	308
2	4	40	17.66	129
2	6	36	15.7	147
2	6	38	15.7	167
2	8	32	13.73	161
3	4	40	17.66	127
3	6	36	15.7	151
3	6	38	15.7	152
3	8	32	13.73	149
3	8	38	15.7	194
3	8	38	17.66	212

Table 5.11: PLAXIS Results of Pullout Tests for $N_a=2$

n_b	H/B	Φ (Degree)	γ (kN/m^3)	Failure Load, P_f (N)
1	4	32	15.7	123
1	6	36	13.73	244
1	6	36	17.66	282
1	6	38	15.7	277
1	8	40	15.7	548
1	8	40	17.66	600
1	6	40	17.66	320
1	8	38	15.7	498
2	4	32	15.7	121
2	6	38	15.7	281
2	6	40	13.73	120
2	8	36	17.66	173
3	4	38	15.7	93.5
3	4	40	17.66	96
3	6	36	15.7	246
3	6	40	17.66	304
3	8	32	13.73	94
3	6	38	15.7	251

Table 5.12: PLAXIS Results of Pullout Tests for $N_a=3$

n_b	H/B	Φ (Degree)	γ (kN/m ³)	Failure Load, P_f (N)
1	4	32	15.7	716
1	4	40	13.73	167
1	6	38	15.7	245
1	6	40	17.66	284
1	8	32	15.7	355
2	4	32	15.7	148
2	6	38	15.7	85
2	6	40	17.66	282
2	8	36	13.73	442
3	4	32	15.7	147
3	4	36	15.7	163
3	4	38	15.7	85
3	6	38	15.7	192
3	6	40	17.66	232
3	8	36	13.73	430
3	8	36	17.66	533

Table 5.13: PLAXIS Results of Pullout Tests for $N_a=4$

n_b	H/B	Φ (Degree)	γ (kN/m ³)	Failure Load, P_f (N)
1	4	38	15.7	213
1	4	40	17.66	235
1	6	38	15.7	362
1	6	40	13.73	346
1	6	40	17.66	432
1	8	32	15.7	112
1	8	36	13.73	392
1	8	36	17.66	595
1	8	38	15.7	489
2	4	32	15.7	169
2	6	40	13.73	340
2	6	40	17.66	422
2	8	36	17.66	193
2	8	38	15.7	583
3	4	32	15.7	94
3	4	38	15.7	179
3	6	40	13.73	326
3	6	40	17.66	411

3	8	36	13.73	461
3	8	36	15.7	529
3	8	36	17.66	584
3	8	38	15.7	569

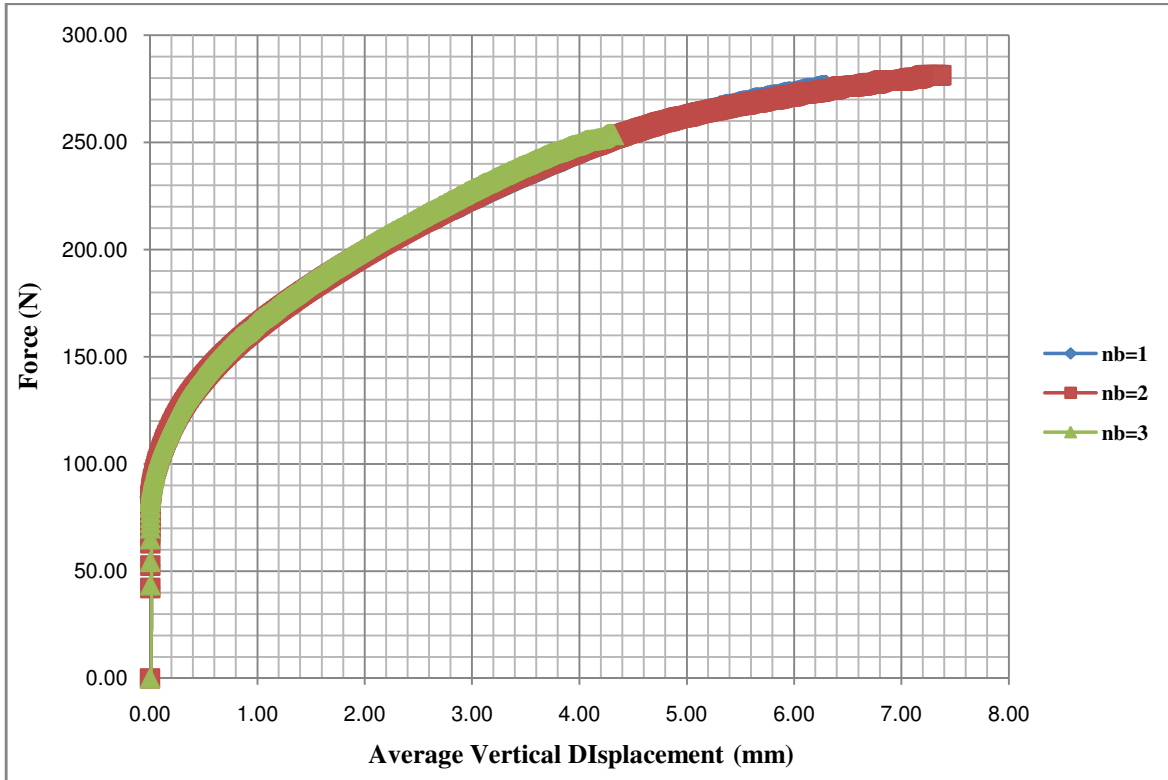


Fig. 5.7: PLAXIS Run in Pullout for $N_a=2$, $H/B=6$ and $n_b=1, 2$ & 3 .

5.6 COMPARISON OF PLAXIS WITH LABORATORY WORK

To validate the results obtained from the laboratory tests, comparison of its results were done with PLAXIS results. This comparison was done in non-dimensional form. For comparison purpose a non-dimensional factor $P_f/(\gamma_d B H \delta_f)$ was defined where P_f is the failure load, γ_d is the unit wt. of sand, B is the diameter of the helical screw of the anchor, H is the embedment depth of the anchor and δ_f is the deformation of the anchor at failure.

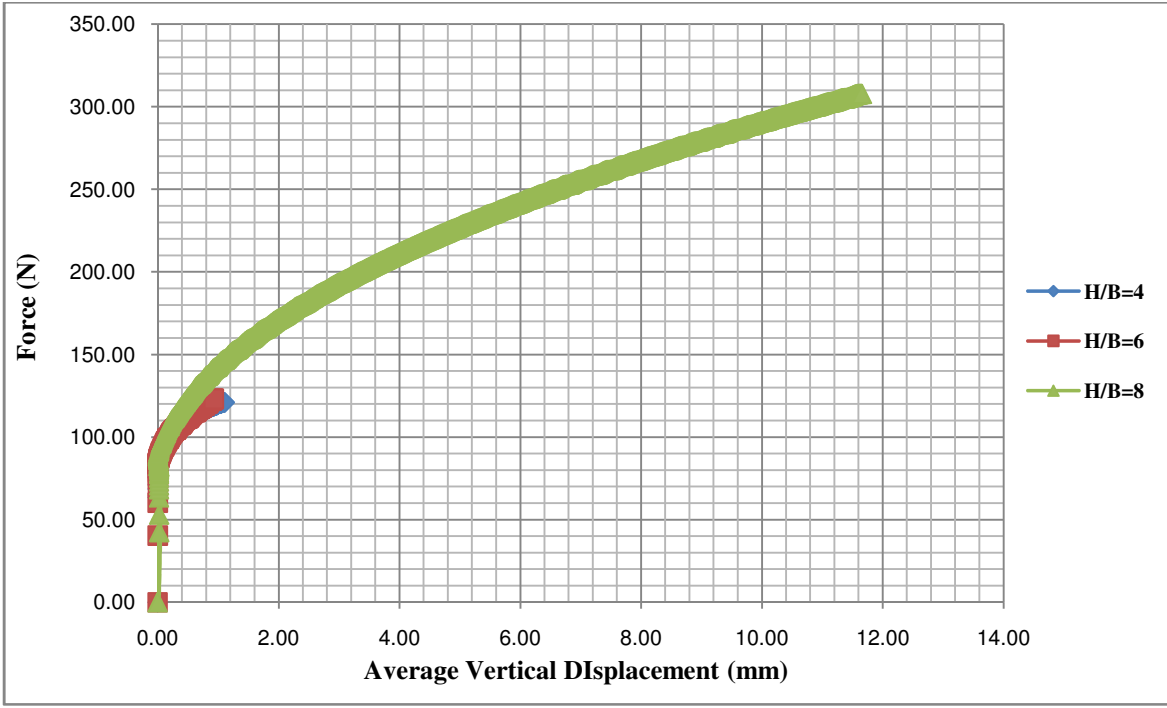


Fig. 5.8: PLAXIS Run in Pullout for $n_b = 1$, $N_a = 1$ and $H/B = 4, 6 \text{ \& } 8$

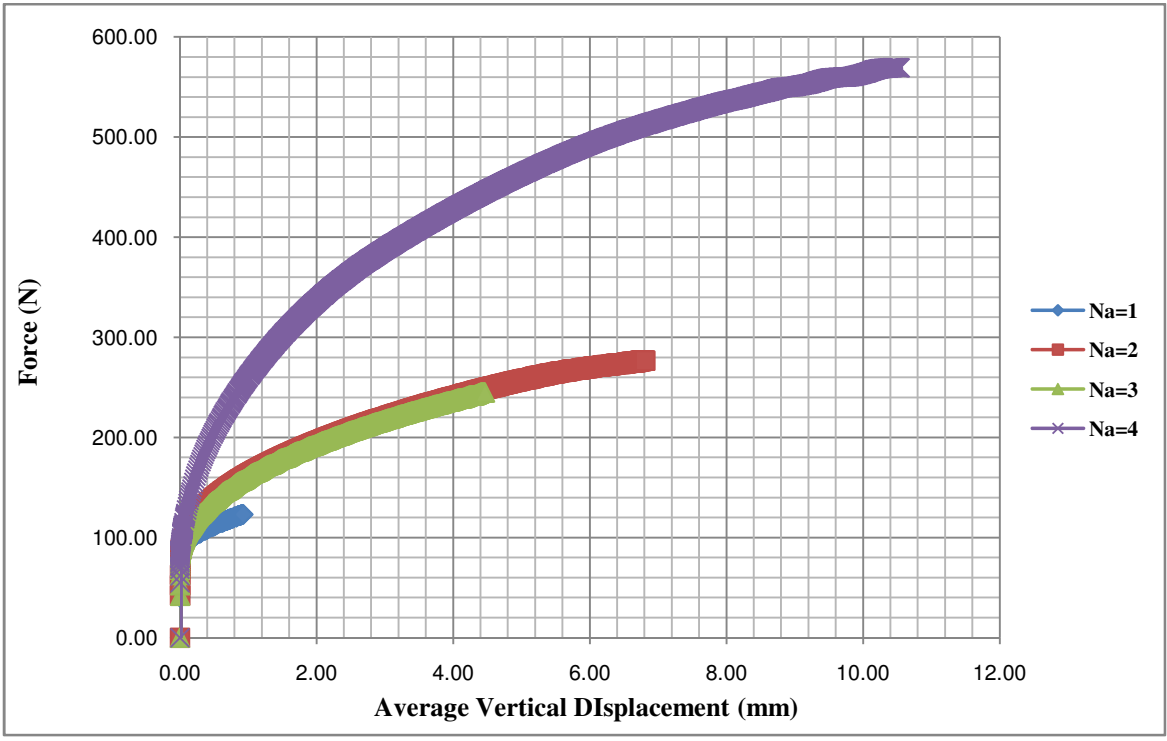


Fig. 5.9: PLAXIS Run in Pullout for $n_b = 1$, $H/B = 6$ and $N_a = 1, 2, 3 \text{ \& } 4$

5.6.1 Comparison with Laboratory Compression Testing

The results obtained by conducting PLAXIS runs on the model similar to the one on which laboratory experiments were conducted were compared with results obtained by laboratory experiments themselves.

Table 5.14 shows the comparison in non-dimensional form. From this table it is clear that the difference between laboratory test and PLAXIS results is within 10% which can be neglected.

Table 5.14: Comparison of Non-dimensional Parameter $P_f/(\gamma_d B H \delta_f)$ from Laboratory Experiment and PLAXIS Run for Compression Tests

N_a	n_b	H/B	$P_f/(\gamma_d B H \delta_f)$		% diff
			LAB Test	PLAXIS	
1	1	4	59535.41	65237.04	8.74
1	1	6	40745.87	44934.23	9.32
1	1	8	32319.35	35575.58	9.15
1	2	6	41649.98	45618.69	8.7
1	3	6	41110.74	45918.67	10.47
2	1	6	41881.16	46110.79	9.17
2	2	6	40895.58	45112.13	9.34
2	3	4	65867.37	72999.35	9.77
3	1	6	35977.61	39389.25	8.66
3	2	8	32936.84	34767.26	8.89
3	3	4	58016.38	62982.96	7.89
4	1	4	60805.28	65573.20	7.27
4	1	6	37383.64	41372.51	9.64
4	2	8	33372.90	37200.84	10.29
4	3	4	56165.46	60037.88	6.45

5.6.2 Comparison with Laboratory Pullout Testing

The results obtained by conducting PLAXIS runs on the model similar to the one on which laboratory experiments were conducted were compared with results obtained by laboratory experiments themselves. Table 5.15 shows the comparison in non-dimensional form. From this table it is clear that the difference between laboratory test and PLAXIS results is within 10% which can be neglected.

Table 5.15: Comparison of Non-dimensional Parameter $P_f/(\gamma_d B H \delta_f)$ from Laboratory Experiment and PLAXIS Run for Pullout Tests

N_a	n_b	H/B	$P_f/(\gamma_d B H \delta_f)$		% diff
			LAB Test	PLAXIS	
1	1	4	759.43	694.32	8.56
1	1	6	529.15	562.21	6.05
1	2	6	203.99	184.14	9.36
1	3	6	304.39	279.05	8.22
2	1	6	208.25	186.61	10.09
2	2	6	179.51	161.88	9.49
2	3	6	289.38	260.78	9.69
3	1	6	258.16	232.95	9.69
3	2	6	305.29	278.83	8.52
3	3	4	1737.88	1923.37	9.62
4	1	4	435.49	400.20	8.04
4	1	6	344.23	311.16	9.59
4	3	4	2956.75	2734.12	7.54

CONCLUSIONS AND RECOMMENDATIONS

In this chapter, summary of research work done on the behaviour of helical screw anchors under compressive and pullout load is presented. The major conclusions of the study are discussed below.

6.0 SUMMARY

Anchors are widely used for variety of structures like transmission towers, buried pipelines, retaining walls, bridges and waterfront structures. Predicting the stability of anchors plays a key role in the design of many civil engineering works. As the current understanding of the behaviour of anchor was unsatisfactory, this made the basis for planning of current research program.

The aims for the study of anchor behaviour presented in this thesis were two fold; firstly, to better understand anchor behaviour and to develop easy stability solutions that can be used to solve practical anchor foundation problems; and secondly, to verify the application of recently developed numerical software, in particular finite element methods based on limit theorems of classical plasticity. With this objective in mind, the present study program was carefully planned and carried out.

The majority of past research on anchor behaviour had been on the basis of experimental study and, as a result, such current design practices are largely based on empirical relationships. Very few rigorous numerical analyses were performed to determine the ultimate compressive and pullout load of anchors. This fact was highlighted in Chapter 2 of the present report. A detailed review of literature on the subject of the axial capacity of the screw anchors narrowed down the study parameters. Anchors were then designed and instrumented for the purpose of studying these parameters. For the test sites, the engineering properties of the sand were obtained by conducting a number of tests in the laboratory tests as outlined in Chapter 3.

In contrast to most previous studies, the significance of a wide range of variables which influence anchor capacity has been investigated. Broadly speaking, the work presented in this thesis can be divided into three distinct categories; namely; the experimental investigation of helical screw anchors under compressive loads; the experimental investigation of helical screw

anchors under pullout load; and the numerical investigation of helical screw anchors using software PLAXIS.

The results obtained from the test indicate that the bearing capacity in compression is much higher than that in tension. The soil above the top helix plate of the anchor is disturbed by the rotary action of the anchor during the installation whereas the soil below the bottom helix plate is not disturbed at all. In compression, bearing capacity component comes from the soil below the bottom helix plate whereas in tension it comes from the soil above the top helix plate. That is why bearing capacity in case of compression are much higher than tension.

6.1 COMPRESSIVE CAPACITY OF HELICAL SCREW ANCHORS

In Chapter 3, the investigations on compressive capacity of helical screw anchors are presented and in chapter 4 these results are discussed thoroughly. For design purposes, parametric equations have been provided that enable the compressive capacity of helical screw anchors to be predicted reliably. Such equations can be used to solve practical design problems.

The major conclusions of experimental and numerical investigations carried out are as given below:

1. With the increase in embedment depth ratio from 2 to 8, the ultimate compressive capacity of helical screw anchor were increased from 981 N to 5150 N for no. of anchors equal to 1 and no. of screw blades in an anchor equal to 3. Here the most important observation is that for initial increase in H/B (i.e. for increase in H/B from 2 to 4), the increase in Q_{uc} is 65%, while for further increase in H/B (i.e. for increase in H/B from 6 to 8); the increase in Q_{uc} is 28% which is quite less than earlier increase.
2. With the increase in no. of anchors from 1 to 4, the ultimate compressive capacity of helical screw anchor were increased from 2796 N to 7848 N for no. of screw blades in an anchor equal to 3 and embedment depth ratio equal to 4. Here the most important observation is that for initial increase in N_a ; the increase in Q_{uc} is 57% (i.e. for increase in N_a from 1 to 2), while for further increase in N_a ; the increase in Q_{uc} is 19% (i.e. for increase in N_a from 3 to 4) which is less than earlier increase.
3. With the increase in no. of screw blades in an anchor from 1 to 3, the ultimate compressive capacity of helical screw anchor were increased from 5346 N to 7848 N

for embedment depth ratio H/B equal to 4 and number of anchors N_a equal to 4. Here the most important observation is that for initial increase in n_b ; the increase in Q_{uc} is 27% (i.e. for increase in n_b from 1 to 2), while for further increase in n_b ; the increase in Q_{uc} is 6% (i.e. for increase in n_b from 2 to 3) which is less than earlier increase.

4. It is clear from the above results that the increase in capacity is prominent with the initial increase of these parameters only. There will not be any significant increase in the capacity with further increase in the values of these parameters.

6.2 PULLOUT CAPACITY OF HELICAL SCREW ANCHORS

In Chapter 3, the investigations on pullout capacity of helical screw anchors are presented and in chapter 4 these results are discussed thoroughly. For design purposes, parametric equations have been provided that enable the pullout capacity of helical screw anchors to be predicted reliably. Such equations can be used to solve practical design problems.

The major conclusions of experimental and numerical investigations carried out are as given below:

1. With the increase in embedment depth ratio from 4 to 10, the ultimate pullout capacity of helical screw anchor were increased from 441 N to 5837 N for no. of anchors equal to 4 and no. of screw blades in an anchor equal to 3. Here the most important observation is that for initial increase in H/B (i.e. for increase in H/B from 4 to 6), the increase in Q_{up} is 73%, while for further increase in H/B (i.e. for increase in H/B from 8 to 10); the increase in Q_{up} is 37% which is quite less than earlier increase.
2. With the increase in no. of anchors from 1 to 4, the ultimate pullout capacity of helical screw anchor were increased from 132 N to 441 N for no. of screw blades in an anchor equal to 1 and embedment depth ratio equal to 4. Here the most important observation is that for initial increase in N_a ; the increase in Q_{up} is 46% (i.e. for increase in N_a from 1 to 2), while for further increase in N_a ; the increase in Q_{up} is 27% (i.e. for increase in N_a from 3 to 4) which is quite less than earlier increase.
3. With the increase in no. of screw blades in an anchor from 1 to 3, the ultimate pullout capacity of helical screw anchor were increased from 2158 N to 3188 N for embedment depth ratio H/B equal to 10 and number of anchors N_a equal to 2. Here

the most important observation is that for initial increase in n_b ; the increase in Q_{up} is 23% (i.e. for increase in n_b from 1 to 2), while for further increase in n_b ; the increase in Q_{up} is 12% (i.e. for increase in n_b from 2 to 3) which is very marginal.

4. It is clear from the above results that the increase in capacity is prominent with the initial increase of parameters only. There will not be any significant increase in the capacity with further increase in the values of these parameters.
5. The value of angle of internal friction increases from 35° for virgin soil to 48° for soil with 4 nos. of double helical screw anchors.
6. Apparent coefficient of friction between the anchor and the soil (f^*) which plays an important role in determining the strength of anchors increases with embedment depth ratio and no. of anchors. For compression it increases from 3.73 to 17.58 (increased by almost 371 % with increase in no. of anchors from 1 to 4, embedment depth ratio from 2 to 8 and no. of screw blades in an anchor from 1 to 3) whereas for pullout it increases from 1.39 to 10.02 (increased by almost 620 % with increase in no. of anchors from 1 to 4, embedment depth ratio from 4 to 10 and no. of screw blades in an anchor from 1 to 3).
7. Theoretical formulation is done for ultimate pullout capacity of anchor for single helical screw anchor. By comparison it can be said that the difference between the theoretical and experimental values is minimal. Hence it can be said that for deep depths, the present theory in this paper predicts the ultimate pullout capacity of multiple helical screw anchors with sufficient accuracy.

6.3 NUMERICAL VALIDATION

In Chapter 5, modeling of the helical screw anchor for compressive and pullout load is presented. These values are compared with the values obtained from laboratory testing. From Tables 5.14 and 5.15 it is clear that the difference between PLAXIS and laboratory values are within 10% which is very marginal.

6.4 SCOPE FOR FUTURE RESEARCH

The research work presented in this thesis is confined to compressive and pullout behaviour of helical screw anchors in sand. In preparing this thesis, several areas of potential future research were identified and these are as discussed below:

1. The sand assumed in this thesis is homogenous, isotropic and behaves in a nonlinear stress strain relationship. Another interesting direction for future research concerns estimating the capacity of anchors in layered soil.
2. Anchors may be tested in actual field conditions and their results be compared with laboratory model tests by using dimensional analysis.

LIST OF REFERENCES

1. Akinmusuru, J.O. (1978), "Horizontally Loaded Vertical Plate Anchors in Sand", *Journal of Geotechnical Engineering Division, ASCE*, Vol.104, No. 2, pp. 283-286.
2. Basudhar, P. K. and Singh, D. N. (1994), "A generalized procedure for predicting optimal lower bound break-out factors of strip anchors", *Geotechnique*, Vol. 44 (2), 307-318.
3. Boominathan, A. and Hari, S. (2002), "Liquefaction strength of fly ash reinforced with randomly distributed fibers", *Soil Dynamics and Earthquake Engineering*, Vol. 22, No. 9, pp. 1027 – 1033.
4. Boominathan, A., Rangaswamy, K. and Rajagopal, K. (2006), "Effect of method of sample preparation on liquefaction resistance of sands in cyclic triaxial testing", *Proceedings of Indian Geotechnical Conference, IIT Madras*, Vol. 2, pp. 833-836.
5. Bouazza, A. and Finlay, T. W. (1990), "Uplift capacity of plate anchors buried in a two-layered sand", *Geotechnique*, Vol. 40 (2), 293-297.
6. Brinkgreve, R. B. J., Engin, E. and Swolfs, W. M. (2013), "PLAXIS 3D 2013", Delft, Netherlands.
7. Chandra, S., Iyengar, N.G.R., and Valsangkar, A.J. (1982), "Flexural Response of Footings on Bilinear Foundation", *Journal of Inst. of Engineers (India)*, Vol. 63, pt. C12, pp. 49-55
8. Chandra, S., Madhav, M. R. and Iyengar, N. G. R. (1984), "Trapezoidal Footings on Nonlinear Subgrades", *Int. Journal of Numerical and Analytical Methods in Geomechanics*, Vol. 8, No. 6, pp. 519 – 529.

9. Chandra, S. and Ojha, P.N. (2005), "Time Dependent Behaviour of Geosynthetic Reinforced Granular Fill-Soft Soil System Subjected to Strip Loading", *Indian Geotechnical Journal*, Vol.35, No.3, pp. 267-282.
10. Chattopadhyay, B. C., and Pise, P. J. (1986), "Uplift capacity of pile in sand" *J. Geotech. Eng.*,112 (9), 888–904.
11. Choudhury, D. and Katdare, A. D. (2013), "New approach to determine seismic passive resistance on retaining walls considering seismic waves", *International Journal of Geomechanics*, ASCE, Vol. 13, No. 6, pp. 852-860.
12. Clemence, S.P., Crouch, L.K., and Stephenson, R.W. (1994), "Prediction of Uplift Capacity for Helical Anchors in Sand", *Proceedings of the 2nd Geotechnical Engineering Conference*, Cairo, Vol. 1, pp. 332-343.
13. Das, B. M., Seeley, G. R. and Das, S. C. (1976), "Ultimate resistance of deep vertical anchors in sand", *Soils and Foundations*, Vol. 17, 52-56.
14. Dash, B. K. and Pise, P. J. (2003), "Effect of compressive load on uplift capacity of model piles", *ASCE*, Vol. 129, No. 11, pp. 987 – 992.
15. Deshmukh, V. B., Dewaikar, D. M. and Choudhury, D. (2010), "Analysis of rectangular and square anchors in cohesionless soil", *International Journal of Geotechnical Engineering*, Vol. 2, No. 4, pp. 79-87.
16. Deshmukh, V. B., Dewaikar, D. M. and Choudhury, D. (2011), "Uplift Capacity of Horizontal Strip Anchors in Cohesionless Soil", *Geotech Geol Engg*, Vol. 29, No. 4, 977-988.
17. Dickin, E.A. and Laman, M. (2007), "Uplift response of strip anchors in cohesionless soil", *Advances in Engineering Software*, Elsevier, Vol. 38, No. 1, pp. 618-625.

18. Elsherbiny, Z. H. and Naggar, M. H. EI. (2013), "Axial compressive capacity of helical piles from field tests and numerical study", Canadian Geotechnical Journal, Vol. 50, No. 12, pp. 1191-1203.
19. Gavin, K., Doherty, P. and T. Ali (2014), "Field investigation of the axial resistance of helical piles in dense sand", Canadian Geotechnical Journal, Vol. 51, No. 10, pp. 1343 – 1354.
20. Geddes, J. D. and Murray E. J. (1996), "Plate anchor groups pulled vertically in sand", J. Geotech. Engg, ASCE, Vol. 122 (7), 509-516.
21. Ghaly, A. M. and Hanna, A. (1991), "Experimental and theoretical studies on installation torque of screw anchors", Canadian Geotechnical Journal, Vol. 28, No. 3, pp. 353 – 364.
22. Ghaly, A. M., Hanna, A. and Hanna, M. (1991), "Uplift behavior of screw anchors in sand.1: Dry Sand", J. Geotech. Engg, ASCE, Vol. 117(5), 773-793.
23. Ghaly, A. M. and Hanna, A. M. (1994), "Ultimate Pullout Resistance of Single Vertical Anchors", Can. Geotech. J., Vol. 31, No. 5, 661–672.
24. Hanna, T.H. and Carr, R.W. (1971), "The Loading Behaviour of Plate Anchors in Normally and Over Consolidated Sands", Proc. 4th Inter Conf. on Soil Mech. & Found Engg. Budapest, 589–600.
25. Hanna, T. H., Sparks, R., and Yilmaz, M. (1972), "Anchor behavior in sand", J. Geotech. Engg, ASCE, 98(11), 1187-1208.
26. Hanna, A. and Ghaly, A. M. (1992), "Effects of K_o and overconsolidation on uplift capacity", J. Geotech. Engg, ASCE, 118(9), 1449-1469.

27. Hanna, A. M. and Ghaly, A. M. (1994), "Ultimate Pullout Resistance of groups of Vertical Anchors", *Can. Geotech. J.*, Vol. 31, No. 5, 673–682.
28. Hanna, A., Ayadat, T. and Sabry, M. (2007), "Pullout resistance of single vertical shallow helical and plate anchors in sand", *Geotech Geol Engg*, Springer, Vol. 25, No. 5, pp. 559-573.
29. Ilamparuthi, K. and Muthukrishnaiah, K. (1999), "Anchors in sand bed: delineation of rupture surface", *Ocean Engineering*, Elsevier, Vol. 26, 1249-1273.
30. Ilamparuthi, K., Dickin, E.A. and Muthukrishnaiah, K. (2002), "Experimental investigation of the uplift behavior of circular plate anchors embedded in sand", *Can. Geotech. J.*, Vol. 39 (3), 648–664.
31. Indian Standard IS: 2720 (Part XIV, 1968), Bureau of Indian Standards, New Delhi.
32. Indian Standard IS: 1498 – 1970 (reaffirmed 1987), Bureau of Indian Standards, New Delhi.
33. Khatri V.N. and Kumar, J. (2011), "Effect of anchor width on pullout capacity of strip anchors in sand", *Canadian Geotechnical Journal*, Vol. 48 (3), 511-517.
34. Koprivica, S. (2009), "Uplift behavior of shallow horizontal plate anchors in sand", *International Journal of Geotechnical Engg*, Vol. 3 (4), 485-491.
35. Kumar, J. (2003), "Uplift resistance of strip and circular anchors in a two layered sand", *Soils and foundations*, Vol. 43, No. 1, pp. 101-107.
36. Kumar, J. (2006), "Uplift response of strip anchors in sand using FEM", *Iranian Journal of Science & Technology*, Vol. 30, No. B4, pp. 475 – 486.

37. Kumar, J. and Bhoi, M. K. (2008), "Interference of Multiple Strip Footings on Sand Using Small Scale Model Tests", *Geotech Geol Engg*, Springer, Vol. 26, No. 4, pp. 469-477.
38. Kumar, J., and Kouzer, K. M. (2008a), "Vertical uplift capacity of a group of shallow horizontal anchors in sand", *Geotechnique*, Vol. 58, No. 10, pp. 821-823.
39. Kumar, J., and Kouzer, K. M. (2008b), "Vertical uplift capacity of horizontal anchors using upper bound limit analysis and finite elements", *Canadian Geotechnical Journal*, Vol. 45, No. 5, pp. 698-704.
40. Kumar, J. and Bhoi, M. K. (2009), "Vertical Uplift Capacity of Equally Spaced Multiple Strip Anchors in Sand", *Geotech Geol Engg*, Springer, Vol. 27, No. 3, pp. 461-472.
41. Kumar, J., and Kouzer, K. M. (2009), "Vertical uplift capacity of two interfering horizontal anchors in sand using an upper bound limit analysis", *Computers and Geotechnics*, Elsevier, Vol. 36, No. 6, pp. 1084-1089.
42. Kumar, J. and Bhoi, M. K. (2010), "Vertical uplift resistance of a group of two strip anchors in sand from model tests", *International Journal of Geotechnical Engg*, Vol. 4, No. 2, pp. 269-277.
43. Kumar, J., and Bhattacharya, P. (2012), "Horizontal Pullout Capacity of a Group of Two Vertical Strip Anchors Plates Embedded in Sand", *Geotech Geol Engg*, Springer, Vol. 30, No. 2, pp. 513 – 521.
44. Kumar, J., and Naskar, T. (2012), "Vertical uplift capacity of a group of two coaxial anchors in a general $c-\Phi$ soil", *Canadian Geotechnical Journal*, Vol. 49, No. 2, pp. 367–373.

45. Kumar, J., and Sahoo, J. P. (2012 a), "Vertical uplift resistance of two horizontal strip anchors with common vertical axis", International Journal of Geotechnical Engg, Vol.4, No. 6, pp. 485-495.
46. Kumar, J., and Sahoo, J. P. (2012 b), "Upper Bound Solution for Pullout Capacity of Vertical Anchors in Sand Using Finite Elements and Limit Analysis", International Journal of Geomechanics, ASCE, Vol. 12, No. 3, pp. 333-337.
47. Kumar, J., and Sahoo, J. P. (2014), "Vertical uplift resistance of two closely spaced horizontal strip anchors embedded in cohesive-frictional weightless medium", Canadian Geotechnical Journal, Vol. 51, No. 2, pp. 223- 230.
48. Latha, G.M. and Amit Somwanshi (2009) "Effect of reinforcement form on the performance of square footings on sand ", Geotextiles and Geomembranes, Vol. 27, pp. 409-422.
49. Latha, G.M., Somawanshi, A. and Reddy, K.H. (2013)"A Multiple Regression Equation for Prediction of Bearing Capacity of Geosynthetic Reinforced Sand Beds", Indian Geotechnical Journal, Springer, Vol. 43, No. 4, pp. 331-343.
50. Latha, G. M. and Varman, A. M. N. (2014)"Geosynthetics in unpaved roads", International Journal of Geotechnical Engineering, Special Issue on Geosynthetics, Vol. 8, No. 3, 209-306.
51. Liu, J., Liu, M. and Zhu Z. (2012), "Sand deformation around an uplift plate anchor", J. Geotech. Engg, ASCE, Vol. 138, No. 6, pp. 728 – 737.
52. Livneh, B. and Naggar, M. H. EI (2008), "Axial testing and numerical modeling of square shaft helical piles under compressive and tensile loading", Canadian Geotechnical Journal, Vol. 45 (3), 1142-1155.

53. Lutenecker, A. J. (2011), "Behavior of Multi-Helix Screw Anchors in Sand", In Proceedings of the 14th Pan-American Conference on Soil Mechanics and Geotechnical Engineering, Toronto, Ont. [CD ROM].
54. Madabhushi, S. P. G. and Zeng, X (1998), "Seismic response of gravity quay walls II: numerical modeling", ASCE, Journal of Geotechnical and Geoenvironmental Engineering, Vol. 124. pp. 418-427.
55. Madabhushi, S. P. G. (2007), "Ground improvement methods for liquefaction remediation", Ground Improvement, 11. pp. 195-206.
56. Madabhushi, S. P. G. and Haigh, SK (2010), "Effect of superstructure stiffness on liquefaction-induced failure Mechanisms", International Journal of Geotechnical Earthquake Engineering, 1. pp. 71-87.
57. Malik, R. (2007), "Performance study of anchor piles in load tests (Pull out and lateral)", M. Tech. Dissertation, IIT Roorkee, India.
58. Merifield, R. S., Lyamin, A. V. and Sloan, S. W. (2006), "Three-dimensional lower-bound solutions for the stability of plate anchors in sand", Geotechnique, Vol. 56 (2), 123-132.
59. Merifield, R. S. (2011), "Ultimate uplift capacity of multi plate helical type anchors in clay", J. Geotech. Engg, ASCE, Vol. 137(7), 704-716.
60. Meyerhof, G. G., and Adams, J. I. (1968), "The ultimate uplift capacity of foundations", Canadian Geotech. J., Vol. 5, No. 4, 224-244.
61. Meyerhof, G. G. (1973), "Uplift resistance of inclined anchors and piles", Proceedings of 8th ICSMFE, Vol. 2, 167-172.

62. Mitsch, M. P. and Clemence, S.P. (1985), “The uplift capacity of helical anchors in sand”, Uplift Behavior of Anchor Foundations in Soil, Editor, S.P. Clemence, ASCE, New York, pp. 26 – 47.
63. Mittal, S., Shekhar S. and Ganjoo B. (2010), “Static Equilibrium of screw anchor pile under lateral load in sands”, Geotech&Geol Eng., Springer, Vol. 28, 717-725.
64. Mittal, S. (2013), “An Introduction to Ground Improvement Engineering”, SIPL Publications, New Delhi, India.
65. Mittal, S. and Shukla, J. P. (2013), “Soil Testing for Engineers”, CBS Publishers & Distributors, Delhi – 110006.
66. Murray, E. J. and Geddes, J. D. (1987), “Uplift of anchor plates in Sand”, J. Geotech. Engg, ASCE, Vol. 113, No. 3, pp. 202 – 215.
67. Nazir, R., Chuan, H. S., Niroumand, H. and Kassim, K. A. (2014), “Performance of single vertical helical anchor embedded in dry sand”, Elsevier, Vol. 49, No. 3, pp. 42 - 51.
68. Neely, W. J., Stewart, J. G. & Graham, J. (1973), “Failure loads of vertical anchor plates in sand”, J. Geotech. Engg, ASCE, Vol. 99(9), 669-685.
69. Popadopolou, K., Saroglou, H. and Popadopoulos, V. (2014), “Finite element analysis and experimental investigation of helical micropiles”, Geotechnical and Geological Engg., Springer, Vol. 32, No. 4, pp. 949-963.
70. Powrie, W. and Cox, S. (2001), “Horizontal wells for leachate control in landfill”, Ground Engineering, Vol. 34, No. 1, 18-19.
71. Powrie, William and White, James(2004), “Landfill process modelling”, Waste Management, Vol. 24, No. 3, pp. 225-226.

72. Powrie, W. and Daly, M.P. (2007),“Centrifuge modelling of embedded retaining walls with stabilizing bases”, *Geotechnique*, Vol. 57, No. 6, 485-497.
73. Puppala, A.J., Porbaha, A., Bhadriraju, V, (2004), “In Situ Methods and Their Quality Assessments in Ground Improvement Projects.” *Proceedings, 2nd International Conference on Site Characterization, Portugal.*
74. Puppala, A.J., Saride, S. Dronamraj, V., Pulijan, V., Cai, G., and Perrin, L. (2010), “Assessment of Stabilization Methods to Control Surficial Slope Failures”, *Transportation Research Board Annual Meeting, Washington, DC, CDROM Proceedings*
75. Puppala, A.J., Saride, S., and Chittoori, B.S. (2012),“Sulfate Induced Heaving: A Hurdle for Light Infrastructure Development.” *Indian Geotechnical Journal, Springer Publishers, Volume 42.*
76. Ranjan, G and Rao, A. S. R. (2000), “Basic and Applied Soil mechanics”, *New Age International Publishers.*
77. Reddy, K.R., Hettiarachchi, H., Gangathulasi, J., and Bogner, J.E. (2011). “Geotechnical properties of municipal solid waste at different phases of degradation”,*Waste Management*, 31(11), 2275-2286.
78. Reddy, K.R., Kulkarni, H.S., and Khire, M.V. (2013). “Two-phase modeling of leachate recirculation using vertical wells in bioreactor landfills.”,*Journal of Hazardous, Toxic and Radioactive Waste*, 17(4), 272-284.
79. Reddy, K.R., Xie, T., and Dastgheibi, S. (2014), “Adsorption of mixed nutrients and heavy metals from simulated urban stormwater by different filter materials”, *Journal of Environmental Science & Health*, Vol. 49, No. 5, pp. 524-539.

80. Rowe, R. K. and Davis, E. H. (1982), "The behaviour of anchor plates in sand", *Geotechnique*, Vol. 32, No. 1, pp. 25 – 41.
81. Sakai, T. and Tanaka, T. (1998), "Scale effect of a shallow circular anchors in dense sand", *Soils and foundations*, Vol. 38 (2), 93-99.
82. Sakai, T. and Tanaka, T. (2007), "Experimental and Numerical Study of Uplift Behavior of Shallow Circular Anchor in Two-Layered Sand", *J. Geotech. Engg, ASCE*, Vol. 133 (4), 469-477.
83. Sakr, M. (2009), "Performance of helical piles in oil sand", *Canadian Geotechnical Journal*, Vol. 46, No. 8, pp. 1046 – 1061.
84. Saran, S. (2006), "Analysis and design of substructures", Oxford and IBH Publishing Co. Ltd.
85. SubbaRao, K. S. and Kumar J. (1994), "Vertical uplift capacity of horizontal anchors", *J. Geotech.Engg, ASCE*, Vol. 120 (7), 1134-1147.
86. Suganthi, A. and Boominathan, A. (2006), "Seismic response studies of Chennai City using geotechnical borehole data and GIS", *Proceedings of Indian Geotechnical Conference, IIT Madras*, Vol. 2, pp. 831-832.
87. Tagaya, K., Tanaka, A., and Aboshi, H. (1983), "Application of finite element method to pullout resistance of buried anchor", *Soils and Found., Japan*, Vol. 23, No. 3, pp. 91-104.
88. Tatsuoka,F., Lo Presti,D.C.F. and Kohata,Y. (1995), "Deformation characteristics of soils and soft rocks under monotonic and cyclic loads and their relationships", *SOA Report, Proc. of the Third Int. Conf. on Recent Advances in Geotechnical Earthquake Engineering and Soil Dynamics, St Luois(Prakash eds.)*, Vol.2, pp.851-879.

89. Tatsuoka, F. (2008), “Recent practice and research of geosynthetic-reinforced earth structures in Japan”, *Journal of GeoEngineering*, Vol. 3, No. 3, pp. 47-67.
90. Tatsuoka, F. (2010), “Cement-based soils in Trans-Tokyo Bay Highway project”, *Soils and Foundations*, Vol. 50, No. 6, pp. 785-804.
91. Terzaghi, K. (1943), “Theoretical soil mechanics”, John Wiley & Sons, New York.
92. Trofimendkov, J. G. and Mariupolskii, L. G. (1965), “Screw piles used for mast and tower foundations”, *Proceedings of Sixth International Conference on Soil Mechanics and Foundation Engineering*, Montreal, Quebec, Vol. 11, pp. 328 -332.
93. Tsuha, C. H. C. and Aoki N. (2010), “Relationship between installation torque and uplift capacity of deep helical piles in sand”, *Can. Geotech. J.*, Vol. 47, No. 5, pp. 635–647.
94. Vanapalli, S.K., Sedano, J.I., and Garga, V.K. (2003), “A rigorous approach of predicting the shear strength of unsaturated soils”, *Proceedings of the 2nd Asian Conference on Unsaturated soils, UNSAT-ASIA*, Osaka, Japan, pp. 253-258
95. Vanapalli, S.K., and Catana, M.C. (2005), “Estimation of the soil-water characteristic curve of coarse grained soils using one point measurement and simple properties”, *International Symposium on Advanced Experimental Unsaturated Soil Mechanics*, Trento, Italy. pp. 401-407.
96. Vanapalli, S.K., Nicotera, M. V., and Sharma, R. S. (2008), “Axis translation and negative water column techniques for suction control”, *Geotech Geol Engg*, Springer, Vol. 26, No. 6, pp. 645 – 660.

PAPERS PUBLISHED FROM CURRENT RESEARCH WORK

Papers in International Journal

1. Mukherjee, S. & Mittal, S. (2015), “Behaviour of Group of Helical Screw Anchors under Compressive Loads”, *Geotech & Geological Engg.*, Springer, Vol. 33, No. 1, pp. 575 - 592.

Papers in National Journal

1. Mukherjee, S. & Mittal, S. (2014), “Vertical Uplift Capacity of a Group of Helical Screw Anchors in Sand: An Empirical Approach”, *Springer*, Vol. 44, No. 4, pp. 480 - 488.
2. Mukherjee, S. & Mittal, S. (2013), “Vertical Uplift Capacity of a Group of Helical Screw Anchors in Sand”, *Springer*, Vol. 43, No. 3, pp. 238 - 250.

Papers in International Conference

1. Mukherjee, S. & Mittal, S. (2015), “Vertical Uplift Capacity of a Group of Equally Spaced Helical Screw Anchors in Sand”, Accepted for publication in ICGE 2015 Colombo Conference.

RESUME

1. **Name:** Sanjeev Mukherjee
2. **Sex:** Male
3. **Father's Name:** Late Dr. Santosh Kumar Mukherjee
4. **Mother's Name:** Mrs. Jaba Mukherjee
5. **Date of Birth:** 1st March 1977
6. **Marital Status:** Married
7. **Nationality:** Indian
8. **Education Qualification:**

Examination	Institute	Period	Marks	Remarks
Master of Engineering [Geotechnical Engineering]	IISc, Bangalore	May '99- Jan '01	7.6 CGPA (Out of 8)	Gold Medal
Bachelor of Engineering [Civil Engineering]	B.I.T. Sindri, Bihar	June '95 - Mar '99	75	First Class with Distinction
H.S. Examination (Science 12 th Standard)	G.L.A. College, Daltonganj	1993	67	First Class
Madhyamik Pariksha (10 th Standard)	Palamau Zila School, Daltonganj	1991	74.1	First Class with Distinction

9. Professional Experience:

Total: 1.5 year (Teaching) + ~8 years (Industry) \approx Total 9.5 years

Amity University, Noida (UP) July '15 - present

Seemanta Engineering College, Baripada (Odisha)

Asst. Professor (Civil Engg) Sep '09 – Dec '10

INFOSYS Technologies Limited, Pune (Maharashtra) Feb '08 – Apr '09

INFOSYS Technologies Limited, Bangalore (Karnataka) Mar '01 – Jan '08

10. Scholarship and Honor

- (a) Recipient of **MHRD scholarship** by **Govt. of India** for pursuing **PhD** for **Financial Years 2011-2014**
- (b) Received **Best Employee Award** from **Finacle** in the **Financial Year 2008 – 09**.
- (c) Recipient of **Gold Medal** from **Indian Institute of Science, Bangalore** pursuing **M.E.** in the **Financial Year 2001**.
- (d) Recipient of **MHRD scholarship** by **Govt. of India** for pursuing **ME** for **Financial Years 1999-2001**.
- (e) Received **All India rank of 20** in **GATE Exam** in **CIVIL Engineering** achieving **99.65 percentile** marks in the **Financial Year 1999**.

11. Memberships of Professional Bodies:

- I. Life Member –Indian Geotechnical Society

12. Papers Published

(a) International Journal

Mukherjee, S. & Mittal, S. (2015), “Behaviour of Group of Helical Screw Anchors Under Compressive Loads”, *Geotech & Geol Eng.*, Springer, Accepted (In Press).

(b) National Journal

Mukherjee, S. & Mittal, S. (2013), “Vertical Uplift Capacity of a Group of Helical Screw Anchors in Sand”, *Indian Geotechnical Journal*, Springer, Vol. 43, No. 3, pp. 238 - 250.

Mukherjee, S. & Mittal, S. (2014), “Vertical Uplift Capacity of a Group of Helical Screw Anchors in Sand: An Empirical Approach”, *Indian Geotechnical Journal*, Springer, Vol. 44, No. 4, pp. 480 - 488.

(c) International Conference

Mukherjee, S. & Mittal, S. (2015), “Vertical Uplift Capacity of a Group of Equally Spaced Helical Screw Anchors in Sand”, Accepted for publication in **ICGE 2015 Colombo Conference**.

(d) National Conference

Mukherjee, S., Rao. P. R. and Murthy, B. R. S. (2001), "Behaviour of large size vertical strip anchors in sand", Proc. Indian Geotechnical Conference - 2001, Indore, Vol. 1, pp. 432 - 435.